Lead Optimization of Highly Potent and Selective CYP11B1 Inhibitors for the Treatment of Cushing's Syndrome and Chronic Wounds

Dissertation

zur Erlangung des Grades

des Doktors der Naturwissenschaften

der Naturwissenschaftlich-Technischen Fakultät

der Universität des Saarlandes

von

M. Sc. Juliette Emmerich

Saarbrücken

2017

Tag des Kolloquiums: 02.03.2018

Dekan: Prof. Dr. Guido Kickelbick

Berichterstatter:

Prof. Dr. R. W. Hartmann

Prof. Dr. Gerhard Wenz

Vorsitz: Prof. Dr. Claus Jacob

Akad. Mitarbeiter: Dr. Stefan Boettcher

Dedicated to My Parents

Acknowledgements

Results described in this thesis were prepared under the guidance of Prof. Dr. Rolf W. Hartmann. The work was conducted at the Department of Pharmaceutical and Medicinal Chemistry of Saarland University and the Helmholtz Institute for Pharmaceutical Research Saarland (HIPS) from November 2010 till February 2015.

Manuscripts included in this thesis

The main part of this thesis consists of three chapters, which were published in peer-reviewed journals or are accepted for publication.

Chapter 3.1.

Cushing's Syndrome: Development of Highly Potent and Selective CYP11B1 Inhibitors of the (Pyridylmethyl)pyridine Type

Emmerich, J.; Hu, Q.; Hanke, N.; Hartmann, R. W.

Journal of Medicinal Chemistry **2013**, *56* (15), 6022-6032.

Chapter 3.2.

Lead Optimization Generates CYP11B1 Inhibitors of Pyridylmethyl Isoxazole Type with Improved Pharmacological Profile for the Treatment of Cushing's Disease

Emmerich, J.; van Koppen, C. J.; Burkhart, J. L.; Hu, Q.; Siebenbürger L.; Boerger, C.; Scheuer, C.; Laschke, M. W.; Menger, M. D.; Hartmann, R. W.

Journal of Medicinal Chemistry **2017,** *60* (12), 5086-5098.

Chapter 3.3.

Accelerated Skin Wound Healing by Selective 11β-Hydroxylase (CYP11B1) Inhibitors.

Emmerich, J.; van Koppen C. J.; Burkhart, J. L.; Engeli, R.; Hu, Q.; Odermatt, A.; Hartmann, R. W.

European Journal of Medicinal Chemistry **2018**, *143*, 591-597.

Further publication that is not part of this thesis

Novel Pyridyl- or Isoquinolinyl-Substituted Indolines and Indoles as Potent and Selective Aldosterone Synthase Inhibitors.

Yin, L.; Hu, Q.; Emmerich, J.; Lo, M. M.; Metzger. E., Ali. A.; Hartmann, R. W.

Journal of Medicinal Chemistry **2014**, *57* (12), 5179-5189.

Summary

The key characteristic of Cushing's syndrome is an abnormally elevated cortisol plasma level. This can be controlled by inhibition of 11β-hydroxylase (CYP11B1), the enzyme catalyzing the last step of the biosynthesis of cortisol.

In the present thesis, lead optimization of the first reported selective CYP11B1 inhibitors resulted in an inhibitor with a 50-fold improved potency for human CYP11B1 (IC_{50}= 2 nM). Additional investigations revealed a promutagenic potential of the inhibitor and a low oral bioavailability in rats (F= 2%). Subsequent structural modifications resulted in a similarly potent and selective compound exhibiting no toxicity and a high oral bioavailability in rats (F= 50%). A good candidate for further *in vivo* studies was identified, which exceeds the clinically used inhibitor metyrapone in terms of CYP11B1 potency and selectivity.

Previous studies have shown that inhibition of cortisol biosynthesis in skin leads to accelerated wound healing. Here, CYP11B1 inhibitors were optimized for topical application to avoid systemic side effects. The resulting very potent, selective CYP11B1 inhibitor exhibited high stability toward human plasma (as a substitute for wound fluid) and low stability toward HLS9 ($t_{1/2}$ = 19 min) for rapid metabolic clearance after absorption. The inhibitor was able to accelerate wound healing in human skin at the applied concentration of 5 µM.

Zusammenfassung

Charakteristisch für die Krankheit Morbus Cushing ist ein abnormal erhöhter Cortisol-Plasmaspiegel. Dieser kann durch Hemmung des Enzyms 11β-Hydroxylase (CYP11B1), welches den letzten Schritt der Biosynthese von Cortisol katalysiert, reguliert werden.

Hier führte eine gezielte Strukturoptimierung von CYP11B1-Inhibitoren zu einer 50-fach potenteren Verbindung bezüglich des humanen CYP11B1-Enzyms. Zusätzliche Untersuchungen offenbarten ein promutagenes Potential des Inhibitors und eine geringe orale Bioverfügbarkeit in Ratten (F = 2%). Nachfolgende strukturelle Modifikationen resultierten in einer ähnlich potenten und selektiven Verbindung, die keine Toxizität aufweist und eine hohe orale Bioverfügbarkeit in Ratten (F = 50%) zeigt. Somit gelang die Identifizierung eines geeigneten Kandidaten für weitere *in vivo* Studien, welcher den klinisch verwendeten Inhibitor Metyrapon bezüglich CYP11B1-Potenz und -Selektivität übertrifft.

Untersuchungen haben gezeigt, dass eine Hemmung der Cortisol-Biosynthese in der Haut zu einer beschleunigten Wundheilung führt. Hierfür wurden CYP11B1-Inhibitoren für eine Anwendung auf der Haut optimiert. Die dabei erhaltene Verbindung zeigte sowohl eine hohe Stabilität gegenüber menschlichem Plasma (als Ersatz für Wundflüssigkeit) als auch eine geringe metabolische Stabilität für eine schnelle Ausscheidung nach der Absorption. Der Inhibitor war in der Lage, die Wundheilung in der menschlichen Haut bei einer Anwendungskonzentration von 5 µM zu beschleunigen.

Abbreviations

11β-HSD1	11β-Hydroxysteroid dehydrogenase type 1
11β-HSD2	11β-Hydroxysteroid dehydrogenase type 2
AIBN	Azobisisobutyronitrile
BINAP	2,2'-Bis-(diphenylphosphino)-1,1'-binaphthyl
CD	Cushing's disease
CDI	1,1'-Carbonyldiimidazole
CS	Cushing's syndrome
CYP11B1	11β-Hydroxylase
CYP11B2	Aldosterone synthase
CYP17A1	17α-Hydroxylase-17,20-lyase
CYP19A1	Aromatase
CL_{int}	Intrinsic clearance
DBPO	Dibenzoyl peroxide
dppf	1,1'-Bis(diphenylphosphino)ferrocene
FFD	Factional factorial design
GC	Glucocorticoid
HLS9	Human liver S9 fraction
HPA	Hypothalamic-pituitary-adrenal
MIF	Molecular interaction fields
NBS	*N*-bromosuccinimide
NMP	*N*-methyl-2-pyrrolidone
n.d.	Not determined
PAPS	3'-Phosphoadenosine-5'-phosphosulfate
PLS	Partial least- squares analysis
QSAR	Quantitative structure–activity relationship
Ref	Reference
RT	Retention time
rt	Room temperature
SAR	Structure–activity relationship
SDEC	Standard deviation of error of calculation
SDEP	Standard deviation of error of prediction
SF	Selectivity factor = $IC_{50\ CYP11B2}/\ IC_{50\ CYP11B1}$
SPhos	2-Dicyclohexylphosphino-2',6'-dimethoxybiphenyl
SRD	Smart region definition
StAR	Steroidogenic acute regulatory protein
$t_{1/2}$	Half-life

Table of Content

1. Introduction

Hormones are an essential part of the communication system within the body. They are signaling molecules which are produced by specific cells and subsequently transported by the circulatory system to reach their distinct target receptors (endocrine signaling). This leads to the activation of associated signal transduction pathways and cell type-specific responses. Among the diverse structural classes of hormones, steroids represent one main class. These, in turn, are classified according to the receptors to which they bind, such as mineralocorticoids, androgens, estrogens, progestogens and glucocorticoids. Cortisol is a crucial glucocorticoid affecting almost every cell in the body. This hormone is released in response to stress and influences the blood pressure, increases blood sugar, controls the metabolism of fats, proteins and carbohydrates and supresses inflammation. Its secretion is mainly controlled by the hypothalamus in the brain, the pituitary gland situated at the base of the brain and the adrenal glands, which are located above the kidneys (hypothalamic-pituitary-adrenal axis).[1]

1.1. Hypothalamic-Pituitary-Adrenal Axis

The production of the glucocorticoid cortisol is usually mediated through the hypothalamic-pituitary-adrenal (HPA) axis (Figure 1). In the event of stress, corticotropin-releasing factor (CRF), which is secreted by the paraventricular nucleus of the hypothalamus, binds to receptors on the pituitary corticotropes. Consequently, adrenocorticotropic hormone (ACTH) is released into the systemic circulation and binds to receptors located in the adrenal cortex. Thereby, the cyclic adenosine monophosphate (cAMP) level increases, which in turn leads to activation of a cAMP-dependent protein kinase. The associated cholesterol esterase is activated through phosphorylation, which leads to cholesterol release from the lipid droplet storage.[2-3]

Further, cholesterol transport from the outer membrane to the inner membrane in mitochondria of the adrenal cortex is mediated by ACTH-induced gene transcription and subsequent phosphorylation of the steroidogenic acute regulatory protein (StAR).[3] In the following, cholesterol is transformed to cortisol in a multi-step biosynthesis (see chapter 1.2.). Cortisol is then secreted, suppressing ACTH as well as CRF production (negative feedback of the HPA axis) and regulating cardiovascular, immune and metabolic processes (Figure 1).[2]
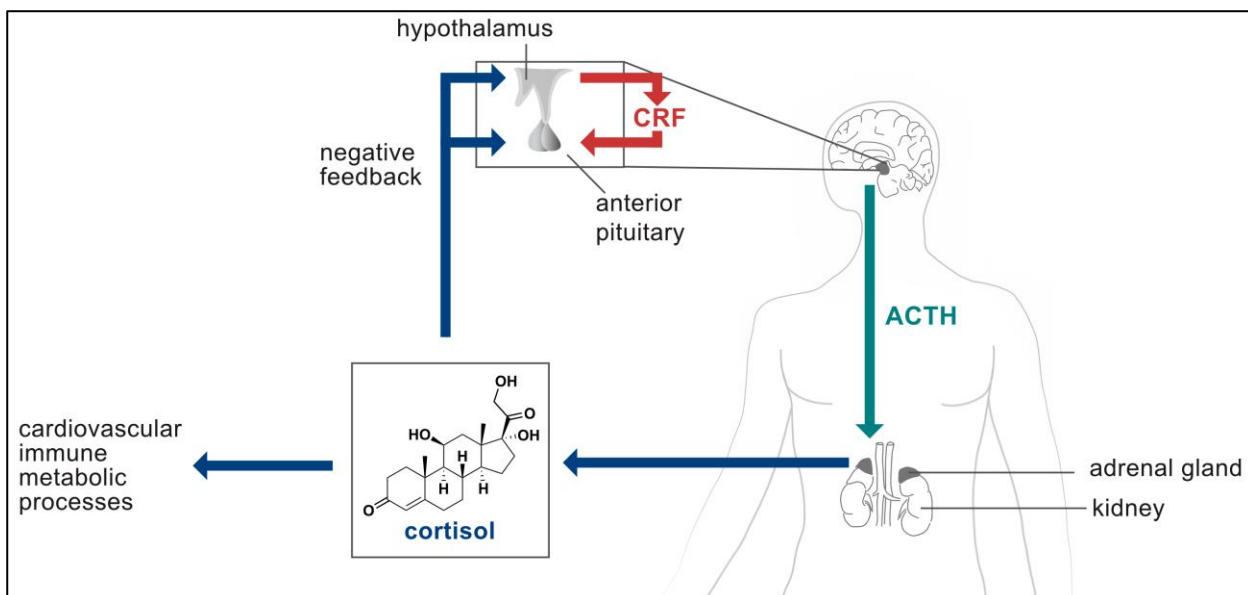
Figure 1. The HPA axis. Modified from ref[4].

1.2. Steroidogenesis

Steroid hormones such as cortisol are synthesized from cholesterol catalyzed by various cytochromes P450 and hydroxysteroid dehydrogenases (HSDs) in the adrenal glands.[5] Cytochromes P450 are a large superfamily of heme-containing enzymes catalyzing mixed-function oxidation reactions. They alter their lipophilic substrates via introduction of molecular oxygen using electrons of the cofactor nicotinamide adenine dinucleotide phosphate (NADPH).[5] HSDs are oxidoreductases using $NADP^+$ or NAD^+ as cofactors. In contrast to HSD mediated reactions, hydroxylation, oxidation and carbon-carbon bond cleavage reactions catalyzed by CYP450s are mechanistically irreversible.[3] After transport to the inner mitochondrial membrane, cholesterol is transformed to pregnenolone (Figure 2) in a rate-limiting first step, which is catalyzed by the cholesterol side chain cleavage enzyme (P450scc, CYP11A1).[3] Further, pregnenolone is then either hydroxylated to 17α-hydroxypregnenolone by 17α-hydroxylase-17,20-lyase (CYP17A1) or converted to progesterone by 3β-hydroxysteroid dehydrogenase/Δ^{5-4} isomerase (3β-HSD). Both precursors can be modified with the help of either CYP17A1 or 3β-HSD to obtain 17α-hydroxyprogesterone. Additional hydroxylation by 21-hydroxylase (CYP21A1) leads to 11-deoxycortisol. Last, an oxidation reaction to generate the glucocorticoid cortisol is conducted by 11β-hydroxylase (CYP11B1). The mineralocorticoid aldosterone, which is responsible for the regulation of blood pressure[5], is formed from intermediate progesterone via successive hydroxylations in positions C-21 (to deoxycorticosterone by CYP21A1) and C-11 (to

corticosterone by CYP11B1 or aldosterone synthase (CYP11B2)).[5-6] Subsequently, corticosterone is further hydroxylated and oxidized in position C-18 catalyzed by aldosterone synthase.[5-6]
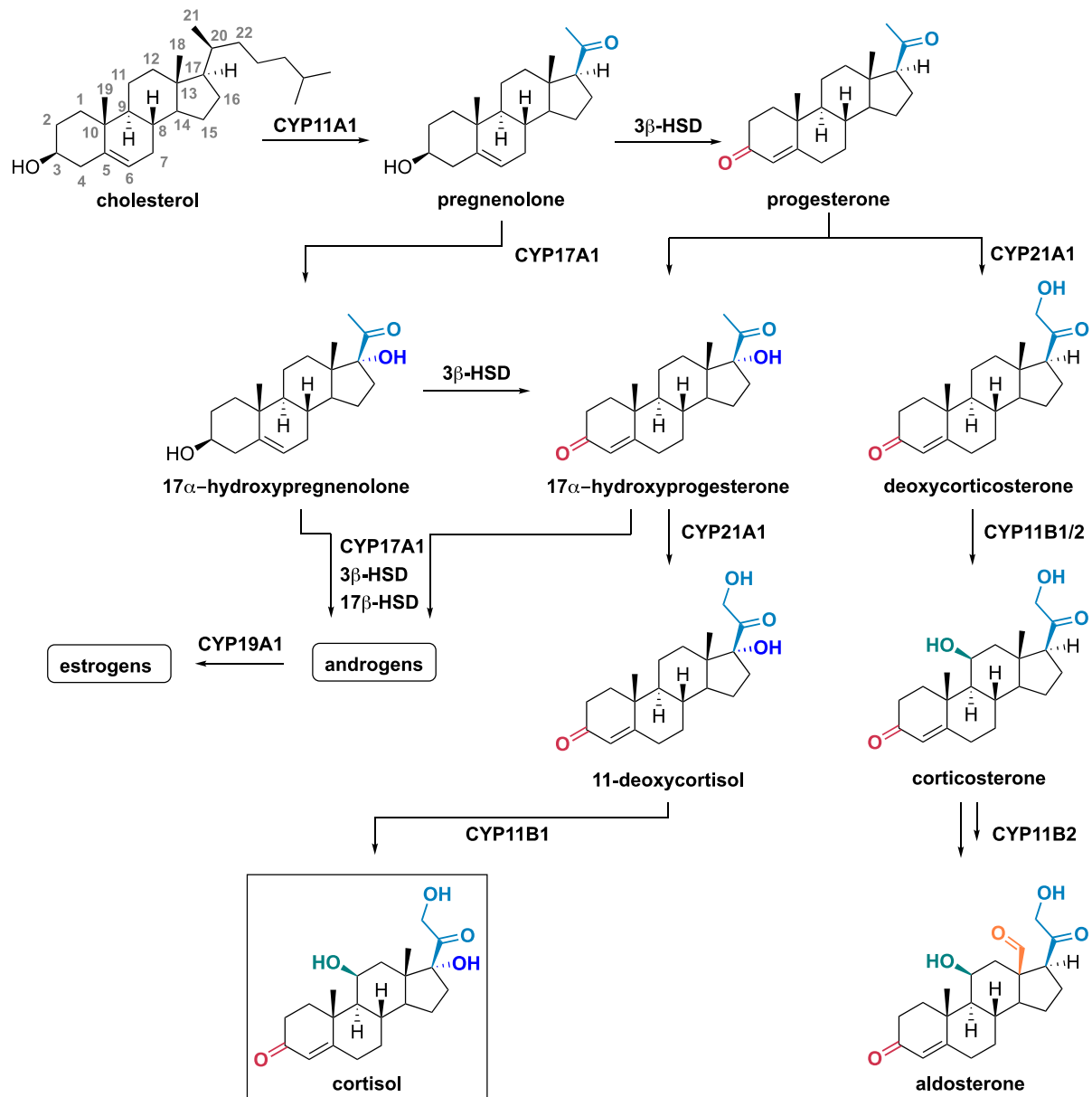
Figure 2. Steroidogenesis.

Precursors of the sex hormones (androgens and estrogens) are formed as well from the intermediates 17α-hydroxypregnenolone and 17α-hydroxyprogesterone catalyzed by CYP17A1 and 3β-HSD. Afterwards, these precursors are transformed to estrogens and androgens in the gonads by 17β-hydroxysteroid dehydrogenases (17β-HSD) and additionally by aromatase (CYP19A1) in the case of estrogens.[5]

1.3. Cortisol and 11β-HSD

In general, the plasma concentration of cortisol is 100–1000-fold higher compared to the aldosterone concentration. Both hormones show similar binding affinities for the mineralocorticoid receptor *in vitro*.[7] Thus, excessive cortisol would trigger, for instance, hypertension by occupying the mineralocorticoid receptor *in vivo*.[8]
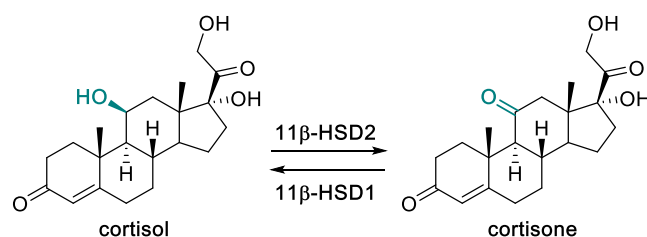
Figure 3. Regulation of the local cortisol concentrations.

To overcome this problem, cortisol is converted to the inactive storage form cortisone catalyzed by the enzyme 11β-HSD2 (Figure 3). If necessary, cortisone can be reactivated by 11β-HSD1. Thus, the local concentration of cortisol is regulated by these enzymes.[8] 11β-HSD1 is expressed in a variety of glucocorticoid target tissues such as liver, adrenal, gonad, brain, skin and adipose tissue.[9] In contrast, 11β-HSD2 expression is mainly limited to aldosterone-selective tissues such as kidney, colon, placenta, sweat and salivary glands.[10]

1.4. Cushing's Syndrome

First described in the 1930s[11], Cushing's syndrome (CS) is associated with elevated plasma levels of the stress hormone cortisol. In the case of CS, plasma cortisol levels are often abnormally elevated due to a long-term, high-dose treatment with adrenocorticotrophic hormone (ACTH) or a glucocorticoid (exogenously).[8] In rare cases (0.7-5 cases per year per million population)[8, 12], the overproduction can be caused within the body (endogenously). This mainly originates from pituitary (70%, termed Cushing disease (CD)) or ectopic tumors (10%) generating ACTH (ACTH-dependent), which leads to an increase of cortisol. Less frequently, the disease is caused by cortisol producing adrenal adenomas (10%) or adrenocortical carcinomas (5%) (ACTH-independent).[8, 13] Especially in the case of CD and adrenal adenomas, females are much more often affected than males (3.5:1 ratio).[12]

Diagnosis is challenging as the development of a full symptomatology lasts months to years and signs are not necessarily related with CS.[8] Truncal obesity (96%), facial fullness (82%), carbohydrate intolerance or diabetes type II (80%), gonadal dysfunction (74%), hirsutism or acne (72%), hypertension (68%), muscle weakness (64%), skin atrophy and bruising (62%) as well as mood disorders (58%) are typical symptoms of the disease.[8, 14] Particularly, the associated cardiovascular and infection risk results in increased morbidity and mortality for the patients.[15] Symptoms differ among patients and even the most frequently occurring ones are missing in some cases.[14]

In addition, metabolic syndrome, which is affecting probably one fourth of the world population,[16] shares common manifestations with CS such as hypertension, visceral obesity and insulin resistance.[16-17] However, plasma cortisol levels in metabolic syndrome patients are not elevated to the diagnostic threshold of CS.[16-17] To ensure the diagnosis of CS over metabolic syndrome, three main tests are available. As the normal circadian rhythm of cortisol production is disturbed in CS, 24 hours urinary-free cortisol tests as well as midnight plasma or late-night salivary cortisol measurements are applied. Furthermore, as dexamethasone is a potent agonist for the glucocorticoid receptor, a low-dose dexamethasone-suppression test should decrease cortisol levels in healthy patients.[12] None of the aforementioned tests is reliable, but one or more abnormal results give strong evidence that CS is present.[12, 14]

For the treatment of exogenous CS, at least gradual reduction of administered corticosteroids to the lowest effective dose is required. A complete discontinuation of corticosteroid medication is dangerous, as the natural steroids might not be produced endogenously anymore due to their high external supply, which could result in Addison's disease.[18]

In the case of pituitary or ectopic carcinomas leading to an overproduction of cortisol (endogenous CS), surgical tumor removal is the first-line treatment associated with a 65-90% remission rate and low morbidity.[8, 19] However, around 25% of patients suffer from a relapse within 10 years.[19-20] Post-operative treatment with glucocorticoid replacements is necessary for 6-12 months until HPA axis normalization.[8] Another effective rapid action is a unilateral or bilateral adrenalectomy, especially in cases of cortisol producing adrenal adenomas and carcinomas. Nevertheless, corticotroph adenoma progression is discovered in about 30% of cases and a lifelong well-balanced replacement of glucocorticoids and mineralocorticoids is required.[19]

For patients which are unsuitable for surgery as well as for inaccessible or invisible tumors, radiotherapy is applied.[12] Pituitary irradiation treatment lasts up to two years and is associated with inherent side effects such as hypopituitarism.[12, 20]

Until radiotherapy is effective, medical treatment is required as the patients are still exposed to glucocorticoid excess. Furthermore, cortisol-controlling drugs are needed for the preparation of

patients before surgery to prevent complications (e.g. bleeding tendency), if tumor resection was unsuccessful and for the period until CS diagnosis is assured.[20-21]

1.5. Medical Treatment of Cushing's Syndrome

1.5.1. Pituitary-Targeted Drugs

There are several approaches to target the tumor and the resulting ACTH overproduction in the pituitary by inhibition of the receptors overexpressed in the tumor. For instance, administration of the selective somatostatin receptor subtype 5 (sst5) ligand pasireotide (Signifor[R], Novartis, Figure 4) normalized the urinary free cortisol (UFC) level after 12 months in 19.1% of CD patients and improved blood pressure and body weight. However, this treatment also resulted in hyperglycemia in 73% of cases.[22] Pasireotide was approved in the EU and the US in 2012 for use in patients with CD for whom surgery is not an option or has failed.[19, 23]

It was also shown that dopamine subtype 2 (D2) receptors are expressed in 80-89% of pituitary tumors.[24] Cabergoline (Figure 4), a D2 receptor agonist, showed normalization of cortisol levels in 37% of patients.[22]
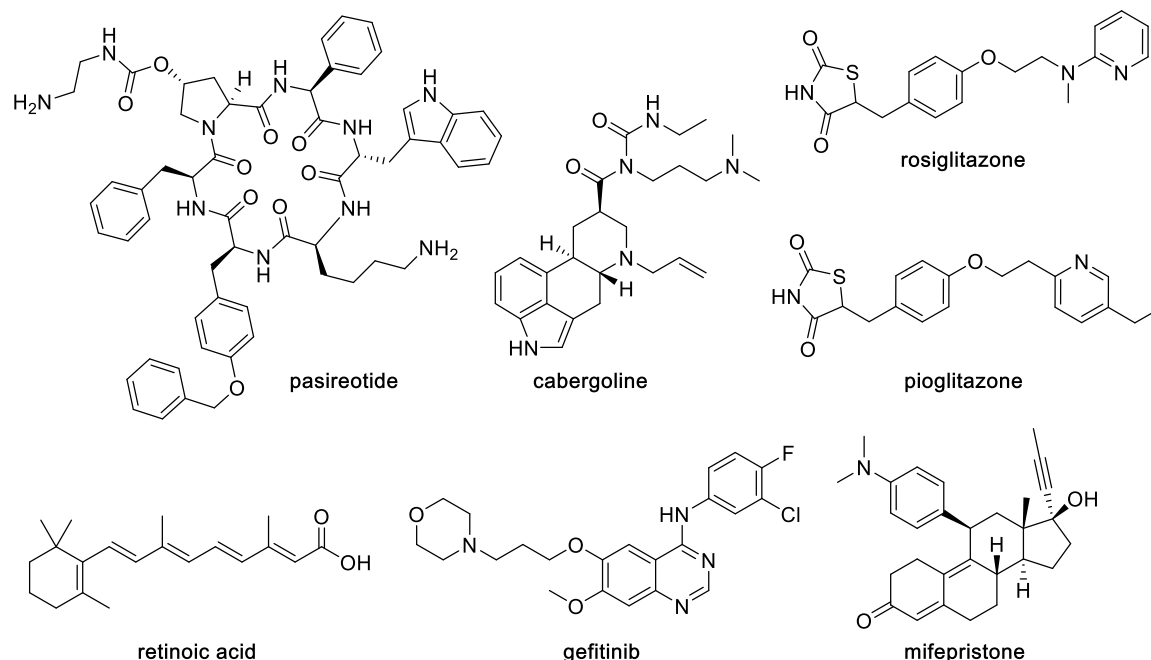
Figure 4. Pituitary-Targeted Drugs and Mifepristone

Studies published so far did not report any severe side effects (the most frequent among them were nausea and dizziness), however, larger multi-center studies to confirm efficacy and safety are

missing.[25] Peroxisome proliferator-activated receptor-gamma (PPAR-γ, functions as a transcription factor) ligands have been demonstrated to inhibit the growth of several kinds of tumors.[19] Unfortunately, efficiency observed *in vitro* with PPAR-γ ligands such as rosiglitazone and pioglitazone (Figure 4) on ACTH secretion and corticotroph tumor cell proliferation has not been reproduced in CD patients.[22, 26]

Inhibition of ACTH release and tumor growth *in vitro* and *in vivo* was achieved through action on POMC gene transcription by retinoic acid (Figure 4). The compound was well tolerated regarding adverse events in a small prospective study (7 patients), but again larger studies are necessary.[25] Another approach (still under research) suggested the tyrosine kinase inhibitor gefitinib (Figure 4) as a potential drug for treatment as it blocks the epidermal growth factor receptor (EGFR), which is overexpressed in a significant proportion of pituitary corticotroph adenomas.[27]

1.5.2. Glucocorticoid Receptor Antagonists

Instead of targeting the ACTH overproducing tumor, the effect of cortisol excess can also be prevented by blocking the glucocorticoid (GC) receptor with an antagonist such as mifepristone (Figure 4).[26] Indeed, clinical symptoms of CS were significantly improved, which is why mifepristone was approved by the FDA in 2012 to control hyperglycemia in endogenous CS patients. In analogy to pasireotide, the treatment with mifepristone is limited to patients who are not suitable candidates for surgery or in whom surgery has failed.[26] However, an abnormally high level of cortisol is still present, which results in mineralocorticoid receptor binding and, therefore, in hypokalemia, increased blood pressure, edema and worsening of salt retention.[28] Furthermore, the negative feedback mechanism of the HPA axis, usually triggered by cortisol binding to the GC receptor, is interrupted leading to an increase of plasma ACTH and cortisol levels.[26, 28]

1.5.3. Cortisol Secretion Inhibitors

Another promising approach is the inhibition of cortisol overproduction by blocking steroidogenic enzymes, especially CYP11B1. As mentioned before, the enzyme catalyzes the last step of the biosynthesis of cortisol (Figure 5). Selective inhibition of CYP11B1 is challenging as human CYP11B1 and CYP11B2 exhibit a 93% sequence identity[29] on the protein level and only differ in 29 out of 479 residues, which are situated outside the substrate recognitions sites.[5, 30] The co-crystal structure of human CYP11B2 and deoxycorticosterone was recently published,[6] but no crystal structure of CYP11B1 is resolved so far.
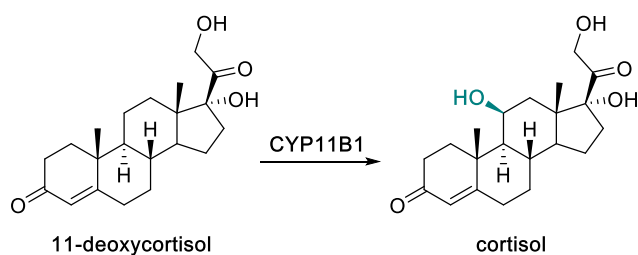
Figure 5. Last step of the biosynthesis of cortisol

According to a homology model, the position of the heme varies slightly in both enzymes as the side chains and their binding loop orientations influence the heme environment differently.[5] In addition, the active site of CYP11B1 was predicted to be bigger compared to that of CYP11B2.[5] In general, selective inhibition of CYP enzymes is difficult to achieve as they all contain one common motif, an iron chelating heme in the active site. Thus, inhibitors interacting with the heme can be unselective.[31-32]

Despite induced side effects caused by unselective inhibition, CYP11B1 inhibitors are commonly used in the clinic and rapidly relieve hypercortisolism and related complications.[5, 21, 33]
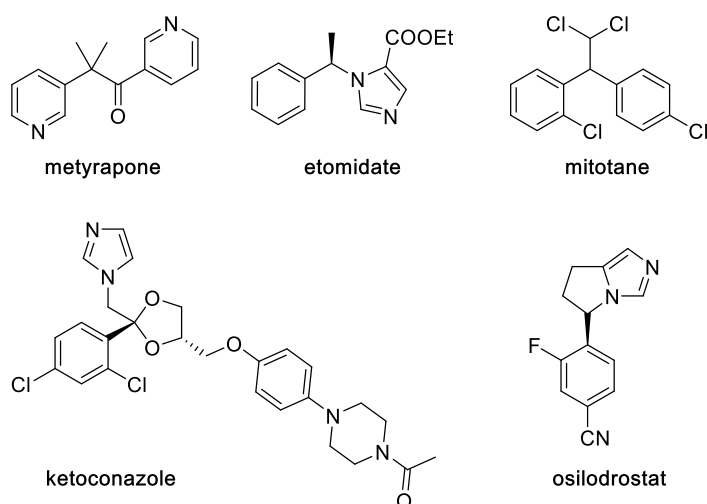
Figure 6. CYP11B1 inhibitors in clinical use or trial

For instance, after initial dosing with the potent CYP11B1 inhibitor metyrapone (Figure 6), cortisol levels drop within four hours.[21] However, at low doses, which do not influence the cortisol synthesis, a strong, CYP11B2-associated effect on aldosterone synthesis was observed.[34] Therefore, treatment with metyrapone may result in accumulation of 11-deoxycorticosterone, the precursor of aldosterone, which binds to the mineralocorticoid receptor leading to hypokalemia, hypertension and edema.[5] As the cortisol synthesis is blocked as well, the negative feedback mechanism for ACTH is reduced. Subsequently, production of ACTH increases, which leads to elevated levels of mineralocorticoid precursors and androgens. The latter causes acne, hirsutism

and voice deepening, which limits longer treatments in women.[24, 35] If overtreatment and hypoadrenalism (deficiency of cortisol causing, e.g., dizziness and nausea) are avoided, the drug is tolerated well in most patients.[21] Therefore, cortisol levels are usually reassessed after administration of a routine starting dose and if necessary, the dose is adjusted until a mean cortisol level between 150 and 300 nmol/L is reached.[21]

Ketoconazole (Figure 6) is another commonly used steroidogenesis inhibitor, which was originally developed as an oral antifungal agent. The risks of overtreatment and hypoadrenalism are lower as it shows a low onset of action.[21] In contrast to metyrapone, it does not only unselectively inhibit CYP11B1 and CYP11B2, but also CYP17A1, CYP11A1 and some hepatic CYP enzymes such as CYP3A4.[21, 36] Side effects such as gastrointestinal adverse effects, gynecomastia, hypogonadism and rash are observed.[26] More importantly, occurrence of liver enzyme dysfunction in some cases leads to severe hepatotoxicity and associated deaths.[21, 26, 37]

The anesthetic agent etomidate (Figure 6) shows an effective and rapid effect by blocking CYP11B1, but as well inhibits CYP11B2, CYP17A1 and CYP11A1.[21] Its use is limited to seriously sick patients due to the observed sedative effect and as it has to be administered intravenously.[21]

The unselective 11β-hydroxylase and CYP11A1 inhibitor mitotane (Figure 6) possesses a slow onset of action and may persist in circulation over months after finishing treatment.[21, 38] As mitotane is teratogenic, pregnancy should be avoided for a long time after discontinuation.[21] Furthermore, adverse effects such as diarrhoea, anorexia, nausea, adrenal insufficiency and dizziness are observed during treatment.[21]

The steroidogenesis inhibitors described above have already been in use for decades. Recently, osilodrostat (LCI699) was developed and is currently undergoing a Phase III clinical trial to evaluate efficacy and safety for Cushing's disease patients. However, besides potent inhibition of CYP11B1, it strongly effects CYP11B2 as well. In Phase II clinical trials, osilodrostat effectively and rapidly normalized cortisol levels.[23, 39] Side effects such as fatigue, nausea, headache, diarrhoea, adrenal insufficiency, hirsutism and acne were reported so far.[23, 39] It was demonstrated that osilodrostat is already effective at much lower doses (~100 times) compared to metyrapone.[23] Nevertheless, due to CYP11B2 inhibition, the plasma concentration of 11-deoxycorticosterone increased and it was assumed that the resulting hypermineralcorticism may in turn result in hypokalemia in some patients.[23] Despite the observed hypermineralcorticism, hypertension did not seem to be a serious issue, which might be due to the benefit of lower levels of circulating cortisol.[23] Both Phase II studies were conducted in a small number of patients and the effect of the drug still has to be assessed in a larger patient population.[39] Extensive clinical trials are difficult to conduct due to the rarity of Cushing's disease.[38] Nevertheless, steroidogenic CYP

enzyme inhibitors are most promising for the medical treatment of Cushing's disease so far, as response rates for metyrapone (75%, one study), mitotane (72%, one small study) and osilodrostat (79-90%, two small Phase II studies) are higher than for the pituitary-targeting drugs pasireotide (17-29%, only one assessed in randomized trial) and cabergoline (25-50%, 4 studies).[38-39] The glucocorticoid receptor antagonist mifepristone was evaluated in a study including patients with CD and other forms of CS and showed response rates of 38-60%.[38]

1.5.4. First Selective CYP11B1 Inhibitors

In 2010, the potent CYP11B1 and CYP11B2 inhibitor R-etomidate (see chapter 1.5.3., IC_{50} CYP11B1= 0.5 nM, IC_{50} CYP11B2= 0.1 nM, Figure 7) was structurally optimized aiming for selective CYP11B2 inhibitors.[40-41] Despite the existing high sequence identity of both enzymes (93%)[29], elimination of the ester and methyl substituents resulted in the slightly selective CYP11B1 inhibitor **1** (IC_{50} CYP11B1= 135 nM, selectivity factor (SF): IC_{50} CYP11B2/IC_{50} CYP11B1= 3.4, Figure 7).[40-41]
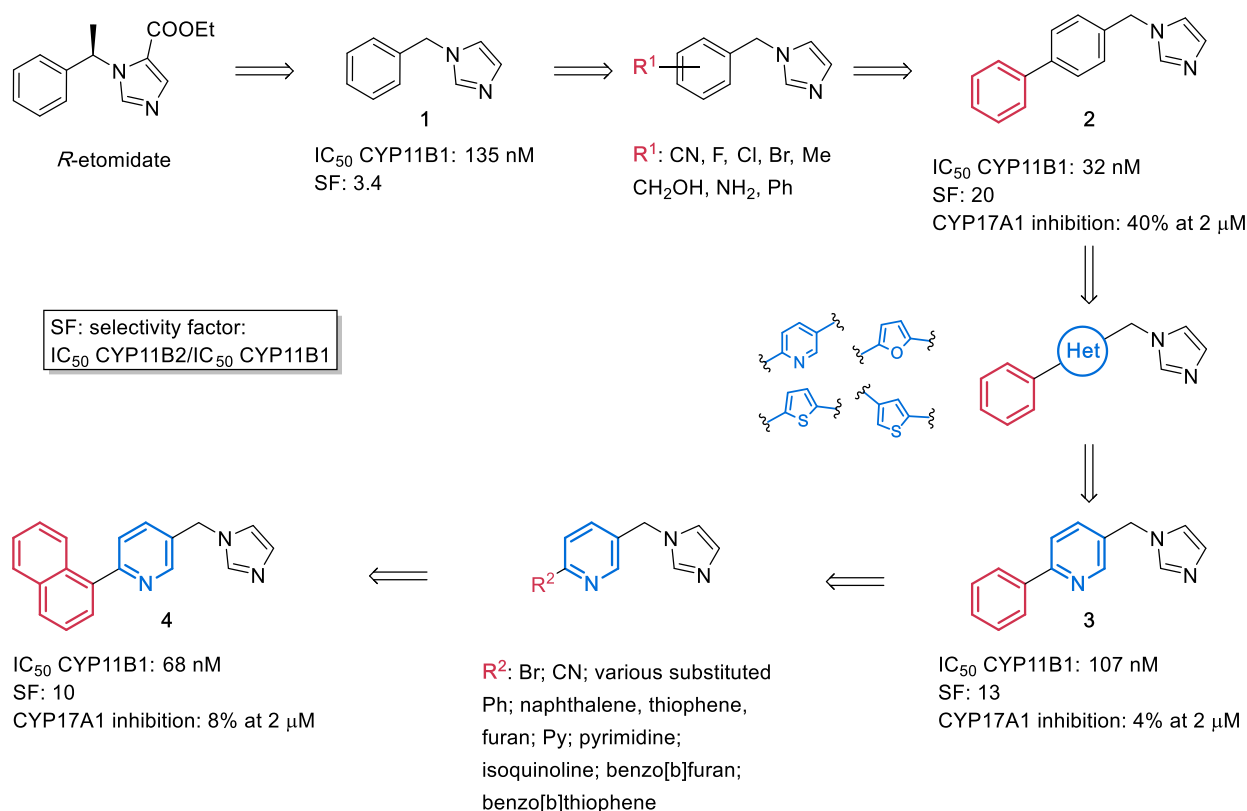
Figure 7. Development of the first selective CYP11B1 inhibitors.

Modification of the phenyl in various positions with substituents differing in electronic properties and H-bond acceptor and donor characteristics led to inhibitor **2** (IC_{50} CYP11B1= 32 nM, SF= 20,

Figure 7), which exhibits increased CYP11B1 potency and selectivity towards CYP11B2.[40-41] As the compound inhibits CYP17A1 as well (40% at 2 µM), further optimization was performed.[41] Exchange of the central phenyl ring of compound **2** by the heterocycles pyridine, thiophene and furan resulted in the first selective CYP11B1 inhibitor **3** (IC_{50} CYP11B1= 107 nM, SF= 13, CYP17A1 inhibition: 4% at 2 µM, Figure 7).[41-42] Further attempts to improve potency and selectivity via replacement of the phenyl in pyridine **3** with various substituted phenyls or heterocycles resulted in the slightly more potent and similarly selective inhibitor **4** (IC_{50} CYP11B1= 68 nM, SF= 10, CYP17A1 inhibition: 8% at 2 µM, Figure 7).[42-43] The selectivity factors described here for **3** and **4** were re-determined for the studies presented in the following and differ from the originally published data due to different enzyme sources. Nevertheless, compared to the CYP11B1 inhibitors used in the clinic, **3** and **4** are similarly potent as ketoconazole (IC_{50} CYP11B1= 127 nM, SF= 0.5) but exhibit much higher selectivity towards CYP11B2 and CYP17A1.[41-43] Therefore, they are promising lead compounds for further optimization studies.

1.6. Role of Cortisol during Skin Wound Healing

The epidermis is the outermost layer of the skin and functions as a shield against mechanical, biological and chemical harms. In case of an injury, the complex wound healing process is accomplished by the highly controlled and timed phases of hemostasis, inflammation, proliferation, and remodeling.[44] Interference of this system results in impaired tissue repair and, therefore, in delayed acute or chronic wounds associated with pathologic inflammation and severe pain.[44] In the USA alone, 3 to 6 million people suffer from chronic wounds, which mainly occur as ulcers (70%) caused by diabetes mellitus, ischemia, pressure or venous insufficiency.[44-45] Especially elderly people are affected and with the increasing occurrence of diabetes and obesity in an aging society, this is an urgent problem requiring immediate care.[44] Current treatments are often ineffective and cause a financial burden for the patients and the health care system.[44, 46] Glucocorticoids play an important role in regulating migration and proliferation of keratinocytes following wound closure.[44, 47] In case of stress, the wound healing process is significantly delayed due to the up-regulation of systemic cortisol levels, which is associated with reduced levels of pro-inflammatory cytokines and suppressed immune response, fibroblast proliferation and collagen synthesis.[44] Keratinocytes, which are the main components of the epidermis (90%),[47] synthesize cortisol *de novo* from cholesterol.[46-47] All components for an independent glucocorticoid synthesis are present such as the cholesterol transporter StAR, ACTH, CYP11A1, CYP17A1, 3β-

HSD1, CYP21A1 and CYP11B1.[47] Here, cortisol seems to function as a local negative feedback for proinflammatory cytokine IL-1β production and associated signaling molecules, which are important for activating keratinocyte migration and proliferation. However, persistent IL-1β production would lead to excessive inflammation and further tissue damage.[46] Therefore, IL-1β triggers the release of ACTH and subsequently the expression of CYP11B1, which is responsible for cortisol synthesis during wound healing.[46] Fine-tuning of the cortisol concentration in skin is possible in the same manner as described for the steroidogenesis in the adrenals. The enzymes 11β-HSD1 and 11β-HSD2 catalyze the transformation of inactive cortisone to active cortisol and reversely (Figure 3).[46] In acute wounds (human and porcine), it was demonstrated that CYP11B1 and cortisol levels gradually increase for 48 hours to control the proinflammatory signals and are normalized again by 96 hours after wounding to avoid delay of wound healing.[46] It was shown that cortisol synthesis can be blocked by the CYP11B1 inhibitor metyrapone, which resulted in increased interleukin IL-1β expression and accelerated wound healing *ex vivo* in human skin explants and *in vivo* in porcine skin.[46] Additional experiments in mice revealed an increase of 11β-HSD1 levels during wound healing and enhanced wound repair through blockade of this enzyme.[48] Interestingly, CYP11B1 is not expressed in rodent skin and metyrapone is known to inhibit 11β-HSD1 as well.[48] A promising approach for new treatments of chronic non-healing wounds could be the inhibition of CYP11B1 as the enzyme is overexpressed and the glucocorticoid receptor pathway is activated at any time.[49-50] However, further extensive investigations are necessary to clarify the individual beneficial effect of CYP11B1 or 11β-HSD1 inhibition during wound healing in human skin. It is worth mentioning that CYP17A1 and CYP19A1 are expressed in skin as well and positively influence wound healing through the synthesis of estrogens, which accelerate wound healing, retain skin moisture and avoid skin aging. [47, 51-52]

2. Aim of the Thesis

The development of improved or novel treatments for rare diseases such as endogenous Cushing's syndrome is limited due to the small number of patients concerned and the associated little interest by the profit-oriented pharmaceutical industry. CYP11B1 inhibitors which are in clinical use for Cushing's disease have been applied for decades but show severe side effects due to unselective inhibition of other steroidogenic or hepatic CYP enzymes (see chapter 1.5.3.). A few years ago, the first potent and selective CYP11B1 inhibitors, such as **3** and **4** (Chart 1), were reported.[41-43] They exceed known CYP11B1 inhibitors regarding selectivity towards CYP11B2 and other steroidogenic CYP enzymes.[41-43] However, investigation of their efficiency in a proof of concept study in rats was limited due to poor inhibition of rat CYP11B1 ($IC_{50} > 10000$ nM).[42] Furthermore, the compounds required improvement of human CYP11B1 inhibitory activity ($IC_{50} = 68$-107 nM) to decrease the doses which have to be administered, thus reducing the risks of off-target effects. As part of the present thesis, rational lead optimization of compounds **3** and **4** was to be performed (Chart 1) aiming at more potent inhibitors of human and rat CYP11B1 while maintaining the important selectivity towards CYP11B2.

Chart 1. Possibilities for structural lead optimization of **3** and **4**.
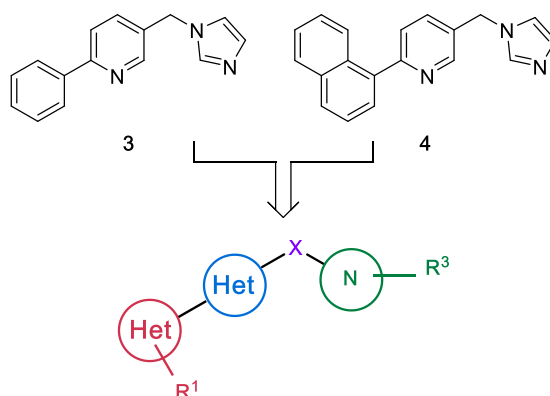
Further, the efficacy of CYP11B1 inhibitors for the acceleration of wound healing in human skin was to be investigated. For this purpose, compounds obtained from the previous optimization were to be modified for topical application to avoid systemic side effects. Rapid metabolic clearance after absorption, stability towards human plasma (as a substitute for wound fluid) and selectivities over 11β-HSD1 and CYP19A1 were further requirements which were aimed to be achieved in this project.

3. Results and Discussion

3.1. Cushing's Syndrome: Development of Highly Potent and Selective CYP11B1 Inhibitors of the (Pyridylmethyl)pyridine Type

Results described in this chapter were published in 2013 in J. Med. Chem.
https://pubs.acs.org/doi/abs/10.1021/jm400240r

The following persons also contributed to the results described in this chapter:

1. Dr. Qingzhong Hu: Performance of the 3D-QSAR study.
2. Dr. Nina Hanke: Coordination and performance of the CYP11B1, CYP11B2, CYP17A1, CYP19A1, CYP2A6, CYP3A4 inhibition assays.
3. Dr. Marco Gargano: Coordination and performance of the metabolic stability assays in human and rat liver S9 fraction.
4. Dr. Jörg Haupenthal: Performance of the cytotoxicity assay.
5. Dr. Ahmed Saad: Performance of the metabolic stability assays in human and rat plasma.

INTRODUCTION

Cortisol is involved in many important physiological processes. However, excessive cortisol leads to Cushing's syndrome that is characterized by visceral obesity, hypertension, and diabetes. Nearly all cases of endogenous Cushing's syndrome are caused by tumors in the hypothalamus, the adrenals or, most frequently, the pituitary. Cases of the last origin are specifically termed Cushing's disease, in which a pituitary adenoma overproduces adrenocorticotropic hormone (ACTH), leading to an elevation of plasma cortisol concentrations. Surgical removal of the tumor is therefore the first-line treatment. If the tumor recurs or resection is not feasible due to the size or location of the tumor, radiotherapy is applied. However, the inherent side effects of irradiation make a safe medication therapy desirable.[19] In addition, blockade of steroidogenesis with drugs before surgery lowers circulating cortisol levels, leading to a reversion of the metabolic consequences of cortisol excess and thus reduces the surgical risks.[21] In the case of metabolic syndrome, which shares some symptoms with Cushing's syndrome and is also accompanied by excessive cortisol, albeit in adipose and liver tissue rather than in circulation, 11β-hydroxysteroid dehydrogenase type 1 (11β-HSD1) inhibitors are promising therapeutics.[53] However, it is doubtful whether 11β-HSD1 inhibitors are able to reduce elevated cortisol plasma levels. By contrast, metyrapone, which is in clinical use for the treatment of Cushing's syndrome, can normalize plasma cortisol levels by inhibiting 11β-hydroxylase (CYP11B1).[19] This enzyme catalyzes the last step of cortisol biosynthesis: the hydroxylation of 11-deoxycortisol to cortisol. However, metyrapone is not selective enough over aldosterone synthase (CYP11B2), which is crucial in aldosterone production, and this might lead to hypokalemia.[34, 54] Consequently, novel and selective CYP11B1 inhibitors are urgently needed. However, selective inhibition of CYP11B1 or CYP11B2 is very challenging due to the high degree of homology (93%) between them.[55] In spite of this difficulty, we have developed selective CYP11B2 inhibitors.[56-59] A CYP11B1 inhibitor **3**[41, 43] was also identified recently, which is potent (IC_{50} = 107 nM) and selective over 17α-hydroxylase-17,20-lyase (CYP17A1), aromatase (CYP19A1) and in particular CYP11B2, for which a selectivity factor (SF = $IC_{50\,CYP11B2}/IC_{50\,CYP11B1}$) of 13 was achieved. In comparison to the most selective inhibitor in clinical use, metyrapone (IC_{50} = 15 nM, SF = 4.8), selectivity was improved. Still, our inhibitors require further enhancement of inhibitory potency to decrease the doses which have to be administered, thus reducing the risks of off-target effects. Because the introduction of substituents at the methylene bridge of a similar compound class resulted in a very potent and selective inhibitor **5**[60] (IC_{50} = 2 nM, SF = 11), various groups, in particular alkyl moieties, were introduced onto the methylene bridge of the current scaffold (Chart 2).

Chart 2. Metyrapone and the Concept of Inhibitor Design.

Het: Pyridine, Pyridazine, Pyrazine, Pyrimidine, Isoquinoline,

N: Imidazole, Pyridine, Isoquinoline, Pyrimidine

metyrapone

20-29

R^1: Ph, Thiophen-3-yl, Naphtalen-1-yl

R^2: Alkyl, Ph, Furan-2-yl

48-54, 57

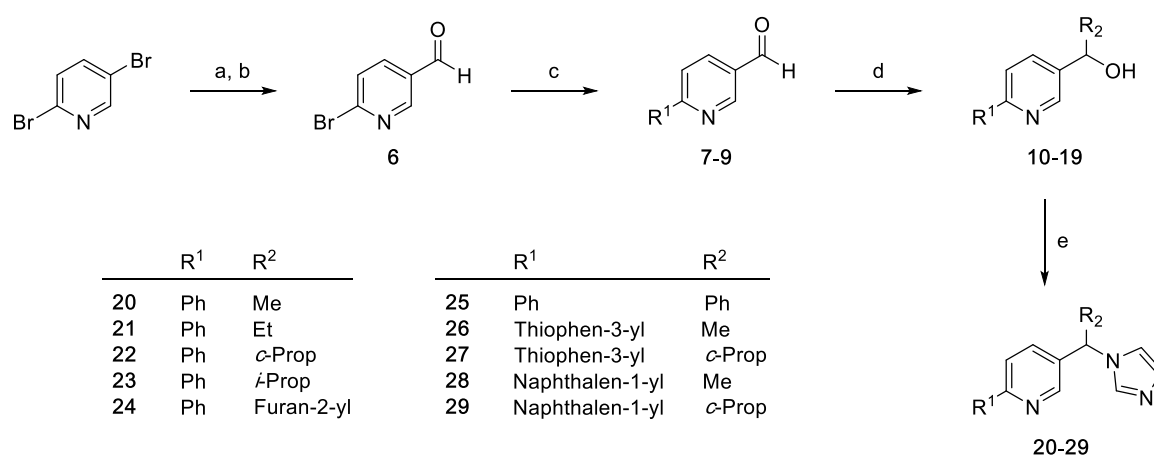R^3: Ph, OMe, $CONH_2$, F, OH, Me(5-Me, 49)

60, 61

X: O, NH
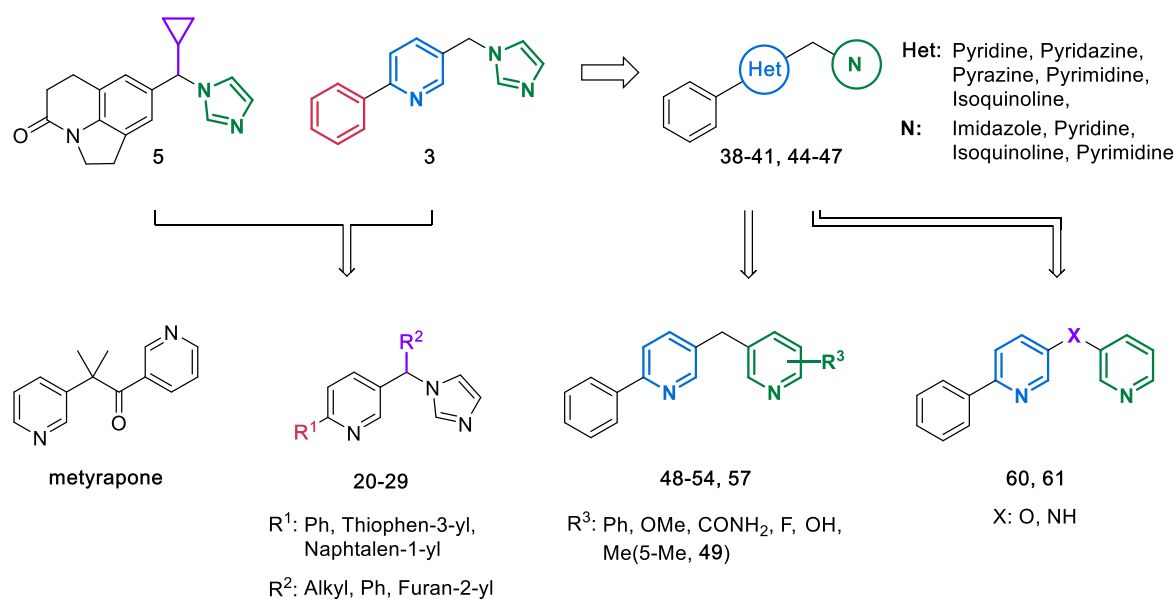
Furthermore, the central pyridine ring was replaced by other heterocycles, preserving the aromatic N because it was deemed to be important for selectivity.[41] After the most suitable core had been identified, the heme-complexing imidazolyl[31] was exchanged by various heterocycles containing an sp^2-hybridized N. Moreover, isosteric exchange of the methylene bridge by O or NH as well as the introduction of substituents at the distal N-containing heterocycle was also performed. These efforts led to 28 novel compounds (Chart 2), which were evaluated for inhibition of CYP11B1 and selectivities over CYP11B2, CYP17A1 and CYP19A1. Selective compounds were further evaluated for metabolic stability, inhibition of hepatic CYP3A4 and CYP2A6 and cytotoxicity. Although **3** was potent toward human CYP11B1 ($IC_{50} = 107$ nM), it showed a poor inhibition of the rat enzyme ($IC_{50} > 10000$ nM), which makes it impossible to use rats for pharmacodynamic experiments and proof of concept. Therefore, the most potent and selective compound of this series was evaluated for rat CYP11B1 inhibition and metabolic stability in rat plasma and S9 fraction to identify a candidate for further *in vivo* studies.

CHEMISTRY

Final compounds **20−29** were synthesized from commercially available 2,5-dibromopyridine (Scheme 1). After the transformation of one bromine substituent into a formyl group via lithium−halogen exchange followed by a nucleophilic formylation, the aromatic ring R^1 was introduced via a Suzuki coupling reaction leading to intermediates **7−9**. Grignard reactions were employed to insert various substituents on the methylene bridge, and the resulting alcohols were subsequently converted to compounds **20−29** via a nucleophilic substitution by reacting with 1,1-carbonyldiimidazole (CDI).

Scheme 1: Synthesis of Compounds **20−29**.[a]

	R^1	R^2		R^1	R^2
20	Ph	Me	25	Ph	Ph
21	Ph	Et	26	Thiophen-3-yl	Me
22	Ph	c-Prop	27	Thiophen-3-yl	c-Prop
23	Ph	i-Prop	28	Naphthalen-1-yl	Me
24	Ph	Furan-2-yl	29	Naphthalen-1-yl	c-Prop

[a]Reagents and conditions: (a) n-BuLi, Et$_2$O, −80 °C, 1 h; (b) DMF, −80 °C, 1 h, HCl; (c) method A, R^1B(OH)$_2$, Pd(PPh$_3$)$_4$, Na$_2$CO$_3$, toluene/EtOH/H$_2$O, reflux, 5 h; (d) method B, R^2MgCl or R^2MgBr, THF; (e) method C, CDI, NMP, 170 °C.

For the synthesis of compounds with different central rings (**38−41**), the heterocyclic intermediates **30−33** were obtained via different routes (Scheme 2). Pyridazine compound **30** was synthesized from commercially available 3-chloro-6-methylpyridazine and phenylboronic acid via a Suzuki reaction, whereas pyrazine intermediate **31** was yielded by nucleophilic addition of propane-1,2-diamine to phenylglyoxal. A condensation between benzamidine and (*E*)-3-ethoxy-2-methylacrylaldehyde led to pyrimidine compound **32**. The isoquinoline intermediate **33**, in contrast, was built via a Wittig reaction of *o*-bromoacetophenone followed by a bromine−lithium exchange and a subsequent nucleophilic substitution by benzonitrile for the ring closure.
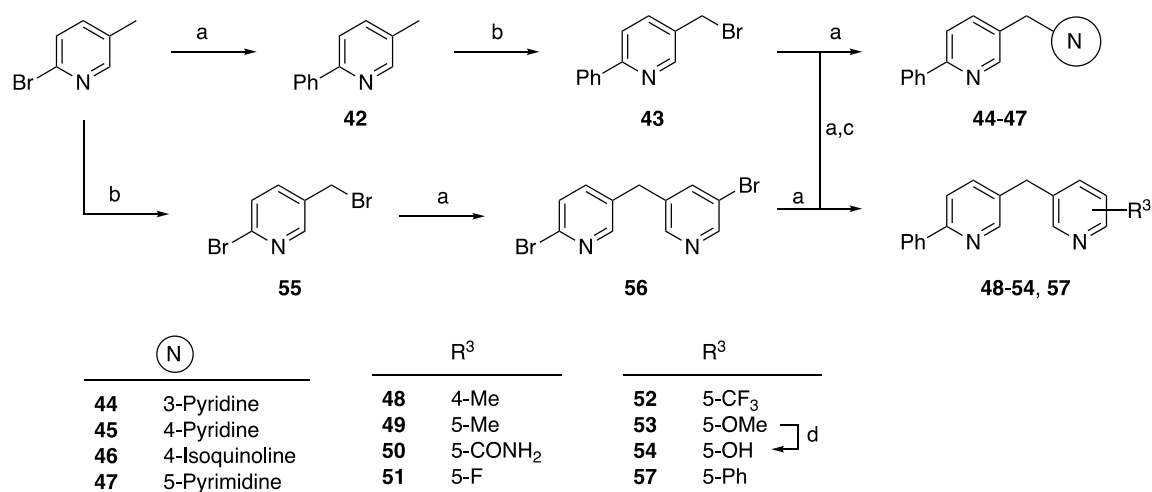
Scheme 2. Synthesis of Compounds **38−41**.[a]
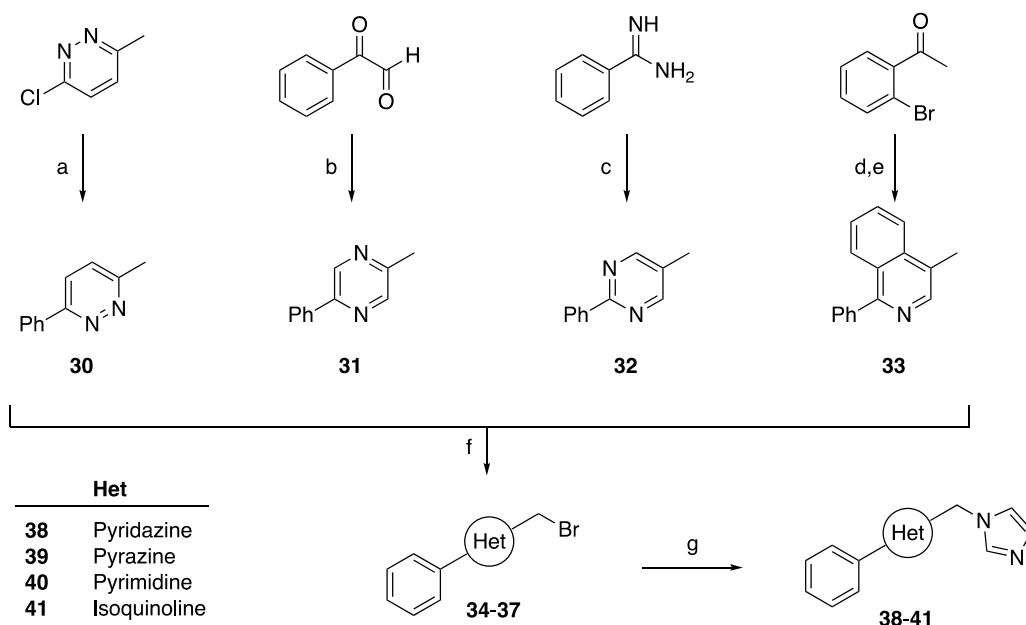
[a]Reagents and conditions: (a) method A, PhB(OH)$_2$, Pd(PPh$_3$)$_4$, Na$_2$CO$_3$, toluene/EtOH/H$_2$O, reflux, 5 h; (b) propane-1,2-diamine, EtOH, KOH; (c) NaOMe, MeOH, (*E*)-3-ethoxy-2-methylacrylaldehyde, H$_2$O, RT; (d) (methoxymethyl)triphenylphosphonium chloride, KO*t*-Bu, THF; (e) *n*-BuLi, PhCN; (f) method D, NBS, DBPO, CCl$_4$, reflux, 12 h; (g) method E, imidazole, K$_2$CO$_3$, DMF, 120 °C, 2 h.

These methyl intermediates **30−33** were subsequently brominated under Wohl−Ziegler conditions and modified with imidazolyl via a nucleophilic substitution with imidazole to yield the desired final compounds **38−41**. Moreover, a common building block **43** was synthesized from 2-bromo-5-methylpyridine using a Suzuki reaction with phenylboronic acid followed by a Wohl−Ziegler bromination (Scheme 3). Further Suzuki coupling of **43** with the boronic acids of the corresponding N-containing heterocycles yielded final compounds **44−54**. An exception was compound **57**, where *m*-bromopyridyl was inserted first, followed by simultaneous Suzuki couplings (method A) at both pyridyl moieties to introduce the phenyl groups. It should be noted that in the synthesis of compounds **50−54**, PdCl$_2$(dppf) was used as the catalyst instead of Pd(PPh$_3$)$_4$ and microwave irradiation was employed to facilitate the reaction (method F) because of the low yields resulting from the conventional Suzuki coupling conditions with thermal heating (method A). The hydroxy compound **54** was obtained from ether cleavage of the methoxy precursor **53**.

Scheme 3. Synthesis of Compounds **44−54** and **57**.[a]

	(N)
44	3-Pyridine
45	4-Pyridine
46	4-Isoquinoline
47	5-Pyrimidine

	R³
48	4-Me
49	5-Me
50	5-CONH₂
51	5-F

	R³
52	5-CF₃
53	5-OMe
54	5-OH
57	5-Ph

[a]Reagents and conditions: (a) method A, corresponding boronic acid, Pd(PPh₃)₄, Na₂CO₃, toluene/EtOH/H₂O, reflux, 5 h; (b) method D, NBS, DBPO, CCl₄, reflux, 12 h; (c) method F, corresponding boronic acid, PdCl₂(dppf), Cs₂CO₃, DME/H₂O/EtOH, 150 °C, 150 W, 18 bar, 20 min, microwave; (d) HBr, 130 °C, 12 h.

To obtain the O (**60**) and NH (**61**) isosters of the methylene compound (**44**), intermediate **58** was prepared via selective Suzuki coupling at the 2-position of 5-bromo-2-iodopyridine. A halogen exchange converting 5-bromo to iodo (**59**) was performed, and the latter compound was subsequently coupled with 3-hydroxypyridine using CuI, picolinic acid and K₃PO₄ as catalysts to obtain the final compound **60**. For the amination of **59** with 3-aminopyridine, Pd-BINAP and excessive Cs₂CO₃ as a base had to be employed instead to give compound **61** (Scheme 4).

Scheme 4. Synthesis of Compounds **60** and **61**.[a]
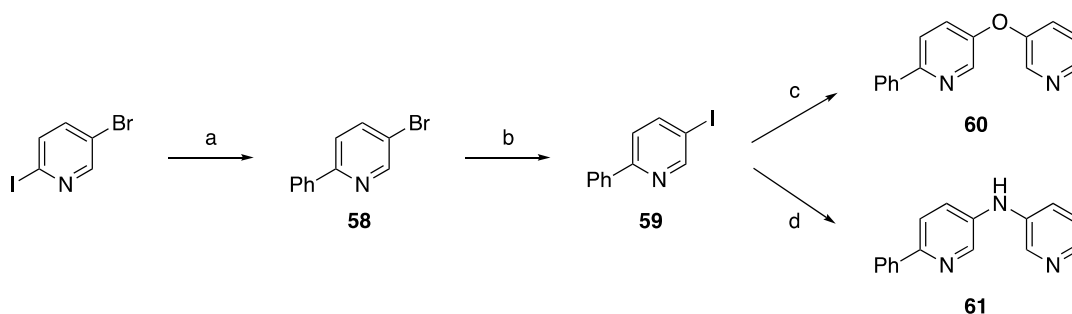
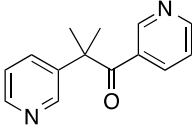[a]Reagents and conditions: (a) method A, PhB(OH)₂, Pd(PPh₃)₄, Na₂CO₃, toluene/EtOH/H₂O, reflux, 5 h; (b) CuI, *N,N'*-dimethylethylenediamine, NaI, dioxane, 110 °C; (c) CuI, 2-picolinic acid, 3-hydroxypyridine, K₃PO₄, DMSO; (d) Pd(OAc)₂, (±)BINAP, 3-aminopyridine, Cs₂CO₃, toluene.
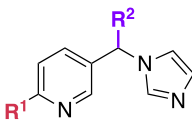
BIOLOGICAL RESULTS AND DISCUSSION

Inhibition of CYP11B1 and CYP11B2. Compounds **20−29**, **38−41**, **44−54**, **57**, **60**, and **61** were evaluated for their inhibitory activities in V79 MZh cells expressing either human CYP11B1 or CYP11B2. The IC$_{50}$ values (n ≥ 3, relative standard deviations < 25%) are presented in tables 1−3 in comparison to metyrapone. As expected, the introduction of alkyl groups onto the methylene bridge of **3** (IC$_{50}$= 107 nM) significantly increased CYP11B1 inhibition up to 9-fold (compounds **20−23**; IC$_{50}$ values ranging from 12 to 33 nM). Here, the trend can be observed that with increased bulkiness of the alkyl groups (Me < Et < *c*-prop < *i*-prop), inhibition of CYP11B1 is enhanced.
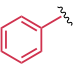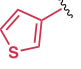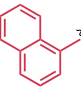
Table 1. Inhibition of CYP11B1 and CYP11B2 by Compounds **20−29**.[a]

metyrapone   3, 4, 20-29, 62

Comp	R^1	R^2	CYP IC$_{50}$ (nM)[a,b]		SF[c]
			11B1	11B2	
3[d]		H	107	1423	13.3
20		Me	33	200	6.1
21		Et	28	92	3.4
22	phenyl	*c*-Prop	21	25	1.2
23		*i*-Prop	12	28	2.4
24		Furan-2-yl	69	74	1.1
25		Ph	124	110	0.9
62[d]		H	181	1017	5.6
26	thiophen-3-yl	Me	21	151	9.1
27		*c*-Prop	11	31	2.8
4[d]		H	68	656	9.7
28	naphthyl	Me	60	273	4.6
29		*c*-Prop	151	220	1.5
metyrapone			15	42	4.8

[a]Mean value of at least three experiments. The deviations were <25%. [b]Hamster fibroblasts expressing human CYP11B1 or CYP11B2; substrate 11-deoxycorticosterone, 100 nM. [c]SF: IC$_{50}$ $_{CYP11B2}$ /IC$_{50}$ $_{CYP11B1}$. [d]See ref[43], IC$_{50}$ values differ due to different enzyme sources.

This is probably caused by occupation of an additional hydrophobic pocket near the heme. Similarly, introduction of alkyl substituents onto the methylene bridge of **62** (IC$_{50}$ = 181 nM) led to significant increases in CYP11B1 inhibition as well (**26**, Me, IC$_{50}$ = 21 nM; **27**, *c*-prop, IC$_{50}$ = 11 nM). By contrast, the naphthalene analogues showed similar (**28**, Me, IC$_{50}$ = 60 nM) or reduced

(29, *c*-prop, IC_{50} = 151 nM) potency compared to non-substituted 4 (IC_{50} = 68 nM), probably indicating different binding modes of the phenyl or thienyl compounds. Interestingly, introduction of aromatic substituents onto the methylene bridge of 3, such as 2-furan (24, IC_{50} = 69 nM) and phenyl (25, IC_{50} = 124 nM), entailed weaker inhibition of the target enzyme compared to the alkyl analogues, as was similarly observed in the compound class of 5.[60] However, the improvement of selectivity over CYP11B2 via introduction of substituents onto the methylene bridge, as seen in the compound class of 5,[60] was not observed. Instead, these modifications increased CYP11B2 inhibition by 3−28-fold, thus leading to a reduction of selectivity (Table 1). Replacement of the central pyridine moiety by other heterocycles, with the N remaining at the same position to retain selectivity[41] (Table 2), reduced the potency compared to 3 (IC_{50} = 107 nM), as it was observed with the pyridazine (38), pyrazine (39) and pyrimidine (40) compounds. This might be due to the electron withdrawing property of the additional nitrogens altering the electrostatic potential of the whole molecule. Interestingly, annulation of a benzene moiety resulting in isoquinoline (41) slightly increased inhibition (IC_{50} = 87 nM) at the expense of selectivity, which was reduced to 3.5.

Table 2. Inhibition of CYP11B1 and CYP11B2 by Compounds 38−41.

Comp	Het	CYP IC_{50} (nM)^{a,b}		SF^c
		11B1	11B2	
3^d		107	1423	13.3
38		1711	4539	2.7
39		610	1025	1.7
40		1122	> 5000	> 5
41		87	302	3.5
metyrapone		15	42	4.8

^{a}Mean value of at least three experiments. The deviations were <25%. ^{b}Hamster fibroblasts expressing human CYP11B1 or CYP11B2; substrate 11-deoxycorticosterone, 100 nM. ^{c}SF: $IC_{50\ CYP11B2}$/$IC_{50\ CYP11B1}$. ^{d}See ref[43], IC_{50} values differ due to different enzyme sources.

Therefore, the pyridine moiety was considered as the most suitable central ring balancing potency and selectivity and was retained in the further optimization process. Subsequently, the exchange of the heme-complexing imidazolyl by other N-containing heterocycles was investigated as well (Table 3). 3-Pyridine (**44**) and isoquinoline (**46**) significantly enhanced the inhibitory potency to 32 and 6 nM, respectively, compared to imidazole **3** (IC$_{50}$ = 107 nM), whereas the 4-pyridine compound **45** showed a similar inhibition of CYP11B1 with an IC$_{50}$ value of 98 nM. By contrast, the exchange of imidazolyl by pyrimidine (**47**) led to a reduction of inhibition (IC$_{50}$ = 240 nM), probably due to the fact that the electron density on the heme-coordinating N was reduced by the withdrawing effect of the second N. Although both 3-pyridine and isoquinoline enhanced inhibition, only the 3-pyridyl analogue **44** preserved a similar selectivity factor of 10 compared to **3** (SF = 13), whereas the isoquinoline compound **46** exhibited a reduced selectivity of 4.

Table 3. Inhibition of CYP11B1 and CYP11B2 by Compounds **44−54**, **57**, **60**, and **61**.

Comp	N	R^3	CYP IC$_{50}$ (nM)^{a,b}		SF^c
			11B1	11B2	
3^d			107	1423	13.3
44			32	322	10.1
45			98	621	6.4
46			6	23	4.2
47			240	3111	12.9
48		4-Me	8	19	2.4
49		5-Me	2.2	33.2	15.1
50		5-CONH$_2$	427	2924	6.9
51		5-F	125	419	3.4
52		5-CF$_3$	38	116	3.0
53		5-OMe	5	25	5.1
54		5-OH	51	836	16.4
57		5-Ph	1.3	0.5	0.4
60			1015	1800	1.9
61			> 5000	> 5000	
metyrapone			15	42	4.8

^{a}Mean value of at least three experiments. The deviations were <25%. ^{b}Hamster fibroblasts expressing human CYP11B1 or CYP11B2; substrate 11-deoxycorticosterone, 100 nM. ^{c}SF: IC$_{50}$ $_{CYP11B2}$ /IC$_{50}$ $_{CYP11B1}$. ^{d}See ref[43], IC$_{50}$ values differ due to different enzyme sources.

Moreover, the isosteric exchange of the methylene bridge by O (**60**) or NH (**61**) led to a dramatic reduction of activity (IC_{50} values of 1015 and > 5000 nM, respectively). This probably indicates a hydrophobic region around the bridge, where these polar moieties are not tolerated. Therefore, optimizations of **3** (IC_{50} = 107 nM, SF = 13) via substitution on the methylene bridge, replacement of the central pyridine moiety by other N-containing heterocycles and isosteric exchange of the methylene bridge led to an increase of CYP11B1 inhibition in some cases. However, selectivity over CYP11B2 decreased. In contrast, the exchange of the heme-complexing imidazolyl by 3-pyridyl resulted in a more potent but similarly selective compound **44** (IC_{50} = 32 nM, SF = 10), which was regarded as a suitable scaffold for further optimization. Additional substituents with various profiles in terms of bulkiness, electronic properties, and H-bond acceptor and donor characteristics were introduced to the 3-pyridyl ring. The electron withdrawing groups 5-$CONH_2$ and 5-F (compounds **50** and **51**) strongly reduced CYP11B1 inhibition by 13- and 4-fold to 427 and 125 nM, respectively, compared to the non-substituted compound **44** (IC_{50} = 32 nM). Similar effects have also been observed in other classes of CYP11B inhibitors.[60-61] By contrast, compound **52** (5-CF_3), as an exception, showed a similar inhibition of CYP11B1 (IC_{50} = 38 nM) as the non-substituted compound **44**. However, the electron-rich groups significantly improved the inhibitory potency, resulting in IC_{50} values lower than 10 nM. The 4-Me compound **48** showed an IC_{50} value of 8 nM but a reduced selectivity of 2.4 compared to the nonsubstituted compound **44** (SF = 10). Shifting of the Me group into the 5-position (compound **49**) further elevated the inhibitory potency, leading to an IC_{50} value of 2 nM, which is over 50-fold more potent than **3**. More important is that the selectivity was also enhanced to 15. 5-Ph substitution at the pyridyl led to the most potent compound in this study (compound **57**, IC_{50} = 1.3 nM), albeit with a reduced SF of 0.4. These results are probably caused by the bulky phenyl group occupying an additional hydrophobic pocket near the heme, leading to the elevated inhibition of both CYP11B1 and CYP11B2. As expected, a 5-OMe substituent (**53**) improved the inhibition to 5 nM, whereas the SF was reduced to 5.1. By contrast, compound **54**, hydroxylated in the 5-position, exhibited a slightly reduced inhibition of CYP11B1 (IC_{50} = 51 nM) compared to the parent compound but achieved the highest SF in this study of 16.4. The optimization process yielded many compounds that are more potent than the lead compound **3**. Some compounds (**23**, **27**, **46**, **48**, **49**, **53**, and **57**) are more potent than the clinically used drug metyrapone (IC_{50} = 15 nM, SF = 4.8). More importantly, among them, compound **49** is also more selective (SF = 15) than metyrapone.

3D-QSAR Study. The CYP11B1 crystal structure is not resolved yet, however, a homology model was reported before.[29] We decided to employ a ligand based approach to further illustrate the structure–activity relationship and built a 3D-QSAR model using the software Open3DQSAR.[62] Compounds **22**, **40**, **46**, **49**, and **51** were used as the test set to validate the predicting ability of the model, whereas the remaining 26 compounds including **3**, **4**, and **62** were employed as the training set. Molecular interaction fields (MIF) regarding steric effects and electrostatic potential were calculated for all compounds within a grid box around the molecules with a 0.5 Å step size and a 5.0 Å margin. The MIF parameters were subsequently regressed with inhibitory potency (pIC$_{50}$) using partial least-squares analysis (PLS). The model was further improved by using smart region definition (SRD) and fractional factorial design (FFD) methods. The cross validation of the model using the leave-many-out paradigm and challenging the model with the test set compounds revealed a $q^2_{L20\%O}$ value of 0.836 with a standard deviation of error of calculation (SDEC) of 0.315 and an r^2 value of 0.958 with a standard deviation of error of prediction (SDEP) of 0.207, indicating a high accuracy of prediction (Figure 8).
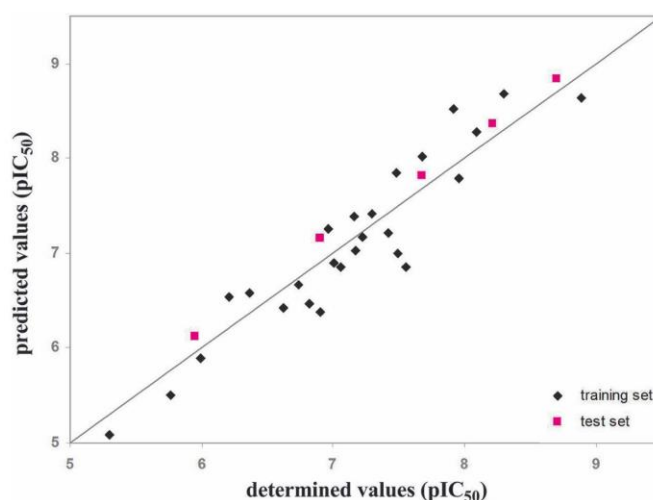
Figure 8. Predicted vs. determined pIC$_{50}$ values for both training set (black) and test set compounds (purple).

The 3D-QSAR model revealed that in area 1, which is located around the distal pyridyl and opposite to the N atom, bulky groups are advantageous (Figure 9A, area 1, green). Above the methylene bridge, medium-sized groups are favored (Figure 9A, area 2, green), whereas right outside of these regions, bulky substituents are prohibited (Figure 9A, area 3, yellow). Areas beneath the methylene bridge and near the sp^2-hybridized N do not tolerate bulky groups either (Figure 9A, area 3, yellow). Moreover, discrete regions around the heme-coordinating pyridyl, the methylene bridge and the core show preference for groups with positive partial charges (Figure 9B, cyan). In contrast, no predilection for negative partial charges was observed at the same level. No suggestions were made around the western aromatic moiety due to the limited number of

33

different rings in this area present in the training set. According to these results, further modifications seem to be reasonable to potentiate the inhibitory potency, such as introduction of bulky substituents onto the *meta-* or *para-*positions of the distal pyridine as well as hydrophobic groups of suitable size onto the methylene bridge. However, one should have in mind that these modifications would increase lipophilicity of the compounds with eventual adverse effects on pharmacokinetic properties.
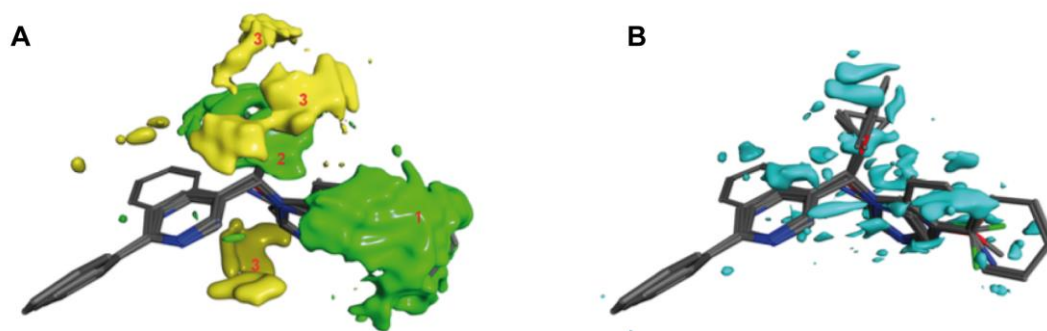
Figure 9. Illustration of the PLS pseudo-coefficient contour maps of the 3D-QSAR model with the superposed compounds from both training and test sets. (A) Steric effects. Green (level: 0.015) indicates bulky groups are favored, whereas yellow (level: −0.015) indicates bulky moieties are prohibited. (B) Electrostatic potential. Cyan (level: 0.005) indicates groups with positive partial charges are favored.

Selectivities over CYP17A1 and CYP19A1. Because of the crucial roles of CYP17A1 and CYP19A1 in the biosynthesis of androgens and estrogens, the inhibitors of CYP17A1[63-64] and CYP19A1[65-68] have been applied in clinic for the treatment of prostate and breast cancer, respectively.

Table 4. Inhibition of CYP17A1 and CYP19A1 by Compounds **20**, **44**, and **49**.

Comp	inhibition (%)[b]	
	CYP17A1[a,c]	CYP19A1[a,d]
3	2	0
20	13	1
44	4	0
49	5	1
metyrapone	3	0

[a]Mean value of at least three experiments. The deviations were <25%. [b]Compound concentrations 2 μM. Inhibition values ≤5% are not significant. [c]E. coli expressing human CYP17A1; substrate progesterone, 25 μM. [d]Human placental CYP19A1; substrate androstenedione, 500 nM.

However, as for CYP11B1 inhibitors, the inhibition of these enzymes would lead to severe side effects due to the same reason. The selectivities over CYP17A1 and CYP19A1 are therefore important safety criteria, and inhibition of these enzymes by the selected compounds **20**, **44**, and **49** was determined (Table 4). As the tested inhibitors exhibited IC_{50} values below 35 nM toward human CYP11B1, a more than 50-fold higher concentration (2 μM) was regarded as sufficient for the determination of CYP17A1 and CYP19A1 inhibition. Compound **20** showed only 13% inhibition of CYP17 at a concentration of 2 μM, whereas compounds **44** and **49** were considered as inactive as they exhibited no significant inhibition (≤5% at 2 μM). Because these compounds are very potent against CYP11B1 ($IC_{50} < 35$ nM), they were regarded to be selective over CYP17A1. As for CYP19A1, none of the compounds showed inhibitory effects at a concentration of 2 μM. These selectivity profiles guarantee no interference with the production of androgens and estrogens under therapeutic doses.

Selectivities over Hepatic CYP2A6 and CYP3A4. Because CYP2A6 and CYP3A4 play important roles in the metabolism of xenobiotics and drugs, compound **49** was tested for inhibition of these enzymes. **49** showed IC_{50} values of 106 μM for CYP2A6 and 1.1 μM for CYP3A4, respectively. In spite of the moderate CYP3A4 inhibition, the safety margin should be sufficient due to the high potency toward CYP11B1 ($IC_{50} = 2$ nM, factor of 550).

Inhibition of Rat CYP11B1. As **3** showed a poor inhibition of the rat enzyme ($IC_{50} > 10000$ nM), compound **49** was evaluated for rat CYP11B1 inhibition to identify a new candidate for *in vivo* experiments in rats. Indeed, compound **49** not only elevated the inhibition of human CYP11B1 but also enhanced the inhibition of the rat enzyme to an IC_{50} of 2440 nM (mean value of more than three repeats). As we have observed with aldosterone synthase (CYP11B2) inhibitors, *in vitro* activities in this range are sufficient to elicit biological effects in rats.[56]

In Vitro Metabolic Stability. Compound **49** showed a moderate metabolic stability toward rat liver S9 fraction with a half−life ($t_{1/2}$) of 16 min (mean value of more than three repeats) as well as an extraordinary metabolic stability toward human liver S9 fraction ($t_{1/2} > 150$ min) and human and rat plasma ($t_{1/2} > 150$ min). These properties make compound **49** an appropriate candidate for a further proof of concept in rats.

Cytotoxicity. The cytotoxicity of compound **49** was evaluated in HEK293 cells with doxorubicin as positive control and rifampicin as negative control. After 24 h of incubation, the compounds showed LC_{50} values of 61.4, 4.3, and >100 μM (mean value of more than three repeats),

respectively. Thus, the cytotoxic effect of compound **49** was only weak and should not give rise to problems *in vivo* due to the strong *in vitro* CYP11B1 inhibitory activity of **49** and the low therapeutic doses necessary.

CONCLUSION

For a better management of Cushing's syndrome, CYP11B1 inhibitors that are more potent and selective than the clinically used drug metyrapone are urgently needed. Optimizations have been performed with the previously identified CYP11B1 inhibitor **3** regarding the potency toward the human enzyme as well as the selectivity over CYP11B2 (SF = 13). Modifications such as the introduction of various substituents onto the methylene bridge and the heme Fe-complexing pyridyl ring, replacement of the central pyridine moiety and the imidazolyl ring by other heterocycles and the isosteric exchange of the methylene bridge with NH or O have been performed. These efforts resulted in potent CYP11B1 inhibitors with IC_{50} values lower than 10 nM (compounds **46**, **48**, **49**, **53** and **57**). Among them, compound **49** turned out to be the best one, with an IC_{50} value of 2 nM toward CYP11B1 (50-fold more potent than **3**). This compound also showed selectivities over CYP11B2 (SF = 15), CYP17A1, and CYP19A1 as well as hepatic CYP2A6 and CYP3A4. To facilitate proof of concept (*in vivo*) studies with the best compound **49**, inhibition of rat CYP11B1 was investigated and a moderate activity was found (IC_{50} of 2440 nM, **3** > 10000 nM). Satisfying metabolic stabilities in both plasma and liver S9 fractions from human and rat origin as well as a negligible cytotoxicity were observed. Because these profiles are clearly superior to that of metyrapone and **3**, compound **49** can be considered as a candidate for further *in vivo* studies in rats.

3.2. Lead Optimization Generates CYP11B1 Inhibitors of Pyridylmethyl Isoxazole Type with Improved Pharmacological Profile for the Treatment of Cushing's Disease

Results described in this chapter were published in 2017 in J. Med. Chem.

https://pubs.acs.org/doi/abs/10.1021/acs.jmedchem.7b00437

The following persons also contributed to the results described in this chapter:

1. Dr. Chris J. van Koppen: Performance of the cytotoxicity, mutagenicity, aryl hydrocarbon receptor activation, hepatic CYP enzyme inhibition and hERG assays. Coordination and performance of the pharmacokinetic studies in rats for compounds **90** and **91** (with the help of Dr. Claudia Scheuer, Julia Parakenings and Prof. Dr. Matthias Laschke)
2. Dr. Jens L. Burkhart: Coordination and performance of the synthesis of compounds **67**, **68**, **70**, **71** and **73**-**77** and the corresponding intermediates.
3. Dr. Franck Lach: Synthesis of compounds **69** and **72** and the corresponding intermediates.
4. Lorenz Siebenbürger: Performance of the metabolic stability assays in human and rat liver S9 fraction and plasma.
5. Dr. Nina Hanke: Coordination and performance of the CYP11B1, CYP11B2, CYP17A1, CYP19A1 and hepatic CYP enzyme inhibition assays.
6. Employees of Cerep (France): Performance of the AMES fluctuation assay for compound **49**.
7. Employees of Pharmacelsus (Germany): Performance of the pharmacokinetic study in rat for compound **49**.

INTRODUCTION

Cushing's disease, a rare endogenous syndrome with an incidence of 1–2 cases per million population[69], is mainly caused by a pituitary adenoma overproducing adrenocorticotropic hormone (ACTH).[12] As a consequence, plasma cortisol levels are abnormally elevated and patients suffer from diabetes mellitus, hypertension, osteoporosis or psychological dysfunctions.[69] Usually, surgical removal of the tumor is the first-line treatment with remission rates of 65–90%.[70] However, the recurrence rate is about 10-20%[70] and surgery bears the risk of pituitary gland damage. In addition, tumors are not always accessible. Alternatively used radiation therapy exhibits a delayed response (2–5 years) and high risk of hypopituitarism.[38] Medications which are targeting steroid 11β-hydroxylase (CYP11B1, catalyzes the last step of cortisol biosynthesis, Scheme 5), such as the inhibitors metyrapone and ketoconazole (Figure 10), are widely used in the clinic.[20]

Scheme 5. Biosynthesis of cortisol and aldosterone
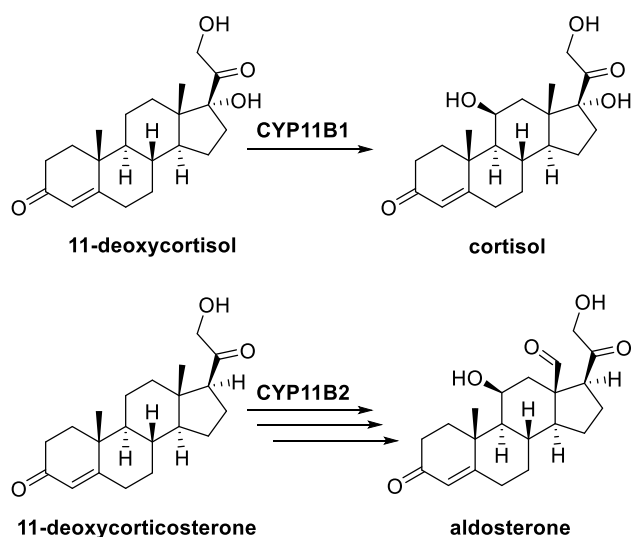
Furthermore, the potent 11β-hydroxylase inhibitor osilodrostat (LCI699, Figure 10) was investigated in a phase 2 study as potential new treatment for Cushing's disease.[23] However, all of them induce various side-effects (e.g. hirsutism, acne, hypertension, hypokalemia, hypogonadism, rash) caused by additional inhibition of other steroidogenic CYP enzymes such as aromatase (CYP19A1), 17α-hydroxylase-17,20-lyase (CYP17A1) or aldosterone synthase (CYP11B2).[23, 38, 71] In fact, selective inhibition is challenging especially towards CYP11B2 (catalyzes the last steps of aldosterone biosynthesis, Scheme 5) since CYP11B1 exhibits a sequence identity of 93% to its isoenzyme.[29]
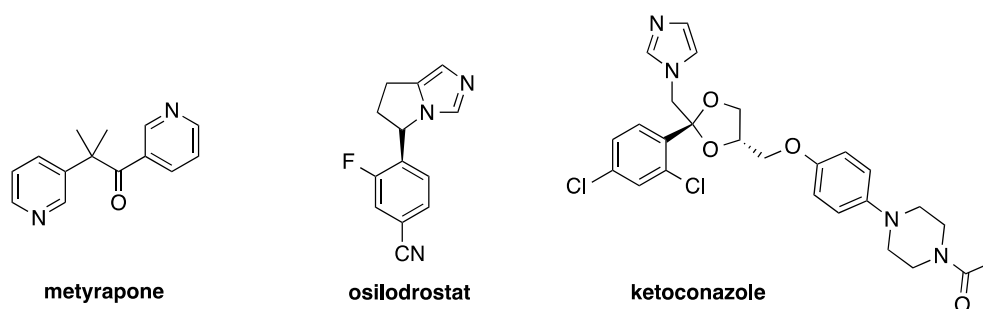
Figure 10. CYP11B1 inhibitors.

Nevertheless, beside the successful development of selective CYP17A1[63-64, 72-73] and CYP19A1 inhibitors[65-68], we identified highly potent and selective CYP11B2 inhibitors[56, 61, 74-78] which are active *in vivo*.[56] In addition, we recently published the first selective human CYP11B1 inhibitors.[41-43, 60] In the class of imidazolylmethyl pyridine type of compounds, **3-4** and **63-66** (Chart 3, IC_{50}= 47–122 nM, SF (IC_{50}CYP11B2/ IC_{50}CYP11B1)= 6–15)[41, 43] were the most active and selective ones, which were subsequently optimized regarding potency and selectivity. [Chapter 3.1[42]] Exchange of the heme-complexing imidazol-1-yl ring for 5-Me- or 5-OMe-pyridin-3-yl led to improved compounds regarding potency (**49** and **53**, Chart 3, IC_{50}= 2–4 nM, SF= 6–17). [Chapter 3.1[42]] Inhibitor **49** exhibited selectivities over CYP17A1, CYP19A1 and hepatic CYP enzymes (CYP2A6, CYP3A4) as well as negligible cytotoxicity and satisfying metabolic stability in human and rat liver S9 fraction. [Chapter 3.1[42]]

Subsequent biological results of 49. Despite the previously shown good *in vitro* pharmacological profile of **49** [Chapter 3.1[42]] in subsequent studies, it became apparent that **49** is a promutagen in the TA98 strain (frameshift mutation) of *Salmonella typhimurium* and, therefore, a potential carcinogen. Furthermore, a pharmacokinetic study in rats revealed a very low oral bioavailability (F= 2%) of **49**. Associated calculated pharmacokinetic parameters of **49** after a single dose in rats are summarized in table 5. After intravenous application (i.v., 1 mg/kg), a maximum plasma concentration (Cmax) of 4.4 µM and a moderate half-life ($t_{1/2}$) of 1.5 h was determined. Previously identified **49** showed a rat CYP11B1 IC_{50} of 2.44 µM [Chapter 3.1[42]] (*in vitro*) and hence plasma levels required for a therapeutic effect were reached after i.v. administration. In contrast, following peroral application (p.o., 2 mg/kg), only low plasma levels (Cmax= 0.1 µM) were obtained. Based on the resulting poor oral bioavailability (F= 2%), **49** was rejected as a potential candidate for preclinical development.

Table 5. Key pharmacokinetic parameters of **49** after a single dose in rats.[a,b]

49
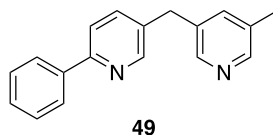
Route	Dose [mg/kg]	C_{max} [μM]	T_{max} [h]	$T_{1/2}$ [h]	V_{dss} [L/kg]	CL [mL/min·kg]	$AUC_{0-\infty}$ [ng·h/mL]	F [%]
i.v. (n=2)	1	4.4		1.5	2.8	21.7	775	
p.o. (n=3)	2	0.1	0.3	0.9			28.4	2

[a]Data are mean values. [b]Abbreviations: i.v., intravenous; p.o., per oral; Cmax, peak plasma concentration of a drug after administration; Tmax, time to reach Cmax; $T_{1/2}$, elimination half-life; Vdss, volume of distribution at steady state; CL, plasma clearance; AUC, area under the concentration−time curve; F, bioavailability.

DESIGN CONCEPT FOR LEAD OPTIMIZATION

Due to the low oral bioavailability in rats of **49**, the inhibitor is a poor candidate for preclinical development. This encouraged us to perform lead optimization of **49** to obtain other candidates for *in vivo* studies with the challenge to retain CYP11B1 selectivity and potency. There are several possible reasons for low oral bioavailability *in vivo* such as low aqueous solubility, low permeability, high first-pass metabolism in the liver or high renal clearance.

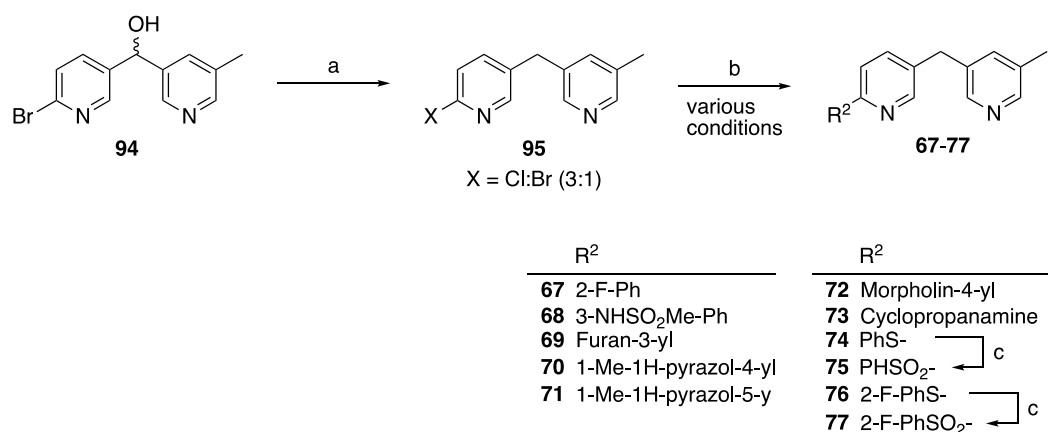**Chart 3.** Lead optimization to find suitable candidates for *in vivo* evaluations.
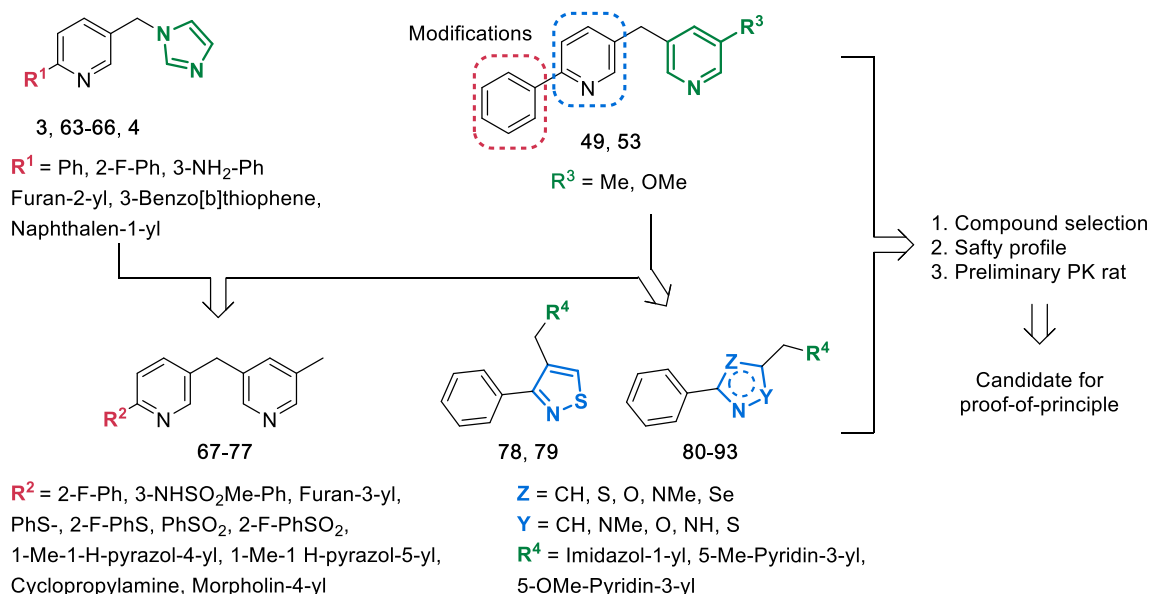
The calculated log D (pH= 7.4) value for **49** is 3.7[79] and, therefore, structural optimization aiming for more polar compounds should balance solubility and permeability properties of the inhibitors

40

under *in vivo* conditions. Furthermore, the modification of electronic properties and molecular geometry of **49** was expected to influence CYP11B1 potency, selectivity over CYP11B2 and *in vivo* pharmacokinetics. Previously, the influence of substitution at the central pyridine ring of the imidazolylmethyl pyridine class was explored extensively.[43] Substituents in 2-position of pyridine exemplified in **3**-**4** and **63**-**66** (R^1, Chart 3) improved CYP11B1 inhibition and exhibited the best effect on selectivity over CYP11B2 (Table 6). However, a distinct trend within these inhibitors could not be identified as the introduced substituents vary in terms of polarity, electronic properties and size. Consequently, the phenyl moiety in **49** was substituted with the most promising of these substituents (2-F-Ph, furan-3-yl). The 3-NH_2-Ph, benzo[*b*]thiophene and naphthalene-1-yl compounds were not synthesized due to anticipated toxicity (carcinogenicity)[80] and solubility (lipophilicity) issues. As the possible carcinogen **64** (3-NH_2-Ph) exhibited the highest selectivity in this series, further hydrophilic substituents differing in size and electronic properties such as N-phenylmethanesulfonamide, pyrazoles or polar non-aromatic cycles were introduced. To investigate the influence of the molecular shape on selectivity, heteroatom linkers (-S-, -SO_2-) were used. In the imidazolylmethyl pyridine class exchange of the pyridine core by furan or thiophene caused an increase in CYP11B1 potency, but a loss of selectivity towards CYP17A1 or CYP19A1.[41] Hence, it could be assumed that the aromatic N is essential for selectivity and change of the molecular geometry by introduction of 5-membered heterocycles is beneficial for CYP11B1 potency. For further investigation, several azoles differing in electronic and steric properties were introduced into the selective lead compounds **3** and **49** with the phenyl substituent next to the aromatic N. The optimized central core was subsequently incorporated into very potent and moderately selective **53** to get a variety of candidates for further biological evaluation. Thus, 27 structurally diverse novel compounds were obtained and evaluated for inhibition of CYP11B1 and selectivity towards CYP11B2. Selected inhibitors were further tested for CYP17A1 and CYP19A1 inhibition, metabolic stability, toxicity and inhibition of hepatic CYP enzymes (CYP1A2, 2B6, 2C9, 2C19, 2D6 and 3A4). Candidates which exhibited a good pharmacological profile were also tested for inhibition of rat CYP11B1 and metabolic stability in rat liver S9 fraction. Preliminary pharmacokinetic experiments were performed with the best inhibitors to find a suitable candidate for clinical use.

CHEMISTRY

The synthesis of the (5-Me-pyridin-3-yl)pyridine derivatives **67–77** (Scheme 6) was performed using the common building block **95**, a 3:1 mixture of 2-chloro and 2-bromo compounds. **95** was accessible from racemic alcohol **94**, which was converted into the chloride by thionyl chloride and reductively dehalogenated to obtain **95**. The aromatically substituted target compounds **67-71** were synthesized using **95** and the corresponding organoboranes under cross coupling conditions.

Scheme 6. Synthesis of compounds **67-77**[a]

	R²			R²
67	2-F-Ph		**72**	Morpholin-4-yl
68	3-NHSO₂Me-Ph		**73**	Cyclopropanamine
69	Furan-3-yl		**74**	PhS-
70	1-Me-1H-pyrazol-4-yl		**75**	PHSO₂-
71	1-Me-1H-pyrazol-5-y		**76**	2-F-PhS-
			77	2-F-PhSO₂-

[a]Reagents and conditions: (a) thionyl chloride, 60 °C, 3 h, then Zn, CH₃COOH, rt, 24 h. (b) various coupling conditions= for **68**, **69**: method A: corresponding boronic acid, Pd(PPh₃)₄, Na₂CO₃, toluene/ EtOH/ H₂O, reflux, 4 h or overnight; for **67**, **71**: method G: corresponding boronic acid or boronic acid pinacol ester, Pd(OAc)₂, SPhos, LiOH (2M), dioxane, 90 °C, 20 h; for **70**: boronic acid pinacol ester, Cs₂CO₃, PdCl₂(dppf), DME, water, reflux, overnight; for **72**, **73**: corresponding amine, NaOEt, Pd(OAc)₂, SPhos, toluene, 80 °C or reflux, overnight; for **74**, **76**: corresponding thiol, Cs₂CO₃, DMSO or dimethylacetamid, 90 °C or 150 °C, overnight. (c) corresponding thioether, potassium peroxymonosulfate, EtOAc, rt, 4 h.

In terms of the *N*-substituted compounds **72** and **73** Buchwald-Hartwig amination of **95** was applied, whereas thioethers **74** and **76** were synthesized via nucleophilic attack of the corresponding thiolate at **95**. Oxidation of thioethers **74** and **76** with potassium peroxymonosulfate resulted in the final sulfone compounds **75** and **77**. The synthesis of the 4- and 5- substituted 3-phenylisothiazoles **78–81** (Scheme 7) was performed from the ester-substituted isothiazoles **97** and **98**, which were obtained by decarboxylation of the oxathiazolone **96** and subsequent 1,3-dipolar cycloaddition with ethyl propiolate.[81] Subsequently, the esters **97** and **98** were reduced to the alcohols, transferred into the bromines **99**, **100** and reacted to the target compounds **78–81** via nucleophilic substitution or Suzuki reaction.
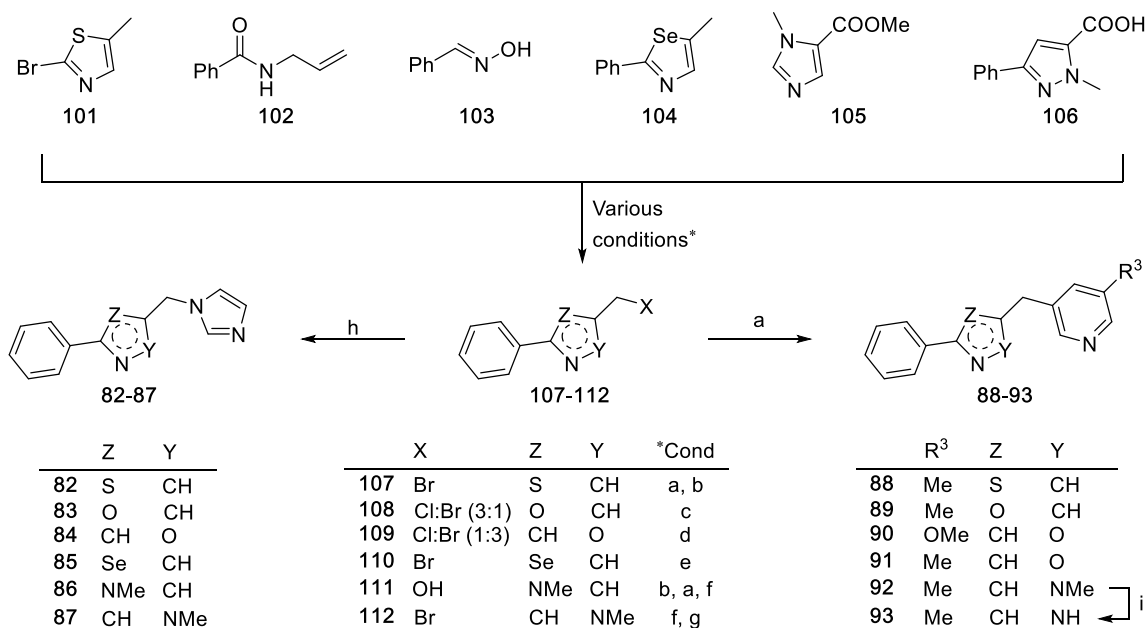
Scheme 7. Synthesis of compounds **78-81**[a]

78, 80   Imidazol-1-yl
79, 81   5-Me-pyridin-3-yl
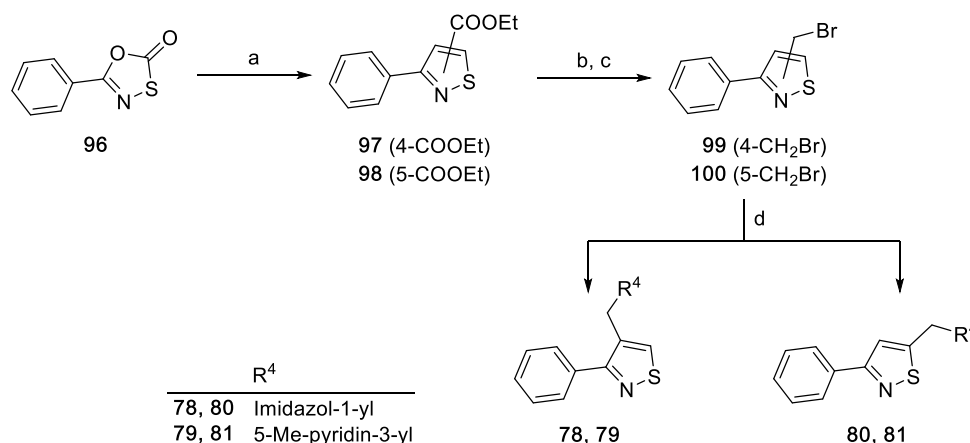
[a]Reagents and conditions: a) ethyl propiolate, CH₃Cl, 160 °C, 25 min, 300 W, microwave oven. b) LiAlH₄, THF, -40 °C, 1 h. c) PPh₃, CBr₄, DCM, 0 °C–rt, 1 h. d) for **78, 80**: method E: imidazole, K₂CO₃, DMF, 120 °C, 2 h; for **79, 81**: method A: corresponding boronic acid, Pd(PPh₃)₄, Na₂CO₃, toluene/ EtOH/ H₂O, reflux, 4h or overnight.

The 5-membered heteroaromatic derivatives **82**–**93** (Scheme 8) were synthesized applying different routes, in which corresponding halogenomethyl or hydroxymethyl compounds **107**–**112** were common intermediates. Bromomethyl thiazole **107** was prepared from 2-bromo-5-methylthiazole **101** by coupling with phenylboronic acid and subsequent bromination under Wohl-Ziegler conditions. Intramolecular oxidative cyclization of *N*-allylbenzamide **102** using *N*-bromosuccinimide (NBS)[82] led to a chloride and bromide (3:1) oxazole mixture **108**, whereas 1,3-dipolar cycloaddition of (*E*)-benzaldehyde oxime **103** and propargyl bromide[83] resulted in a chloride and bromide (1:3) isoxazole mixture **109**. In terms of the bromomethyl selenazole **110**, propargyl selenoamide was first cycloisomerized to methyl selenazole **104** and then brominated with NBS.[84] Introduction of bromine to methyl 1-methyl-1*H*-imidazole-5-carboxylate (**105**) under Wohl- Ziegler conditions, Suzuki coupling and subsequent reduction led to hydroxymethyl imidazole **111**. Furthermore, reduction of 1-methyl-3-phenyl-1*H*-pyrazole-5-carboxylic acid **106** to the alcohol and further reaction with phosphorus tribromide resulted in the bromomethyl pyrazole **112**. Finally, the desired imidazol-1-yl and pyridin-3-yl derivatives **82**–**92** were obtained either by substitution of the halogen or hydroxyl with an imidazol-1-yl or Suzuki reaction of intermediates **107**–**112**. Moreover, N-demethylation of 1-Me-pyrazole **92** using pyridine hydrochloride resulted in the pyrazole **93**.

Scheme 8. Synthesis of compounds **82-93**[a]

	Z	Y
82	S	CH
83	O	CH
84	CH	O
85	Se	CH
86	NMe	CH
87	CH	NMe

	X	Z	Y	*Cond
107	Br	S	CH	a, b
108	Cl:Br (3:1)	O	CH	c
109	Cl:Br (1:3)	CH	O	d
110	Br	Se	CH	e
111	OH	NMe	CH	b, a, f
112	Br	CH	NMe	f, g

	R^3	Z	Y
88	Me	S	CH
89	Me	O	CH
90	OMe	CH	O
91	Me	CH	O
92	Me	CH	NMe
93	Me	CH	NH

[a]Reagents and conditions: a) method A: corresponding boronic acid, Pd(PPh$_3$)$_4$, Na$_2$CO$_3$, toluene/ EtOH/ H$_2$O, reflux, 4 h; for **91**: corresponding boronic acid pinacol ester, PdCl$_2$(dppf), Cs$_2$CO$_3$, DME/ H$_2$O/ EtOH, 150 W, 150 °C, 20 min, microwave oven. (b) method D: NBS, DBPO, CCl$_4$, 60 °C or reflux, 12 h or 48 h. c) NBS, 1,2-dichloroethane, 100 °C, 24 h. d) propargyl bromide (80% in toluene), Et$_3$N, DCM, 12% aq. sodium hypochlorite, rt, 8 h. e) AIBN, NBS, CCl$_4$, hv (300 W) for 2 h, then 12 h, rt. f) THF, LiAlH$_4$, 0 °C or 0 °C–rt, 1 h or 12 h. g) PBr$_3$, THF, 0 °C - rt, 20 h. h) method E: imidazole, K$_2$CO$_3$, DMF, 120 °C, 2 h; for **20**: NMP, CDI, 190 °C, 16 h. i) pyridine hydrochloride, 2.5 h, 200 °C, 200 W, microwave oven.
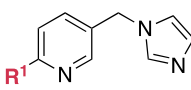
IN VITRO BIOLOGICAL RESULTS AND DISCUSSION

Inhibition of Human CYP11B1 and CYP11B2. Inhibitory potencies of the target compounds **67–93** were determined using V79MZ cells expressing either recombinant human CYP11B1 or CYP11B2, with [³H]-labeled 11-deoxycorticosterone as substrate. Obtained IC$_{50}$-values are shown in tables 6–7 in comparison to metyrapone and osilodrostat. *Ortho*-substitution of the phenyl moiety in **49** (IC$_{50}$= 2 nM, SF (IC$_{50}$CYP11B2/ IC$_{50}$CYP11B1)= 17) with electron withdrawing and lipophilic fluorine led to the similarly potent, but less selective compound **67** (Table 6, IC$_{50}$= 3 nM, SF= 9). In case of substitution in 3-position with an electron withdrawing, but hydrophilic methylsulfonamide a very similar result was obtained (**68**, IC$_{50}$= 2 nM, SF= 8). Exchange of phenyl for π-electron rich and hydrophilic furan-3-yl (**69**, IC$_{50}$= 4 nM, SF= 7) was not appropriate to increase selectivity towards CYP11B2 either. Introduction of π-electron rich and hydrophilic 1-Me-pyrazoles resulted in a loss of potency towards both enzymes (**70**, **71**, IC$_{50}$= 16–42 nM, SF= 4–6). Interestingly, exchange of the phenyl by the non-aromatic, hydrophilic, H-bond acceptor morpholin-4-yl (**72**) or the hydrophilic H-bond donor cyclopropylamine (**73**) did not change the inhibitory potency for CYP11B1 and CYP11B2 much (Table 6, IC$_{50}$= 4–22 nM, SF= 4–8). Moreover, introduction of a -S- or -SO$_2$- linker (**74**, **75**) between the central pyridine and the phenyl
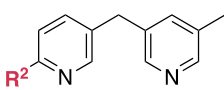
44

moiety led to similar findings (Table 6). *Ortho*-fluorine inserted into the phenyl moiety of **74** and **75** enhanced inhibitory potency for CYP11B1, but did not improve selectivity (**76, 77**, IC_{50}= 2–3 nM, SF= 8–9). Hence, structural diverse substituents in 2-position of the central pyridine core exhibiting various profiles concerning electronic properties, bulkiness and H-bond acceptor or donor properties were tolerated by both enzymes. Nevertheless, six compounds (**67–69, 73, 76, 77**) inhibited CYP11B1 with IC_{50}-values of less than 5 nM and exhibited good selectivity over CYP11B2 (SF= 7–9), thus exceeding the references metyrapone (IC_{50}= 15 nM, SF= 5) and osilodrostat (IC_{50}= 3 nM, SF= 0.07).
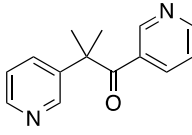
Table 6. Inhibition of CYP11B1 and CYP11B2 by compounds **67**–**77**.
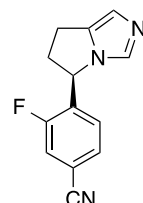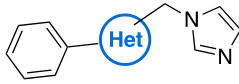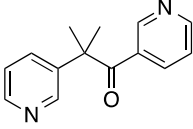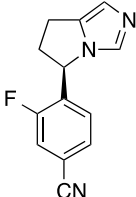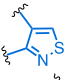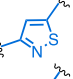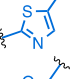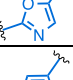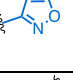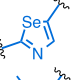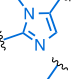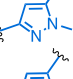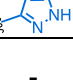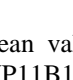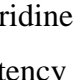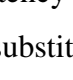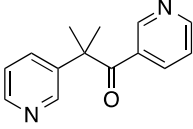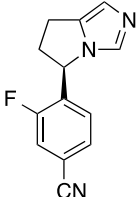
Comp	R^1/R^2	CYP IC_{50} (nM)[a,b]		SF^c
		11B1	11B2	
3[d]	Ph	107	1423	13
63[d]	2-F-Ph	122	767	6
64[d]	3-NH_2-Ph	85	1243	15
65[d]	Furan-3-yl	112	775	7
66[d]	3-Benzo[*b*]thiophene	47	375	8
4[d]	Naphthalen-1-yl	68	656	10
49[e]	Ph	2	33	17
67	2-F-Ph	3	27	9
68	3-$NHSO_2Me$-Ph	2	16	8
69	Furan-3-yl	4	28	7
70	1-Me-1*H*-pyrazol-4-yl	42	182	4
71	1-Me-1*H*-pyrazol-5-yl	16	97	6
72	Morpholin-4-yl	22	90	4
73	Cyclopropanamine	4	32	8
74	PhS-	5	30	6
75	$PhSO_2$-	20	173	9
76	2-F-PhS-	3	24	8
77	2-F-$PhSO_2$-	2	17	9
metyrapone		15	72	5
osilodrostat		3	0.2	0.07

[a]Mean value of at least two experiments. The deviations were <25%. [b]Hamster fibroblasts expressing human CYP11B1 or CYP11B2; substrate 11-deoxycorticosterone, 100 nM. [c]SF: IC_{50} $_{CYP11B2}$ / IC_{50} $_{CYP11B1}$. [d]See reference [43], IC_{50} values differ due to different enzyme sources. [e]See chapter 3.1[42].

Replacement of the central pyridine in imidazolylmethyl pyridine **3** (IC$_{50}$= 107 nM, SF= 13) by π-electron rich 5-membered heterocycles led to differing results (Table 7).

Table 7. Inhibition of CYP11B1 and CYP11B2 by compounds **78–93**.

Het	Comp	CYP IC$_{50}$ (nM)^{a,b}		SF^c	Comp	R^3	CYP IC$_{50}$ (nM)^{a,b}		SF^c
		11B1	11B2				11B1	11B2	
	3^d	107	1423	13	**49**^{d}	Me	2	33	17
					53^d	OMe	4	25	6
	78	57	174	3	**79**	Me	48	152	3
	80	14	120	9	**81**	Me	1	8	8
	82	62	459	7	**88**	Me	9	24	3
	83	150	520	4	**89**	Me	14	116	8
	84	148	1304	9	**90**	Me	5	82	16
					91	OMe	2	27	14
	85	104	657	6					
	86	516	507	1					
	87	58	215	4	**92**	Me	1	6	6
					93	Me	137	586	4
-	**metyrapone**	15	72	4					
-	**osilodrostat**	3	0.2	0.07					

^{a}Mean value of at least two experiments. The deviations were <25%. ^{b}Hamster fibroblasts expressing human CYP11B1 or CYP11B2; substrate 11-deoxycorticosterone, 100 nM. ^{c}SF: IC$_{50\,CYP11B2}$ / IC$_{50\,CYP11B1}$. ^{d}See chapter 3.1[42].

Pyridine isosteres isothiazoles **78** and **80** and thiazole **82** caused increased CYP11B1 inhibitory potency (IC$_{50}$= 14–62 nM), but also a loss of selectivity towards CYP11B2. Here, the 3,5-disubstituted isothiazole **80** (IC$_{50}$= 14 nM, SF= 9) demonstrated a 4-fold increased potency for the target enzyme with a better selectivity compared to the 3,4-disubstituted compound **78** (IC$_{50}$= 57

nM, SF= 3). Interestingly, bioisosteric selenazole **85** (IC$_{50}$= 104 nM, SF= 6) was not as potent and selective as thiazole **82**. Exchange of the thiazole for the more electronegative and less bulky oxazole (**83**) or isoxazole (**84**) led to decreased CYP11B1 inhibition (IC$_{50}$= 148–150 nM). Here, differences regarding electronegativity (O > S, Se) or molecular geometry (size: Se, S > O) might influence interaction with the target enzyme. Furthermore, introduction of 1-Me-imidazole (**86**) led to a significant decrease in CYP11B1 inhibition (IC$_{50}$= 516 nM) with improved potency for CYP11B2 (SF=1). Obviously, the *N*-methyl group is not tolerated by the CYP11B1 enzyme in this position, in contrast to the *N*-methylated pyrazole **87** (IC$_{50}$= 58 nM). However, **87** is less active than the corresponding isothiazole compound **80**, which showed an 8-fold improvement of CYP11B1 inhibition compared to **3**, but a slight loss of selectivity over CYP11B2. Compared to the imidazolylmethyl class, similar results were obtained by exchange of the central pyridine in **49** with π-electron rich 5-membered heterocycles (Table 7). In compounds of the pyridylmethyl class, introduction of thiazole did not lead to an enhanced inhibition of the target enzyme (**88**, IC$_{50}$= 9 nM, SF= 3), though. The isoxazole compound **90** showed only a slight decrease of potency, but a retained selectivity (IC$_{50}$= 5 nM, SF= 16). Hence, isoxazole is a suitable replacement for the central pyridine of **49** and derivatization according to **53** was performed (exchange of 5-Me by 5-OMe) to obtain another potent and selective candidate. Thereby, CYP11B1 inhibition could be enhanced (**91**, IC$_{50}$= 2 nM, SF= 14). The pyrazole **93** exhibited reduced activity towards the target enzyme, indicating that a hydrogen bond donor is not well tolerated. Modification of the central pyridine in **49** led to four novel inhibitors with IC$_{50}$ values of ≤ 5 nM (**81**, **90**–**92**) with isoxazoles **90** and **91** (IC$_{50}$= 2–5 nM, SF= 14–16) showing similar selectivity over CYP11B2 as **49** (IC$_{50}$= 2 nM, SF= 17). It is worth mentioning that **90** and **91** were more potent and selective than the clinically used inhibitor metyrapone (IC$_{50}$= 15 nM, SF= 5) or the recently published osilodrostat (IC$_{50}$= 3 nM, SF= 0.07). Albeit significant improvement of CYP11B1 inhibitory potency was achieved in the imidazolylmethyl class, the 5-Me-pyridin-3-ylmethyl analogues showed stronger inhibition of the target enzyme. Compounds **90** (IC$_{50}$= 5 nM) and **91** (IC$_{50}$= 2 nM), exhibiting selectivity factors above 10, were chosen for further biological evaluation.

Inhibition of Rat CYP11B1. Inhibition of rat CYP11B1 by isoxazoles **90** and **91** was determined in V79MZ cells expressing recombinant rat CYP11B1 as a precondition for *in vivo* proof-of-principle experiments. Both inhibitors revealed similar improved potencies towards rat CYP11B1 (**90**, IC$_{50}$= 4.0 μM; **91**, IC$_{50}$= 1.8 μM) compared to metyrapone (IC$_{50}$= 4.6 μM). The 1.000-fold lower rat CYP11B1 potency is in accordance with the low sequence identity between human and rat CYP11B1 (64%).[29]

Metabolic Stability. To achieve sufficient plasma concentrations of the parent compounds, metabolic stability in rat and human liver S9 fraction was determined. Isoxazoles **90** and **91** exhibited good stabilities in human liver S9 fraction with half-lives of 145 min and 125 min, respectively. Furthermore, inhibitors **90** and **91** showed increased metabolic stability in rat liver S9 fraction (**90**: $t_{1/2}$= 30 min, **91**: $t_{1/2}$= 23 min) compared to **49** ($t_{1/2}$= 16 min) and metyrapone ($t_{1/2}$= 12 min).

IN VITRO TOXICITY EVALUATION

Selectivities over Human CYP17A1 and CYP19A1. Since both 17α-hydroxylase-17,20-lyase (CYP17A1) and aromatase (CYP19A1) are essential for the production of the sex steroids, their inhibition might cause severe side-effects such as hypogonadism[85] or hyperandrogenism,[86] respectively. Assays for CYP17A1 and CYP19A1 inhibition were performed with compound concentrations of 2 μM.[87-89] This rather high concentration was chosen to provide a selectivity factor of at least 400 for the highly potent CYP11B1 inhibitors **90** and **91** showing IC_{50} values of 5 nM and 2 nM (Table 7). Compounds **90** and **91** exhibited no significant inhibition (Table 8, ≤ 9% at 2 μM) and are considered as inactive.

Table 8. Inhibition of CYP17A1 and CYP19A1 by compounds **90** and **91**.

Comp	inhibition (%)[a]	
	CYP17A1[b]	CYP19A1[c]
49	5	1
90	2	3
91	4	9
metyrapone	3	0

[a]Compounds concentration 2 μM. Inhibition ≤ 9 % is not significant. [b]E. coli expressing human CYP17A1; substrate progesterone, 25 μM. [c]Human placental CYP19A1; substrate androstenedione, 500 nM.

Selectivities over Human Hepatic CYP Enzymes. Hepatic CYP enzymes play an eminent role in the metabolism of drugs and their inhibition could result in adverse drug reactions or toxicity. Thus, derivatives **90** and **91** were tested for inhibition of a series of relevant metabolizing CYP enzymes, comprising CYP1A2, CYP2B6, CYP2C9, CYP2C19, CYP2D6 and CYP3A4. Tested at a concentration of 1 μM, compound **90** showed percent inhibition values of 54%, 3%, 28%, 8%, 0% and 61% and, compound **91** values of 23%, 19%, 17%, 17%, 8% and 33% for CYP1A2, 2B6,

2C9, 2C19, 2D6 and 3A4, respectively. Hence, selectivity over hepatic CYP enzymes should be sufficient for the highly active compounds.

Cytotoxicity. The effect of compounds **90** and **91** on cell viability was tested in an MTT assay using HEK293 cells. No effect on cellular viability was observed up to 28 µM and 42 µM (IC$_{20}$ values) after 66 h of incubation for compounds **90** and **91**, respectively. Given the strong CYP11B1 inhibition of these compounds (IC$_{50}$ ≤ 5 nM), it is expected that no cytotoxic effects will be observed at therapeutic concentrations.

Mutagenicity. For determination of the mutagenic potential of compounds **90** and **91**, AMES II tests were performed using TA98 (frameshift mutation) or TAMix (base-pair substitution, TA7001-TA7006) strains of *Salmonella typhimurium* in the presence or absence of rat liver S9 fraction. The inhibitors **90** and **91** showed no mutagenic potential up to the highest tested concentration of 100 µM in the absence or presence of rat liver S9 fraction.

Aryl Hydrocarbon Receptor Activation. Activation of the aryl hydrocarbon receptor (AhR) induces several biochemical responses, such as expression of CYP1A1 and CYP1A2. Both are responsible for the metabolic activation of promutagens, which is a potential risk for cancer development.[90] Compounds **90** and **91** did not show activation of the AhR in HepG2 hepatocellular carcinoma cells at a concentration of 3.16 µM and, therefore, no interference with the receptor is expected at pharmacologically relevant concentrations.

Cardiotoxicity. Drug-induced arrhythmia caused by blocking the cardiac potassium ion channel hERG (human ether-a-go-go related gene) is a potential cause for sudden death among patients. Compound **91** was tested using a hERG fluorescence polarization assay[91] and showed an IC$_{50}$ value of 23 µM. Due to the high CYP11B1 potency of **91** (IC$_{50}$= 2 nM), the safety margin can be considered as sufficient.

IN VIVO BIOLOGICAL RESULTS AND DISCUSSION

Preliminary Evaluation of Plasma Concentrations of 90 and 91 in Rats. Based on the *in vitro* biological evaluation, inhibitors **90** and **91** are promising candidates for a proof-of-principle study in rats. Both compounds exhibit different physicochemical properties due to distinct scaffolds compared to **49**. For instance, the calculated log D (pH= 7.4) value was changed from 3.7 for **49** to 3.1 and 2.8 for **90** and **91**, respectively.[79] This should balance solubility and permeability

properties of the compounds under *in vivo* conditions. In the light of the poor oral bioavailability of **49** (F= 2%) in rats, preliminary pharmacokinetic experiments for the novel inhibitors **90** and **91** were performed first to show their suitability for extensive *in vivo* experiments. Both compounds should be soluble under these conditions as they exhibited good aqueous solubility (>200 µM). Plasma concentrations of **90** and **91** in rats were determined using a single dose of 100 mg/kg (perorally) per inhibitor (Figure 11). Interestingly, the 5-OMe compound **91** showed much higher plasma concentrations of 19.7 µM and 106.4 µM at 1 h and 4 h, respectively, than 5-Me derivative **90** (1 h, 2.5 µM; 4 h, 0.3 µM). The required plasma levels for a therapeutic effect in rats on the basis of the *in vitro* assay (**91**, IC_{50}= 2 µM; **90**, IC_{50}= 4 µM) were achieved in case of **91** and, therefore, the oral bioavailability of **91** was determined in rats.
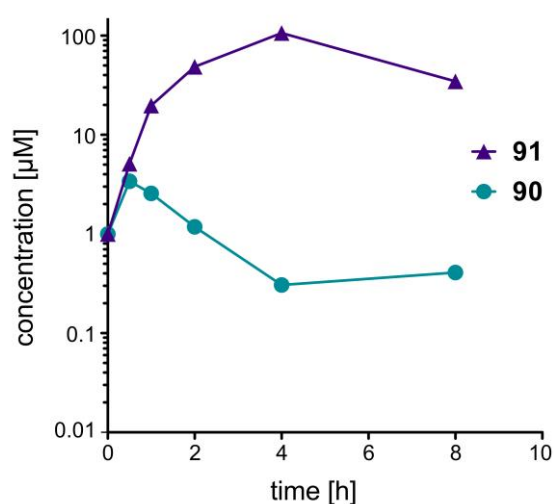
Figure 11. Plasma concentration [µM] in rat versus time after oral application (100 mg/kg) of compounds **90** and **91** in single dosing experiments (n=1).

Oral Bioavailability Study of 91 in Rats. The pharmacokinetic parameters of **91** were determined after intravenous (5 mg/kg, n= 2) and oral (28 mg/kg, n= 2) application in rats (mean values are listed in table 9). Mean maximal concentrations of 27.8 µM (i.v.) and 6.4 µM (p.o.) were achieved. As depicted in figure 12, plasma concentrations above the *in vitro* IC_{50} value for rat CYP11B1 (2 µM) were obtained for a duration of up to 7 hours. The compound exhibited long half-lives of 4.8 hours (i.v.) and 3.3 hours (p.o.) as well as a moderate plasma clearance of 22.6 mL/min·kg. Most importantly, absolute oral bioavailability (F) was determined to be 50%. In a previously published paper, metyrapone (IC_{50} *in vitro* rat= 5 µM) showed an ED_{50} of 40 mg/kg and EC_{50} of 3.6 µM for inhibition of the corticosterone biosynthesis (CYP11B1 catalyzes the last step of corticosterone biosynthesis in rats) in an 8 h experiment.[92] Hence, it can be assumed that inhibitor **91** is able to reduce corticosterone plasma levels in rats at higher doses due to high plasma concentrations and, therefore, it is a good candidate for a following proof-of-principle study.

50

Table 9. Key pharmacokinetic parameters of **91** after a single dose in rats.[a,b]
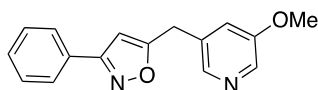
91

Comp	Route	Dose [mg/kg]	C_{max} [µM]	T_{max} [h]	$T_{1/2}$ [h]	V_{dss} [L/kg]	CL [mL/min·kg]	$AUC_{0-\infty}$ [ng·h/mL]	F [%]
91	i.v. (n=2)	5	27.8		4.8	3.1	22.6	3677	
	p.o. (n=2)	28	6.4	2.5	3.3			10220	50

[a]Data are mean values. [b]Abbreviations: i.v., intravenous; p.o., per oral; Cmax, peak plasma concentration of a drug after administration; Tmax, time to reach Cmax; $T_{1/2}$, elimination half-life; Vdss, volume of distribution at steady state; CL, plasma clearance; AUC, area under the concentration−time curve; F, bioavailability.
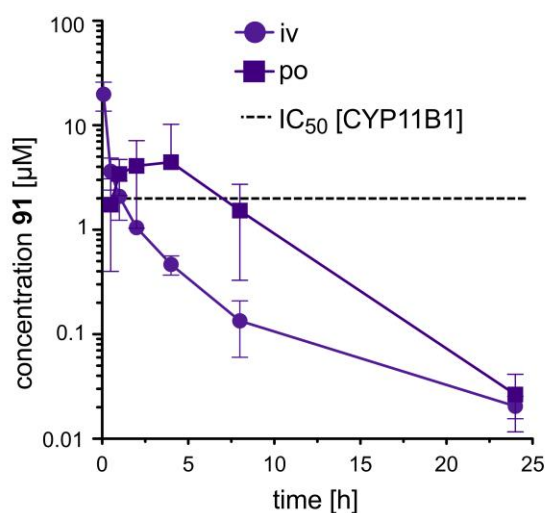
Figure 12. Mean profile (±) SD of plasma concentration [µM] in rat versus time after oral (28 mg/kg) and intravenous (5 mg/kg) application of compound **91** in single dosing experiments (n=2). At 4 h peroral SD = 4107 nM. Dashed line represents the *in vitro* CYP11B1 IC$_{50}$ value for **91** in rat.

CONCLUSION

For the treatment of Cushing's disease, the steroid 11β-hydroxylase (CYP11B1) inhibitor metyrapone is used in the clinic. Very high (500-6000 mg per day) and frequent dosing (every 8 hours) of metyrapone is needed and it causes severe side-effects due to unselective inhibition of other steroidogenic CYP enzymes.[38, 71] Previously, we identified the selective and very potent CYP11B1 inhibitor **49** (IC_{50}= 2 nM, SF= 17), which exceeded metyrapone in CYP11B1 potency and selectivity (IC_{50}= 15 nM, SF= 5) and exhibited an acceptable *in vitro* pharmacological profile. [Chapter 3.1[42]] However, further determination of mutagenicity identified **49** as promutagen in the TA98 strain (frameshift mutation) of *Salmonella typhimurium* and a pharmacokinetic study in rats revealed a poor oral bioavailability of **49** (F= 2%). Optimizations of **49** and the less potent, but selective compound **3** (IC_{50}= 107 nM, SF= 13) were performed to obtain other candidates for further *in vivo* studies with at least similar CYP11B1 potency and selectivity. For this purpose, the phenyl moiety of **49** was exchanged by various substituents and the central pyridine cores of selective **3** and **49** were replaced by several azoles differing in electronic and steric properties. Out of the 27 synthesized compounds, derivatives **67–69**, **73**, **74**, **76**, **77**, **81**, **90–92** showed IC_{50} values of ≤ 5 nM. Among them, isoxazoles **90** and **91** exhibited the highest selectivity over CYP11B2 (SF > 10) and, therefore, showed an improved inhibitory profile compared to the clinically used metyrapone (IC_{50}= 15 nM, SF= 5) or the recently published CYP11B1 inhibitor osilodrostat (IC_{50}= 3 nM, SF= 0.07). Both inhibitors showed selectivities over CYP17A1, CYP19A1 and hepatic CYP enzymes (CYP1A2, 2B6, 2C9, 2C19, 2D6 and 3A4), metabolic stability in human liver S9 fraction, negligible cytotoxicity, no interference with the aryl hydrocarbon receptor and for **91** negligible inhibition of the cardiac potassium ion channel hERG. Furthermore, both compounds exhibited increased metabolic stability in rat liver S9 fraction (**90**: $t_{1/2}$= 30 min, **91**: $t_{1/2}$= 23 min) compared to **49** ($t_{1/2}$= 16 min) and metyrapone ($t_{1/2}$= 12 min) and moderately inhibited rat CYP11B1 (**90**, IC_{50}= 4 μM; **91**, IC_{50}= 2 μM). Compounds **90** and **91** showed no mutagenic potential and *in vivo* PK evaluation in rats revealed sufficiently high plasma concentrations (1 h, 19.7 μM; 4 h, 106.4 μM) for therapeutic effects in case of inhibitor **91** (100 mg/kg, perorally). Further pharmacokinetic study of orally applied **91** in rats demonstrated plasma levels above the required concentration for a therapeutic effect for up to 7 hours (28 mg/kg, perorally) and, thus, a significantly improved oral bioavailability of 50%. It is worth mentioning that in spite of the fact that compound **91** is much less active towards the rat than the human enzyme (factor of 1000), plasma levels are even high enough in rats to expect biological activity. Hence, a novel selective and very potent CYP11B1 inhibitor was identified, exhibiting high lipophilic efficiency (LiPE= 5.9) and a good pharmacological profile with expected ability to reduce corticosterone plasma levels *in vivo*.

3.3. Accelerated Skin Wound Healing by Novel 11β-Hydroxylase (CYP11B1) Inhibitors

Results described in this chapter were published in 2018 in Eur. J. Med. Chem.
https://doi.org/10.1016/j.ejmech.2017.11.018

Reprinted with permission from *Eur. J. Med. Chem.* **2018**, *143*, 591−597.
Copyright: © 2017 Elsevier Masson SAS

The following persons also contributed to the results described in this chapter:

1. Dr. Jens L. Burkhart: Synthesis of compounds **118** and **119** and the corresponding intermediates.
2. Dr. Roger T. Engeli: Performance of the 11β-HSD1 and 11β-HSD2 inhibition assays.
3. Lorenz Siebenbürger: Performance of the metabolic stability assays in human and rat liver S9 fractions and plasma.
4. Dr. Chris J. van Koppen: Coordination and performance of the CYP11B1, CYP11B2, CYP17A1, CYP19A1 inhibition assays. Performance of the AMES II mutagenicity assay.
5. Employees of BIOalternatives (France) and Dr. Chris J. van Koppen: Coordination and performance of the wound healing and cytotoxicity experiments.

INTRODUCTION

Chronic wounds arise from disorders of the tightly regulated skin healing process comprising the overlapping phases of hemostasis, inflammation, proliferation and tissue remodeling .[93] The skin defect lasts more than 6 weeks or frequently recurs.[94] Non-healing wounds are mainly ulcers (~70%) induced by ischemia, diabetes mellitus, venous stasis disease, or pressure.[45] It is an enormous burden for the patient and the health care system as approximately 37 million people are affected worldwide.[94] Due to the aging population and a rise in obesity or diabetes, the number of patients is expected to increase further.[95] Associated costs for global wound care management are estimated to reach \$22 billion per year by 2020.[96] Therefore, new therapeutic approaches are urgently needed to accelerate the wound healing process and to reduce costs. It has been shown that human skin is a steroidogenic organ expressing the corresponding enzymes for the synthesis of glucocorticoids, androgens and estrogens.[51] To regulate the wound healing process, the glucocorticoid cortisol is formed *de novo* from cholesterol by keratinocytes,[46, 97] which make up 90% of the epidermis.[47] In general, excess cortisol (endogenous or exogenous) negatively influences the epidermal growth factor signaling, epidermal cell migration and re-epithelialization as well as angiogenesis, which results in inhibition of wound healing.[48, 98-99] It was demonstrated that in the case of an acute wound, the levels of cortisol and the enzyme catalyzing its last step of biosynthesis (Figure 13), 11β-hydroxylase (CYP11B1), are gradually increased in human (*ex vivo*) and porcine skin (*in vivo*) with a maximum at 48 h and then return to normal levels within the next 24 h.[46]
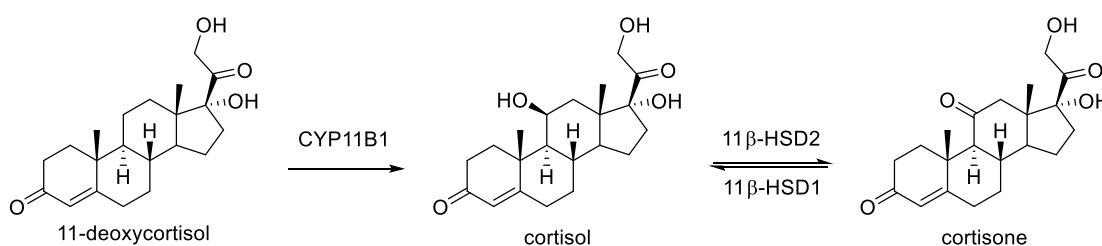
Figure 13. Biosynthesis and regulation of local concentrations of cortisol in human.

Acceleration of wound healing in these models was observed by topical application of high concentrations (1 mM) of metyrapone (Figure 14)[46], a potent CYP11B1 inhibitor (IC$_{50}$ CYP11B1= 15 nM). Another study in mice skin showed an increase of 11β-hydroxysteroid dehydrogenase type 1 (11β-HSD1, reduces 11-dehydrocorticosterone to corticosterone in rodents) expression, but a lack of CYP11B1 expression during wound healing.[48] Blockade of 11β-HSD1 by subcutaneous application of **113** (IC$_{50}$ 11β-HSD1= 1.1 nM, Figure 14)[100] resulted in enhanced wound healing in mice (*in vivo*).[101]
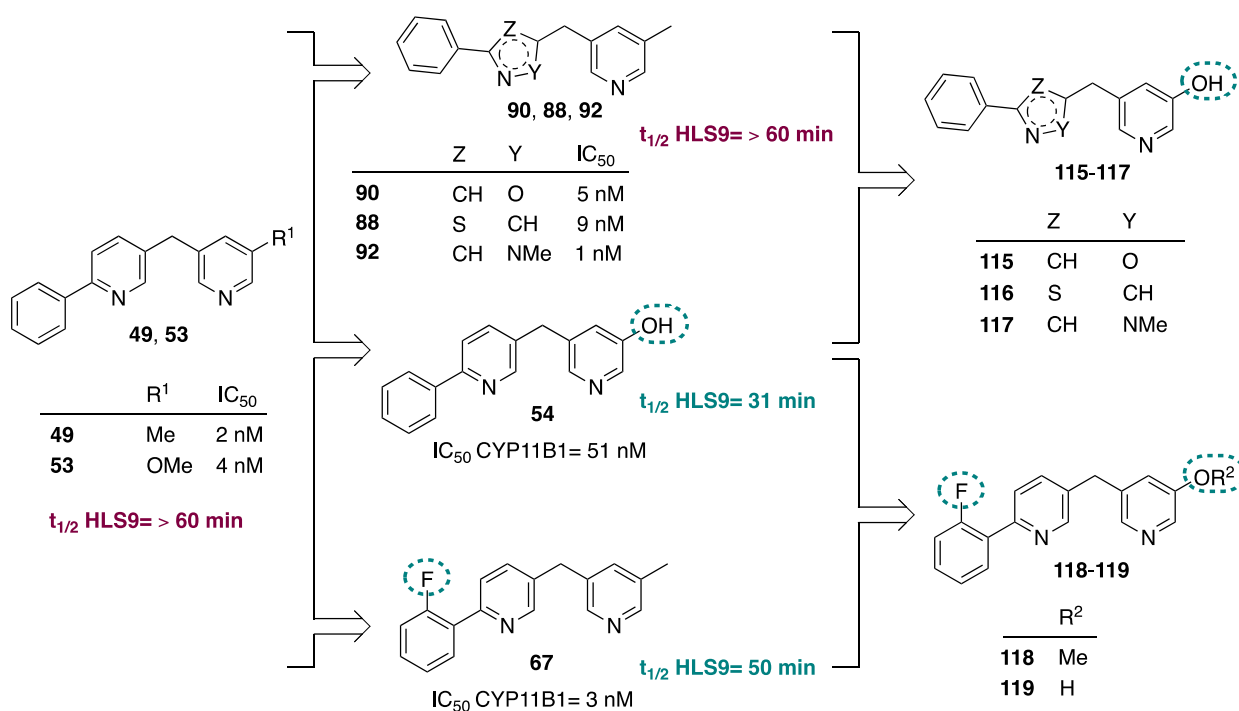
54
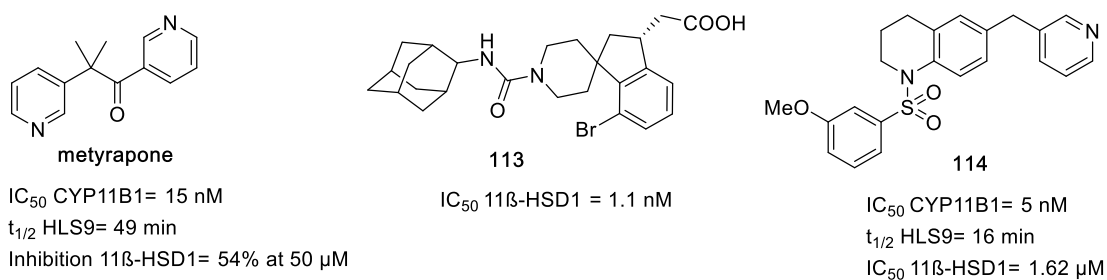
Figure 14. CYP11B1 and 11β-HSD1 inhibitors for wound healing.

In fact, metyrapone is a non-selective inhibitor of CYP enzymes[102] and, in our studies, inhibits 11β-HSD1 (54% at 50 µM and 70% at 200 µM, Figure 14) as well. Hence, it remains unclear whether improved wound healing of human skin results from CYP11B1 or 11β-HSD1 (reduces cortisone to cortisol in human, Figure 13) inhibition. However, blockade of cortisol synthesis in skin seems to be a promising approach for the treatment of chronic wounds where CYP11B1 expression is permanently increased and does not normalize, thereby blocking re-epithelialization, re-vascularization and wound healing.[49-50] The aim of this study was to identify an appropriate potent CYP11B1 inhibitor which is selective over 11β-HSD1 and demonstrates acceleration of wound healing in a human skin explant.

INHIBITOR REQUIREMENTS AND OPTIMIZATION

Usually, selectivity of CYP11B1 inhibitors over aldosterone synthase (CYP11B2, 93% homology)[55] is challenging to achieve.[41-43, 58, 60, 103-105] However, selectivity is not needed for dermal application as CYP11B2 expression and activity have not been identified in human skin.[51, 106] In contrast, estrogens exhibit an essential role in wound healing as they influence the inflammatory phase, act mitogenically on keratinocytes, enhance re-epithelialization and raise collagen synthesis.[107] To ensure that there is no interference with this system, selectivity of CYP11B1 inhibitors is a precondition. Accordingly, the key enzymes 17α-hydroxylase-17,20-lyase (CYP17A1) and aromatase (CYP19A1) should not be inhibited. Additionally, we aimed to achieve selectivity over 11β-HSD1 to study whether the wound healing effect can be obtained by selective CYP11B1 inhibition. Selectivity over 11β-hydroxysteroid dehydrogenase 2 (11β-HSD2) should also be achieved to avoid inhibition of the conversion of cortisol to inactive cortisone. Furthermore, to exclude degradation in wound fluid and related poor *in vivo* efficacy, an ideal candidate should be stable in plasma, whose composition is comparable to wound fluid.[108] As the application site is not well defined (intact and injured skin), resorption of a CYP11B1 inhibitor after dermal application on wounded skin is expected.

Chart 4. Design Concept to Reduce Metabolic Stability

90, 88, 92

t$_{1/2}$ **HLS9= > 60 min**

	Z	Y	IC$_{50}$
90	CH	O	5 nM
88	S	CH	9 nM
92	CH	NMe	1 nM

49, 53

	R^1	IC$_{50}$
49	Me	2 nM
53	OMe	4 nM

t$_{1/2}$ **HLS9= > 60 min**

54

t$_{1/2}$ **HLS9= 31 min**

IC$_{50}$ CYP11B1= 51 nM

67

t$_{1/2}$ **HLS9= 50 min**

IC$_{50}$ CYP11B1= 3 nM

115-117

	Z	Y
115	CH	O
116	S	CH
117	CH	NMe

118-119

|	R^2
118	Me
119	H

Therefore, rapid systemic clearance of the absorbed potent inhibitor is desired to avoid effects on the adrenal steroidogenesis. Metyrapone (Figure 14) exhibits the desired stability in human plasma (t$_{1/2}$= > 150 min), but can be significantly improved, as it shows a relatively long half-life of 49 min in human liver S9 fractions (HLS9), which is likely to result in systemic side effects after dermal application on wounded skin. Previously, we discovered **114** (Figure 14) featuring an improved potency for CYP11B1 (IC$_{50}$= 5 nM), a half-life of 16 min in HLS9 and stability in human plasma (t$_{1/2}$= > 150 min).[52] However, beside weak CYP19A1 inhibition by **114** (26% at 2 μM)[52], our further studies revealed that the compound inhibits 11 β -HSD1 with an IC$_{50}$-value of 1.62 μM (Figure 14). The published wound healing experiments were performed with a high concentration of metyrapone (1 mM).[46] Inhibitor **114** would still inhibit 11 β -HSD1 and CYP19A1 even if a 100-fold lower concentration is used in the described wound healing experiment. Due to these drawbacks, **114** is not the most appropriate candidate for a proof of concept study. The structurally different and very potent CYP11B1 inhibitors **49**, **53**, **88**, **90** and **92** (Chart 4) [Chapter 3.1[42], Chapter 3.2[104]] are more suitable candidates for further optimization due to their high selectivity over CYP19A1 (0-3% at 2 μM, Table 10). They mainly differ in their central core and were all metabolically stable (t$_{1/2}$ HLS9= > 60 min). However, exchange of 5-Me-pyridin-3-yl (**49**, IC$_{50}$= 2 nM) by a 5-OH- pyridin-3-yl moiety in **54** [Chapter 3.1[42]], which is able to undergo conjugation reactions by Phase II enzymes, resulted in an expected reduced half-life of 31 min in HLS9. Since this modification led to a strong decrease of potency towards CYP11B1 (**54**, IC$_{50}$= 51 nM),

exchange of 5-Me by 5-OH was also performed in **88**, **90** and **92**, [Chapter 3.2[104]] aiming at metabolically labile as well as potent inhibitors (**115-117**). Introduction of an *ortho*-fluorine into the phenyl moiety of **49** ($t_{1/2}$ HLS9= > 60 min) led to **67** [Chapter 3.2[104]] exhibiting a decreased half-life of 50 min in HLS9. For further investigations, an *ortho*-fluorine was introduced at the phenyl moiety of the potent 5-OMe derivative **53**, which is prone to ether cleavage by Phase I enzymes and subsequent rapid Phase II metabolism, and the labile compound **54** (5-OH) leading to compounds **118** and **119**. Inhibitors **115-119** were biologically evaluated for CYP11B1 inhibition and half-life in HLS9. Subsequently, selectivities over CYP17A1, CYP19A1, 11β-HSD1 and 11β-HSD2 as well as plasma stability and toxicity were investigated for the most promising compounds. One selected CYP11B1 inhibitor was further evaluated for its ability to accelerate wound healing in human skin.

CHEMISTRY

Hydroxy compounds **115-117** were accessible *via* a two-step synthesis starting from the previously described halogenomethyl derivatives **109**, **107** and **112** [Chapter 3.2[104]] and (5-methoxypyridin-3-yl)boronic acid pinacol ester using Suzuki conditions under microwave irradiation (Scheme 9). Subsequently, the crude ether intermediates obtained were cleaved under acidic conditions leading to the final compounds **115-117**. Coupling of 2-bromo-5-methyl-pyridine with (2-fluorophenyl)boronic acid resulted in compound **120**, which was further brominated under Wohl-Ziegler conditions.

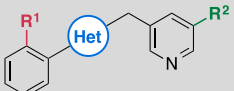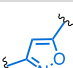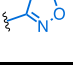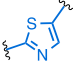**Scheme 9**. Synthesis of compounds **115–119**.[a]

	Z	Y
115, 109	CH	O
116, 107	S	CH
117, 112	CH	NMe

X = Cl:Br (1:3) or Br
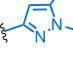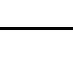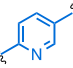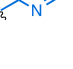
	R^2
118	Me
119	H
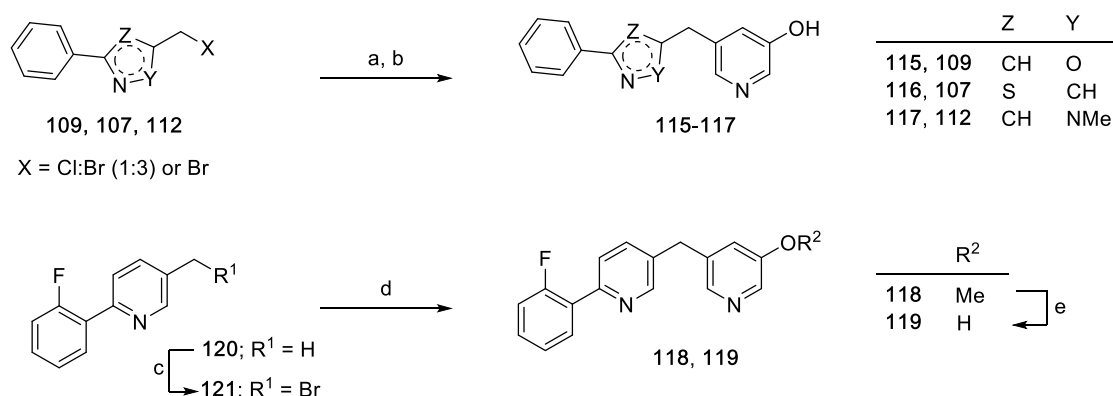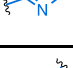
[a]Reagents and conditions: (a) Reagents and conditions: (a) (5-methoxypyridin-3-yl)boronic acid pinacol ester, PdCl$_2$(dppf), Cs$_2$CO$_3$, DME/H$_2$O/EtOH, 150 °C, 150 W, 18 bar, 20 min, microwave. (b) HBr (48% in water), 130 °C, 12 h. (c) NBS, AIBN, CCl$_4$, 80 °C, 7 h. (d) (5-methoxypyridin-3-yl)boronic acid pinacol ester, Pd(PPh$_3$)$_4$, Na$_2$CO$_3$, toluene/EtOH/H$_2$O, 100 °C, 22 h. (e) BBr$_3$, DCM, -78 °C–rt, 21 h.

The bromine intermediate **121** was coupled with the corresponding organoborane resulting in the desired methoxy compound **118**. In addition, hydroxy derivative **119** was available *via* ether cleavage using boron tribromide (Scheme 9).

BIOLOGICAL RESULTS AND DISCUSSION

Inhibition of Human CYP11B1. The final compounds **115**-**119** were evaluated for inhibitory potency using V79MZ cells expressing recombinant human CYP11B1 with [³H]-labeled 11-deoxycorticosterone as substrate.[109] The IC_{50}-values obtained are shown in table 10 in comparison to metyrapone, **114**, **49**, **53**, **88**, **90**, **92**, **54** and **67**.

Table 10. Inhibition of CYP11B1, CYP19A1 and metabolic stability data of metyrapone and compounds **49**, **53**, **54**, **67**, **88**, **90**, **92** and **114**-**119**.

Comp	R^1	Het	R^2	CYP11B1 IC_{50} (nM)[a]	$t_{1/2}$ HLS9 (min)[b]	CYP19A1[c] inhibition (%)[d]
90[e]	H		Me	4.6 ± 0.6	>60 min	3 ± 2
115	H		OH	120 ± 35	n.d.	n. d.
88[e]	H		Me	8.7 ± 1.8	>60 min	0 ± 0
116	H		OH	77 ± 27	n.d.	n. d.
92[e]	H		Me	1.3 ± 0.2	>60 min	2 ± 2
117	H		OH	17 ± 0.4	33	0 ± 0
49[f]	H		Me	2.2 ± 0.5	>60 min	1 ± 2
53[f]	H		OMe	4.4 ± 0.7	>60 min	0 ± 0
54[f]	H		OH	51 ± 3	31	0 ± 0
67[e]	F		Me	3 ± 0.6	50	0 ± 0
118	F		OMe	0.8 ± 0.2	19	2 ± 3
119	F		OH	29 ± 1	21	1 ± 1
metyrapone				15 ± 2	49	0 ± 0
114[g]				5 ± 0.7	16	26 ± 2

[a]V79 hamster fibroblasts heterologously expressing human CYP11B1, substrate 11-deoxycorticosterone, 100 nM, mean ± SD, n≥ 2. [b]HLS9, human liver S9 fractions. [c]Human placental CYP19A1; substrate androstenedione, 500 nM. [d]Compound concentrations 2 µM. Inhibition values ≤10% are not significant, mean ± SD, n≥ 2. [e]See [chapter 3.2[104]]. [f]See [chapter 3.1[42]]. [g]See ref[52]. n. d., not determined.
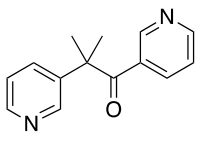
Exchange of lipophilic 5-Me-pyridin-3-yl in **49** (IC_{50}= 2 nM) by hydrophilic, H-bond donating 5-OH-pyridin-3-yl (**54**) resulted in a 26-fold decrease of potency (IC_{50}= 51 nM) [Chapter 3.1[42]]. The same modification (5-Me to 5-OH) in **88**, **90** and **92** (IC_{50}= 1-9 nM), which vary in electronic and steric properties due to the different central cores, likewise led to a 9 to 24-fold loss of inhibitory activity (**115-117**, IC_{50}= 17-120 nM). Nevertheless, compound **117** is more potent than **54**. Following this trend, the fluorine-containing compound **119** (5-OH, IC_{50}= 29 nM) demonstrated weaker inhibition of CYP11B1 than the 5-Me derivative (**67**, IC_{50}= 3 nM). However, inhibitor **119** (5-OH) was more potent than **54** (5-OH) lacking fluorine substitution. Since 5-OMe pyridin-3-yl compound **53** exhibited a slight decrease of potency compared to **49** (5-Me), the same was expected for fluorinated 5-OMe inhibitor **118**.

In fact, **118** showed an improved IC_{50}-value of 0.8 nM compared to **67** (5-Me, IC_{50}= 3 nM) and exceeds metyrapone (IC_{50}= 15 nM) and **114** (IC_{50}= 5 nM). The most potent inhibitors (**117-119**) were further tested for metabolic stability.

Stability in human liver S9 fraction and plasma. For topical application, a suitable inhibitor should be stable in wound fluid but have a rapid metabolic clearance in the liver to avoid systemic side effects. In analogy to **54**, the hydroxyl compounds **117** ($t_{1/2}$= 33 min, Table 1) and **119** ($t_{1/2}$= 21 min), were more rapidly metabolized in HLS9 compared to the corresponding 5-Me inhibitors **92** ($t_{1/2}$= > 60 min) and **67** ($t_{1/2}$= 50 min), respectively. The rapid metabolism is expected due to their ability to undergo conjugation reactions by Phase II enzymes. Additional influence of the *ortho*- fluorine and hydroxyl group on half-life can be observed for compound **119**. The same effect was observed for the 5-OMe derivative, which is also susceptible towards rapid Phase II metabolism after ether cleavage in the liver. Introduction of an *ortho*-fluorine enhanced metabolism for the 5-OMe compound from over 60 min (**53**) to 19 min (**118**). Compounds **118** and **119** were metabolized twice as fast as metyrapone ($t_{1/2}$= 49 min). We selected inhibitor **118** for further biologically evaluation as it was 36-fold more potent than **119** at inhibiting CYP11B1. Compound **118** exhibited a long half-life in human plasma ($t_{1/2}$=> 150 min). This was expected, as no typical functional groups prone to plasma degradation are present in compound **118**.[110] Wound fluid and plasma have a comparable composition[108] and, therefore, **118** can be expected to be stable in wound fluid.
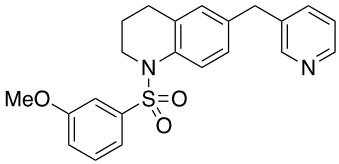
***Selectivity over human CYP17A1 and CYP19A*1.** Estrogens play a crucial role in the wound healing process. Therefore, enzymes which are essential for the biosynthesis of estrogens in skin such as CYP17A1 and CYP19A1 should not be influenced by compound **118**. Previously described assays for CYP17A1 and CYP19A1 inhibition were therefore performed with **118**.[87-89]

Due to the high CYP11B1 potency of **118** with an IC$_{50}$ value of 0.8 nM, a 2500-fold higher concentration (2 μM) was used to ensure no interference with this system. Compound **118** demonstrated no significant inhibition of both enzymes (CYP17A1, 5% at 2 μM; CYP19A1, 2% at 2 μM, Table 11) and, therefore, was considered inactive. In contrast, the previously discovered **114** inhibited CYP19A1 by 26% at 2 μM. Here, inhibitor **118** showed a clearly superior safety profile for CYP19A1 at higher concentrations.
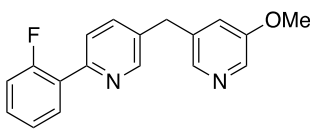
Table 11. Inhibition of CYP17A1, CYP19A1, 11β-HSD1 and 11β-HSD2 by metyrapone and compounds **114** and **118**.

Comp	CYP11B1	CYP17A1[b]	CYP19A1[c]	11β-HSD1[d]	11β-HSD2[e]
	IC$_{50}$	inhibition (%)			
	(nM)[a]	at 2 μM		at 200 μM	
metyrapone	15 ± 2	3 ± 3	0 ± 0	70 ± 6	n. i.
114	5 ± 0.7	10 ± 5	26 ± 2	IC$_{50}$ 1.62 ± 0.2 μM	n. i. at 10 μM
118	0.8 ± 0.2	5 ± 6	2 ± 3	48 ± 1	n. i.

[a]V79 hamster fibroblasts heterologously expressing human CYP11B1, substrate 11-deoxycorticosterone, 100 nM, mean ± SD, n≥ 2. [b]E. coli expressing human CYP17A1; substrate progesterone, 25 μM. mean ± SD, n≥ 2. [c]Human placental CYP19A1; substrate androstenedione, 500 nM. Inhibition values ≤10% are not significant, mean ± SD, n≥ 2. [d]Lysates of human embryonic kidney cells (HEK-293) transfected with human 11β-HSD1; substrate [1,2-^{3}H]-cortisone, 200 nM; n= 3, in triplicates; for IC$_{50}$ n= 3, independent measurements. [e]Lysates of HEK-293 cells transfected with human 11β-HSD2; substrate [1,2,6,7-^{3}H]-cortisol, 50 nM; a residual enzyme activity of more than 70% was considered as no inhibition. n. i., no inhibition.

Selectivity over human 11β-HSD1 and 11β-HSD2. It is unclear whether accelerated wound healing occurs from CYP11B1 or 11β-HSD1 inhibition. Therefore, 11β-HSD1 inhibitory activity was measured to ensure that compound **118** selectively inhibits CYP11B1. This was performed as previously described using lysates of stably transfected cell lines expressing 11β-HSD1.[111] Compound **118** exhibited 48% inhibition of 11β-HSD1 only at 200 μM (Table 11), which ensures selective inhibition of CYP11B1 at low concentrations due to the high inhibitory potency of **118** (IC$_{50}$ CYP11B1= 0.8 nM). In contrast, metyrapone and **114** showed much higher inhibition of 11β- HSD1 (metyrapone, 54% at 50 μM, 70% at 200 μM; **114**, IC$_{50}$ 11β-HSD1=

1.62 μM, Table 11). Inhibition of the transformation of cortisol to inactive cortisone by 11β-HSD2 should be avoided, as an additional cortisol reducing effect might be beneficial for wound healing. In a previously described assay,[111] compound **118** showed no inhibition at 200 μM and can be considered inactive (Table 11).

In vitro toxicity. Cytotoxicity of compound **118** was tested in a MTT reduction assay using normal human epidermal keratinocytes. After 72 h of incubation in the presence of up to 11 μM of **118**, no effect on cell viability was observed (87% cell viability at 11 μM). Therefore, no cytotoxic effect is expected at therapeutic concentrations due to the strong CYP11B1 inhibitory potency of compound **118** (IC_{50}= 0.8 nM). Mutagenic potential of **118** was evaluated using an AMES II mutagenicity assay containing TA98 and TA7001-TA7006 strains of *Salmonella typhimurium* in the presence or absence of rat liver S9 fractions. The inhibitor exhibited no mutagenic potential up to the highest tested concentration of 100 μM with or without metabolic activation.

Wound healing. The effect of compound **118** on wound healing was investigated in a human skin explant as described previously.[46, 112-113] In order to simulate acute wounds, 2 mm biopsy punches on the explants were performed. Subsequently, inhibitor **118** was topically applied once per day (5 μM, n= 3) over 3 days and the rate of re-epithelization was evaluated (Figure 15). Control skin explants showed progressively increased wound healing over 3 days (24 h, 13%; 48 h, 28%; 72 h, 100%). The newly epithelialized regions could be identified due to their typical morphological appearance, characterized by the presence of two or three cell layers of keratinocytes associated with a thin or absent stratum corneum layer. Topical application of compound **118** had no significant effect after 24 h (10% re-epithelialization). However, after 48 h, a 3-fold accelerated wound closure (89%) was observed compared to the control (28%). The effect was expected to be most pronounced after 48 h, since CYP11B1 expression is known to gradually increase during wound healing with a maximum after 2 days and drop to the control values at 72 h.[46] As seen in the control, re-epithelization was complete after 72 h. This clearly shows that a CYP11B1 inhibitor which is selective over 11β-HSD1 is able to accelerate wound healing at the applied concentration of 5 μM.
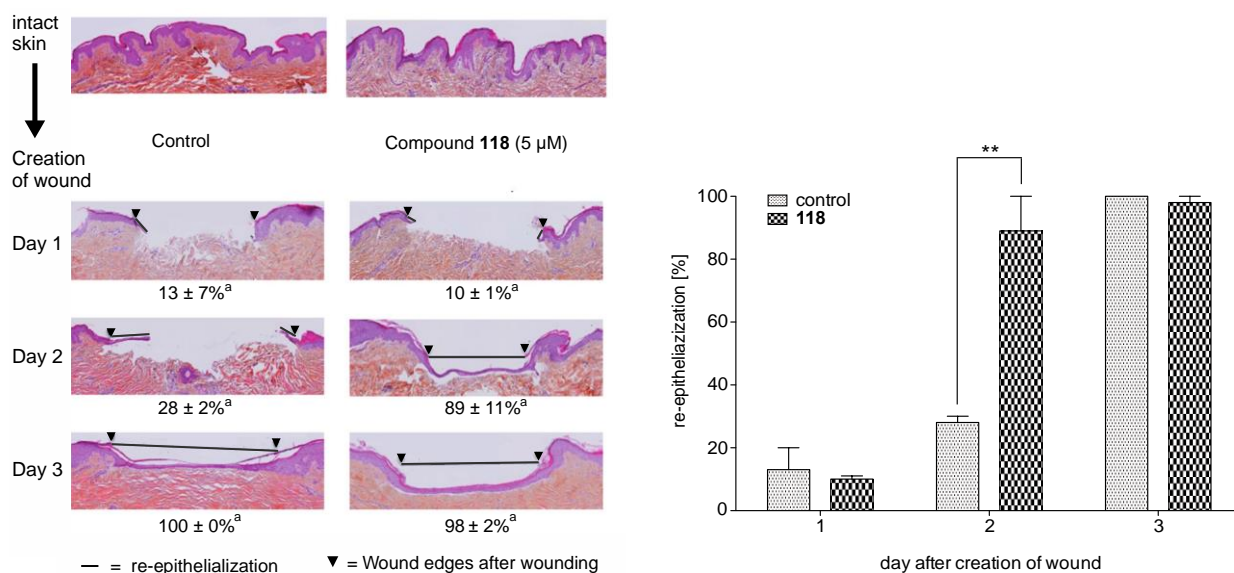
Figure 15. Acceleration of wound closure by **118** in *ex vivo* human skin experiment. [a]Percentage of re-epithelialization, mean ± SEM, n= 3; the inter-group comparisons were performed by an unpaired Student's t-test. [**]P= 0.001 to 0.01, very significant.

CONCLUSION

Chronic wounds cause an extensive period of suffering for patients and immense costs for the health care system.[96] Recently, it has been shown that inhibition of cortisol synthesis in skin resulted in accelerated wound healing.[46, 101] It remained unclear whether this effect occurs from the blockade of CYP11B1 or 11β-HSD1. In the current study, the previously described very potent CYP11B1 inhibitors **49**, **53**, **88**, **90** and **92** [Chapter 3.1[42], Chapter 3.2[104]] were optimized for topical application on wounds. Here, stability in plasma (comparable composition to wound fluid[107]) and rapid systemic clearance of absorbed compound are requirements to ensure safety and efficacy. An increase of metabolism in the HLS9 fractions was achieved by exchange of the 5-Me groups of **49** and **92** ($t_{1/2}$= > 60 min) by 5-OH substituents (**54**, **117**, $t_{1/2}$= 31-33 min). Introduction of an *ortho*-fluorine into the labile hydroxy compound **54** ($t_{1/2}$= 31 min) and the potent compound **53** ($t_{1/2}$> 60 min) further decreased the half-life (**118-119**; $t_{1/2}$= 19-21 min). In comparison to the CYP11B1 inhibitor metyrapone ($t_{1/2}$= 49 min), **118** and **119** were metabolized twice as fast and, therefore, exhibited the required reduced metabolic stability. Furthermore, compound **118** showed the highest CYP11B1 potency in this series (IC_{50}= 0.8 nM) and exceeds CYP11B1 inhibitors previously described for wound healing not only in potency (metyrapone, IC_{50}= 15 nM and **114**, IC_{50}= 5 nM), but also in selectivity over 11β-HSD1 (**118**, 48% at 200 μM; metyrapone, 54% at 50 μM; **114**, IC_{50}= 1.62 μM). This fact allowed the usage of **118** as a tool to study the effect on wound healing *via* selective blockade of CYP11B1-catalyzed cortisol synthesis. In addition, selectivity over CYP19A1 was also clearly improved (**118**, 2% at 2 μM; **114**, 26% at

62

2 μM) and **118** was stable in plasma, non-cytotoxic to human keratinocytes at >10 μM, and non-mutagenic. For the first time, it has been shown that a CYP11B1 inhibitor **118** is able to accelerate wound healing in human skin without affecting 11 β -HSD1 (proof of concept) at the applied concentration of 5 μM. Thus, compound **118** is a promising candidate for the treatment of chronic wounds and can be considered for further *in vivo* experiments.

4. Final Discussion

New medical treatments for Cushing's disease, characterized by abnormally high plasma cortisol levels, are urgently needed. CYP11B1 inhibitors in clinical use, which block the last step of cortisol biosynthesis, are effective due to the high response rates in affected patients (over 70%).[38-39] However, selectivity of these inhibitors over CYP11B2 and other steroidogenic or hepatic CYP enzymes has to be increased to avoid related severe side effects (see chapter 1.5.3.). Starting from the known CYP11B1 inhibitor etomidate, the novel compounds **3** and **4** (Table 12) were identified.[41-43] They exceeded known inhibitors regarding selectivity over CYP11B2 and exhibited no or minor inhibition of CYP17A1 and CYP19A1 (Table 12). In contrast, human CYP11B1 inhibitory potency still needs to be improved in order to reduce the administration dose, thus lowering the risks of off-target effects. Furthermore, the compounds showed no inhibition of rat CYP11B1, which is a prerequisite for a proof of concept study in rats.[42]

Table 12. Inhibition of human CYP11B1 and CYP11B2 by clinically used and reported inhibitors.

| Comp | IC$_{50}$ (nM)^{a,b} | | SF^c | Inhibition (%)^d | |
	CYP11B1	CYP11B2		CYP17A1^e	CYP19A1^f
3	107	1422	13	2	0
4	68	656	10	2	24
metyrapone	15	72	4.8	3	0
osilodrostat	3	0.2	0.07	n. d.	n. d.
ketoconazole	127	67	0.5	IC$_{50}$= 2.78 μM	0^g
etomidate	0.5	0.1	0.5	1	0^g

^{a}Mean value of at least two experiments. The deviations were < 25%. ^{b}Hamster fibroblasts expressing human CYP11B1 or CYP11B2; substrate 11-deoxycorticosterone, 100 nM. ^{c}SF: IC$_{50}$ CYP11B2 / IC$_{50}$ CYP11B1. ^{d}Compound concentration 2 μM. Inhibition ≤ 10 % is not significant. ^{e}*E. coli* expressing human CYP17A1; substrate progesterone, 25 μM. ^{f}Human placental CYP19A1; substrate androstenedione, 500 nM. ^{g}Compound concentration 0.5 μM. n. d., not determined.

To overcome these drawbacks, further structural optimization of this compound class was performed in the course of the present thesis. In this final discussion, only those structural changes are reviewed that had a pronounced impact on the human CYP11B1 inhibitory potency and selectivity. The hitherto most selective and potent CYP11B1 inhibitor **3** (IC_{50}= 107 nM, SF (IC_{50} CYP11B2/ IC_{50} CYP11B1)= 13, no significant inhibition of CYP17A1 and CYP19A1, Chart 5) was an appropriate lead structure for further development. Previous studies with this compound class (see chapter 1.5.4.) revealed the importance of the central pyridine ring for selectivity towards CYP17A1 and CYP19A1. Concluding that electronic and steric properties of the central core strongly influence CYP11B1 inhibitory activity and selectivity, the impact of a second nitrogen in the ring system was further investigated (Chart 5). Hence, the pyridine moiety was replaced by pyridazine (→**38**), pyrazine (→**39**) and pyrimidine (→**40**), with the first nitrogen remaining at the same position as in compound **3**. The additional electron-withdrawing effect probably altered the electrostatic potential of the whole molecule, which resulted in a drop of CYP11B1 potency (IC_{50}= 610-1711 nM). This indicates that π-electron rich central cores containing one nitrogen are needed for CYP11B1 potency and selectivity. Previously discovered potent thiophene and furan derivatives are π-electron rich and exhibit a different molecular geometry. To balance the observed loss of selectivity of these inhibitors, several azoles differing in electronic and steric properties were introduced into lead compound **3**, retaining the nitrogen in the same position (Chart 5). Indeed, the 3,5-substituted pyridine isostere isothiazole **80** showed an 8-fold increase of CYP11B1 potency and a moderate selectivity towards CYP11B2 (IC_{50}= 14 nM, SF= 9). On the contrary, bioisostere selenazole **85** showed no improvement of CYP11B1 potency (IC_{50}= 104 nM). In case of the more electron-poor and less bulky oxazole **83** and isoxazole **84**, a loss of CYP11B1 potency and selectivity was obtained (IC_{50}= 148-150 nM, SF= 4-9). Interestingly, the less selective *N*-methylated pyrazole **87** exhibited moderate inhibition of CYP11B1 (IC_{50}= 58 nM), whereas Me-imidazole **86** was less tolerated by the enzyme (IC_{50}= 516 nM). Compound **3** was used for further optimizations as it still shows the highest selectivity over CYP11B2 within this series.

In another study of a similar compound class, the introduction of alkyl or aromatic substituents onto the methylene bridge resulted in the potent and selective CYP11B1 inhibitor **5** (Chart 5, IC_{50}= 2 nM, SF= 11).[60] The same modifications were performed on the current scaffold expecting an increase of CYP11B1 potency and selectivity (Chart 5). In fact, strongly enhanced CYP11B1 inhibition was achieved by introduction of alkyl substituents (**20-23**, IC_{50}= 12-33 nM). Due to the trend observed when comparing CYP11B1 potency and bulkiness of the substituents (Me (IC_{50}= 33 nM) < Et (IC_{50}= 28 nM) < *c*-prop (IC_{50}= 21 nM) < *i*-prop (IC_{50}= 12 nM)), it was assumed that

a hydrophobic pocket near the heme was occupied. However, introduction of furan-2-yl only slightly increased CYP11B1 potency (**24,** IC$_{50}$= 69 nM), whereas the phenyl substituent caused a loss of activity (**25,** IC$_{50}$= 124 nM) compared to **3** (IC$_{50}$= 107 nM). In contrast to the previously described compound class of **5**, selectivity towards CYP11B2 was strongly reduced upon these modifications (SF= 0.9-6.1). Thus, alterations of the central pyridine core and the methylene bridge resulted in some more potent but less selective compounds (Chart 5).

Chart 5. Lead optimization of **3** to improve CYP11B1 potency and selectivity.
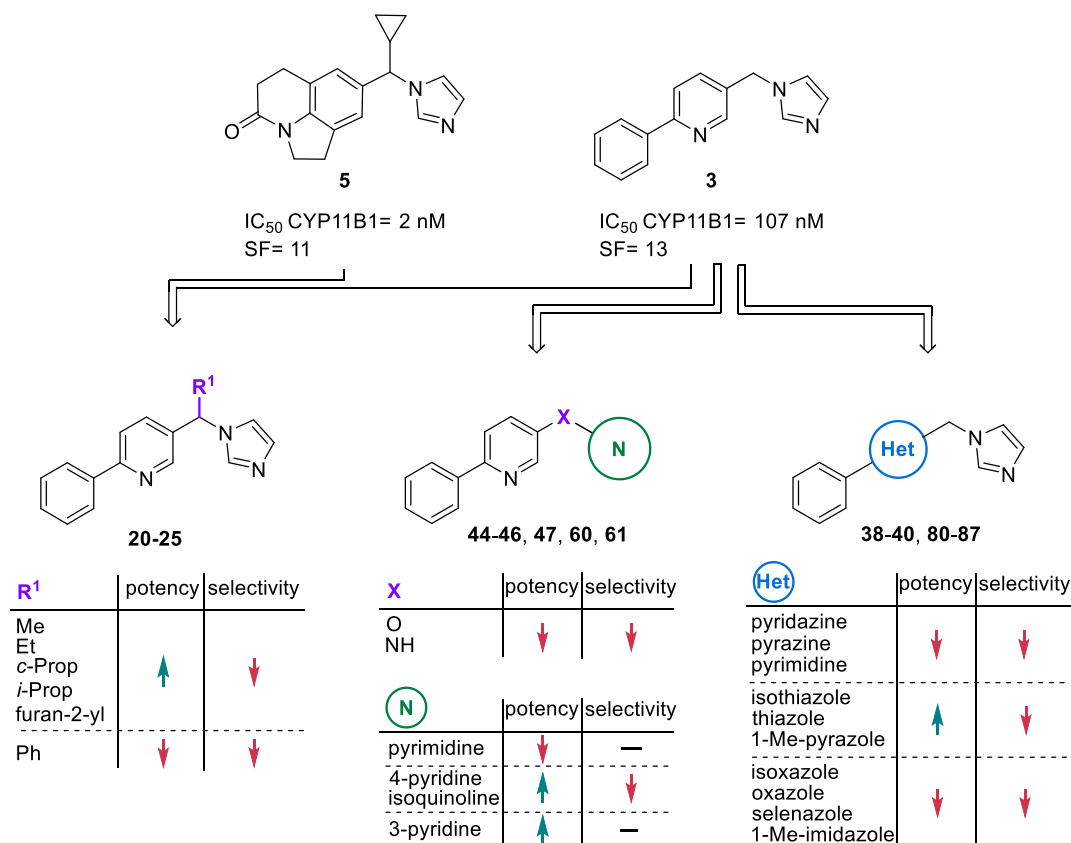
Subsequently, the imidazolyl of **3** (IC$_{50}$= 107 nM, SF = 13) was replaced by several heterocycles containing an sp^2-hybridized nitrogen, as it probably coordinates to the heme complex within the CYP enzyme and, therefore, is essential for affinity (Chart 5).[31] Introduction of pyrimidinyl (→**47**) resulted in a loss of CYP11B1 potency (IC$_{50}$= 240 nM), which is likely caused by the electron-withdrawing effect of the second nitrogen associated with reduced electron density on the heme-coordinating nitrogen. Exchange of imidazolyl by 4-pyridinyl resulted in the similarly potent but less selective inhibitor **45** (IC$_{50}$= 98 nM, SF= 6.4). In contrast, 3-pyridine **44** showed a 3.3-fold increase of CYP11B1 potency with almost complete retention of selectivity towards CYP11B2 (IC$_{50}$= 32 nM, SF= 10). The influence of the methylene bridge was further investigated for this compound. Isosteric exchange of -CH$_2$- in **44** by -O- (→**60**) or -NH- (→**61**) resulted in a

strong drop of inhibitory activity (IC_{50}= 1015 nM and > 5000 nM, respectively). This is in line with the finding that introduction of lipophilic alkyl groups to the methylene bridge of **3** led to an increase of CYP11B1 potency. Polar moieties are probably not tolerated as there is a hydrophobic region around the bridge. Annulation of the 3-pyridine to isoquinoline (→**46**) enhanced CYP11B1 inhibition by 18-fold compared to **3**, but resulted in a loss of selectivity (IC_{50}= 6 nM, SF= 4.2). Therefore, the influence of substitution of **44** was further investigated (Chart 6). Substituents differing in their steric and electronic properties and H-bond acceptor and donor characteristics were introduced. In analogy to pyrimidine **47** (IC_{50}= 240 nM), electron-withdrawing effects caused by 5-$CONH_2$ (→**50**) and 5-F (→**51**) strongly decreased CYP11B1 potency (IC_{50}= 125-427 nM) compared to **44** (IC_{50}= 32 nM). Interestingly, the lipophilic and electron-deficient 5-CF_3 derivative **52** exhibited a similar CYP11B1 potency but a reduced selectivity towards CYP11B2 (IC_{50}= 38 nM, SF = 3.0). As expected, electron-rich groups such as 5-OMe (→**53**) and bulky 5-Ph (→**57**) strongly enhanced CYP11B1 inhibitory activity by 6.4 to 25-fold. In case of the 5-Ph substituent, this might as well be caused by occupying an additional hydrophobic pocket near the heme. However, enhanced inhibition of both enzymes was observed (SF= 0.4-5.1). In contrast, the polar electron- and H-bond-donating substituent 5-OH improved selectivity for CYP11B1 but likewise caused a loss of potency (**54**, IC_{50}= 51 nM, SF= 16). Introduction of the lipophilic and electron-donating 5-Me substituent (→**49**) resulted in the most potent and selective inhibitor of this series (Chart 6, IC_{50}= 2 nM, SF = 17). The same modification in 4-position improved the inhibitory potency for both enzymes (**48**, IC_{50}= 8 nM, SF= 2.4). In summary, exchange of the imidazolyl of **3** (IC_{50}= 107 nM, SF = 13) by 5-Me-pyridin-3-yl resulted in **49** showing an 54-fold increase of CYP11B1 potency and selectivities over steroidogenic CYP11B2 (SF= 17), CYP17A1 (5% inhibition at 2 μM), and CYP19A1 (1% inhibition at 2 μM) as well as hepatic CYP2A6 (IC_{50}= 106 μM) and CYP3A4 (IC_{50}= 1.1 μM). Further, the inhibitor showed metabolic stability toward human and rat liver S9 fraction ($t_{1/2}$= > 150 min and 16 min, respectively), negligible cytotoxicity and the desired enhanced inhibition of the rat CYP11B1 enzyme (IC_{50}= 2.4 μM) compared to **3** (IC_{50}= > 10 μM). Due to the promising *in vitro* profile of **49**, a pharmacokinetic study in rat was conducted. There, very low oral bioavailability was observed (F= 2%), and in addition, the compound exhibited promutagenic potential in an AMES test using TA98 strains of *Salmonella typhimurium*. As compound **49** was identified as a poor candidate for preclinical development, further structural optimization was necessary to obtain other candidates for *in vivo* studies (Chart 6). Low bioavailability can be caused, inter alia, by poor aqueous solubility and low permeability. To balance both properties, inhibitor **49**, which exhibited a calculated log D (pH= 7.4) value of 3.7, was modified to obtain more polar derivatives.

Chart 6. Optimization of **44** to improve CYP11B1 potency and selectivity.

44
IC$_{50}$ CYP11B1= 32 nM
SF= 10

48-57

R^3	potency	selectivity
CONH$_2$		
F		
CF$_3$	↓	↓
OH		
OMe	↑	↓
Ph		
Me	↑	↑

49
IC$_{50}$ CYP11B1= 2 nM
SF= 17

Drawbacks:
- Oral bioavailability in rat = 2%
- Promutagen

R^2	potency	selectivity
2-F-Ph		
3-NHSO$_2$Me-Ph		
furan-3-yl		
PhS		
2-F-PhS		
PhSO$_2$	↓	↓
2-F-PhSO$_2$		
1-Me-1-H-pyrazol-4-yl		
1-Me-1-H-pyrazol-5-yl		
cyclopropylamine		
morpholin-4-yl		

67-77

79-90, 93

Het	potency	selectivity
thiazole		
oxazole	↓	↓
pyrazole		
isothiazole	↑	↓
1-Me-pyrazole		
isoxazole	↑	↑

90
IC$_{50}$ CYP11B1= 5 nM
SF= 16

91
IC$_{50}$ CYP11B1= 2 nM
SF= 14

However, CYP11B1 potency and selectivity was to be retained. Previously conducted extensive structure activity relationship studies in the imidazolyl compound class of **3** revealed that substitution of the phenyl moiety with polar 3-NH$_2$ resulted in a potent and selective CYP11B1 inhibitor. As this structural motif is likely to cause toxicity (carcinogenicity) and to vary several molecular properties, other hydrophilic groups differing in size and electronic characteristics such as pyrazoles (→**70** and **71**), *N*-phenylmethanesulfonamide (→**68**) or polar non-aromatic cycles (→**72** and **73**) were introduced to **49**. Further, the phenyl moiety of **49** was replaced by 2-F-Ph (→**67**) and furan-3-yl (→**69**), as both derivatives in the imidazolyl class showed good CYP11B1 potency and selectivity. In the current thesis, it was demonstrated that electronic properties and molecular geometry strongly influence CYP11B1 potency and selectivity. Therefore, heteroatom linkers such as -S- (→**74** and **76**) and -SO$_2$- (→**75** and **77**) were introduced between the central pyridine and the phenyl substituents. Many of the thereby obtained derivatives (**67**-**69**, **73**-**74**, **76**-**77**) differing in polarity, electronic properties and size exhibited similar CYP11B1 inhibitory activity (IC$_{50}$= 2-5 nM), but selectivity towards CYP11B2 was not retained (SF= 6-9). A clear

trend within the novel synthesized inhibitors (**67-77**) was not identified. To further investigate the influence of the molecular shape and electronic properties, the central pyridine core was replaced by similar azoles as for the imidazolyl class before. Interestingly, isothiazole **81**, isoxazole **90** and 1-Me-pyrazole **92** exhibited similar CYP11B1 inhibitory activities (IC$_{50}$= 1-5 nM), but only the isoxazole retained selectivity towards CYP11B2 (SF= 16) compared to **49** (IC$_{50}$= 2 nM, SF= 17). Deprotection of the pyrazole (→**93**) resulted in a strong loss of CYP11B1 potency (IC$_{50}$= 137 nM) indicating that a hydrogen bond donor in this position is not well tolerated. As described previously, substitution of the 3-pyridine core with electron-donating moieties increased CYP11B1 potency. Replacement of the 5-Me-pyridin-3-yl of isoxazole **90** to 5-OMe-pyridin-3-yl (→**91**) resulted in a similarly potent and selective derivative (IC$_{50}$= 2 nM, SF= 14). Thus, the two novel, potent and selective compounds **90** and **91** (IC$_{50}$= 2-5 nM, SF= 14-16), which differ in their structure and, therefore, physicochemical properties from **49** were obtained. They exceed inhibitors on the market such as metyrapone (IC$_{50}$= 15 nM, SF= 4.8) and ketoconazole (IC$_{50}$= 127 nM, SF= 0.5) in terms of CYP11B1 potency and selectivity towards CYP11B2. Further, the compounds are similarly potent and much more selective than osilodrostat (IC$_{50}$= 3 nM, SF= 0.07), which is currently undergoing a phase III clinical trial. Inhibitors **90** and **91** demonstrated an enhanced rat CYP11B1 inhibition (IC$_{50}$= 1.8-4 μM) and selectivities over steroidogenic (CYP17A1 and CYP19A1, ≤9% at 2 μM) and hepatic CYP enzymes (CYP1A1, CYP2B6, CYP2C19, CYP2D6 and CYP3A4, see chapter 3.2. for values). Both compounds are stable towards human liver S9 fraction (t$_{1/2}$= 125-145 min) and exhibited enhanced metabolic stability in rat liver S9 fraction (t$_{1/2}$= 23-30 min) compared to **49** (t$_{1/2}$= 16 min). *In vitro* tests for cytotoxicity, cardiotoxicity or induction of hepatic CYP enzymes such as CYP1A1 and CYP1A2 were performed and both compounds showed a satisfying profile (for further details see chapter 3.2.). Most importantly, the compounds exhibited no mutagenic potential in the AMES II test up to the highest tested concentration of 100 μM, with or without metabolic activation, in contrast to **49**. The inhibitors were expected to show an improved pharmacokinetic profile in rats as the calculated log D values (pH=7.4) were reduced (3.7 for **49**; 3.1 for **90**; 2.8 for **91**). Thus, balance between permeability and solubility under *in vivo* conditions should be improved. Indeed, the compounds exhibited a good aqueous solubility (> 200 μM). Plasma concentrations of **90** and **91** in rats were evaluated after perorally administration of 100 mg/kg (single dose) per inhibitor. Only **91** demonstrated sufficiently high plasma concentration (1 h, 19.7 μM; 4 h, 106.4 μM) for therapeutic effect in rats on the basis of the *in vitro* assay (IC$_{50}$ CYP11B1 in rat= 1.8 μM). Subsequently performed pharmacokinetic study in rats revealed a significantly improved oral bioavailability of **91** (F= 50%) compared to **49** (F= 2%). Summarized, successful, rational lead optimization of CYP11B1 inhibitor **3** (IC$_{50}$= 107 nM) resulted in a novel selective compound **91** exhibiting a 54-fold

70

improved potency for human CYP11B1 (IC_{50}= 2 nM) and enhanced inhibition of the rat enzyme (**91**, IC_{50}= 1.8 µM; **3**, IC_{50}= >10 µM). Inhibitor **91** demonstrated a good *in vitro* pharmacological profile and high oral bioavailability in rats (F=50%). Thus, an excellent candidate for further *in vivo* studies was obtained.

Besides the application of CYP11B1 inhibitors in Cushing's disease, they could be used for the treatment of chronic wounds, which are an enormous burden for the patients and cause immense costs for the health care system. It was demonstrated that cortisol levels are elevated in acute and chronic wounds of human skin. Topical application of high concentrations of the CYP11B1 inhibitor metyrapone (1 mM) resulted in acceleration of wound healing in human (*ex vivo*) and porcine skin (*in vivo*). Further investigations are necessary, as metyrapone not only blocks CYP11B1 but also 11β-HSD1 at high concentrations (54% at 50 µM), impeding a clear identification of the mode of action. Inhibitors developed in the present thesis are not appropriate for topical application as they likely cause systemic side effects due to their metabolic stability ($t_{1/2}$= > 60 min in HLS9). Metyrapone as well exhibits a relatively long half-life of 49 min. Fast resorption of the compounds was expected due to the not well-defined application site (injured skin and intact skin) of wounds. Therefore, potential candidates for a proof-of-concept study have to be rapidly cleared after absorption and exhibit selectivity over 11β-HSD1. Another key prerequisite is the stability of the compounds towards human plasma as a substitute for wound fluid. Replacement of the 5-Me in compound **49** for a metabolically labile group such as 5-OH, which is able to undergo conjugation reactions by Phase II enzymes, caused, as expected, a reduced half-life in HLS9 (→**54**, $t_{1/2}$= 31 min). However, inhibitory potency for CYP11B1 was decreased by 26-fold (**54**, IC_{50}= 51 nM). The same modifications were performed for the very potent CYP11B1 inhibitors **88**, **90** and **92** differing in their molecular geometry and electronic properties with the aim to obtain metabolically labile but potent inhibitors. Loss of CYP11B1 potency was observed as well (9-26-fold). Nevertheless, compound **117** still exhibited an inhibitory activity below 20 nM (IC_{50}= 17 nM) and the desired reduced half-life in HLS9 ($t_{1/2}$= 33 min). Interestingly, introduction of an *ortho*-fluorine to the phenyl substituent of **49** caused a slightly reduced metabolic stability (→**67**, $t_{1/2}$= 50 min) with negligible effects on CYP11B1 potency (IC_{50}= 3 nM). For further investigation of this effect, *ortho*-fluorine was also introduced to the labile, 5-OH-substituted compound **54** and the very potent 5-OMe derivative **53**. Indeed, in both cases, a decreased metabolic stability was obtained (→**118** and **119**, $t_{1/2}$= 19-21 min), whereas CYP11B1 potency was even enhanced by 6 or 2-fold, respectively (**118**, IC_{50}= 0.8 nM; **119**, IC_{50}= 29 nM). Only inhibitor **118** was further evaluated, as it exhibited the highest CYP11B1 potency of this series (Figure 16, 21-36-fold more potent than **117** and **119**).
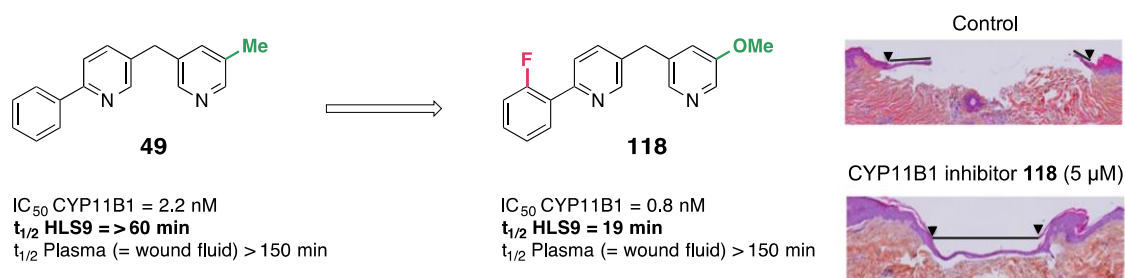
Figure 16. Optimization of CYP11B1 inhibitors for wound healing.

The compound is expected to be stable in wound fluid as it demonstrated a long half-life in human plasma ($t_{1/2}$= >150 min). Importantly, it showed enhanced selectivity towards 11β-HSD1 (48% inhibition at 200 μM) in comparison with metyrapone (70% inhibition at 200 μM and 54% at 50 μM). The inhibitor is selective towards CYP17A1 and CYP19A1 as well. This is important, as those enzymes are catalyzing the biosynthesis of estrogens, which play a crucial role in the wound healing process. Selectivity over CYP11B2 was not required for dermal application as the enzyme has not been identified in human skin. No cytotoxicity in human keratinocytes was observed up to a concentration of 11 μM of **118**. In contrast to the structurally similar derivative **49**, compound **118** exhibited no mutagenic potential up to a concentration of 100 μM with or without metabolic activation. The inhibitor showed the desired *in vitro* pharmacological profile and was a suitable candidate for a proof-of-concept study. For the first time, acceleration of wound healing in human skin (*ex vivo*) was demonstrated at a low applied concentration of 5 μM without affecting 11β-HSD1 (Figure 16). This clearly shows the potential of selective CYP11B1 inhibitors for the treatment of chronic wounds.

5. Outlook

Lead optimization of CYP11B1 inhibitor **3** (IC$_{50}$= 107 nM, SF= 13) for the treatment of Cushing's syndrome resulted in the novel compound **91** exhibiting a 54-fold improved potency for human CYP11B1 (IC$_{50}$= 2 nM), a good *in vitro* pharmacological profile and a high oral bioavailability in rats (F=50%). To enhance the therapeutic window and reduce possible side effects, improvement of selectivity towards CYP11B2 is still an issue. Further, other structurally different candidates are needed in case **91** fails in the upcoming *in vivo* studies in rats and other species. The central pyridine was replaced by several azoles differing in electronic properties and molecular geometry. Depending on the central core, strong influences on CYP11B1 potency and selectivity were obtained. So far, replacement of the central pyridine core by *N*-substituted or unprotected pyrrol was not successful, which likely has a significant impact on the enzyme as well. Further synthetic routes or purification methods of the final product have to be investigated.

Chart 7. Recently published selective CYP11B1 inhibitors and possible examples to be synthesized.
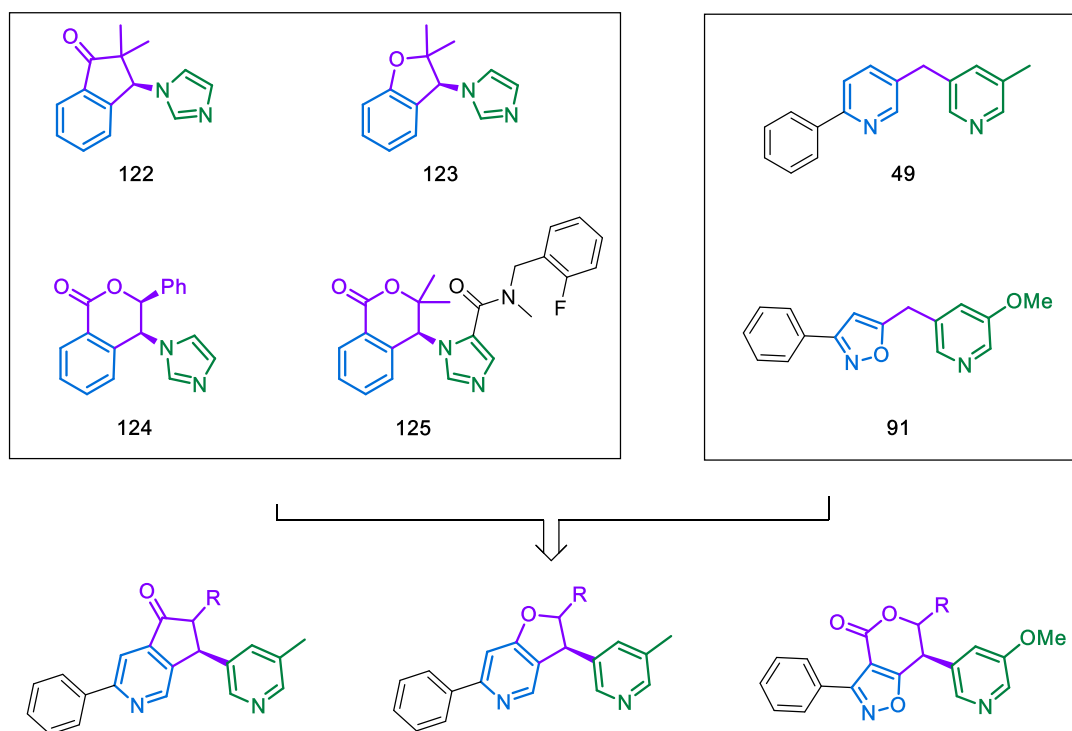
As substitution or exchange of the methylene bridge resulted in significant changes of CYP11B1 potency and selectivity, prolongation (e.g. CH$_2$CH$_2$) or removal of the linker should be studied. In addition, based on the observed SAR of the current compound class, a hydrophobic protein region near the methylene bridge was assumed (see chapter 3.1). Thus, substitution of the hydrogens by

fluorine, which is known to increase the lipophilicity, could have a strong impact on CYP11B1 inhibition. Recently, rigidification of the linker (derivatives **122**-**125**, Chart 7) was demonstrated to be beneficial for CYP11B1 selectivity.[114] Similar modifications can be applied to inhibitors **91** and **49** as exemplified in Chart 7.

In terms of the wound-healing project, the metabolite of the tested inhibitor **118** has to be identified, synthesized and evaluated regarding toxicity and selectivity to exclude undesired side effects. The dose dependency of **118** in comparison to metyrapone for the acceleration of wound healing in human skin (*ex vivo*) has to be investigated. Afterwards, inhibitor **118** can be tested for skin wound healing in other species such as pig or monkey (*in vivo*).

6. General Experimental Details

Biological Test Procedures

Inhibition of CYP11B1 and CYP11B2. V79MZh cells expressing human or rat CYP11B1 or CYP11B2 were incubated with [1,2-^{3}H]-11-deoxycorticosterone (100 nM) as the substrate and inhibitor at different concentrations. The assay was performed as previously described.[109, 115]

CYP17A1 Preparation and Assay. Human CYP17A1 was expressed in *E. coli* (coexpressing human CYP17 and rat NADPH-P450 reductase), and the assay was performed using the method previously described with progesterone (25 μM) as the substrate and NADPH as the cofactor.[87-88]

CYP19A1 Preparation and Assay. Human CYP19A1 was obtained from microsomal preparations of human placenta, and the assay was performed using the ^{3}H$_2$O-method as previously described with [1β-^{3}H]androstenedione (500 nM) as substrate and fadrozole and aminoglutethimid as references.[89]

11β-HSD1 and 11β-HSD2 Preparation and Assay. Lysates of human embryonic kidney cells (HEK-293) transfected with human 11β-HSD1 were incubated with [1,2-^{3}H]-cortisone (200 nM) as the substrate and NADPH (500 μM) as the cofactor. A similar procedure was used in case of 11β-HSD2, but using [1,2,6,7-^{3}H]-cortisol (50 nM) as the substrate and NAD$^+$ (500 μM) as the cofactor. The assay was performed using glycyrrhetinic acid as positive control and as previously described.[111]

CYP2A6 and CYP3A4 Assay of 49. The inhibition of CYP2A6 was determined using the CYP2A6/coumarin inhibitor screening kit (BD Gentest) with coumarin (3 μM) as the substrate. Similarly, the inhibition of CYP3A4 was determined using the CYP3A4/BFC inhibitor screening kit (BD Gentest) with 7-benzyloxy-trifluorome-thylcoumarin (50 μM) as the substrate. Both assays were performed according to the manufacturer's instruction.

Human Hepatic CYP Enzyme Assays of 90 and 91. The inhibition of hepatic CYP enzymes CYP1A2, CYP2B6, CYP2C9, CYP2C19, CYP2D6 and CYP3A4 was determined in microsomes

of baculovirus-infected insect cells expressing the recombinant human enzyme according to the manufacturer's instruction (BD Gentest).

Metabolic Stability Tests in Human and Rat Liver S9 Fraction. For the evaluation of Phase I and II metabolic stability, the compound (1 μM) was incubated with 1 mg/mL pooled mammalian liver S9 fraction (BD Gentest), 2 mM NADPH regenerating system, 1 mM UDPGA, and 0.1 mM PAPS at 37 °C for 0, 5, 15, and 60 min. The incubation was stopped by precipitation of S9 enzymes with 2 volumes of cold acetonitrile containing an internal standard. Concentration of the remaining test compound at the different time points was analyzed by LC-MS/MS and used to determine half−life ($t_{1/2}$) and intrinsic clearance (CL_{int}).

Metabolic Stability Tests in Human and Rat Plasma. For the evaluation of mammalian plasma stability, the compound (1 μM) was incubated with mammalian plasma (pooled, heparinized) of the indicated species at 37 °C for 0, 10, 30, 60, and 150 min. The incubation was stopped by precipitation of plasma proteins with 5 volumes of cold acetonitrile containing an internal standard, and the remaining compound concentration was analyzed by LC-MS/MS.

Cytotoxicity Assay. HEK 293 cells (2×10^5 cells per well) were seeded in 24-well flat-bottom plates. Culturing of cells, incubations, and OD measurements were performed as described previously[116] with minor modifications. 4 or 24 h after seeding the cells, the incubation was started by addition of the compounds in a final DMSO concentration of 1%. Fluorescence was measured in a BMG Labtech Pherastar FS reader. The decrease in fluorescence (at 570 nm) in the presence of the test compound compared to the fluorescence in the presence of the vehicle control (1% DMSO) was determined after 24 or 66 h followed by the calculation of LC_{50} or IC_{20} values using GraphPad Prism curve fitting.

For compound **118**: normal human epidermal keratinocytes were incubated with MTT reduced in blue formazan crystals by mitochondrial enzymes. This reduction is proportional to the enzymes activity. After cell dissociation and formazan crystal solubilisation using DMSO, the optical density of the extracts at 540 nm, which is proportional to the number of living cells and their metabolic activity, was recorded with a microplate reader (VERSAmax, Molecular Devices). The decrease in fluorescence (at 540 nm) in the presence of the test compound compared to the fluorescence in the presence of the vehicle control (1% DMSO) was determined after 72 h.

Mutagenicity Testing. Compound **49** was tested at Cerep in the Cerep's AMES fluctuation assay (according to manufacturer's instruction) containing TA98, TA1537 (frameshift mutation) and

TA100 as well as TA1535 (base-pair substitution) strains of *Salmonella typhimurium* in the presence or absence of rat liver S9 fraction. The Cerep's AMES fluctation assay is equivalent to the AMES II mutagenicity assay. Thereby, **49** was identified as a promutagen in TA98 strain in the presence of rat liver S9 fraction for compound concentrations of 5-100 µM.

Mutagenic potential of **90, 91** and **118** was evaluated using Xenometrix AMES II mutagenicity assay kit containing TA98 and TA7001−TA7006 strains of Salmonella typhimurium in the presence or absence of rat liver S9 fraction according to the manufacturer's instruction.

HERG Cardiotoxicity Evaluation. Compound **91** was tested using the predictor[TM] hERG fluorescence polarization assay kit (Invitrogen) according to the manufacturer's instruction. The high-affinity hERG ligands quinidine and E-4031 were used as positive controls and atenolol served as the negative control. Controls and the tested compound were incubated for 3.5 hours.

Aryl Hydrocarbon Receptor Assay. The aryl hydrocarbon receptor agonistic activity of compounds was determined in a human hepatocellular carcinoma cell line (HepG2) by measuring the CYP1A1 activity. Cells were split on a 24 well plate (each compound in quadruplicate) and incubated for 16-24 hours before compounds or vehicle were added to a final DMSO concentration of 0.1%. After 48 hours of incubation with the compound (3.16 µM) or vehicle, cells were washed with 1 mL of warm PBS (37 °C). Then, 500 µL of 3-cyano-7-ethoxycoumarin (CEC, specific CYP1A1 substrate), which forms a fluorescent product, was added to the cells at a final concentration of 40 µM in DME medium with 10% fetal calf serum + 1% penicillin + streptomycin (37 °C). After an incubation of 30 minutes, fluorescence was measured in the BMG Labtech Clariostar reader (excitation: 409 nm; emission 460 nm). The increase in fluorescence induced by the test compound was expressed relative to the increase induced by the reference compound, omeprazole (50 µM).

Solubility Determination. Aqueous solubility was evaluated as previously described[117]. Briefly, final concentrations of 5, 15, 50, 100 and 200 µM of **90** and **91** in an aqueous solution containing 2% DMSO were prepared and the solution clarity and potential compound precipitation were determined after 1 h and 24 h at room temperature (19-24 °C).

Pharmacokinetic Study of 49 in Rats. A pharmacokinetic study in rats was conducted to ensure that a scaffold like **49** is capable to enter the systemic circulation with sufficiently high plasma concentrations for a therapeutic effect after peroral application. All animal procedures were performed in accordance with the Guide for the Care and Use of Laboratory Animals. The

pharmacokinetic study of **49** was performed by Pharmacelsus using male Sprague-Dawley rats (body weight 250–350 g). Animals were maintained in a 12 h light/12 h dark cycle and housed in a separate temperature-controlled room (20-24°C). The test compound was administered at 1 mg/kg (n= 2, intravenously) or 2 mg/kg (n= 3, perorally) in a mixture of ethanol, PEG300 and water (10:60:30). Blood was sampled predose and after 15, 30, 60 minutes and 2, 4, 6, 8 and 24 hours via a catheter in the jugular vein (inserted 2-3 days prior to blood sampling). Until analysis, the obtained plasma samples were stored at -20 °C. Mean key pharmacokinetic parameters were estimated by noncompartmental analysis using the computer software Kinetica 5.0.

In Vivo **Rat Pharmacokinetics of 90 and 91.** All animal procedures were approved by the local government animal care committee and performed in accordance with the Guide for the Care and Use of Laboratory Animals. Pharmacokinetic analysis of **90** and **91** was conducted on female Sprague-Dawley rats (body weight 244–299 g) purchased from Charles River Laboratory (Sulzfeld, Germany). After an acclimatization period of 1 week, compounds were administered orally at a dose of 100 mg/kg (1 animal) or 28 mg/kg (2 animals) and intravenously at a dose of 5 mg/kg (2 animals). For oral administration, suspensions of the inhibitors in 0.5% porcine gelatin/5% mannitol (w/w) in water were freshly prepared followed by 15 min sonication 60-90 min before administration. For i.v. administration, **91** was dissolved in PEG300/ethanol/water (60/10/30). Before i.v. application (1 mL solution/kg body weight) and oral application (4 mL suspension/kg body weight), rats were anesthetized with 2% isoflurane. Blood samples (50 µL) were taken from the tail vein and collected in 0.2 mL Eppendorf tubes containing 5 µL of 106 mM sodium citrate buffer. After centrifugation at 5000 rpm at 4 °C, the plasma samples were first frozen at -20 °C and stored at -80 °C within 24 h. For bioanalysis, plasma samples were thawed and 10 µL of plasma were added to 50 µL of acetonitrile containing diphenhydramine (750 nM) as internal standard. Samples and calibration standards (in rat plasma) were centrifuged at 2400 xg for 5 min at 4 °C. The solutions were transferred to fresh vials for HPLC-MS/MS analysis (Accucore RP-MS, TSQ Quantum triple quadrupole mass spectrometer, electrospray interface). After injection of 10 µL (performed in duplicate), data were analyzed based on the ratio of the peak areas of analyte and internal standard. Mean key pharmacokinetic parameters were estimated by non-compartmental analysis using the computer software Phoenix WinNonlin. Cmax and Tmax were obtained directly from the plasma concentration-time curve. All other parameters ($t_{1/2}$, Vdss, CL, AUC and F) were calculated.

3D-QSAR Study. Ligands were built and energy minimized in the MMFF94s force field with MOE before being aligned using the flexible alignment module. Among the top three solutions,

78

which showed similar average strain energy (dU < 0.03), the one with the highest similarity (dF = 0.0000) was selected as the final alignment. The aligned compounds were subsequently imported into Open3DQSAR, where a grid box around the molecules with a 0.5 Å step size and a 5.0 Å margin was set up. Molecular interaction fields regarding steric factors and electrostatic potential were then calculated. After importing the corresponding activity data, compounds 17, 35, 41, 44, and 46 were assigned to the test set, while the rest of the compounds were employed as the training set. The MIF parameters were pretreated with zeroing (level = 0.05), max/min cutoff (level = ±30), standard deviation cutoff, N-level variable elimination and block unscaled weighting before regression with pIC_{50} data using partial least-squares analysis (PLS). The model was further improved with variable selection procedures using smart region definition (SRD) and fractional factorial design (FFD) methods. It was subsequently cross-validated using the leave-many-out paradigm and challenged with the test set compounds. The PLS pseudocoefficient contour maps were finally illustrated with MOE.

Wound Healing Experiments. This study was performed at BIOalternatives (Gencay, France). Wound healing was evaluated on human skin explants obtained from mammary plastic surgery of one patient. Upon receipt of skin biopsy, 30 punches of 8 mm diameter were performed and put on 6-well plates. Three punches were set aside for the non-wounded day 0 control. Then, on the remaining 18 punches, a 2 mm diameter punch was performed on the epidermis layer in order to create an acute wound. The skin specimens were laid in DMEM supplemented with L-glutamine, penicillin-streptomycin and delipidized fetal calf serum (thus not containing steroid hormones like cortisol) with the epidermis layer above the culture medium. Compound **118** (5 μM, each time freshly prepared in culture medium with a final DMSO concentration of 0.1%) was topically applied in the 2 mm diameter "hole" on a daily basis until day 3. Control explants were generated in parallel by treating the explants with culture medium containing 0.1% DMSO only. The explants were incubated for 24, 48 and 72 hours. All experimental conditions were performed in triplicate. After 1, 2 and 3 days of incubation, the explants were paraffin-embedded, sectioned and stained using hematoxylin-eosin-saffron. The wound healing was then measured by image analysis (NIKON E400 microscope) of the stained sections. To determine the extent of re-epithelialization, the linear distance covered by the new epithelium was measured and divided by the linear distance between the original wound edges. Measurements were performed using Image J software and inter-group comparisons were performed by an unpaired Student's test.[46, 112-113]

HPLC Purity Control of Final Compounds. A SpectraSystems® LC system consisting of a pump, an autosampler and a PDA detector was employed. Mass spectra (LC/MS) were measured on an

MSQ® electro spray mass spectrometer (ThermoFisher, Dreieich, Germany). An RP-C18 NUCLEODUR® 100-5 (125x3 mm) column (Macherey-Nagel GmbH, Düren, Germany) was used as stationary phase. All solvents were HPLC grade. The system was operated by the standard software Xcalibur®. In a gradient run, the percentage of acetonitrile in water (supplemented with 0.1% trifluoroacetic acid)[a] was increased from an initial concentration of 0% at 0 min to 100% at 15 min and kept at 100% for 5 min. For a part of the compounds, both solvents were used without trifluoroacetic acid or with 0.1% formic acid.[b] The injection volume was 10 µL and the flow rate was set to 800 µL/min. MS analysis was carried out at a spray voltage of 3800 V, a capillary temperature of 350 °C and a source CID of 10 V. Spectra were acquired in positive mode from 100 to 1000 m/z and at 254 nm for the UV trace. The relative peak area in the UV chromatogram was used to determine the purity of the compounds.

Comp	RT [min]	Purity [%]	Comp	RT [min]	Purity [%]	Comp	RT [min]	Purity [%]
20	5.68[a]	99	50	5.75[a]	99	79	7.80[a]	99
21	6.31[a]	98	51	7.14[a]	98	80	7.77[a]	98
22	6.09[a]	97	52	7.97[a]	99	81	8.77[a]	99
23	6.92[a]	98	53	6.18[a]	99	82	7.20[a]	99
24	7.28[a]	99	54	5.52[a]	98	83	6.51[a]	99
25	7.82[a]	99	57	7.33[a]	99	84	7.08[a]	99
26	4.99[a]	99	60	5.92[a]	99	85	7.47[a]	99
27	5.98[a]	98	61	6.13[a]	98	86	2.61[a]	98
28	7.88[a]	99	67	11.53	99	87	6.89[a]	99
29	8.68[a]	97	68	7.20[b]	99	88	8.09[a]	99
28	4.39[a]	99	69	4.87[a]	99	89	7.40[a]	99
39	6.45[a]	99	70	8.15[b]	98	90	8.09[a]	99
40	6.37[a]	98	71	5.70[a]	99	91	8.59[a]	99
41	6.09[a]	99	72	9.09[b]	99	92	7.92[a]	99
44	6.24[a]	99	73	4.05[a]	98	93	7.55[a]	99
45	7.70[a]	99	74	12.30[b]	99	115	4.7[c]	99
46	5.91[a]	99	75	6.36[b]	99	116	4.5[c]	97
47	5.86[a]	99	76	13.76[b]	98	117	4.5[c]	98
48	5.22[a]	98	77	7.42[a]	98	118	5.2[c]	99
49	5.31[a]	99	78	11.58[b]	99	119	4.2[c]	98

For compounds **115**-**119**, the following method was used: A Dionex Ultimate 3000 HPLC coupled to a Bruker amaZon SL (Thermo Scientific, Germany) system consisting of a pump, an autosampler and a UV detector (254 nm) was employed. An RP-18 column (100/2 Nucleoshell RP18plus, 2.7 µm from Machery Nagel, Germany) was used as stationary phase. All solvents were HPLC grade. In a gradient run, the percentage of acetonitrile in water was increased from an initial concentration of 5% at 0 min to 95% at 15 min and kept at 95% for 5 min, both solvents contained 0.1% formic acid[c]. The injection volume was 10 µL and the flow rate was set to 600 µL/min. The relative peak area in the UV chromatogram was used to determine the purity of the compounds (DataAnalysis (Bruker Daltonics, Bremen, Germany). The purity of all compounds was ≥95%.

Chemistry

General Experimental. Reagents and solvents were used as obtained from commercial suppliers without further purification or drying. All reactions were performed under a nitrogen atmosphere unless otherwise indicated. Yields refer to purified products and are not optimized. Flash chromatography was performed on silica gel 60 (40−60 μm). Melting points of samples were determined in open capillaries using a SMP3 Melting Point Apparatus of Bibby Sterilin and are uncorrected. Microwave irradiation experiments were performed in sealed tubes in a CEM Discover Explorer 12 microwave reactor. ^{1}H NMR and ^{13}C spectra were recorded on a Bruker DRX-500 or Bruker Fourier 300 instrument. Chemical shifts are given in parts per million (ppm) and spectra are obtained from DMSO-d$_6$, CDCl$_3$ or aceton-d$_6$ solutions, in which the hydrogenated residues of deuterated solvents were used as internal standard (CDCl$_3$: δ = 7.27, 77.00. Aceton-d$_6$: δ = 2.05, 29.92. DMSO-d$_6$: δ = 2.50, 39.51). The following abbreviations are used to denote signal multiplicities: s= singlet, d= doublet, dd= doublet of doublet, t = triplet, q = quartet and m = multiplet. All coupling constants (*J*) are given in Hertz (Hz). Several signals were assigned with the help of ^{1}H, ^{1}H-COSY, ^{1}H, ^{13}C-HSQC and ^{1}H, ^{13}C-HMBC experiments. Mass spectra (LC/MS) were measured on an MSQ$^{®}$ electro spray mass spectrometer (ThermoFisher, Dreieich, Germany). High resolution mass spectra were obtained on a Bruker maxis 4G hr-QqToF spectrometer and low resolution mass spectra were recovered on a Bruker amaZon SL spectrometer. The data were analyzed using DataAnalysis (Bruker Daltonics, Bremen, Germany).

Method A: Suzuki coupling. The corresponding brominated aromatic compound (1 equiv) and the boronic acid (1.5 equiv) were dissolved in toluene (10 mL), ethanol (10 mL), and aq Na$_2$CO$_3$ (2.0 M, 2.5 mL). The mixture was degassed under reduced pressure and flushed with N$_2$ for three times before Pd(PPh$_3$)$_4$ (5 mol%) was added. The resulting suspension was then heated under reflux for 4-12 h. After cooling down, the phases were separated, and the aqueous phase was extracted two times with EtOAc. The combined organic extracts were dried over MgSO$_4$ and concentrated under reduced pressure to give the crude product, which was purified with flash chromatography on silica gel.

Method B: Grignard reaction. To a solution of the Grignard reagent (2 equiv) in dry diethyl ether (10 mL), the corresponding carbonyl compound (1 equiv) in dry diethyl ether (5 mL) was added dropwise. The reaction mixture was heated to reflux for 2 h. Afterward, ice was added followed by the addition of HCl (1 M) until the resulting precipitate disappeared. The phases were separated, and the aqueous phase was extracted twice with diethyl ether. The combined organic layers were

washed with saturated sodium hydrogen carbonate solution and brine. After drying over MgSO$_4$ and concentration under vacuum, the crude product was purified by flash chromatography on silica gel.

Method C: CDI reaction. To a solution of the corresponding alcohol (1 equiv) in NMP, CDI (5 equiv) was added. Then the solution was heated to reflux for 16 h. After cooling to room temperature, the reaction mixture was diluted with EtOAc and washed with water and brine. The organic phase was dried over MgSO$_4$ and concentrated under vacuum. The crude product was purified by flash chromatography on silica gel.

Method D: Wohl−Ziegler bromination. The methyl heteroaromatic compound was dissolved in 20 mL of dry carbon tetrachloride. To this solution, *N*-bromosuccinimide (NBS) (1.1 equiv) and benzoyl peroxide (5 mol%) were added and the mixture was refluxed overnight. After cooling, the succinimide was removed by filtration and the filtrate was concentrated under vacuum. The crude product was purified by flash chromatography on silica gel.

Method E: S$_N$ reaction. K$_2$CO$_3$ (5 equiv), imidazole (4 equiv), and the corresponding methyl heteroaromatic bromide were suspended in DMF (1 mL/mmol) or acetonitrile (1 mL/mmol). The resulting mixture was heated to 120 °C for 2 h. After cooling, water (10 mL) was added and the aqueous layer was extracted with EtOAc (3 × 10 mL). The combined organic layers were washed with brine (10 mL), dried over MgSO$_4$, and evaporated in vacuo. The crude product was purified by column chromatography using SiO$_2$.

Method F: Suzuki coupling using microwave irradiation. A mixture of the brominated aromatic compound (1 equiv), the corresponding boronic acid or boronic acid pinacolester (1.2 equiv), Cs$_2$CO$_3$ (3 equiv) and PdCl$_2$(dppf) (5 mol%) were dissolved in DME/H$_2$O/EtOH (1 mL/1 mL/1 mL). The reaction mixture was stirred for 20 min at 150 °C, 150 W and 18 bar in the microwave oven. After addition of H$_2$O (10 mL) and extraction with ethyl acetate (3 × 15 mL), the combined organic phases were dried over MgSO$_4$ and concentrated under reduced pressure. The purification was performed by flash chromatography using SiO$_2$. After flash chromatography, the product was dissolved in ethyl acetate and a few drops of conc. HCl and water were added. After stirring for 30 min the phases were separated and the aqueous phase was neutralized with aqueous Na$_2$CO$_3$ solution (2M). After extraction with ethyl acetate and drying over MgSO$_4$, the solvent was removed under vacuum.

Method G: Suzuki-Reaction using palladium(II) acetate. The corresponding brominated aromatic compound (1.0 eq) was dissolved in degassed 1,4-dioxane (7 mL/mmol) under N_2. Subsequently, the boronic acid or boronic acid pinacolester (1.7 eq), palladium(II) acetate (0.7 mol%), SPhos (2 mol%) and 2 M aqueous, degassed LiOH solution (3.5 eq) were added. The reaction mixture was stirred at 90 °C for 20 h. After cooling to room temperature water and ethyl acetate were added and the suspension was filtered over celite. The phases were separated and the aqueous phase was extracted with ethyl acetate thrice. The combined organic layers were washed with 1 M aqueous NaOH solution, water and brine, dried over Na_2SO_4 and concentrated in vacuum. The purification was performed by flash chromatography using SiO_2.

Method H: Suzuki-Coupling and ether cleavage. A mixture of brominated aromatic compound (1 eq), corresponding boronic acid pinacolester (1.2 eq), Cs_2CO_3 (3 eq) and $PdCl_2(dppf)$ (5 mol %) were dissolved in DME/ H_2O/ EtOH (2 mL/ 2 mL/ 2 mL). The reaction mixture was stirred for 20 min at 150°C, 150 W and 18 bar in the microwave oven. After addition of H_2O (10 mL) and extraction with ethyl acetate (3 × 15 mL), the combined organic phases were dried over $MgSO_4$ and concentrated under reduced pressure. Without further purification the crude product was suspended in HBr (48 % in water, 10 mL) and the mixture was stirred at 130 °C overnight. After cooling down, the aqueous phase was washed with EtOAc and then basified with saturated Na2CO3 solution. After extraction with EtOAc, the combined organic phases were dried over MgSO4, filtered and concentrated under reduced pressure. Subsequent purification was performed by flash chromatography using SiO2.

6-Bromonicotinaldehyde (6). To a suspension of 2,5-dibromopyridine (2.00 g, 8.44 mmol) in dry

diethyl ether (25 mL) was added *n*-BuLi (3.55 mL, 8.87 mmol, 2.5 M solution in hexane) at −80 °C under a nitrogen atmosphere. After stirring for 1 h at −80 °C, dry DMF (0.68 mg, 9.28 mmol) was added. Reaction mixture was stirred for an additional hour at −80 °C, warmed slowly to 0 °C, and HCl (18.0 mL, 1 M) was added. After stirring for 15 min, the phases were separated and aqueous layer was extracted twice with diethyl ether. The combined organic layers were washed with water (50 mL) and brine (50 mL) and dried over MgSO₄. The organic phase was concentrated under reduced pressure, and the crude product was purified by flash chromatography on silica gel using a mixture of hexane/ethyl acetate (8:1) as eluent. White solid. Yield: 1.03 g, 66%. ^{1}H NMR (CDCl₃, 500 MHz): δ_H (ppm) = 7.67−7.71 ppm (m, 1H), 8.02 (dd, *J* = 8.2, 2.5 Hz, 1H), 8.84 (dd, *J* = 2.5, 0.6 Hz, 1H), 10.10 (s, 1H). [13]C
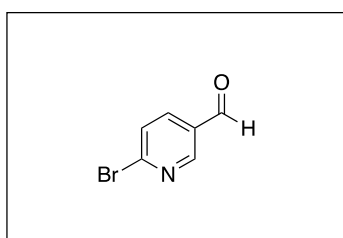
NMR (CDCl₃, 125 MHz): δ_C (ppm) =129.0, 130.6, 137.5, 148.3, 152.5, 189.4. MS (ESI): m/z = 187.19 [M + H]⁺.

6-Phenylnicotinaldehyde (7). Synthesized using compound **6** (1.20 g, 6.44 mmol) and phenylboronic acid (1.18 g, 9.65 mmol) according to method A. Crude product was purified by flash chromatography on silica gel using a mixture of hexane/ethyl acetate (10:1) as eluent. Light-yellow solid. Yield: 1.10 g, 94%. ¹H NMR (CDCl₃, 500 MHz): δ_H (ppm) = 7.44−7.52 ppm (m, 3H), 7.87 (d, J = 8.2 Hz, 1H), 8.04−8.08 (m, 2H), 8.20 (dd, J = 8.2, 2.2 Hz, 1H), 9.10 (dd, J = 2.2, 0.6 Hz, 1H), 10.11 (s, 1H). ¹³C NMR (CDCl₃, 125 MHz): δ_C (ppm) = 120.5, 127.5, 129.0, 129.8, 130.4, 136.5, 138.0, 152.4, 162.2, 190.4. MS (ESI): m/z = 184.31 [M + H]⁺.
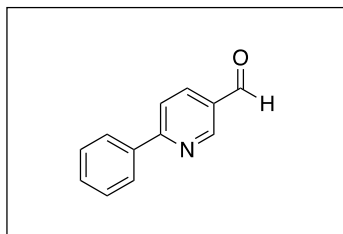
6-(Thiophen-3-yl)nicotinaldehyde (8). Synthesized using compound **6** (840 mg, 4.52 mmol) and thiophen-3-ylboronic acid (867 g, 6.77 mmol) according to Method A. Crude product was purified by flash chromatography on silica-gel using a mixture of hexane / ethyl acetate (8:2) as eluent. Orange solid. Yield: 556 mg, 65%. ¹H NMR (CDCl₃, 500 MHz): δ_H (ppm) = 7.45 (dd, J = 5.0, 2.8 Hz, 1H), 7.72–7.80 (m, 2H), 8.11 (dd, J = 2.8, 1.3 Hz, 1H), 8.19 (dd, J = 8.2, 2.2 Hz, 1H), 9.06 (dd, J = 2.2, 0.9 Hz, 1H), 10.11 (s, 1H); ¹³C NMR (CDCl₃, 125 MHz): δ_C (ppm) = 120.3, 126.3, 126.4, 126.9, 129.6, 136.5, 141.1, 152.6, 158.0, 190.2; (ESI): m/z = 190.27 [M + H]⁺.
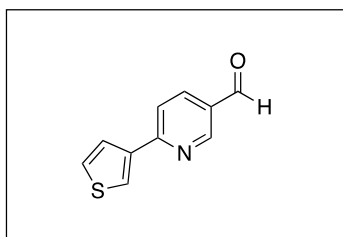
6-(Naphthalen-1-yl)nicotinaldehyde (9). Synthesized using compound **6** (720 mg, 3.87 mmol) and 1-naphthalenboronic acid (1.00 g, 5.81 mmol) according to Method A. Crude product was purified by flash chromatography on silica-gel using a mixture of hexane / ethyl acetate (8:1) as eluent. Orange solid. Yield: 733 mg, 81%. ¹H NMR (CDCl₃, 500 MHz): δ_H (ppm) = 7.50–7.62 (m, 3H), 7.65–7.69 (m, 1H), 7.77–7.81 (m, 1H), 7.92–8.00 (m, 2H), 8.10– 8.14 (m, 1H), 8.31 (dd, J = 7.9, 2.2 Hz, 1H), 9.25 (dd, J = 2.2, 0.9 Hz, 1H), 10.22 (s, 1H); ¹³C NMR (CDCl₃, 125 MHz): δ_C (ppm) = 125.1, 125.2, 125.4, 126.2, 127.0, 128.0, 128.5, 129.7, 130.0, 130.7, 134.0, 136.1, 137.2, 152.1, 164.6, 190.5; MS (ESI): m/z = 234.29 [M + H]⁺.
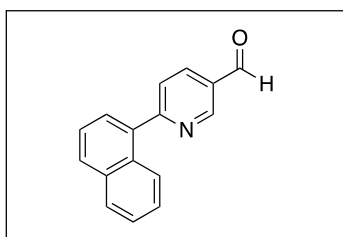
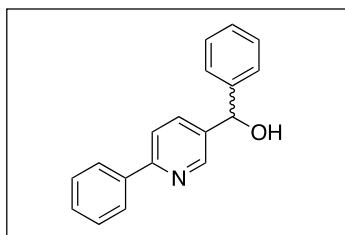**1-(6-Phenylpyridin-3-yl)ethanol (10).** Synthesized using compound **7** (210 mg, 1.15 mmol) and methylmagnesium bromide (2.29 mL, 2.29 mmol, 1 M in THF) according to method B. Crude product was purified by flash chromatography on silica gel using a mixture of hexane/ethyl acetate (2:1) as eluent. Light-yellow solid. Yield: 201 mg, 88%. ^{1}H NMR (CDCl$_3$, 500 MHz): δ_H (ppm) = 1.51 (d, J = 6.6 Hz, 3H), 3.05 (br, s, 1H), 4.92 (q, J = 6.6 Hz, 1H), 7.38−7.50 (m, 3H), 7.65 (d, J = 7.9 Hz, 1H), 7.74 (dd, J = 8.2, 2.2 Hz, 1H), 7.91−7.97 (m, 2H), 8.58 (d, J = 2.2 Hz, 1H). ^{13}C NMR (CDCl$_3$, 125 MHz): δ_C (ppm) = 25.0, 67.8, 120.4, 126.9, 128.7, 128.9, 134.0, 139.0, 139.5, 147.2, 156.6. MS (ESI): m/z = 200.32 [M + H]$^+$.
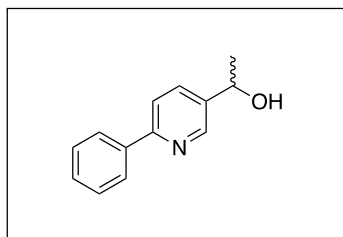
1-(6-Phenylpyridin-3-yl)propan-1-ol (11). Synthesized using compound **7** (313 mg, 1.71 mmol) and ethylmagnesium bromide (3.42 mL, 3.42 mmol, 1 M in THF) according to Method B. Crude product was purified by flash chromatography on silica-gel using a mixture of hexane / ethyl acetate (3:1) as eluent. Light yellow solid. Yield: 298 mg, 82%. ^{1}H NMR (CDCl$_3$, 500 MHz): δ_H (ppm) = 0.90–0.95 (m, 3H), 1.71–1.88 (m, 2H), 4.62 (t, J = 6.62 Hz, 1H), 7.38–7.43 (m, 1H), 7.43–7.49 (m, 2H), 7.64–7.67 (m, 1H), 7.69–7.73 (m, 1H), 7.92–7.96 (m, 2H), 8.54 (d, J = 2.21 Hz, 1H); ^{13}C NMR (CDCl$_3$, 125 MHz): δ_C (ppm) = 9.9, 31.7, 73.2, 120.3, 126.8, 128.7, 128.8, 134.5, 138.3, 139.0, 147.7, 156.5; MS (ESI): m/z = 214.28 [M + H]$^+$.
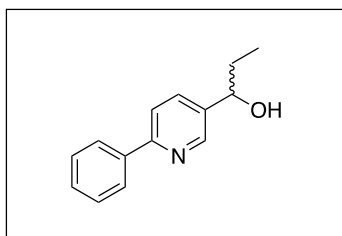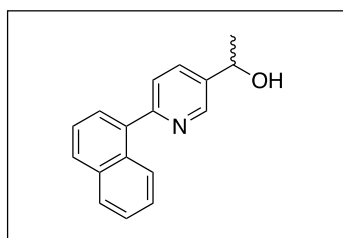
Cyclopropyl(6-phenylpyridin-3-yl)methanol (12). Synthesized using compound **7** (227 mg, 1.24 mmol) and cyclopropylmagnesium bromide (4.96 mL, 2.48 mmol, 0.5 M in THF) according to Method B. Crude product was purified by flash chromatography on silica-gel using a mixture of hexane / ethyl acetate (3:1) as eluent. Light yellow solid. Yield: 234 mg, 84%. ^{1}H NMR (CDCl$_3$, 500 MHz): δ_H (ppm) = 0.35–0.44 (m, 1H), 0.49 (dq, J = 9.4, 4.7 Hz, 1H), 0.55–0.68 (m, 2H), 1.21 (qt, J = 8.1, 5.0 Hz, 1H), 3.00 (br, s, 1H), 4.05 (d, J = 8.2 Hz, 1H), 7.38–7.44 (m, 1H), 7.44–7.50 (m, 2H), 7.66–7.70 (m, 1H), 7.80–7.85 (m, 1H), 7.94–8.00 (m, 2H), 8.64–8.69 (m, 1H); ^{13}C NMR (CDCl$_3$, 125 MHz): δ_C (ppm) = 2.8, 3.6, 19.0, 75.9, 120.3, 126.8, 128.7, 128.8, 134.5, 137.7, 139.1, 147.6, 156.5; MS (ESI): m/z = 226.28 [M + H]$^+$.
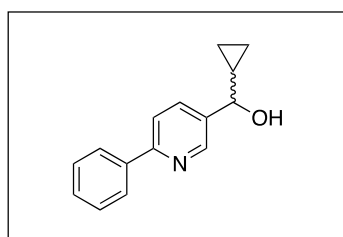
2-Methyl-1-(6-phenylpyridin-3-yl)propan-1-ol (13). Synthesized using compound **7** (283 mg, 1.55 mmol) and isopropylmagnesium chloride (1.55 mL, 3.10 mmol, 2 M in THF) according to Method B. Crude product was purified by flash chromatography on silica-gel using a mixture of hexane / ethyl acetate (4:1) as eluent. Orange solid. Yield: 138 mg, 40%. ^{1}H NMR (CDCl$_3$, 500 MHz): δ_H (ppm) = 0.82–0.93 (m, 3H), 1.02 (d, J = 6.6 Hz, 3H), 1.95– 2.08 (m, 1H), 4.46 (d, J = 6.6 Hz, 1H), 7.39–7.44 (m, 1H), 7.45–7.50 (m, 2H), 7.68–7.75 (m, 2H), 7.96–8.01 (m, 2H), 8.57 (d, J = 1.9 Hz, H); MS (ESI): m/z = 228.26 [M + H]$^+$.
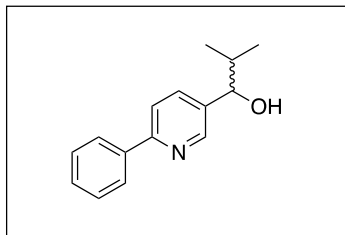
Furan-2-yl(6-phenylpyridin-3-yl)methanol (14). Synthesized using compound **7** (650 mg, 3.75 mmol) and furan-2-ylmagnesium bromide (1.85 g, 10.8 mmol, 2 M in THF) according to Method B. Crude product was purified by flash chromatography on silica-gel using a mixture of hexane / ethyl acetate (6:1) as eluent. Yellow solid. Yield: 631 mg, 67%. ^{1}H NMR (CDCl$_3$, 500 MHz): δ_H (ppm) = 3.62 (br. s., 1H), 5.86 (s, 1H), 6.17 (d, J = 3.4 Hz, 1H), 6.33 (dd, J = 3.0, 1.8 Hz, 1H), 7.33–7.51 (m, 4H), 7.69 (d, J = 7.9 Hz, 1H), 7.83 (dd, J = 8.2, 1.8 Hz, 1H), 7.88–7.99 (m, 2H); ^{13}C NMR (CDCl$_3$, 125 MHz): δ_C (ppm) = 66.7, 106.7, 109.3, 119.4, 126.0, 127.7, 128.0, 134.0, 134.3, 137.9, 141.8, 147.1, 154.1, 156.1; (ESI): m/z = 251.87 [M + H]$^+$.
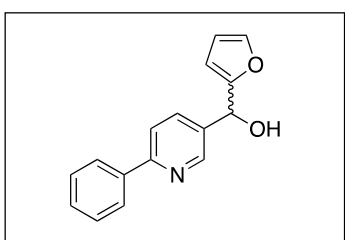
Phenyl(6-phenylpyridin-3-yl)methanol (15). Synthesized using compound **7** (300 mg, 1.73 mmol) and phenylmagnesium bromide (1.73 mL, 3.46 mmol, 2 M in THF) according to Method B. Crude product was purified by flash chromatography on silica-gel using a mixture of hexane / ethyl acetate (3:1) as eluent. Yellow solid. Yield: 138 mg, 42%. ^{1}H NMR (CDCl$_3$, 500 MHz): δ_H (ppm) = 5.91 (s, 1H), 7.29–7.34 (m, 1H), 7.35–7.50 (m, 7H), 7.68 (dd, J = 8.2, 0.6 Hz, 1H), 7.73–7.78 (m, 1H), 7.94–7.99 (m, 2H), 8.68 (dd, J = 1.6, 0.6 Hz, 1H); ^{13}C NMR (CDCl$_3$, 125 MHz): δ_C (ppm) = 74.1, 120.3, 126.5, 126.9, 128.0, 128.7, 128.7, 128.9, 135.0, 137.6, 139.0, 143.0, 148.2, 156.7; (ESI): m/z = 261.97 [M + H]$^+$.

**1-(6-(Thiophen-3-yl)pyridin-3-yl)ethanol (16).** Synthesized using compound **8** (260 mg, 1.37
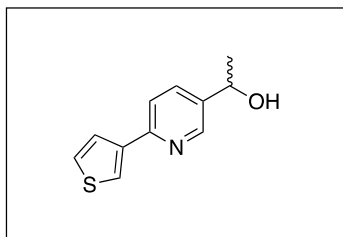
mmol) and methylmagnesium bromide (2.74 mL, 2.74 mmol, 1 M in THF) according to Method B. Crude product was purified by flash chromatography on silica-gel using a mixture of hexane / ethyl acetate (1:1) as eluent. Yellow solid. Yield: 240 mg, 85%. ^{1}H NMR (CDCl$_3$, 500 MHz): δ_H (ppm) = 1.50 (d, J = 6.6 Hz, 3H), 4.90 (q, J = 6.3 Hz, 1H), 7.38 (dd, J = 5.0, 2.8 Hz, 1H), 7.55 (d, J = 8.2 Hz, 1H), 7.61 (dd, J = 5.0, 1.3 Hz, 1H), 7.70 (dd, J = 8.2, 2.2 Hz, 1H), 7.85 (dd, J = 2.8, 1.3 Hz, 1H), 8.48 (d, J = 2.2 Hz, 1H); ^{13}C NMR (CDCl$_3$, 125 MHz): δ_C (ppm) = 25.2, 68.0, 120.4, 123.6, 126.4, 126.5, 134.3, 139.5, 142.0, 147.4, 152.9; (ESI): m/z = 206.29 [M + H]$^+$.

Cyclopropyl(6-(thiophen-3-yl)pyridin-3-yl)methanol (17). Synthesized using compound **8** (270
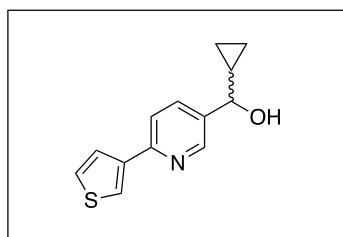
mg, 1.43 mmol) and cyclopropylmagnesium bromide (5.72 mL, 2.86 mmol, 0.5 M in THF) according to Method B. Crude product was purified by flash chromatography on silica- gel using a mixture of hexane / ethyl acetate (1:1) as eluent. Yellow solid. Yield: 138 mg, 42%. ^{1}H NMR (CDCl$_3$, 500 MHz): δ_H (ppm) = 0.37–0.45 (m, 1H), 0.50 (dq, J = 9.7, 4.8 Hz, 1H), 0.57–0.71 (m, 2H), 1.18–1.29 (m, 1H), 2.48 (br. s., 1H), 4.06 (d, J = 8.2 Hz, 1H), 7.39 (dd, J = 5.0, 3.2 Hz, 1H), 7.60 (dd, J = 8.2, 0.6 Hz, 1H), 7.64–7.68 (m, 1H), 7.78–7.85 (m, 1H), 7.89 (dd, J = 3.0, 1.4 Hz, 1H), 8.60–8.64 (m, 1H); ^{13}C NMR (CDCl$_3$, 125 MHz): δ_C (ppm) = 2.8, 3.6, 19.1, 76.1, 120.0, 123.4, 126.2, 126.3, 134.5, 137.2, 141.9, 147.6, 152.8; (ESI): m/z = 232.26 [M + H]$^+$.

1-(6-(Naphthalen-1-yl)pyridin-3-yl)ethanol (18). Synthesized using compound **9** (231 mg, 0.99

mmol) and methylmagnesium bromide (1.98 mL, 1.98 mmol, 1 M in THF) according to Method B. Crude product was purified by flash chromatography on silica-gel using a mixture of hexane / ethyl acetate (2:1) as eluent. White solid. Yield: 172 mg, 70%. ^{1}H NMR (CDCl$_3$, 500 MHz): δ_H (ppm) = 1.59 (d, J = 6.1 Hz, 3H), 5.00 (m, 1H), 7.44–7.62 (m, 5H), 7.80–7.86 (m, 1H), 7.90–7.96 (m, 2H), 8.07 (d, J = 7.9 Hz, 1H), 8.74 (s, 1H); (ESI): m/z = 250.29 [M + H]$^+$.

Cyclopropyl(6-(naphthalen-1-yl)pyridin-3-yl)methanol (19). Synthesized using compound **9**
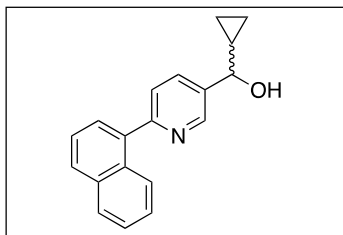
(253 mg, 1.09 mmol) and cyclopropylmagnesium bromide (4.34 mL, 2.17 mmol, 0.5 M in THF) according to Method B. Crude product was purified by flash chromatography on silica- gel using a mixture of hexane / ethyl acetate (3:1) as eluent. Light yellow solid. Yield: 239 mg, 80%. ^{1}H NMR (CDCl$_3$, 500 MHz): δ_H (ppm) = 0.39–0.54 (m, 2H), 0.60–0.72 (m, 2H), 1.22–1.29 (m, 1H), 4.04–4.14 (m, 1H), 7.42–7.60 (m, 5H), 7.86–7.92 (m, 3H), 8.04–8.08 (m, 1H), 8.77 (d, J = 2.2 Hz, 1H); ^{13}C NMR (CDCl$_3$, 125 MHz): δ_C (ppm) = 3.3, 3.9, 14.4, 60.6, 125.0, 125.5, 125.9, 126.1, 126.7, 127.7, 128.6, 129.1, 134.2, 137.8, 138.5, 147.8, 158.5, 171.4; MS (ESI): m/z = 276.34 [M + H]$^+$.
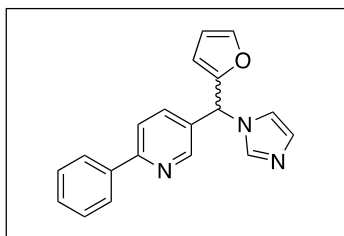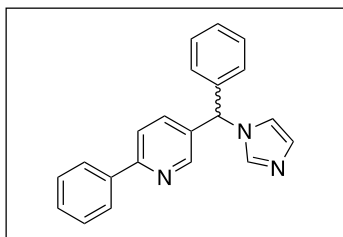
5-(1-(1H-Imidazol-1-yl)ethyl)-2-phenylpyridine (20). Synthesized using compound **10** (164 mg,
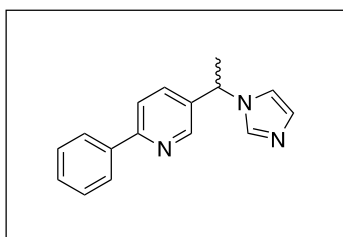
0.82 mmol), CDI (667 mg, 4.12 mmol), and NMP (8 mL) according to method C. Crude product was purified by flash chromatography on silica gel using a mixture of ethyl acetate/ methanol (9:1) as eluent. White solid. Yield: 20 mg, 10%. Melting point: 64−67 °C (ethyl acetate). ^{1}H NMR (CDCl$_3$, 500 MHz): δ_H (ppm) = 1.93 (d, J = 7.3 Hz, 3H), 5.45 (q, J = 6.9 Hz, 1H), 6.97 (t, J = 1.4 Hz, 1H), 7.11−7.15 (m, 1H), 7.40−7.51 (m, 4H), 7.64 (s, 1H), 7.71 (dd, J = 8.2, 0.6 Hz, 1H), 7.95−8.00 (m, 2H), 8.58 (dd, J = 1.6, 0.6 Hz, 1H). ^{13}C NMR (CDCl$_3$, 125 MHz): δ_C (ppm) = 21.8, 54.2, 117.7, 120.5, 126.9, 128.8, 129.3, 129.9, 134.3, 135.3, 135.9, 138.5, 147.5, 157.4. MS (ESI): m/z = 250.26 [M + H]$^+$.

5-(1-(1H-Imidazol-1-yl)propyl)-2-phenylpyridine (21). Synthesized using compound **11** (275
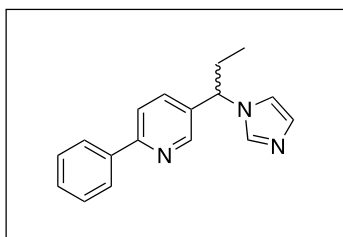
mg, 1.29 mmol), CDI (1.05 g, 6.45 mmol), and NMP (10 mL) according to method C. Crude product was purified by flash chromatography on silica gel using a mixture of ethyl acetate/me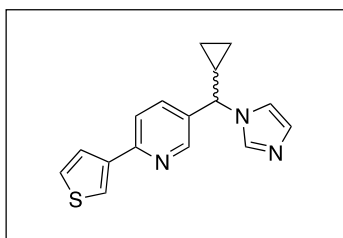thanol (9:1) as eluent. Beige solid. Yield: 114 mg, 34%. Melting point: 103−104 °C (ethyl acetate). ^{1}H NMR (CDCl$_3$, 500 MHz): δ_H (ppm) = 0.76 (t, J = 7.3 Hz, 3H), 1.98−2.13 (m, 2H), 4.87 (t, J = 7.7 Hz, 1H), 6.75 (t, J = 1.1 Hz, 1H), 6.89 (s, 1H), 7.16−7.33 (m, 4H), 7.41 (s, 1H), 7.47 (d, J = 8.2 Hz, 1H), 7.71−7.79 (m, 2H), 8.37 (d, J = 2.2 Hz, 1H). ^{13}C NMR (CDCl$_3$, 125 MHz): δ_C (ppm) = 10.9, 28.4, 60.8, 117.4, 120.4, 126.8, 128.8, 129.2, 130.0, 134.1, 134.7, 136.3, 138.5, 148.0, 157.4. MS (ESI): m/z = 264.37 [M + H]$^+$.

5-(Cyclopropyl(1H-imidazol-1-yl)methyl)-2-phenylpyridine **(22).** Synthesized using compound **12** (200 mg, 0.89 mmol), CDI (720 mg, 4.44 mmol), and acetonitrile (12 mL) according to method C. Crude product was purified by flash chromatography on silica gel using a mixture of hexane/ethyl acetate (1:3) as eluent. White solid. Yield: 45 mg, 18%. Melting point: 122−124 °C (ethyl acetate). ^{1}H NMR (CDCl$_3$, 500 MHz): δ_H (ppm) = 0.50−0.61 (m, 2H), 0.81−0.95 (m, 2H), 1.58 (m, 1H), 4.49 (d, J = 9.5 Hz, 1H), 6.98 (t, J = 1.3 Hz, 1H), 7.13 (t, J = 0.9 Hz, 1H), 7.40−7.51 (m, 4H), 7.72 (dd, J = 9.9, 1.4 Hz, 2H), 7.97−8.02 (m, 2H), 8.63 (d, J = 2.2 Hz, 1H). ^{13}C NMR (CDCl$_3$, 125 MHz): δ_C (ppm) = 4.9, 5.2, 16.2, 63.8, 118.2, 120.4, 126.8, 128.8, 129.2, 129.7, 134.0, 134.9, 136.4, 138.5, 148.0, 157.4. MS (ESI): m/z = 276.28 [M + H]$^+$.
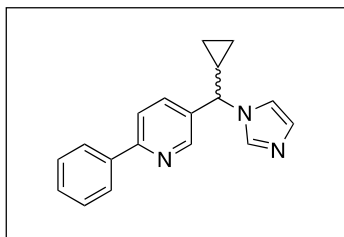
**5-(1-(1H-Imidazol-1-yl)-2-methylpropyl)-2-phenylpyridine (23).** Synthesized using compound **13** (231 mg, 1.02 mmol), CDI (825 mg, 5.09 mmol), and NMP (10 mL) according to method C. Crude product was purified by flash chromatography on silica gel using a mixture of ethyl acetate/methanol (9:1) as eluent. Beige solid. Yield: 71 mg, 25%. Melting point: 127−129 °C (ethyl acetate). ^{1}H NMR (CDCl$_3$, 500 MHz): δ_H (ppm) = 0.93−1.02 (m, 6H), 2.59−2.66 (m, 1H), 4.72 (d, J = 10.4 Hz, 1H), 7.02−7.07 (m, 1H), 7.09 (s, 1H), 7.40−7.51 (m, 3H), 7.62−7.70 (m, 2H), 7.70−7.76 (m, 1H), 7.95− 8.02 (m, 2H), 8.67 (d, J = 2.2 Hz, 1H). ^{13}C NMR (CDCl$_3$, 125 MHz): δ_C (ppm) = 19.9, 20.2, 32.4, 66.6, 117.2, 120.5, 126.8, 128.8, 129.3, 130.0, 133.2, 135.3, 136.4, 138.5, 148.8, 157.4. MS (ESI): m/z = 278.41 [M + H]$^+$.
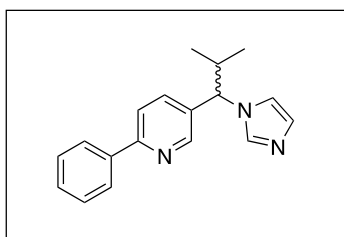
**5-(Furan-2-yl(1H-imidazol-1-yl)methyl)-2-phenylpyridine (24).** Synthesized using compound **14** (631 mg, 2.51 mmol), CDI (2.04 g, 12.56 mmol), and NMP (4 mL) according to method C. Crude product was purified by flash chromatography on silica gel using ethyl acetate/methanol (9:1) as eluent. Brown oil. Yield: 276 mg, 37%. ^{1}H NMR (CDCl$_3$, 500 MHz): δ_H (ppm) = 6.25−6.29 (m, 1H), 6.42 (dd, J = 3.5, 1.9 Hz, 1H), 6.55 (s, 1H), 6.95 (t, J = 1.3Hz, 1H), 7.14 (t, J = 1.1 Hz, 1H), 7.42−7.57 (m, 6H), 7.75 (dd, J = 8.5, 0.6 Hz, 1H), 7.97− 8.04 (m, 2H), 8.54 (dt, J = 1.6, 0.8 Hz, 1H). ^{13}C NMR (CDCl$_3$, 125 MHz): δ_C (ppm) = 56.6, 110.7, 110.8, 118.6, 120.4, 126.9, 128.8, 129.4, 129.9, 131.6, 135.4, 136.8, 138.4, 143.9, 148.4, 150.1, 157.8. MS (ESI): m/z = 301.96 [M + H]$^+$.

5-((1H-Imidazol-1-yl)(phenyl)methyl)-2-phenylpyridine (25). Synthesized using compound **15** (299 mg, 1.14 mmol), CDI (928 mg, 5.72 mmol), and NMP (8 mL) according to method C. Crude product was purified by flash chromatography on silica gel using ethyl acetate as eluent. Beige solid. Yield: 75 mg, 21%. Melting point: 124−126 °C (ethyl acetate). ^{1}H NMR (CDCl$_3$, 500 MHz): δ_H (ppm) = 6.58 (s, 1H), 6.87−6.91 (m, 1H), 7.11−7.19 (m, 3H), 7.34−7.54 (m, 8H), 7.73 (d, J = 8.2 Hz, 1H), 7.98−8.04 (m, 2H), 8.49 (d, J = 2.5 Hz, 1H). ^{13}C NMR (CDCl$_3$, 125 MHz): δ_C (ppm) = 62.6, 119.0, 120.2, 126.8, 127.8, 128.7, 128.8, 129.0, 129.3, 129.8, 133.1, 136.1, 137.2, 138.0, 138.3, 149.2, 157.4. MS (ESI): m/z = 312.01 [M + H]$^+$.

5-(1-(1H-Imidazol-1-yl)ethyl)-2-(thiophen-3-yl)pyridine (26). Synthesized using compound **16** (227 mg, 1.11 mmol), CDI (897.0 mg, 5.53 mmol), and NMP (8 mL) according to method C. Crude product was purified by flash chromatography on silica gel using ethyl acetate/ methanol (9:1) as eluent. Brown oil. Yield: 78 mg, 28%. ^{1}H NMR (CDCl$_3$, 500 MHz): δ_H (ppm) = 1.75 (d, J = 6.9 Hz, 3H), 5.25 (q, J = 7.0 Hz, 1H), 6.79 (t, J = 1.3 Hz, 1H), 6.96 (t, J = 0.9 Hz, 1H), 7.21− 7.28 (m, 2H), 7.40−7.52 (m, 3H), 7.74 (dd, J = 2.8, 1.3 Hz, 1H), 8.34 (d, J = 2.5 Hz, 1H). ^{13}C NMR (CDCl$_3$, 125 MHz): δ_C (ppm) = 21.7, 54.2, 117.6, 120.2, 123.9, 126.1, 126.5, 129.9, 134.3, 134.9, 135.9, 141.4, 147.5, 153.5. MS (ESI): m/z = 256.08 [M + H]$^+$.
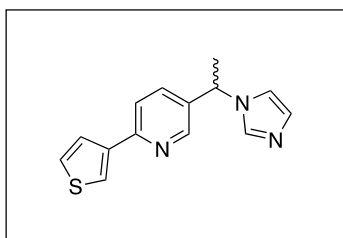
5-(Cyclopropyl(1H-Imidazol-1-yl)methyl)-2-(thiophen-3-yl)-pyridine (27). Synthesized using compound **17** (116 mg, 0.50 mmol), CDI (407 mg, 2.51 mmol), and NMP (5 mL) according to method C. Crude product was purified by flash chromatography on silica gel using ethyl acetate as eluent. Brown oil. Yield: 70 mg, 50%. ^{1}H NMR (CDCl$_3$, 500 MHz): δ_H (ppm) = 0.49−0.60 (m, 2H), 0.83−0.91 (m, 2H), 1.53−1.64 (m, 1H), 4.47 (d, J = 9.5 Hz, 1H), 6.97 (t, J = 1.3 Hz, 1H), 7.12 (t, J = 1.1 Hz, 1H), 7.39−7.46 (m, 2H), 7.59−7.63 (m, 1H), 7.64−7.68 (m, 1H), 7.72 (s, 1H), 7.91 (dd, J = 3.2, 1.3 Hz, 1H), 8.56 (dd, J = 1.6, 0.6 Hz, 1H). ^{13}C NMR (CDCl$_3$, 125 MHz): δ_C (ppm) = 4.9, 5.2, 16.2, 63.8, 118.2, 120.2, 123.9, 126.1, 126.5, 129.8, 133.7, 134.9, 136.4, 141.4, 148.0, 153.5. MS (ESI): m/z = 282.30 [M + H]$^+$.

5-(1-(1H-Imidazol-1-yl)ethyl)-2-(naphthalen-1-yl)pyridine (28). Synthesized using compound
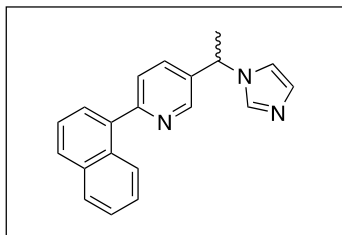
18 (147 mg, 0.59 mmol), CDI (478 mg, 2.95 mmol), and NMP (6 mL) according to method C. Crude product was purified by flash chromatography on silica gel using ethyl acetate as eluent. Brown oil. Yield: 59 mg, 33%. ^{1}H NMR (CDCl$_3$, 500 MHz): δ_H (ppm) = 1.97 (d, J = 7.3 Hz, 3H), 5.50 (q, J = 6.9 Hz, 1H), 7.02−7.06 (m, 1H), 7.16 (s, 1H), 7.45−7.63 (m, 6H), 7.69 (s, 1H), 7.92 (td, J = 4.9, 2.5 Hz, 2H), 8.06 (dd, J = 8.2, 0.9 Hz, 1H), 8.68 (d, J = 2.2 Hz, 1H). ^{13}C NMR (CDCl$_3$, 125 MHz): δ_C (ppm) = 22.1, 54.5, 117.9, 125.3, 125.5, 125.6, 126.2, 126.8, 127.8, 128.6, 129.4, 130.2, 131.2, 134.1, 134.1, 135.6, 136.2, 137.9, 147.6, 159.4. MS (ESI): m/z = 300.03 [M + H]$^+$.

5-(Cyclopropyl(1H-imidazol-1-yl)methyl)-2-(naphthalen-1-yl)-pyridine (29). Synthesized
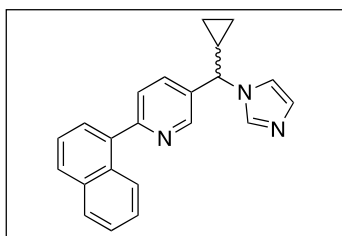
using compound **19** (210 mg, 0.76 mmol), CDI (619 mg, 3.82 mmol), and NMP (8 mL) according to method C. Crude product was purified by flash chromatography on silica gel using a mixture of ethyl acetate/methanol (9:1) as eluent. Brown oil. Yield: 38 mg, 15%. ^{1}H NMR (CDCl$_3$, 500 MHz): δ_H (ppm) = 0.54−0.66 (m, 2H), 0.86−0.98 (m, 2H), 1.61−1.68 (m, 1H), 4.54 (d, J = 9.5 Hz, 1H), 7.06 (s, 1H), 7.17 (s, 1H), 7.46−7.64 (m, 6H), 7.78 (s, 1H), 7.89−7.97 (m, 2H), 8.06−8.12 (m, 1H), 8.75 (dd, J = 1.3, 0.6 Hz, 1H). ^{13}C NMR (CDCl$_3$, 125 MHz): δ_C (ppm) = 5.1, 5.2, 16.4, 64.0, 118.2, 125.0, 125.2, 125.4, 125.9, 126.6, 127.6, 128.4, 129.2, 129.8, 131.0, 133.9, 134.1, 134.5, 136.4, 137.7, 147.8, 159.3. MS (ESI): m/z = 325.96 [M + H]$^+$.

3-Methyl-6-Phenylpyridazine (30). Synthesized using 3-chloro-6-methylpyridazine (1.00 g, 7.78
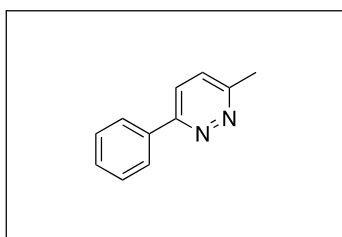
mmol) and phenylboronic acid (1.42 g, 11.67 mmol) according to Method A. Crude product was purified by flash chromatography on silica-gel using a mixture of hexane / ethyl acetate (2:1) as eluent. White solid. Yield: 1.00 g, 76%. ^{1}H NMR (CDCl$_3$, 500 MHz): δ_H (ppm) = 2.76 (s, 3H), 7.39 (d, J = 8.5 Hz, 1H), 7.46–7.55 (m, 3H), 7.76 (d, J = 8.5 Hz, 1H), 8.03–8.09 (m, 2H); ^{13}C NMR (CDCl$_3$, 125 MHz): δ_C (ppm) = 22.0, 123.9, 126.9, 127.2, 128.9, 129.7, 134.4, 136.4, 157.2, 158.5; (ESI): m/z = 170.96 [M + H]$^+$.

2-Methyl-5-phenylpyrazine (31). To a stirred solution of propylenediamine (2.94 g, 0.04 mol) in ethanol (50 mL) was added phenylglyoxal-monohydrate (5.00 g, 0.03 mol) at 0°C within 30 minutes. After stirring for 1.5 hours at room temperature KOH (2.10 g, 0.04 mol) was added and the reaction mixture was refluxed for 12 hours. Then the solvent was removed under vacuum and the residue was extracted with ether. The organic phases were washed with brine and dried over $MgSO_4$. Crude product was purified by flash chromatography on silica- gel using a mixture of hexane / ethyl acetate (7:3→3:7) as eluent. After flash chromatography the product was recrystallized from hexane. White solid. Yield: 780 mg, 15%. ^{1}H NMR (CDCl$_3$, 500 MHz): δ_H (ppm) = 2.57 (s, 3H), 7.38–7.50 (m, 3H), 7.91–7.99 (m, 2H), 8.43– 8.49 (m, 1H), 8.87 (d, J = 1.5 Hz, 1H); ^{13}C NMR (CDCl$_3$, 125 MHz): δ_C (ppm) = 21.2, 126.6, 128.9, 129.4, 136.5, 140.9, 143.8, 149.8, 151.9; (ESI): m/z = 170.94 [M + H]$^+$.
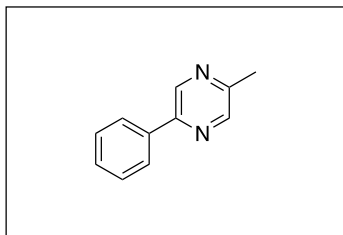
5-Methyl-2-phenylpyrimidine (32). To a solution of benzamidine hydrochloride (500 mg, 3.19 mmol) and 3-ethoxy-2-methylacrylaldehyde (400 mg, 3.51 mmol) in methanol (10 mL) was added a NaOMe solution (30% in methanol) dropwise under stirring over 30 minutes. After stirring for 4 hours, water (20 mL) was added and mixture was stirred for further 30 minutes at room temperature. After filtration, the obtained precipitate was washed with water and dried. White solid. Yield: 220 mg, 41%. ^{1}H NMR (CDCl$_3$, 500 MHz): δ_H (ppm) = 2.34 (s, 3H), 7.44–7.54 (m, 3H), 8.37–8.45 (m, 2H), 8.64 (d, J = 0.6 Hz, 2H); ^{13}C NMR (CDCl$_3$, 125 MHz): δ_C (ppm) = 15.7, 128.1, 128.5, 128.8, 130.6, 137.9, 157.6, 162.7; (ESI): m/z = 170.97 [M + H]$^+$.
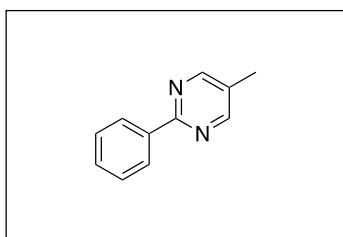
4-Methyl-1-phenylisoquinoline (33). Under nitrogen atmosphere methoxymethyl-triphenylphosphoniumchlorid (11.0 g, 0.03 mol) was suspensed in THF (40 mL) and cooled to -40 °C. Then KO*t*Bu (4.50 g, 0.04 mol) was added so that temperature not rised over -10 °C. After complete addition of KO*t*Bu immediately 2'-bromacetophenon (4.00 g, 2.71 mL, 0.02 mol) in THF (25 mL) was added dropwise at less then -10°C. The reaction mixture was stirred for 1 h at -10 °C and afterwards 18 h at room temperature. Then addition of H_2O (100 mL) and extraction with hexane (10 × 20 mL) were followed. The organic phases were dried over $MgSO_4$ and concentrated under vacuum. The residue was dissolved in methanol (100 mL) and water (75 mL) followed by extraction with hexane (10 × 20 mL). Again the organic phases were dried over $MgSO_4$ and concentrated under vacuum. The obtained 1-
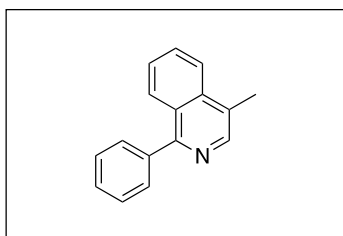
bromo-2-(1-methoxyprop-1-en-2-yl)benzene (orange liquid, 4.05 g) was used directly in the next step without further purification and characterization. To a stirred solution of 1-bromo-2-(1-methoxyprop-1-en-2-yl)benzene (3.13 g, 13.8 mmol) in diethyl ether (30 mL) at 0 °C was added *n*-BuLi (1.6M in hexane, 8.60 mL, 13.8 mmol) dropwise. After 1 h PhCN (1.56 g, 1.56 mL, 15.2 mmol) was added and the reaction temperature was raised to room temperature. H_2O (40 mL) was added and the organic materials were extracted with diethyl ether (2 × 30 mL). The combined extracts were washed with brine (20 mL), dried over $MgSO_4$ and concentrated under vacuum. Crude product was purified by flash chromatography on silica-gel using a mixture of hexane / ethyl acetate (10:1→5:1) as eluent. Yellow oil. Yield: 1.10 g, 36%. ^{1}H NMR (CDCl$_3$, 500 MHz): δ_H (ppm) = 2.66 (d, J = 0.9 Hz, 3 H), 7.44–7.54 (m, 4 H), 7.64–7.68 (m, 2 H), 7.72 (ddd, J = 8.3, 6.9, 1.3 Hz, 1 H), 8.00 (m, 1 H), 8.09 (m, 1 H), 8.45 (d, J = 0.9 Hz, 1 H); ^{13}C NMR (CDCl$_3$, 125 MHz): δ_C (ppm) = 16.0, 123.5, 126.1, 126.7, 128.1, 128.3, 128.3, 129.8, 129.9, 136.1, 139.8, 142.1, 159.3; (ESI): m/z = 219.92 [M + H]$^+$.

3-(Bromomethyl)-6-phenylpyridazine (34). Synthesized using compound **30** (982 mg, 5.77

mmol), NBS (1.13 g, 6.35 mmol) and DBPO (70 mg, 0.29 mmol) in carbon tetrachloride according to Method D. Crude product was purified by flash chromatography on silica-gel using hexane / ethyl acetate (4:1) as eluent. Product was used directly in the next step without further characterization. Orange solid. Yield: 53 mg, 4%. (ESI): m/z = 250.67 [M + H]$^+$.
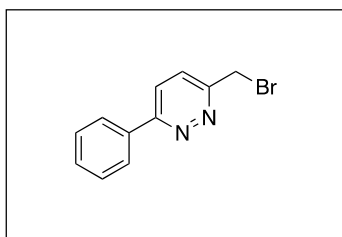
2-(Bromomethyl)-5-phenylpyrazine (35). Synthesized using compound **31** (724 mg, 4.25 mmol), NBS (832 mg, 4.68 mmol) and DBPO (52 mg, 0.21 mmol) in carbon tetrachloride according to

Method D. Crude product was purified by flash chromatography on silica-gel using a mixture of hexane / ethyl acetate (3:1) as eluent. Product was used directly in the next step without further characterization. Yellow solid. Yield: 571 mg, 54%. (ESI): m/z = 250.80 [M + H]$^+$.
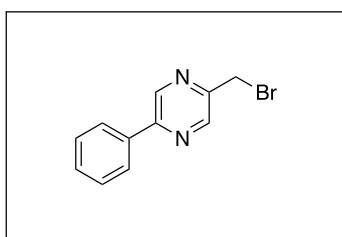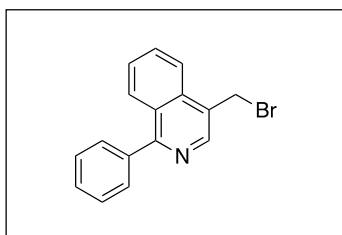
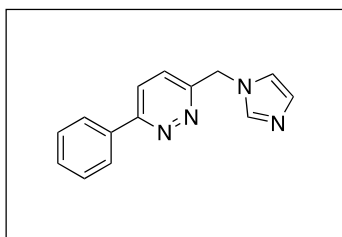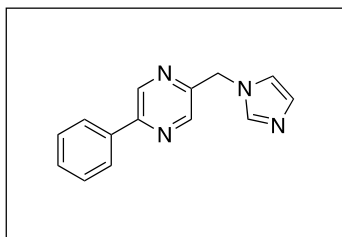**5-(Bromomethyl)-2-phenylpyrimidine (36).** Synthesized using compound **32** (205 mg, 1.20 mmol), NBS (236 mg, 1.32 mmol) and DBPO (14.6 mg, 0.06 mmol) in carbon tetrachloride according to Method D. Crude product was purified by flash chromatography on silica-gel using hexane / ethyl acetate (10:1) as eluent. Product was used directly in the next step without further characterization. White solid. Yield: 89 mg, 30%. (ESI): m/z = 250.68 $[M + H]^+$.
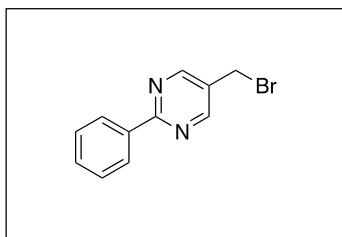
4-(Bromomethyl)-1-phenylisoquinoline (37). Synthesized using compound **33** (4.21 g, 19.2 mmol), NBS (3.76 g, 21.1 mmol) and DBPO (233 mg, 0.96 mmol) in carbon tetrachloride according to Method D. Crude product was purified by flash chromatography on silica-gel using a mixture of hexane / ethyl acetate (8:1→2:1) as eluent. Light yellow solid. Yield: 710 mg, 12%. ^{1}H NMR (CDCl$_3$, 500 MHz): δ_H (ppm) = 4.94 (s, 2 H), 7.47–7.54 (m, 3 H), 7.57 (ddd, J = 8.4, 7.0, 1.1 Hz, 1 H), 7.64–7.67 (m, 2 H), 7.82 (ddd, J=8.4, 7.0, 1.3 Hz, 1 H), 8.14 (m, 1 H), 8.18 (m, 1 H), 8.64 (s, 1 H); ^{13}C NMR (CDCl$_3$, 125 MHz): δ_C (ppm) = 28.5, 123.3, 126.1, 126.7, 127.4, 128.4, 128.4, 128.5, 128.9, 129.9, 130.0, 130.6, 134.6, 139.2, 142.6, 162.3; (ESI): m/z = 299.59 $[M + H]^+$.

3-((1*H*-Imidazol-1-yl)methyl)-6-phenylpyridazine (38). Synthesized using compound **34** (40 mg, 0.16 mmol), imidazole (44 mg, 0.64 mmol) and K$_2$CO$_3$ (111 mg, 0.80 mmol) in acetonitrile according to Method E. The crude product was purified by flash chromatography on silica-gel using ethyl acetate as eluent. After flash chromatography the solid was washed with ethyl acetate. Light orange solid. Yield: 22 mg, 58%. Mp: 145–148 °C (ethyl acetate). ^{1}H NMR (CDCl$_3$, 500 MHz): δ_H (ppm) = 5.58 (s, 2H), 7.08 (s, 1H), 7.17–7.26 (m, 2H), 7.55–7.61 (m, 3H), 7.72 (s, 1H), 7.88 (d, J = 8.8 Hz, 1H), 8.09–8.14 (m, 2H); ^{13}C NMR (CDCl$_3$, 125 MHz): δ_C (ppm) = 50.9, 119.6, 125.1, 125.5, 127.4, 129.4, 130.7, 130.8, 135.8, 137.8, 157.2, 159.3; MS (ESI): m/z = 236.91 $[M + H]^+$.
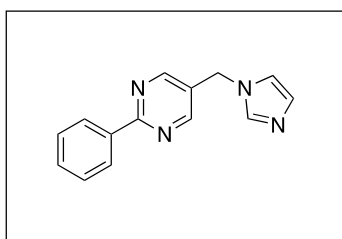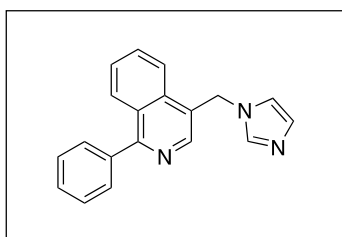
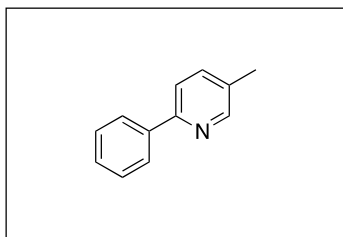**2-((1H-Imidazol-1-yl)methyl)-5-phenylpyrazine (39).** Synthesized using compound **35** (100 mg, 0.40 mmol), imidazole (109 mg, 1.60 mmol) and K_2CO_3 (276 mg, 2.00 mmol) in DMF according to Method E. Crude product was purified by flash chromatography on silica-gel using ethyl acetate as eluent. Light yellow solid. Yield: 69 mg, 73%. Mp: 152–154 °C (ethyl acetate). ^{1}H NMR (CDCl$_3$, 500 MHz): δ_H (ppm) = 5.50 (s, 2H), 7.24 (t, J = 1.3 Hz, 1H), 7.33 (t, J = 1.1 Hz, 1H), 7.64–7.74 (m, 3H), 7.86 (s, 1H), 8.17–8.23 (m, 2H), 8.63 (d, J = 1.3 Hz, 1H), 9.18 (d, J = 1.6 Hz, 1H); ^{13}C NMR (CDCl$_3$, 125 MHz): δ_C (ppm) = 50.0, 119.2, 126.9, 129.1, 130.2, 130.3, 135.7, 137.5, 141.5, 142.3, 152.3; MS (ESI): m/z = 236.91 [M + H]$^+$.

5-((1H-Imidazol-1-yl)methyl-2-phenylpyrimidine (40). Synthesized using compound **36** (70 mg, 0.28 mmol), imidazole (76 mg, 1.12 mmol) and K_2CO_3 (195 mg, 1.41 mmol) in acetonitrile according to Method E. Crude product was purified by flash chromatography on silica-gel using ethyl acetate as eluent. After flash chromatography the product was recrystallized in ethyl acetate. Light yellow solid. Yield: 62 mg, 94%. Mp: 155–157 °C (ethyl acetate). ^{1}H NMR (CDCl$_3$, 500 MHz): δ_H (ppm) = 5.17 (s, 2H), 6.94 (t, J = 1.3 Hz, 1H), 7.15 (t, J = 1.1 Hz, 1H), 7.47–7.54 (m, 3H), 7.61 (s, 1H), 8.41–8.46 (m, 2H), 8.63 (s, 2H); ^{13}C NMR (CDCl$_3$, 125 MHz): δ_C (ppm) = 46.0, 118.8, 127.0, 128.2, 128.7, 130.7, 131.1, 136.8, 137.2, 156.2, 164.8; MS (ESI): m/z = 236.92 [M + H]$^+$.

4-((1H-Imidazol-1-yl)methyl)-1-phenylisoquinoline (41). Synthesized using compound **37** (110 mg, 0.37 mmol), imidazole (101 mg, 1.48 mmol), and K_2CO_3 (256 mg, 1.85 mmol) in DMF according to method E. Crude product was purified by flash chromatography on silica gel using a mixture of ethyl acetate/methanol (9:1) as eluent. White solid. Yield: 30 mg, 28%. Melting point: 138−140 °C (eth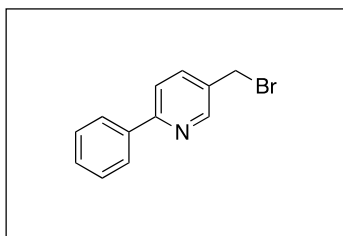yl acetate). ^{1}H NMR (CDCl$_3$, 500 MHz): δ_H (ppm) = 5.56 (s, 2H), 6.96 (m, 1H), 7.09 (m, 1H), 7.49−7.60 (m, 4H), 7.62 (s, 1H), 7.66−7.75 (m, 3H), 7.86 (d, J = 8.2 Hz, 1H), 8.17 (d, J = 8.5 Hz, 1H), 8.49 (s, 1H). ^{13}C NMR (CDCl$_3$, 125 MHz): δ_C (ppm) = 46.5, 119.1, 122.0, 123.4, 126.5, 127.4, 128.3, 128.7, 128.9, 129.8, 129.8, 131.0, 134.7, 137.1, 139.0, 142.5, 162.4. MS (ESI): m/z = 285.96 [M + H]$^+$.

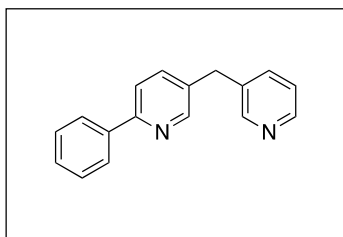**5-Methyl-2-phenylpyridine (42).** Synthesized using 2-bromo-5-methylpyridine (2.92 g, 16.95 mmol) and phenylboronic acid (3.09 g, 25.4 mmol) according to method A. Crude product was purified by flash chromatography on silica gel using a mixture of hexane/ethyl acetate (8:1) as eluent. White solid. Yield: 1.99 g, 70%. ^{1}H NMR (CDCl$_3$, 500 MHz): δ_H (ppm) = 2.38 (s, 3H), 7.37−7.43 (m, 1H), 7.44−7.51 (m, 2H), 7.54−7.60 (m, 1H), 7.60−7.67 (m, 1H), 7.95− 8.00 (m, 2H), 8.51−8.55 (m, 1H). ^{13}C NMR (CDCl$_3$, 125 MHz): δ_C (ppm) = 18.1, 120.0, 126.7, 128.6, 128.7, 131.5, 137.3, 139.4, 150.1, 154.8. MS (ESI): m/z = 169.97 [M + H]$^+$.

5-(Bromomethyl)-2-phenylpyridine (43). Synthesized using compound **42** (760 mg, 4.49 mmol), NBS (878 mg, 4.93 mmol), and DBPO (54 mg, 0.23 mmol) in carbon tetrachloride according to method D. Crude product was purified by flash chromatography on silica gel using hexane/ethyl acetate (8:1) as eluent. White solid. Yield: 297 mg, 73%. ^{1}H NMR (CDCl$_3$, 500 MHz): δ_H (ppm) = 4.54 (s, 2H), 7.42−7.53 (m, 3H), 7.71−7.77 (m, 1H), 7.80−7.85 (m, 1H), 7.98−8.04 (m, 2H), 8.72−8.76 (m, 1H). ^{13}C NMR (CDCl$_3$, 125 MHz): δ_C (ppm) = 29.7, 120.6, 127.0, 128.4, 128.8, 130.1, 137.6, 138.5, 149.6, 157.36. MS (ESI): m/z = 249.66 [M + H]$^+$.

2-Phenyl-5-(pyridin-3-ylmethyl)pyridine (44). Synthesized using compound **43** (100 mg, 0.40 mmol) and 3-pyridineboronic acid (74 mg, 0.61 mmol) according to method A. Crude product was purified by flash chromatography on silica gel using a mixture of hexane/ethyl acetate (2:1) as eluent. After flash chromatography, the product was dissolved in ethyl acetate, and a few drops of conc HCl and water were added. After stirring for 30 min, the phases were separated and aqueous phase was neutralized with aqueous Na$_2$CO$_3$ solution (2M). After extraction with ethyl acetate and drying over MgSO$_4$, the solvent was removed under vacuum. Beige solid. Yield: 32 mg, 32%. Melting point: 86−88 °C (ethyl acetate). ^{1}H NMR (CDCl$_3$, 500 MHz): δ_H (ppm) = 3.80 (s, 2H), 6.99−7.06 (m, 1H), 7.15−7.20 (m, 1H), 7.21− 7.35 (m, 4H), 7.45 (d, J = 8.2 Hz, 1H), 7.72−7.77 (m, 2H), 8.28 (dd, J = 4.7, 1.3 Hz, 1 H), 8.36 (d, J = 1.9 Hz, 1 H), 8.33 (d, J = 1.9 Hz, 1 H). ^{13}C NMR (CDCl$_3$, 125 MHz): δ_C (ppm) = 35.9, 120.4, 123.6, 126.8, 128.7, 128.9, 133.6, 135.4, 136.2, 137.0, 139.0, 148.1, 149.9, 150.1, 155.9. MS (ESI): m/z = 246.98 [M + H]$^+$.
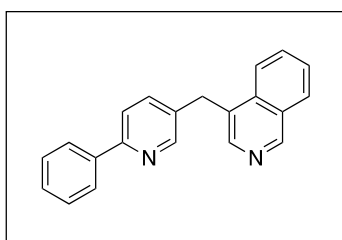
2-Phenyl-5-(pyridin-4-ylmethyl)pyridine (45). Synthesized using compound **43** (355 mg, 1.43 mmol) and 4-pyridineboronic acid (264 mg, 2.15 mmol) according to method A. Crude product was purified by flash chromatography on silica gel using a mixture of hexane/ethyl acetate (2:1) as eluent. After flash chromatography the product was dissolved in ethyl acetate, and a few drops of conc HCl and water were added. After stirring for 30 min, the phases were separated and aqueous phase was neutralized with aqueous Na_2CO_3 solution (2M). After extraction with ethyl acetate and drying over $MgSO_4$, the solvent was removed under vacuum. Beige solid. Yield: 140 mg, 40%. Melting point: 72−75 °C (ethyl acetate). ^{1}H NMR (CDCl$_3$, 500 MHz): δ_H (ppm) = 3.77 (s, 2H), 6.88−6.93 (m, 2H), 7.15−7.21 (m, 1H), 7.21− 7.31 (m, 3H), 7.45 (dd, J = 8.2, 0.9 Hz, 1H), 7.72−7.78 (m, 2H), 8.28−8.33 (m, 2H), 8.33−8.37 (m, 1H). ^{13}C NMR (CDCl$_3$, 125 MHz): δ_C (ppm) = 38.0, 120.3, 124.0, 126.7, 128.7, 128.9, 132.7, 137.1, 138.9, 148.7, 149.9, 150.0, 156.0. MS (ESI): m/z = 246.85 [M + H]$^+$.
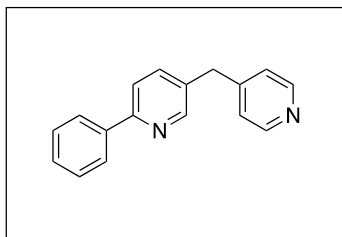
4-((6-Phenylpyridin-3-yl)methyl)isoquinoline (46). Synthesized using compound **43** (109 mg, 0.44 mmol) and 4-isoquinolineboronic acid (114 mg, 0.66 mmol) according to method A. Crude product was purified by flash chromatography on silica gel using a mixture of hexane/ethyl acetate (3:1) as eluent. After flash chromatography, the product was dissolved in ethyl acetate and a few drops of conc HCl and water were added. After stirring for 30 min, the phases were separated and aqueous phase was neutralized with aqueous Na_2CO_3 solution (2M). After extraction with ethyl acetate and drying over $MgSO_4$, the solvent was removed under vacuum. Beige solid. Yield: 20 mg, 19%. Melting point: 133−136 °C (ethyl acetate). ^{1}H NMR (CDCl$_3$, 500 MHz): δ_H (ppm) = 4.43 (s, 2H), 7.37−7.54 (m, 4H), 7.59−7.65 (m, 2H), 7.65−7.75 (m, 1H), 7.89−8.07 (m, 4H), 8.48 (s, 1H), 8.65−8.70 (m, 1H), 9.23 (s, 1H). ^{13}C NMR (CDCl$_3$, 125 MHz): δ_C (ppm) = 33.2, 120.3, 123.1, 126.7, 127.2, 128.4, 128.6, 128.6, 128.7, 128.9, 130.7, 133.6, 134.6, 136.7, 139.0, 143.7, 149.7, 152.3, 155.7. MS (ESI): m/z = 296.95 [M + H]$^+$.
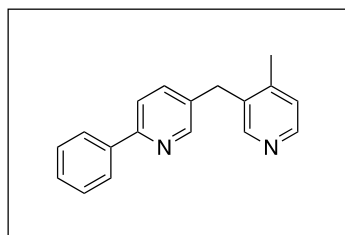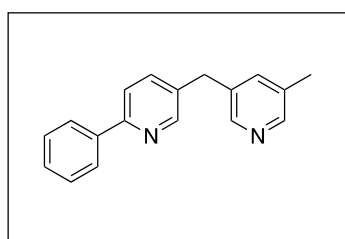
5-((6-Phenylpyridin-3-yl)methyl)pyrimidine (47). Synthesized using compound **43** (219 mg, 0.88 mmol) and pyrimidine-5-boronic acid (164 mg, 1.32 mmol) according to Method A. Crude product was purified by flash chromatography on silica-gel using a mixture of hexane / ethyl acetate (1:1) as eluent. After flash chromatography the product was dissolved in ethyl acetate and a few drops of conc. HCl and water
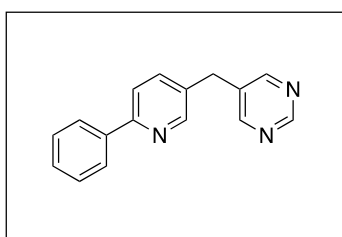
were added. After stirring for 30 minutes the phases were separated and aqueous phase was neutralized with aqueous Na_2CO_3 solution (2M). After extraction with ethyl acetate and drying over $MgSO_4$ the solvent was removed under vacuum. White solid. Yield: 43 mg, 20%. Mp: 128–130 °C (ethyl acetate). ^{1}H NMR ($CDCl_3$, 500 MHz): δ_H (ppm) = 4.02 (s, 2H), 7.39–7.44 (m, 1H), 7.44–7.56 (m, 3H), 7.70 (dd, J = 8.2, 0.9 Hz, 1H), 7.95–8.00 (m, 2H), 8.58–8.67 (m, 3 H), 9.13 (s, 1H); ^{13}C NMR ($CDCl_3$, 125 MHz): δ_C (ppm) = 33.4, 120.5, 126.8, 128.8, 129.1, 132.2, 133.3, 136.9, 138.7, 149.7, 156.4, 156.9, 157.3; MS (ESI): m/z = 247.83 [M + H][+].

5-((4-Methylpyridin-3-yl)methyl)-2-phenylpyridine (48). Synthesized using compound **43** (100 mg, 0.40 mmol) and 4-methylpyridine-3-boronic acid (83 mg, 0.61 mmol) according to method A. Crude product was purified by flash chromatography on silica gel using ethyl acetate as eluent. After flash chromatography, the product was dissolved in ethyl acetate and a few drops of conc HCl and water were added. After stirring for 30 min, the phases were separated and aqueous phase was neutralized with aqueous Na_2CO_3 solution (2M). After extraction with ethyl acetate and drying over $MgSO_4$, the solvent was removed under vacuum. Light-yellow solid. Yield: 54 mg, 52%. Melting point: 82−84 °C (ethyl acetate). ^{1}H NMR ($CDCl_3$, 500 MHz): δ_H (ppm) = 2.22−2.29 (m, 3H), 4.02 (s, 2H), 7.11 (d, J = 5.0 Hz, 1H), 7.37−7.51 (m, 4H), 7.64 (dd, J = 8.2, 0.6 Hz, 1H), 7.95− 8.01 (m, 2H), 8.38−8.46 (m, 2H), 8.52−8.57 (m, 1H). ^{13}C NMR ($CDCl_3$, 125 MHz): δ_C (ppm) = 19.3, 33.8, 120.5, 125.7, 126.9, 129.0, 129.1, 133.2, 133.8, 136.8, 139.2, 146.1, 148.7, 149.9, 150.7, 155.9. MS (ESI): m/z = 260.85 [M + H][+].

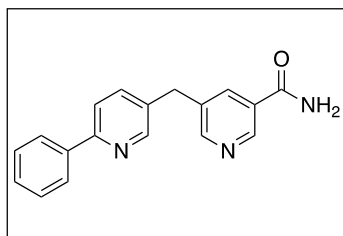**5-((5-Methylpyridin-3-yl)methyl)-2-phenylpyridine (49).** Synthesized using compound **43** (70 mg, 0.28 mmol) and 5-methylpyridine- 3-boronic acid (58 mg, 0.42 mmol) according to method A. Crude product was purified by flash chromatography on silica gel using ethyl acetate as eluent. After flash chromatography, the product was dissolved in ethyl acetate and a few drops of conc HCl and water were added. After stirring for 30 min, the phases were separated and aqueous phase was neutralized with aqueous Na_2CO_3 solution (2M). After extraction with ethyl acetate and drying over $MgSO_4$, the solvent was removed under vacuum. Light-yellow solid. Yield: 56 mg, 77%. Melting point: 79−81 °C (ethyl acetate). ^{1}H NMR ($CDCl_3$, 500 MHz): δ_H (ppm) = 2.30 (d, J = 0.6 Hz, 3H), 3.98 (s, 2H), 7.28−7.32 (m, 1H), 7.38−7.44 (m, 1H), 7.44−7.55 (m, 3H), 7.67 (dd, J = 8.0, 0.8 Hz, 1H), 7.96 − 8.01 (m, 2H), 8.36 (d, J = 1.6 Hz, 1H), 8.33 (d, J = 1.6 Hz, 1H), 8.58 (dd, J = 1.6, 0.6 Hz, 1H). ^{13}C NMR ($CDCl_3$, 125

MHz): δ_C (ppm) = 18.3, 35.7, 120.4, 126.7, 128.7, 128.9, 133.1, 133.8, 134.8, 136.8, 137.0, 139.0, 147.2, 148.6, 149.8, 155.8. MS (ESI): m/z = 260.84 [M + H]$^+$.
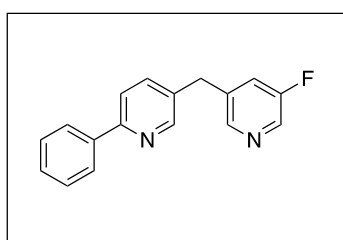
5-((6-Phenylpyridin-3-yl)methyl)nicotinamide (50). Synthesized using compound **43** (57.0 mg, 0.23 mmol) and 5-(4,4,5,5- tetramethyl-1,3,2-dioxaborolan-2-yl)nicotinonitrile (64.0 mg, 0.28 mmol), Cs$_2$CO$_3$ (225 mg, 0.7 mmol), and PdCl$_2$(dppf) (8.40 mg, 0.01 mmol) according to method F. Crude product was purified by flash chromatography on silica gel using a mixture of ethyl acetate/ methanol (10:1) as eluent. White solid. Yield: 18.0 mg, 27%. Melting point: 170−173 °C (ethyl acetate). ^{1}H NMR (DMSO-d$_6$, 500 MHz): δ_H (ppm) = 4.11 (s, 2H), 7.36−7.53 (m, 3H), 7.58 (s, 1H), 7.76 (dd, J = 8.2, 1.9 Hz, 1H), 7.90 (d, J = 7.9 Hz, 1H), 8.05 (d, J = 7.3 Hz, 2H), 8.08−8.22 (m, 2H), 8.61−8.68 (m, 1H), 8.71 (d, J = 1.6 Hz, 1H), 8.90 (d, J = 1.6 Hz, 1H); ^{13}C NMR (DMSO-d$_6$, 125 MHz): δ_C (ppm) = 34.5, 120.1, 126.4, 128.7, 128.9, 129.6, 134.5, 135.2, 135.9, 137.4, 138.4, 146.6, 149.7, 152.0, 154.3, 166.3. MS (ESI): m/z = 290.04 [M + H]$^+$.
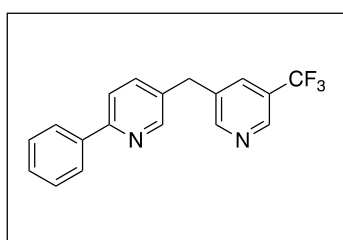
5-((5-Fluoropyridin-3-yl)methyl)-2-phenylpyridine (51). Synthesized using compound **43** (57.0 mg, 0.23 mmol) and 5- fluoropyridine-3-boronic acid (39.0 mg, 0.28 mmol), Cs$_2$CO$_3$ (225 mg, 0.7 mmol), and PdCl$_2$(dppf) (50 mg, 0.07 mmol) according to method F. Crude product was purified by flash chromatography on silica gel using a mixture of hexane/ethyl acetate (2:1) as eluent. White solid. Yield: 20.0 mg, 33%. Melting point: 89−92 °C (ethyl acetate). ^{1}H NMR (CDCl$_3$, 500 MHz): δ_H (ppm) = 4.05 (s, 2H), 7.19−7.23 (m, 1H), 7.39−7.44 (m, 1H), 7.45−7.50 (m, 2H), 7.53 (dd, J = 8.2, 2.5 Hz, 1H), 7.70 (dd, J = 8.2, 0.6 Hz, 1H), 7.96−8.00 (m, 2H), 8.36−8.40 (m, 2H), 8.57−8.60 (m, 1H). ^{13}C NMR (CDCl$_3$, 125 MHz): δ_C (ppm) = 35.6, 120.7, 123.1, 123.3, 127.0, 129.0, 129.2, 133.0, 136.6, 136.8, 137.3, 137.4, 137.4, 139.1, 146.0, 146.1, 150.1, 156.4, 158.8, 160.8. MS (ESI): m/z = 265.00 [M + H]$^+$.

**2-Phenyl-5-((5-(trifluoromethyl)pyridin-3-yl)methyl) pyridine (52).** To a solution of 3-bromo-5-(trifluoromethyl)pyridine (502 mg, 2.22 mmol) in THF (20 mL) was added trimethylborate (240 mg, 26.0 mL, 2.31 mmol) under nitrogen atmosphere. After the mixture was cooled to −78 °C, *n*-BuLi (1.6 M in hexane, 1.45 mL, 2.32 mmol) was added dropwise over 10 min, keeping the temperature below 65 °C. Then the reaction mixture was slowly warmed to room temperature and stirred for 1 h. Afterward, HCl (1M, 10 mL)

was added and the mixture was stirred for 15 min. The phases were separated, and the organic phase was washed with HCl (1M, 20 mL). The aqueous layers are combined and washed with ethyl acetate (2 × 20 mL). Afterward, the aqueous phases were neutralized with sodium hydroxide solution (2M) and extracted with ethyl acetate (2 × 20 mL). The solvent was evaporated in vacuum, and 5-(trifluoromethyl)pyridine-3-boronic acid (113 mg, yellow solid) was obtained. The boronic acid was directly used in the next step without further characterization and purification. A mixture of compound **43** (171 mg, 0.69 mmol), 5-(trifluoromethyl)pyridine-3- boronic acid (113 mg, 0.59 mmol), Cs_2CO_3 (684 mg, 2.10 mmol), and $PdCl_2$(dppf) (26 mg, 0.04 mmol) was used for synthesis according to method F. Crude product was purified by flash chromatography on silica gel using a mixture of hexane/ethyl acetate (5:1) as eluent. White solid. Yield: 22 mg, 10%. Melting point: 95−98 °C (ethyl acetate). ^{1}H NMR (CDCl$_3$, 500 MHz): δ_H (ppm) = 4.11 (s, 2H), 7.40−7.56 (m, 4H), 7.69−7.76 (m, 2H), 7.97−8.02 (m, 2H), 8.58−8.61 (m, 1H), 8.73 (s, 1H), 8.80 (s, 1H). ^{13}C NMR (CDCl$_3$, 125 MHz): δ_C (ppm) = 35.7, 120.6, 126.8, 128.8, 129.1, 132.4, 133.1, 133.1, 135.7, 137.0, 138.8, 144.9, 145.0, 149.8, 153.3, 153.3, 156.4. MS (ESI): m/z = 314.87 [M + H]$^+$.

5-((5-Methoxypyridin-3-yl)methyl)-2-phenylpyridine (53). Synthesized using compound **43**
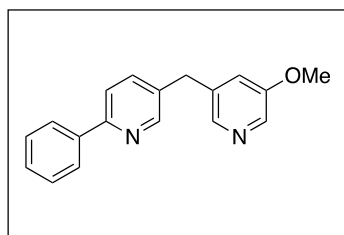
(338 mg, 1.36 mmol), 3-methoxy-5-(4,4,5,5-tetramethyl-1,3,2-dioxaborolan-2-yl)pyridine (413 mg, 1.76 mmol), Cs_2CO_3 (1.33 g, 4.10 mmol), and $PdCl_2$(dppf) (50 mg, 0.07 mmol) according to method F. Crude product was purified by flash chromatography on silica gel using a mixture of hexane/ethyl acetate (1:1→1:2) as eluent. Light-yellow solid. Yield: 145 mg, 39%. Melting point: 102−105 °C (ethyl acetate). ^{1}H NMR (CDCl$_3$, 500 MHz): δ_H (ppm) = 3.82 (s, 3H), 4.01 (s, 2H), 6.98−7.01 (m, 1H), 7.39−7.44 (m, 1H), 7.45−7.50 (m, 2H), 7.53 (dd, J = 8.2, 2.2 Hz, 1H), 7.68 (dd, J = 8.2, 0.9 Hz, 1H), 7.96−7.99 (m, 2H), 8.17 (d, J = 1.6 Hz, 1H), 8.21 (d, J = 2.8 Hz, 1H), 8.59 (dd, J = 1.6, 0.6 Hz, 1H). ^{13}C NMR (CDCl$_3$, 125 MHz): δ_C (ppm)= 35.7, 55.5, 120.4, 120.9, 126.7, 128.7, 128.9, 133.6, 135.7, 136.0, 137.0, 139.0, 142.3, 149.8, 155.8, 155.9. MS (ESI): m/z = 276.95 [M + H]$^+$.

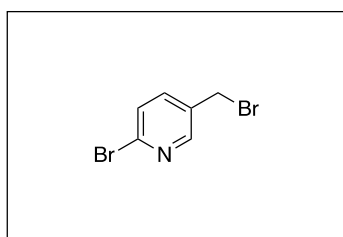**5-((6-Phenylpyridin-3-yl)methyl)pyridin-3-ol (54).** Compound **53** (145 mg, 0.53 mmol) was
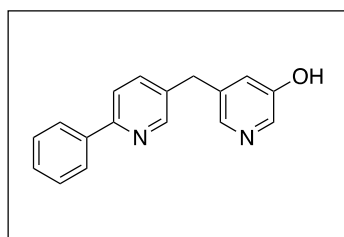
suspended in HBr (48% in water, 5 mL), and the mixture was stirred at 130 °C overnight. After cooling down to room temperature, saturated Na_2CO_3 solution was added to neutralize the mixture. After extraction with ethyl acetate (3 × 10 mL) and drying over $MgSO_4$, the solvent was removed under vacuum. The crude product was dissolved in ethyl acetate, and a few drops of conc HCl and water were added. After stirring for

30 min, the phases were separated and aqueous phase was neutralized with aqueous Na_2CO_3 solution (2M). After extraction with ethyl acetate and drying over $MgSO_4$, the solvent was removed under vacuum. Light-yellow solid. Yield: 100 mg, 72%. Melting point: 181−183 °C (ethyl acetate). ^{1}H NMR (DMSO-d6, 500 MHz): δ_H (ppm) = 3.97 (s, 2H), 7.02 (dd, J = 2.8, 1.9 Hz, 1H), 7.39−7.43 (m, 1H), 7.45−7.50 (m, 2H), 7.72 (dd, J = 8.2, 2.2 Hz, 1H), 7.89 (dd, J = 8.2, 0.6 Hz, 1H), 7.99 (d, J = 2.5 Hz, 1H), 8.01−8.07 (m, 3H), 8.59−8.62 (m, 1H), 9.83 (s, 1H). ^{13}C NMR (DMSO-d6, 125 MHz): δ_C (ppm) = 34.4, 120.0, 122.0, 126.3, 128.7, 128.8, 134.9, 136.1, 136.7, 137.3, 138.5, 140.4, 149.6, 153.6, 154.2. MS (ESI): m/z = 263.00 [M + H]+.
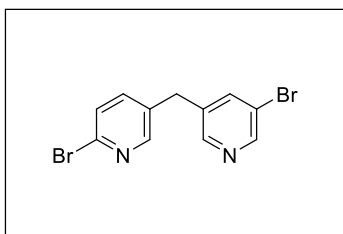
2-Bromo-5-(bromomethyl)pyridine (55). Synthesized using 2-bromo-5-methylpyridine (2.30 g, 13.4 mmol), NBS (2.62 g, 14.7 mmol), and DBPO (162 mg, 0.67 mmol) in carbon tetrachloride according to method D. Crude product was purified by flash chromatography on silica gel using a mixture of hexane/ethyl acetate (15:1→8:1) as eluent. Yellow solid. Yield: 1.50 g, 45%. ^{1}H NMR (CDCl3, 500 MHz): δ_H (ppm) = 4.42 (s, 2H), 7.49 (dd, J = 8.2, 0.9 Hz, 1H), 7.58−7.62 (m, 1H), 8.39 (dd, J = 2.5, 0.6 Hz, 1H). MS (ESI): m/z = 251.62 [M + H]+.
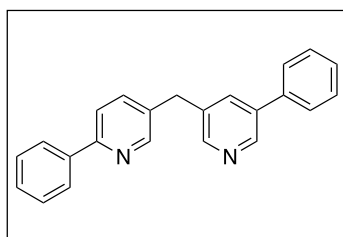
2-Bromo-5-((5-bromopyridin-3-yl)methyl)pyridine (56). Synthesized using compound **55** (283 mg, 1.13 mmol) and 5-bromopyridine-3-boronic acid (228 mg, 1.13 mmol) according to method A. Crude product was purified by flash chromatography on silica gel using a mixture of hexane/ethyl acetate (5:1) as eluent. White solid. Yield: 70.0 mg, 19%. ^{1}H NMR (CDCl3, 500 MHz): δ_H (ppm) = 3.94 (s, 2H), 7.33 (dd, J = 8.2, 2.5 Hz, 1H), 7.45 (d, J = 8.2Hz, 1H), 7.61 (s, 1H), 8.27 (d, J = 2.2 Hz, 1H), 8.42 (s, 1H), 8.58 (s, 1H). ^{13}C NMR (CDCl3, 125 MHz): δ_C (ppm) = 35.0, 121.1, 128.3, 133.7, 136.5, 138.9, 138.9, 140.8, 147.8, 149.3, 150.2. MS (ESI): m/z = 328.64 [M + H]+.

**2-Phenyl-5-((5-phenylpyridin-3-yl)methyl)pyridine (57).** Synthesized using compound **56** (70.0 mg, 0.21 mmol) and phenylboronic acid (96.0 mg, 0.64 mmol) according to method A. Crude product was purified by flash chromatography on silica gel using a mixture of hexane/ethyl acetate (5:1) as eluent. After flash chromatography, the product was dissolved in ethyl acetate and a few drops of conc HCl and water were added. After stirring for 30 min, the phases were separated and aqueous phase was

102

neutralized with aqueous Na_2CO_3 solution (2M). After extraction with ethyl acetate and drying over $MgSO_4$, the solvent was removed under vacuum. White solid. Yield: 49.0 mg, 72%. Melting point: 115−117 °C (ethyl acetate). ^{1}H NMR (CDCl$_3$, 500 MHz): δ_H (ppm) = 4.09 (s, 2H), 7.37−7.44 (m, 2H), 7.44−7.50 (m, 4H), 7.53−7.59 (m, 3H), 7.67−7.70 (m, 2H), 7.97− 8.02 (m, 2H), 8.53 (d, J = 2.2 Hz, 1H), 8.63−8.66 (m, 1H), 8.75 (d, J = 2.2Hz, 1H). ^{13}C NMR (CDCl$_3$, 125 MHz): δ_C (ppm) = 35.8, 120.4, 126.7, 127.1, 128.1, 128.7, 128.9, 129.0, 133.5, 134.6, 135.2, 136.6, 137.0, 137.4, 138.9, 146.6, 148.6, 149.8, 155.9. MS (ESI): m/z = 322.95 [M + H]$^+$.

5-Bromo-2-phenylpyridine (58). Synthesized using 2-iodo-5-bromopyridine (1.79 g, 6.3 mmol) and phenylboronic acid (1 eq, 770 mg, 6.3 mmol) according to Method A. Crude product was
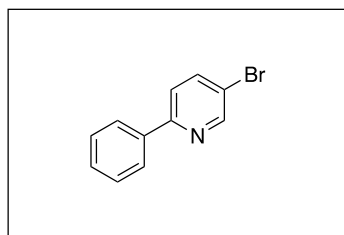
purified by flash chromatography on silica-gel using a mixture of hexane / ethyl acetate (50:1→30:1) as eluent. Product was used directly in the next step without further characterization. White solid. Yield: 841 mg, 57%. MS (ESI): m/z = 235.83 [M + H]$^+$.

5-Iodo-2-phenylpyridine (59). To a mixture of NaI (2.20 g, 14.8 mmol) and CuI (71.0 mg, 0.37
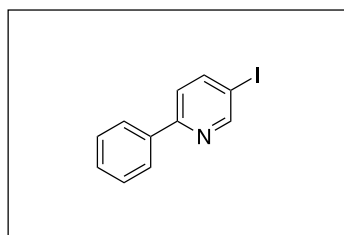
mmol) $N,N^{'}$-dimethylethylendiamin (65.0 mg, 0.74 mmol), **58** (1.74 g, 7.42 mmol) and dioxane (30 mL) were added under nitrogen atmosphere. The reaction mixture was stirred for 21 h at 110 °C followed by the addition of an ammonia solution (30% in water, 5 mL) and water (20 mL). The aqueous phase was extracted with DCM (4 × 30 mL) and then the combined organic phases were dried over $MgSO_4$. The solvent was removed under vacuum and the crude product was purified by flash chromatography on silica-gel using a mixture of hexane / ethyl acetate (40:1) as eluent. Product was used directly in the next step without further characterization. Light yellow solid. Yield: 860 mg, 41%. (ESI): m/z = 281.86 [M + H]$^+$.

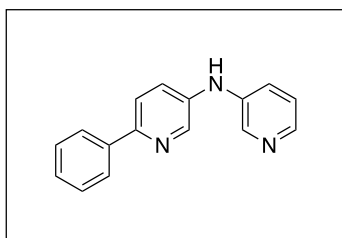**2-Phenyl-5-(pyridine-3-yloxy)pyridine (60).** A mixture of **59** (230 mg, 0.82 mmol), copper(I)
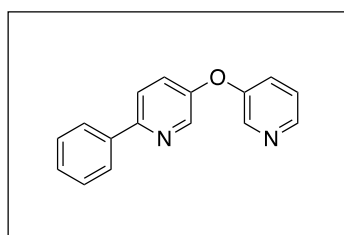
iodide (8.00 mg, 0.04 mmol), 2-picolinic acid (10.0 mg, 0.08 mmol), 3- hydroxypyridine (94.0 mg, 0.98 mmol) and K_3PO_4 (348 mg, 1.64 mmol) was dissolved in DMSO (5 mL) under nitrogen atmosphere. The reaction mixture was stirred for 24 h at 80 °C. After cooling down to room temperature ethyl acetate (10 mL) and H_2O (1mL) were added and the organic layer was separated. The aqueous layer was extracted with ethyl acetate (2 × 10 mL) and the combined organic phases were dried over $MgSO_4$. After filtration the

solvent was evaporated under vacuum and the resulting crude product was purified by flash chromatography on silica-gel using a mixture of hexane / ethyl acetate (2:1) as eluent. Light yellow solid. Yield: 38 mg, 19%. Mp: 150–152 °C (ethyl acetate). ^{1}H NMR (CDCl$_3$, 500 MHz): δ_H (ppm) = 7.29–7.33 (m, 1 H), 7.34–7.43 (m, 3 H), 7.45–7.50 (m, 2 H), 7.73 (m, 1 H), 7.95–7.99 (m, 2 H), 8.43 (dd, J = 4.6, 1.4 Hz, 1 H), 8.49 (d, J = 2.8 Hz, 1 H), 8.51 (m, 1 H); ^{13}C NMR (CDCl$_3$, 125 MHz): δ_C (ppm) = 121.1, 124.2, 125.4, 126.5, 126.6, 128.8, 128.8, 138.5, 141.1, 141.4, 145.1, 151.9, 153.2; MS (ESI): m/z = 249.04 [M + H]$^+$.
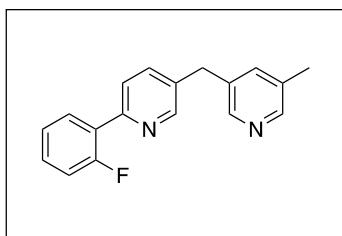
6-Phenyl-*N*-(pyridin-3-yl)pyridin-3-amine (61). A mixture of **59** (91.0 mg, 0.32 mmol), 3-aminopyridine (37.0 mg, 0.38 mmol) and Cs$_2$CO$_3$ (521 mg, 1.60 mmol) was dissolved in toluene (15 mL) under nitrogen atmosphere. Then, a fresh solution of Pd(OAc)$_2$-BINAP (under nitrogen atmosphere) Pd(OAc)$_2$ (2.00 mg, 0.01 mmol) and (±)-BINAP (6.00 mg, 0.01 mmol) were dissolved in toluene (5 mL) and stirred for 20 min at room temperature) in toluene was added. The resulting reaction mixture was heated under reflux overnight. After mixture was cooled down to room temperature, the solid material was filtered off and washed with DCM (100 mL). The filtrate was evaporated and the resulting crude product was purified by flash chromatography on silica-gel using a mixture of hexane / ethyl acetate (1:1→1:2→ ethyl acetate) as eluent. Orange solid. Yield: 47 mg, 52%. Mp: 157–159 °C (ethyl acetate). ^{1}H NMR (CDCl$_3$, 500 MHz): δ_H (ppm) = 6.50 (s, 1 H), 7.21 (dd, J = 8.2, 4.7 Hz, 1 H), 7.34– 7.40 (m, 1 H), 7.42–7.51 (m, 4 H), 7.65 (d, J = 8.5 Hz, 1 H), 7.92–7.96 (m, 2 H), 8.23 (dd, J = 4.7, 1.3 Hz, 1 H), 8.43 (d, J = 2.5 Hz, 1 H), 8.46–8.50 (m, 1 H); ^{13}C NMR (CDCl$_3$, 125 MHz): δ_C (ppm) = 120.7, 123.8, 123.9, 124.8, 126.2, 128.3, 128.7, 137.5, 138.9, 139.0, 140.2, 140.3, 142.6, 150.7; MS (ESI): m/z = 247.97 [M + H]$^+$.

**2-(2-Fluorophenyl)-5-((5-methylpyridin-3-yl)methyl)pyridine (67).** Synthesized using compound **95** (3:1 mixture of chloride and bromide, 150 mg, 0.65 mmol), 2-fluorophenylboronic acid (160 mg, 1.20 mmol), palladium(II) acetate (1.00 mg, 4.45 µmol), SPhos (5.00 mg, 12.2 µmol) and 2 M aqueous LiOH (1.15 mL, 2.30 mmol) according to method G. As the reaction was not completed after 12 h the same amount of boronic acid, SPhos , Pd(OAc)$_2$ and LiOH was added and the reaction mixture was stirred again for 2 h at 90 °C. Crude product was purified by flash chromatography on silica-gel using ethyl acetate as eluent. White solid. Yield: 113 mg, 62%. Mp 71–72 °C. ^{1}H NMR (Aceton-d$_6$, 500 MHz): δ_H (ppm) = 8.67 (d, J = 1.6 Hz, 1 H), 8.40 (d, J = 2.5 Hz, 1 H), 8.30 (d, J = 1.6 Hz,

1 H), 8.05 (td, *J* = 8.0, 1.7 Hz, 1 H), 7.78 (ddd, *J* = 8.2, 2.2, 1.0 Hz, 1 H), 7.73 (dd, *J* = 8.2, 2.2 Hz, 1 H), 7.50 (m, 1 H), 7.45 (m, 1 H), 7.30 (td, *J* = 7.6, 1.3 Hz, 1 H), 7.23 (ddd, *J* = 11.7, 8.3, 1.4 Hz, 1 H), 4.07 (s, 2 H), 2.28 (s, 3 H). ^{13}C NMR (Aceton-d$_6$, 125 MHz): δ_C (ppm) = 161.5 (d, $J_{C,F}$ = 248.4 Hz), 152.1 (d, $J_{C,F}$ = 1.8 Hz), 151.0, 149.3, 148.2, 137.6, 137.4, 136.3, 133.9, 132.0 (2 C), 131.4 (d, $J_{C,F}$ = 9.2 Hz), 128.1 (d, $J_{C,F}$ = 11.9 Hz), 125.5 (d, $J_{C,F}$ = 2.8 Hz), 124.9 (d, $J_{C,F}$ = 10.1 Hz), 117.0 (d, $J_{C,F}$ = 23.8 Hz), 36.1, 18.3. (ESI): m/z = 279 [M+H]$^+$.

N-(3-(5-((5-Methylpyridin-3-yl)methyl)pyridin-2-yl)phenyl)methanesulfonamide (68).
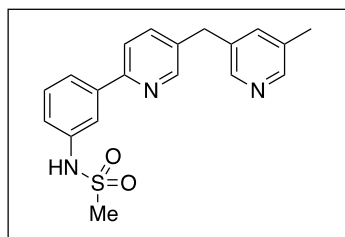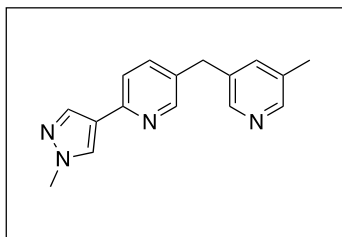

Synthesized using compound **95** (3:1 mixture of chloride and bromide, 100 mg, 0.44 mmol) and (3-(methylsulfonamido)phenyl)boronic acid (120 mg, 0.56 mmol) according to method A. The reaction mixture was stirred for 18 hours at 100 °C. Crude product was purified by flash chromatography on silica-gel using a mixture of dichloromethane/ methanol (95:5) as eluent. Afterwards the product was washed with diethylether. Beige solid. Yield: 101 mg, 65%. Mp 204–206 °C. ^{1}H NMR (CDCl$_3$, 500 MHz): δ_H (ppm) = 9.84 (br s, NH), 8.62 (d, *J* = 1.3 Hz, 1 H), 8.37 (br s, 1 H), 8.27 (br s, 1 H), 7.95 (m, 1 H), 7.83 (d, *J* = 7.8 Hz, 1 H), 7.74 (d, *J* = 7.8 Hz, 1 H), 7.50 (br s, 1 H), 7.43 (t, *J* = 7.9 Hz, 1 H), 7.27 (d, *J* = 8.0 Hz, 1 H), 4.00 (s, 2 H), 3.01 (s, 3 H), 2.25 (s, 3 H). ^{13}C NMR (CDCl$_3$, 125 MHz): δ_C (ppm) = 153.5, 149.6, 147.9, 146.8, 139.5, 138.9, 137.3, 136.5, 135.4, 135.2, 132.8, 129.6, 121.8, 120.1, 120.1, 117.6, 39.2, 34.5, 17.7. (ESI): *m/z* = 354 [M+H]$^+$.

2-(Furan-3-yl)-5-((5-methylpyridin-3-yl)methyl)pyridine (69). Synthesized using compound
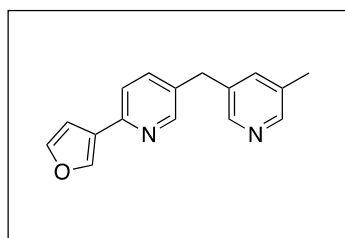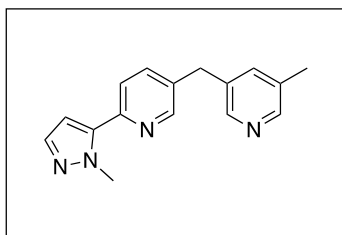

95 (3:1 mixture of chloride and bromide, 200 mg, 0.87 mmol) and furan-3-ylboronic acid (128 mg, 1.14 mmol) according to method A. The reaction mixture was stirred for 20 h at 100 °C. Crude product was purified by flash chromatography on silica-gel using a mixture of dichloromethane/methanol (98:2) as eluent. White solid. Yield: 168 mg, 77%. Mp 69–71 °C. ^{1}H NMR (CDCl$_3$, 500 MHz): δ_H (ppm) = 8.45 (m, 1 H), 8.30–8.31 (m, 2 H), 7.98 (dd, *J* = 1.5, 0.9 Hz, 1 H), 7.46 (t, *J* = 1.7 Hz, 1 H), 7.43 (dd, *J* = 8.1, 2.3 Hz, 1 H), 7.37 (dd, *J* = 8.1, 0.8 Hz, 1 H), 7.24 (m, 1 H), 6.89 (dd, *J* = 1.9, 0.9 Hz, 1 H), 3.92 (s, 2 H), 2.26 (d, *J* = 0.5 Hz, 3 H). ^{13}C NMR (CDCl$_3$, 125 MHz): δ_C (ppm) = 150.1, 149.8, 148.5, 147.1, 143.8, 141.0, 136.8, 136.7, 134.8, 133.4, 133.1, 126.7, 119.9, 108.5, 35.7, 18.2. (ESI): *m/z* = 251 [M+H]$^+$.

2-(1-Methyl-1*H*-pyrazol-4-yl)-5-((5-methylpyridin-3-yl)methyl)pyridine (70). Compound **95** (3:1 mixture of chloride and bromide, 100 mg, 0.44 mmol), 1-methylpyrazole-4-boronic acid pinacol ester (119 mg, 0.57 mmol), Cs_2CO_3 (310 mg, 0.95 mmol) and $PdCl_2$(dppf) (14.0 mg, 19.0 µmol) were dissolved under N_2 in degassed dimethoxyethane (4 mL). The reaction mixture was stirred under reflux overnight, afterwards diluted with water and extracted three times with diethyl ether. The combined organic layers were washed with water, brine, dried over Na_2SO_4, filtered and concentrated in vacuum. Crude product was purified by flash chromatography on silica-gel using a mixture of dichloromethane/methanol (98:2) as eluent. White solid. Yield: 37 mg, 32%. Mp 107–109 °C. ^{1}H NMR (DMSO-d$_6$, 500 MHz): δ_H (ppm) = 8.60–8.94 (m, 2 H), 8.57 (d, J = 2.5 Hz, 1 H), 8.37 (s, 1 H), 8.25 (s, 1 H), 8.07 (s, 1 H), 7.92 (dd, J = 8.4, 2.4 Hz, 1 H), 7.79 (d, J = 8.2 Hz, 1 H), 4.18 (s, 2 H), 3.90 (s, 3 H), 2.42 (s, 3 H). ^{13}C NMR (DMSO-d$_6$, 125 MHz): δ_C (ppm) = 150.1, 148.4, 146.8, 144.8, 141.4, 140.4, 140.1, 137.4, 132.7, 130.2, 120.5, 119.7, 38.8, 33.9, 17.7. (ESI): m/z = 265 [M+H]$^+$.
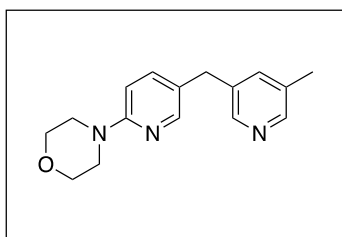
2-(1-Methyl-1*H*-pyrazol-5-yl)-5-((5-methylpyridin-3-yl)methyl)pyridine (71). Synthesized using compound **95** (3:1 mixture of chloride and bromide, 100 mg, 0.44 mmol), 1-methyl-5-(4,4,5,5-tetramethyl-1,3,2-dioxaborolan-2-yl)-1*H*-pyrazole (158 mg, 0.76 mmol), palladium(II) acetate (0.90 mg, 4.01 µmol), SPhos (3.00 mg, 7.31 µmol) and 2 M aqueous LiOH (0.76 mL, 1.52 mmol) according to method G. Crude product was purified by flash chromatography on silica-gel using a mixture of dichloromethane/methanol (92:8) as eluent. White solid. Yield: 60 mg, 52%. Mp 71–73 °C. ^{1}H NMR (Aceton-d$_6$, 500 MHz): δ_H (ppm) = 8.62 (d, J = 1.6 Hz, 1 H), 8.38 (d, J = 1.9 Hz, 1 H), 8.30 (d, J = 1.9 Hz, 1 H), 7.73 (dd, J = 8.2, 2.1 Hz, 1 H), 7.67 (dd, J = 8.2, 0.6 Hz, 1 H), 7.49 (m, 1 H), 7.41 (d, J = 2.2 Hz, 1 H), 6.67 (d, J = 1.9 Hz, 1 H), 4.17 (s, 3 H), 4.05 (s, 2 H), 2.28 (s, 3 H). ^{13}C NMR (Aceton-d$_6$, 125 MHz): δ_C (ppm) = 150.2, 149.3, 149.1, 148.2, 141.6, 138.5, 138.1, 137.4, 136.2, 136.0, 133.9, 123.3, 107.1, 40.0, 36.1, 18.3. (ESI): m/z = 265 [M+H]$^+$.

4-(5-((5-Methylpyridin-3-yl)methyl)pyridin-2-yl)morpholine (72). Compound **95** (3:1 mixture of chloride and bromide, 100 mg, 0.44 mmol) and morpholine (66.4, 0.76 mmol) was dissolved in degassed toluene (3 mL). Afterwards NaOEt (62.7 mg, 0.92 mmol), Pd(OAc)$_2$ (17.7 mg, 78.8 µmol) and SPhos (62.7 mg, 0.15 mmol) were added and the reaction mixture was stirred for 18 h at 80 °C. After cooling to room temperature, the

suspension was diluted with ethyl acetate and filtrated over celite. The solvent was removed in vacuum and the crude product was purified by flash chromatography on silica-gel using a mixture of ethyl acetate/ethanol (9:1) as eluent. White solid. Yield: 72 mg, 61%. Mp 91–92 °C. ^{1}H NMR (Aceton-d$_6$, 500 MHz): δ_H (ppm) = 8.30 (d, J = 1.8 Hz, 1 H), 8.25 (d, J = 1.6 Hz, 1 H), 8.10 (m, 1 H), 7.40–7.43 (m, 2 H), 6.73 (dd, J = 8.7, 0.6 Hz, 1 H), 3.85 (s, 2 H), 3.42–3.44 (m, 4 H), 2.27 (s, 3 H). ^{13}C NMR (Aceton-d$_6$, 75 MHz): δ_C (ppm) = 19.2, 36.5, 47.5, 68.2, 108.7, 127.4, 134.6, 138.0, 138.2, 139.7, 149.0, 149.4, 149.9, 160.5. (ESI): m/z = 270 [M+H]$^+$.

N-Cyclopropyl-5-((5-methylpyridin-3-yl)methyl)pyridin-2-amine (73). Compound **95** (3:1
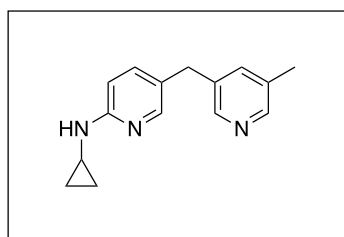
mixture of chloride and bromide, 800 mg, 3.48 mmol) was dissolved under N$_2$ in 40 ml dry toluene and cyclopropylamine (1.27 mL, 1.04 g, 18.2 mmol), sodium ethoxide (556 mg, 8.17 mmol), Pd(OAc)$_2$ (8.00 mg, 35.6 µmol) and SPhos (27.9 mg, 68 µmol) were added. The reaction mixture was stirred under reflux overnight and subsequently quenched with water. After extraction of the water phase with EtOAc thrice the combined organic layers were washed with water, brine, dried over Na$_2$SO$_4$, filtered and concentrated in vacuum. Crude product was purified by flash chromatography on silica-gel using a mixture of ethyl acetate/ethanol (9:1) as eluent. Pale yellow solid. Yield: 182 mg, 22%. Mp 81–83 °C. ^{1}H NMR (CDCl$_3$, 300 MHz): δ_H (ppm) = 8.31 (s, 1 H), 8.28 (s, 1 H), 7.81 (dd, J = 2.1, 0.6 Hz, 1 H), 7.43 (dd, J = 8.8, 2.2 Hz, 1 H), 7.24 (m, 1 H), 6.88 (d, J = 8.8 Hz, 1 H), 6.45 (br s, 1 H), 3.81 (s, 2 H), 2.52 (m, 1 H), 2.29 (d, J = 0.6 Hz, 3 H), 0.82 (m, 2 H), 0.62 (m, 2 H). ^{13}C NMR (CDCl$_3$, 75 MHz): δ_C (ppm) = 156.8, 148.6, 147.0, 142.3, 140.9, 136.7, 134.7, 133.2, 124.7, 108.3, 34.9, 23.9, 18.3, 7.5. (ESI): m/z = 240 [M+H]$^+$.

5-((5-Methylpyridin-3-yl)methyl)-2-(phenylthio)pyridine (74). Compound **95** (3:1 mixture of
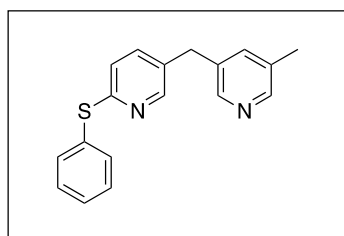

chloride and bromide, 500 mg, 2.18 mmol) was dissolved under N$_2$ in dimethylacetamid (10 mL), followed by addition of caesium carbonate (929 mg, 2.85 mmol) and thiophenol (0.23 g, 2.09 mmol). The reaction mixture was stirred at 90 °C overnight, quenched with water afterwards and extracted with EtOAc thrice. The combined organic layers were washed with water, brine, dried over Na$_2$SO$_4$, filtered and concentrated in vacuum. Crude product was purified by flash chromatography on silica-gel using ethyl acetate as eluent. As product showed some impurities, another column chromatography using a mixture of dichloromethane/methanol (97:3) as eluent was applied. Colorless oil. Yield: 75 mg, 12%. ^{1}H NMR (CDCl$_3$, 500 MHz): δ_H (ppm) = 8.32 (m, 1 H), 8.30 (s, 1 H), 8.28 (s, 1 H), 7.56–7.60 (m,

2 H), 7.37–7.44 (m, 3 H), 7.21–7.25 (m, 2 H), 6.84 (dd, J = 8.5, 0.6 Hz, 1 H), 3.86 (s, 2 H), 2.28 (d, J = 0.6 Hz, 3 H). ^{13}C NMR (CDCl$_3$, 125 MHz): δ_C (ppm) = 159.5, 149.6, 148.6, 147.0, 137.2, 136.7, 134.8, 134.7, 133.1, 131.7, 131.1, 129.6, 129.0, 121.4, 35.4, 18.3. (ESI): m/z = 293 [M+H]$^+$.

5-((5-Methylpyridin-3-yl)methyl)-2-(phenylsulfonyl)pyridine (75). To a solution of thioether
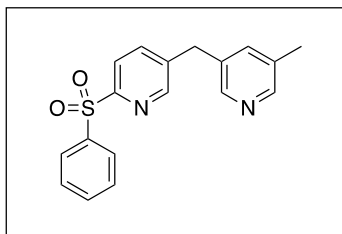
74 (62.0 mg, 0.21 mmol) in ethyl acetate (2 mL) water (2 mL) and potassium peroxymonosulfate (261 mg, 0.85 mmol) were added at room temperature and the reaction mixture was vigorously stirred for 4 h at room temperature. Saturated NaHCO$_3$-solution was added and the mixture was extracted with DCM. The combined organic layers were dried over Na$_2$SO$_4$ and concentrated in vacuum. Crude product was purified by flash chromatography on silica-gel using ethyl acetate as eluent. White solid. Yield: 60 mg, 88%. Mp 128–129 °C. ^{1}H NMR (CDCl$_3$, 500 MHz): δ_H (ppm) = 8.51 (dd, J = 2.2, 0.5 Hz, 1 H), 8.32 (s, 1 H), 8.16 (s, 1 H), 8.12 (d, J = 8.6 Hz, 1 H), 8.03–8.05 (m, 2 H), 7.66 (dd, J = 7.9, 2.2 Hz, 1 H), 7.60 (m, 1 H), 7.52 (m, 2 H), 7.22 (m, 1 H), 3.98 (s, 2 H), 2.27 (s, 3 H). ^{13}C NMR (CDCl$_3$, 125 MHz): δ_C (ppm) = 157.0, 150.7, 149.0, 147.1, 139.6, 138.9, 138.0, 136.8, 133.7, 133.4, 133.2, 129.1, 128.8, 122.2, 35.8, 18.2. (ESI): m/z = 325 [M+H]$^+$.

2-((2-Fluorophenyl)thio)-5-((5-methylpyridin-3-yl)methyl)pyridine (76). Compound **95** (3:1
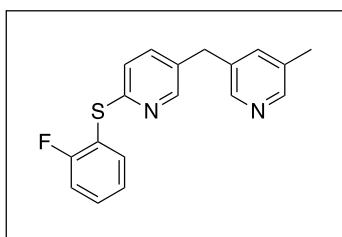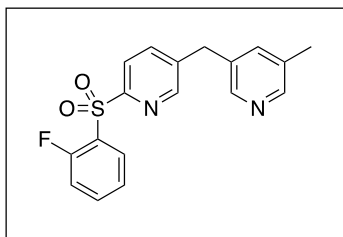

mixture of chloride and bromide, 100 mg, 0.44 mmol) was dissolved under N$_2$ in dimethylacetamid (2 mL), followed by addition of caesium carbonate (371 mg, 1.14 mmol) and 2-fluorothiophenol (45 µL, 4.20 mmol). The reaction mixture was stirred at 90 °C overnight, quenched with sat. NaHCO$_3$-solution afterwards and extracted with EtOAc thrice. The combined organic layers were washed with water, brine, dried over Na$_2$SO$_4$, filtered and concentrated in vacuum. Crude product was purified by preparative thin layer chromatography using a mixture of hexane/ethyl acetate (2:8) as eluent. Pale yellow oil. Yield: 40 mg, 29%. ^{1}H NMR (CDCl$_3$, 500 MHz): δ_H (ppm) = 8.26–8.29 (m, 3 H), 7.57 (td, J = 7.4, 1.6 Hz, 1 H), 7.41 (m, 1 H), 7.28 (m, 1 H), 7.25 (dd, J = 8.2, 2.5 Hz, 1 H), 7.19–7.13 (m, 2 H), 6.87 (d, J = 8.3 Hz, 1 H), 3.86 (s, 2 H), 2.28 (s, 3 H). ^{13}C NMR (CDCl$_3$, 125 MHz): δ_C (ppm) = 162.6 (d, $J_{C,F}$ = 249.3 Hz), 157.4, 149.6, 147.5, 146.0, 137.7, 137.1, 136.9, 135.1, 133.6, 131.7, 131.6, 124.9 (d, $J_{C,F}$ = 3.7 Hz), 121.1, 117.9 (d, $J_{C,F}$ = 18.3 Hz), 116.3 (d, $J_{C,F}$ = 22.0 Hz), 35.3, 18.2. (ESI): m/z = 311 [M+H]$^+$.
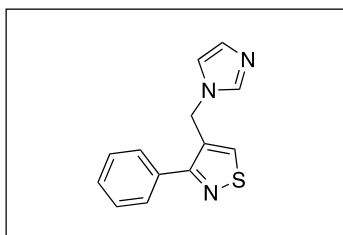
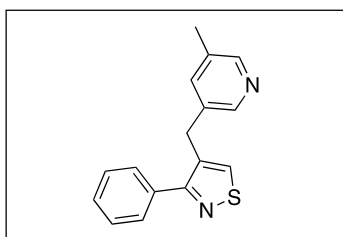**2-((2-Fluorophenyl)sulfonyl)-5-((5-methylpyridin-3-yl)methyl)pyridine (77).** To a solution of thioether **76** (30 mg, 96.7 µmol) in ethyl acetate (2 mL) was added water (2 mL) and potassium peroxymonosulfate (119 mg, 0.39 mmol) at room temperature and the reaction mixture was vigorously stirred for 4 h at room temperature. Saturated NaHCO$_3$-solution was added and the mixture was extracted with DCM. The combined organic layers were dried over Na$_2$SO$_4$ and concentrated in vacuum. Crude product was purified by flash chromatography on silica-gel using ethyl acetate as eluent. Beige solid. Yield: 21 mg, 64%. Mp 144–146 °C. ^{1}H NMR (CDCl$_3$, 300 MHz): δ_H (ppm) = 8.49 (s, 1 H), 8.33 (s, 1 H), 8.28 (s, 1 H), 8.16–8.23 (m, 2 H), 7.73 (d, J = 8.1 Hz, 1 H), 7.62 (m, 1 H), 7.36 (m, 1 H), 7.24 (br s, 1 H), 7.10 (dd, J = 9.6, 8.6 Hz, 1 H), 4.01 (s, 2 H), 2.29 (s, 3 H). ^{13}C NMR (CDCl$_3$, 75 MHz): δ_C (ppm) = 159.5 (d, $J_{C,F}$ = 257.2 Hz), 156.5, 150.5, 149.1, 147.2, 140.2, 138.1, 136.9, 136.5, 136.4, 133.4 (d, $J_{C,F}$ = 13.8 Hz), 131.1, 127.0 (d, $J_{C,F}$ = 13.8 Hz), 124.7 (d, $J_{C,F}$ = 3.8 Hz), 122.8 (d, $J_{C,F}$ = 1.9 Hz), 117.1 (d, $J_{C,F}$ = 20.9 Hz), 35.9, 18.3. (ESI): m/z = 343 [M+H]$^+$.

4-((1H-Imidazol-1-yl)methyl)-3-phenylisothiazole (78). Synthesized using impure compound **99** (100 mg), imidazole (107 mg, 1.57 mmol) and K$_2$CO$_3$ (270 mg, 1.95 mmol) in DMF according to method E. Crude product was purified by flash chromatography on silica-gel using ethyl acetate as eluent. Off-white solid. Yield: 44 mg. Mp 113–115 °C. ^{1}H NMR (CDCl$_3$, 500 MHz): δ_H (ppm) = 8.35 (s, 1H, isothiazole H-5), 7.53–7.47 (m, 5H, Ph H), 7.46 (s, 1H, imidazolyl H-2), 7.09 (s, 1H, imidazolyl H-4), 6.86 (s, 1H, imidazolyl H-5), 5.24 (s, 2H, CH$_2$); ^{13}C NMR (CDCl$_3$, 125 MHz): δ_C (ppm) = 166.6 (isothiazol C-3), 148.1 (isothiazol C-5), 137.1 (imidazolyl C-2), 134.5 (Ph C$_q$), 132.6 (isothiazol C-4), 130.1 (imidazolyl C-4), 129.4 (Ph C), 128.8 (Ph C), 128.2 (Ph C), 118.9 (imidazolyl C-5), 44.4 (CH$_2$); (ESI): m/z = 242 [M+H]$^+$.

4-((5-Methylpyridin-3-yl)methyl)-3-phenylisothiazole (79). Synthesized using impure compound **99** (144 mg) and (5-methylpyridin-3-yl)boronic acid (116 mg, 0.85 mmol) according to method A. Crude product was purified by flash chromatography on silica-gel using ethyl acetate as eluent. Colorless oil. Yield: 61 mg. ^{1}H NMR (CDCl$_3$, 500 MHz): δ_H (ppm) = 8.31 (d, J = 1.6 Hz, 1H, pyridinyl H-2), 8.23 (d, J = 1.6 Hz, 1H, pyridinyl H-6), 8.22 (t, J = 0.8 Hz, 1H, isothiazole H-5) 7.59–7.54 (m, 2H, Ph H), 7.48–7.40 (m, 3H, Ph H), 7.20–7.17 (m, 1H, pyridinyl H-4), 4.05 (s, 2H, CH_2), 2.28 (d, J = 0.6 Hz, 3H,

CH_3); ^{13}C NMR (CDCl$_3$, 125 MHz): δ$_C$ (ppm) = 167.6 (isothiazole C-3),, 148.5 (pyridinyl C-6), 147.1 (pyridinyl C-2), 146.9 (isothiazole C-5), 136.6 (pyridinyl C-4), 135.4 (pyridinyl C-3), 135.3 (Ph C$_q$), 134.5 (isothiazole C-4), 133.0 (pyridinyl C-5), 128.8 (Ph C), 128.5 (Ph C), 128.4 (Ph C), 31.4 (CH$_2$), 18.3 (CH$_3$); (ESI): *m/z* = 267 [M+H]$^+$.

5-((1*H*-Imidazol-1-yl)methyl)-3-phenylisothiazole (80). Synthesized using compound **100** (46 mg, 0.18 mmol), imidazole (49 mg, 0.72 mmol) and K$_2$CO$_3$ (124 mg, 0.90 mmol) in DMF according to method E. Crude product was purified by flash chromatography on silica-gel using ethyl acetate as eluent. White solid. Yield: 17 mg, 40%. Mp 92–94 °C. ^{1}H NMR (CDCl$_3$, 500 MHz): δ$_H$ (ppm) = 7.91–7.86 (m, 2H), 7.64 (s, 1H), 7.47–7.38 (m, 3H), 7.37 (t, *J* = 1.0 Hz, 1H), 7.16 (s, 1H), 7.02 (s, 1H), 5.46–5.41 (m, 2H). ^{13}C NMR (CDCl$_3$, 125 MHz): δ$_C$ (ppm) = 168.1, 163.5, 137.2, 134.2, 130.4, 129.5, 128.8, 126.8, 120.5, 119.0, 43.6. (ESI): *m/z* = 242 [M+H]$^+$.
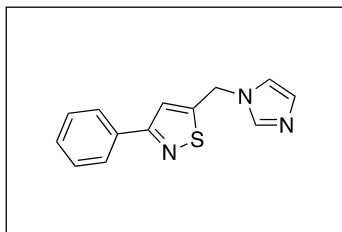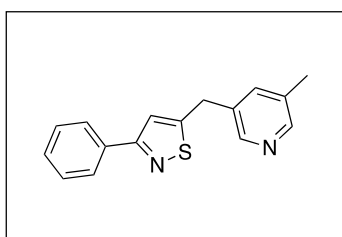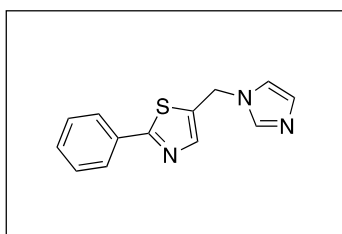
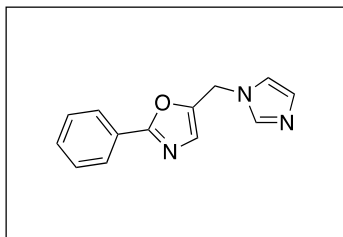**5-((5-Methylpyridin-3-yl)methyl)-3-phenylisothiazole (81).** Synthesized using compound **100** (180 mg, 0.71 mmol) and (5-methylpyridin-3-yl)boronic acid (146 mg, 1.07 mmol) according to method A. Crude product was purified by flash chromatography on silica-gel using ethyl acetate as eluent. Colorless oil. Yield: 40 mg, 21%. ^{1}H NMR (CDCl$_3$, 500 MHz): δ$_H$ (ppm) = 8.40 (s, 1H), 8.38 (s, 1H), 7.94–7.87 (m, 2H), 7.45–7.36 (m, 4H), 7.31 (t, *J* = 1.0 Hz, 1H), 4.23 (s, 2H), 2.35–2.31 (m, 3H). ^{13}C NMR (CDCl$_3$, 125 MHz): δ$_C$ (ppm) = 168.1, 167.6, 149.4, 147.1, 136.8, 134.9, 133.7, 133.5, 129.4, 128.9, 127.0, 120.9, 31.4, 18.5. (ESI): *m/z* = 267 [M+H]$^+$.

5-((1*H*-Imidazol-1-yl)methyl)-2-phenylthiazole (82). Synthesized using compound **107** (103 mg, 0.41 mmol), imidazole (110 mg, 1.62 mmol) and K$_2$CO$_3$ (283 mg, 2.05 mmol) in DMF according to method E. Crude product was purified by flash chromatography on silica-gel using a mixture of ethyl acetate/methanol (9:1) as eluent. Yellow solid. Yield: 52 mg, 53%. Mp 118–120 °C. ^{1}H NMR (CDCl$_3$, 500 MHz): δ$_H$ (ppm) = 7.92–7.87 (m, 2H), 7.74 (s, 1H), 7.60 (s, 1H), 7.47–7.42 (m, 3H), 7.12 (s, 1H), 6.99 (s, 1H), 5.34 (s, 2H). ^{13}C NMR (CDCl$_3$, 125 MHz): δ$_C$ (ppm) = 169.9, 142.7, 136.9, 133.2, 133.1, 130.5, 130.3, 129.0, 126.5, 118.7, 43.1. (ESI): *m/z* = 242 [M+H]$^+$.
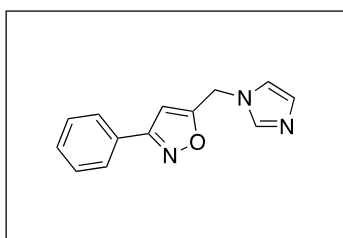
5-((1*H*-Imidazol-1-yl)methyl)-2-phenyloxazole (83). Synthesized using compound **108** (3:1 mixture of chloride and bromide, 160 mg, 0.78 mmol), imidazole (183 mg, 2.69 mmol) and K_2CO_3 (463 mg, 3.35 mmol) in DMF according to method E. Crude product was purified by flash chromatography on silica-gel using a mixture of ethyl acetate/methanol (9:1) as eluent. White solid. Yield: 102 mg, 58%.

Mp 119–121 °C. ^{1}H NMR (CDCl3, 500 MHz): δ_H (ppm) = 8.03–7.96 (m, 2H, Ph H), 7.62 (s, 1H, imidazolyl H-2), 7.49–7.42 (m, 3H, Ph H), 7.17–7.14 (m, 1H, oxazole H-4), 7.13–7.08 (m, 1H, imidazolyl H-4), 7.03–6.99 (m, 1H, imidazolyl H-5), 5.22 (d, *J* = 0.6 Hz, 2H, C*H*2). ^{13}C NMR (CDCl3, 125 MHz): δ_C (ppm) = 162.6 (oxazole C-2), 146.0 (oxazole C-5), 137.0 (imidazolyl C-2), 130.8 (Ph C), 130.1 (imidazolyl C-4), 128.8 (Ph C), 127.0 (oxazole C-4), 126.8 (Ph C_q), 126.4 (Ph C), 118.8 (imidazolyl C-5), 41.4 (CH2). (ESI): *m/z* = 226 [M+H]$^+$.
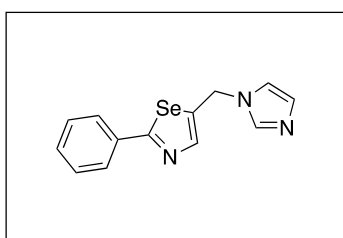
5-((1*H*-Imidazol-1-yl)methyl)-3-phenylisoxazole (84). Synthesized using compound **109** (1:3 mixture of chloride and bromide, 122 mg, 0.54 mmol), imidazole (139 mg, 2.04 mmol) and K_2CO_3 (354 mg, 2.56 mmol) in DMF according to method E. Crude product was purified by flash chromatography on silica-gel using ethyl acetate as eluent. Beige solid. Yield: 89 mg, 74%. Mp 117–119 °C. ^{1}H NMR (DMSO-d6, 500 MHz): δ_H (ppm) = 7.87–7.82 (m, 2H, Ph H), 7.81 (t, *J* = 1.1 Hz, 1H, imidazolyl H-2), 7.52–7.47 (m, 3H, Ph H), 7.28 (t, *J* = 1.3 Hz, 1H, imidazolyl H-5), 6.97–6.94 (m, 2H, imidazolyl H-4, isoxazol H-4), 5.53 (s, 2H, C*H*2). ^{13}C NMR (DMSO-d6, 125 MHz): δ_C (ppm) = 168.9 (isoxazol C-5), 162.1 (Isoxazol C-3), 137.7 (imidazolyl C-2), 130.4 (Ph C), 129.1 (Ph C), 128.9 (imidazolyl C-4), 128.2 (Ph C_q), 126.6 (Ph C), 119.8 (imidazolyl C-5), 101.3 (isoxazol C-4), 41.2 (CH2). (ESI): *m/z* = 226 [M+H]$^+$.

5-((1*H*-Imidazol-1-yl)methyl)-2-phenyl-1,3-selenazole (85). To a stirred solution of **104** (123 mg, 0.55 mmol) in CCl4 (8 mL) was added azo-bis-(isobutyronitril) (91.0 mg, 0.55 mmol) and *N*-bromosuccinimid (108 mg, 0.61 mmol). Subsequently, the reaction mixture was irradiated with hν for 2 h (300 W, tungsten lamp). An ice bath was used to avoid overheating during irradiation and the reaction mixture was stirred for 12 h protected from light afterwards. Subsequently, the succinimide was removed by filtration and the filtrate was concentrated under reduced pressure. The residue was purified by flash chromatography on silica-gel using a mixture of hexane/ethyl acetate (10:1) as eluent. A

suspension of the obtained impure bromine **110** (35 mg, yellow solid), imidazole (32.0 mg, 0.47 mmol) and K_2CO_3 (80.0 mg, 0.58 mmol) in DMF was heated to 120 °C for 2 h. Subsequent work up and purification was performed according to method E. Crude product was purified by flash chromatography on silica-gel using ethyl acetate as eluent. Off-white solid. Yield: 12 mg, 8%. Mp 115–117 °C. ^{1}H NMR (CDCl$_3$, 500 MHz): δ_H (ppm) = 7.86–7.79 (m, 2H, Ph H), 7.70 (t, J = 1.0 Hz, 1H, selenazole H-4), 7.61 (br s, 1H, imidazolyl H-2), 7.46–7.36 (m, 3H, Ph H), 7.10 (br s, 1H, imidazolyl H-4), 6.98 (br s, 1H, imidazolyl H-5), 5.36 (d, J = 1.0 Hz, 2H, CH_2). ^{13}C NMR (CDCl$_3$, 125 MHz): δ_C (ppm) = 177.4 (selenazole C-2), 143.6 (selenazole C-4), 140.5 (selenazole C-5), 137.1 (imidazolyl C-2), 136.1 (Ph C), 131.0 (Ph C), 130.4 (imidazolyl C-4), 129.4 (Ph C), 127.2 (Ph C), 118.4 (imidazolyl C-5), 45.8 (CH$_2$). (ESI): m/z = 290 [M+H]$^+$.

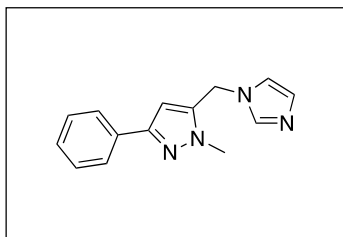**5-((1H-Imidazol-1-yl)methyl)-1-methyl-2-phenyl-1H-imidazole (86).** To a solution of the
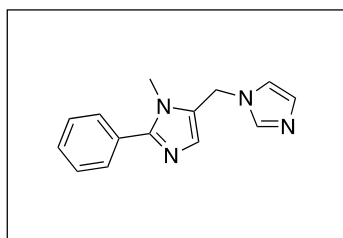
corresponding alcohol **111** (101 mg, 0.54 mmol) in NMP (20 mL/mmol), CDI (436 mg, 2.69 mmol) was added. Then the solution was heated at 190 °C for 16 h. After cooling to room temperature the reaction mixture was diluted with ethyl acetate and washed with water and brine. The organic phase was dried over $MgSO_4$ and concentrated under reduced pressure. The crude product was purified by flash chromatography on silica-gel using a mixture of ethyl acetate/methanol (9:1) as eluent. After flash chromatography the product was dissolved in ethyl acetate and a few drops of conc. HCl and water were added. Mixture was stirred for 5 min followed by separation of the phases and neutralization of the aqueous phase with aq. Na_2CO_3 solution (2.0 M). After extraction with ethyl acetate and drying over $MgSO_4$ the solvent was removed under reduced pressure. White solid. Yield: 35 mg, 27%. Mp 96–98 °C. ^{1}H NMR (CDCl$_3$, 500 MHz): δ_H (ppm) = 7.57 (m, 3H, Ph H, imidazolyl H-2), 7.49–7.42 (m, 3H, Ph H), 7.24 (s, 1H, imidazol H-4), 7.12–7.10 (m, 1H, imidazolyl H-4), 6.94 (t, J = 1.3 Hz, 1H, imidazolyl H-5), 5.18 (s, 2H, CH_2), 3.47 (s, 3H, CH_3). ^{13}C NMR (CDCl$_3$, 125 MHz): δ_C (ppm) = 150.2 (imidazol C-2), 136.7 (imidazolyl C-2), 130.1 (imidazol C-5), 130.1 (Ph C), 129.8 (imidazolyl C-4), 129.2 (imidazol C-4), 128.9 (Ph C), 128.6 (Ph C), 126.5 (Ph C$_q$), 118.6 (imidazolyl C-5), 41.1 (CH$_2$), 31.7 (CH$_3$). (ESI): m/z = 239 [M+H]$^+$.

5-((1H-Imidazol-1-yl)methyl)-1-methyl-3-phenyl-1H-pyrazole (87). Synthesized using compound **112** (112 mg, 0.45 mmol), imidazole (123 mg, 1.81 mmol) and K_2CO_3 (308 mg, 2.23 mmol) in DMF according to meth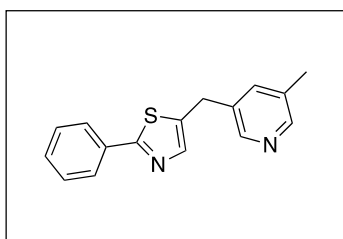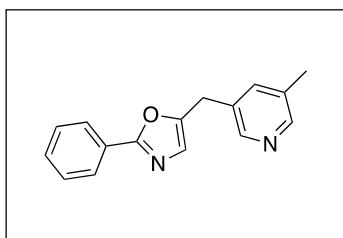od E. Crude product was purified by flash chromatography on silica-gel using a mixture of ethyl acetate/methanol (10:1) as eluent. Colorless oil. Yield: 61 mg, 57%. ^{1}H NMR (CDCl$_3$, 500 MHz): δ_H (ppm) = 7.77–7.73 (m, 2H), 7.55 (s, 1H), 7.42–7.37 (m, 2H), 7.33–7.29 (m, 1H), 7.12 (m, 1H), 6.92 (m, 1H), 6.50 (s, 1H), 5.17 (s, 2H), 3.78 (s, 3H). ^{13}C NMR (CDCl$_3$, 125 MHz): δ_C (ppm) = 150.6, 137.6, 136.9, 132.7, 130.2, 128.7, 127.9, 125.4, 118.8, 104.2, 41.7, 36.5. (ESI): m/z = 239 [M+H]$^+$.

**5-((5-Methylpyridin-3-yl)methyl)-2-phenylthiazole (88).** Synthesized using compound **107** (105 mg, 0.41 mmol) and (5-methylpyridin-3-yl)boronic acid (85 mg, 0.62 mmol) according to method A. Crude product was purified by flash chromatography on silica-gel using a mixture of hexane/ethyl acetate (1:1) as eluent. Light yellow solid. Yield: 60 mg, 55%. Mp 89–91 °C. ^{1}H NMR (CDCl$_3$, 500 MHz): δ_H (ppm) = 8.36 (d, J = 1.5 Hz, 1H), 8.39 (d, J = 1.5 Hz, 1H), 7.92–7.85 (m, 2H), 7.59 (s, 1H), 7.45–7.39 (m, 3H), 7.38–7.36 (m, 1H), 4.16 (s, 2H), 2.32 (s, 3H). ^{13}C NMR (CDCl$_3$, 125 MHz): δ_C (ppm) = 168.0, 149.0, 146.9, 141.5, 137.3, 136.5, 134.3, 133.7, 133.2, 129.9, 128.9, 126.3, 30.4, 18.3. (ESI): m/z = 267 [M+H]$^+$.

5-((5-Methylpyridin-3-yl)methyl)-2-phenyloxazole (89). Synthesized using compound **108** (3:1 mixture of chloride and bromide, 90.0 mg, 0.44 mmol) and (5-methylpyridin-3-yl)boronic acid (78.0 mg, 0.57 mmol) according to method A. Crude product was purified by flash chromatography on silica-gel using a mixture of hexane/ethyl acetate (1:1→ ethyl acetate) as eluent. White solid. Yield: 20 mg, 18%. Mp 86–88 °C. ^{1}H NMR (CDCl$_3$, 500 MHz): δ_H (ppm) = 8.42–8.39 (m, 1H, pyridinyl H-2), 8.37 (s, 1H, pyridinyl H-6),8.03–7.96 (m, 2H, Ph H), 7.47–7.41 (m, 3H, Ph H), 7.41–7.38 (m, 1H, pyridinyl H-4), 6.90–6.89 (m, 1H, oxazole H-4), 4.04 (s, 2H, CH_2), 2.33 (d, J = 0.6 Hz, 3H, CH_3). ^{13}C NMR (CDCl$_3$, 125 MHz): δ_C (ppm) = 161.5 (oxazole C-2), 150.2 (oxazole C-5), 149.0 (pyridinyl C-6), 147.1 (pyridinyl C-2), 136.7 (pyridinyl C-4), 133.2 (pyridinyl C-5), 131.7 (pyridinyl C-3), 130.2 (Ph C), 128.7 (Ph C), 127.4 (Ph C$_q$), 126.1 (Ph C), 125.1 (oxazole C-4), 29.3 (CH$_2$), 18.3 (CH$_3$). (ESI): m/z = 251 [M+H]$^+$.

5-((5-Methylpyridin-3-yl)methyl)-3-phenylisoxazole (90). Synthesized using compound **109**
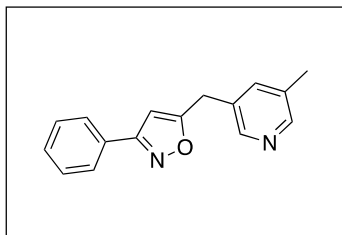
(1:3 mixture of chloride and bromide, 127 mg, 0.56 mmol) and (5-methylpyridin-3-yl)boronic acid (110 mg, 0.80 mmol) according to method A. Crude product was purified by flash chromatography on silica-gel using ethyl acetate as eluent. Yellow solid. Yield: 58 mg, 41%. Mp 62–64 °C. ^{1}H NMR (CDCl$_3$, 500 MHz): δ_H (ppm) = 8.42–8.40 (m, 1H, pyridinyl H-2), 8.40–8.38 (m, 1H, pyridinyl H-6), 7.79–7.74 (m, 2H, Ph H), 7.47–7.40 (m, 4H, Ph H, pyridinyl H-4), 6.26 (t, J = 0.8 Hz, 1H, isoxazol H-4), 4.11 (s, 2H, CH_2), 2.34 (s, 3H CH_3). ^{13}C NMR (CDCl$_3$, 125 MHz): δ_C (ppm) = 171.6 (isoxazol C-5), 162.8 (isoxazol C-3), 149.5 (pyridinyl C-6), 147.3 (pyridinyl C-2), 137.1 (pyridinyl C-4), 133.6 (pyridinyl C-5), 131.3 (pyridinyl C-3), 130.2 (Ph C), 129.2 (Ph C$_q$), 129.1 (Ph C), 127.0 (Ph C), 100.5 (isoxazol C-4), 30.6 (CH$_2$), 18.5 (CH$_3$). (ESI): m/z = 251 [M+H]$^+$.

5-((5-Methoxypyridin-3-yl)methyl)-3-phenylisoxazole (91). A mixture of compound **109** (1:3
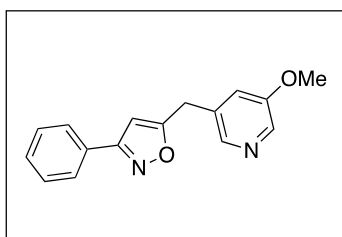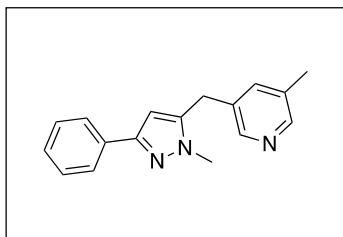

mixture of chloride and bromide, 315 mg, 1.39 mmol), 3-methoxy-5-(4,4,5,5-tetramethyl-1,3,2-dioxaborolan-2-yl)py-ridine (373 mg, 1.59 mmol), Cs$_2$CO$_3$ (1.29 g, 3.96 mmol) and PdCl$_2$(dppf) (48.0 mg, 0.07 mmol) were dissolved in DME/H$_2$O/EtOH (3 mL/ 3 mL/ 3 mL). The reaction mixture was stirred for 20 min at 150°C, 150 W and 18 bar in the microwave oven. After addition of H$_2$O and extraction with ethyl acetate three times, the combined organic phases were dried over MgSO$_4$ and concentrated under reduced pressure. Crude product was purified by flash chromatography on silica-gel using a mixture of hexane/ethyl acetate (1:2) as eluent. After flash chromatography the product was dissolved in ethyl acetate and a few drops of conc. HCl and water were added. After stirring for 30 min the phases were separated and aqueous phase was neutralized with aqueous Na$_2$CO$_3$ solution (2M). After extraction with ethyl acetate and drying over MgSO$_4$ the solvent was removed under reduced pressure. White solid. Yield: 107 mg, 29%. Mp: 71–73 °C. ^{1}H NMR (CDCl$_3$, 500 MHz): δ_H (ppm) = 8.27 (s, 1H, pyridinyl H-6)), 8.21 (s, 1H, pyridinyl H-2), 7.73–7.80 (m, 2H, Ph H), 7.41–7.48 (m, 3H, Ph H), 7.13–7.17 (m, 1H, pyridinyl H-4), 6.28 (t, J = 0.8 Hz, 1H, isoxazol H-4), 4.13 (s, 2H, CH_2), 3.86 (s, 3H, CH_3). ^{13}C NMR (CDCl$_3$, 125 MHz): δ_C (ppm) = 171.1 (isoxazol C-5), 162.6 (isoxazol C-3), 155.8 (pyridinyl C-5), 142.1 (pyridinyl C-2), 136.5 (pyridinyl C-6), 132.1 (pyridinyl C-3), 130.0 (Ph C), 128.9 (Ph C$_q$), 128.9 (Ph C), 126.7 (Ph C), 120.9 (pyridinyl C-4), 100.3 (isoxazol C-4), 55.6 (CH$_3$), 30.4 (CH$_2$). MS (ESI): m/z = 267 [M+H]$^+$.

3-Methyl-5-((1-methyl-3-phenyl-1H-pyrazol-5-yl)methyl)pyridine (92). Synthesized using compound **112** (122 mg, 0.49 mmol) and (5-methylpyridin-3-yl)boronic acid (100 mg, 0.73 mmol) according to method A. Crude product was purified by flash chromatography on silica-gel using ethyl acetate as eluent. White solid. Yield: 65 mg, 50%. Mp 41–43 °C. ^{1}H NMR (CDCl$_3$, 500 MHz): δ_H (ppm) = 8.39–8.37 (m, 1H), 8.36–8.35 (m, 1H), 7.78–7.75 (m, 2H), 7.40–7.36 (m, 2H), 7.31–7.26 (m, 2H), 6.31 (s, 1H), 3.99 (s, 2H), 3.79 (s, 3H), 2.32 (d, J = 0.6 Hz, 3H). ^{13}C NMR (CDCl$_3$, 125 MHz): δ_C (ppm) = 150.2, 148.9, 146.9, 141.5, 136.5, 133.3, 133.3, 132.4, 128.6, 127.5, 125.4, 103.4, 36.5, 29.1, 18.3. (ESI): m/z = 264 [M+H]$^+$.

3-Methyl-5-((3-phenyl-1*H*-pyrazol-5-yl)methyl)pyridine (93). A mixture of **92** (126 mg, 0.48 mmol) and pyridine hydrochloride (700 mg, 6.06 mmol) was stirred for 2.5 h at 200 °C and 200 W in the microwave oven. After cooling to room temperature H$_2$O (10 mL) was added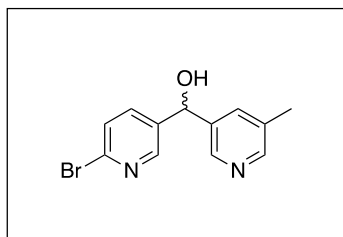 and the obtained mixture was extracted with ethyl acetate twice. The combined organic phases were dried over MgSO$_4$ and concentrated under reduced pressure. Crude product was purified by flash chromatography on silica-gel using ethyl acetate as eluent. After flash chromatography the product was dissolved in ethyl acetate and a few drops of conc. HCl and water were added. After stirring for 5 min the phases were separated and aqueous phase was neutralized with aqueous Na$_2$CO$_3$ solution (2.0 M). After extraction with ethyl acetate and drying over MgSO$_4$ the solvent was removed under reduced pressure. Colorless oil. Yield: 21 mg, 18%. ^{1}H NMR (DMSO-d$_6$, 500 MHz): δ_H (ppm) = 12.87 (br s, 1H, NH), 8.34 (s, 1H, pyridinyl H-2), 8.28 (s, 1H, pyridinyl H-6), 7.73 (d, J = 7.3 Hz, 2H, Ph H), 7.48 (s, 1H, pyridinyl H-4), 7.38 (t, J = 7.7 Hz, 2H, Ph H), 7.31–7.25 (m, 1H, Ph H), 6.48 (s, 1H, pyrazole H-4), 3.96 (s, 2H, C*H*$_2$), 2.26 (s, 3H, C*H*$_3$). ^{13}C NMR (DMSO-d$_6$, 125 MHz): δ_C (ppm) = 147.9 (pyridinyl C-6), 146.8 (pyridinyl C-2), 136.4 (pyridinyl C-4), 134.5 (pyridinyl C-3), 132.6 (pyridinyl C-5), 128.7 (Ph C), 127.5 (PhC), 125.0 (Ph C), 101.2 (pyrazole C-4), 29.4 (CH$_2$), 17.8 (CH$_3$). (ESI): m/z = 250 [M+H]$^+$.
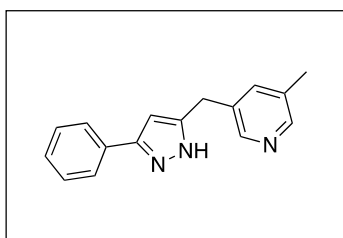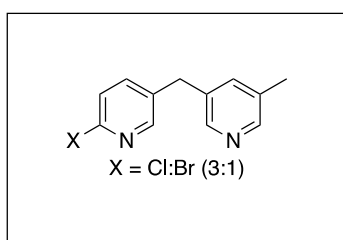
(6-Bromopyridin-3-yl)(5-methylpyridin-3-yl)methanol (94). To a stirred solution of 3-bromo-5-methylpyridine (6.30 mL, 9.39 g, 54.6 mmol) in dry diethyl ether (760 mL) was added *n*-butyllithium (2.5 M in hexane, 20.6 mL, 51.5 mmol) dropwise at –78 °C and the clear solution was stirred for additional 5 min at this temperature. Subsequently a solution of 6-bromonicotinaldehyde (10.1 g, 54.3 mmol) in dry toluene (20 mL) and dry THF (30 mL) was added dropwise and the pale brown suspension was stirred for additional 30 min at -78 °C. The reaction mixture was quenched with sat. aqueous NH_4Cl solution, diluted with water at room temperature and extracted with diethyl ether thrice. The combined organic layers were dried over Na_2SO_4 and concentrated in vacuum. Crude product was purified by flash chromatography on silica-gel using a mixture of ethyl acetate/ethanol (9:1) as eluent. Yellow solid. Yield: 9.76 g, 64%. Mp 126–128 °C. ^1H NMR (Aceton-d_6, 500 MHz): δ_H (ppm) = 8.46–8.47 (m, 2 H), 8.32 (d, J = 1.7 Hz, 1 H), 7.74 (ddd, J = 8.2, 2.5, 0.6 Hz, 1 H), 7.60 (m, 1 H), 7.56 (d, J = 8.2 Hz, 1 H), 5.98 (s, 1 H), 5.41 (br s, 1 H), 3.16 (s, 3 H). ^{13}C NMR (Aceton-d_6, 125 MHz): δ_C (ppm) = 151.2, 150.4, 147.2, 142.7, 141.9, 140.8, 139.1, 136.0, 134.9, 129.7, 72.3, 19.3.

Mixture of 2-Chloro-5-((5-methylpyridin-3-yl)methyl)pyridine and 2-Bromo-5 ((5 methyl pyridin-3-yl)methyl)pyridine (95). Ice cooled alcohol **94** (9.76 g, 35.0 mmol) was dissolved under nitrogen atmosphere in fresh distilled thionyl chloride (43.0 mL, 595 mmol). The reaction mixture was stirred for 3 h at 60 °C. After cooling to room temperature, the thionyl chloride was removed in vacuum, the residue neutralized with sat. aqueous $NaHCO_3$-solution and extracted with ethyl acetate thrice. The combined organic layers were washed successively with sat. $NaHCO_3$ solution, water, brine and dried over Na_2SO_4. The solvent was removed in vacuum and the crude chloride was dissolved under nitrogen atmosphere in degassed glacial acetic acid (90 mL). Zinc-powder was added in small portions and the reaction mixture was stirred for 24 h at room temperature. Afterwards the solvent was evaporated in vacuum, saturated aqueous $NaHCO_3$ solution and ethyl acetate were added to the residue and the mixture was filtered over celite. Subsequently the phases were separated and the aqueous phase was extracted twice with ethyl acetate. The combined organic layers were washed with water and brine, dried over Na_2SO_4 and concentrated in vacuum. Crude product was purified by flash chromatography on silica-gel using ethyl acetate as eluent to yield an inseparable mixture of 2-Chloro-5-((5-methyl-pyridin-3-yl)methyl)pyridine and 2**-**Bromo-5-((5-methylpyridin-3-yl)methyl)pyridine (3:1). White solid. Yield: 6.25 g, 78%. **2-Chloro-5-((5-methylpyridin-3-yl)methyl)pyridine.** ^1H NMR (CDCl$_3$, 300 MHz): δ_H (ppm) = 8.31 (s, 1 H),

8.27 (s, 1 H), 8.25 (d, J = 2.5 Hz, 1 H), 7.40 (dd, J = 8.2, 2.5 Hz, 1 H), 7.20–7.24 (m, 2 H), 3.90 (s, 2 H), 2.27 (s, 3 H). ^{13}C NMR (CDCl$_3$, 75 MHz): δ$_C$ (ppm) = 149.7, 149.6, 148.8, 147.0, 139.1, 136.6, 134.3, 134.1, 133.2, 124.2, 35.2, 18.2. (ESI): m/z = 219 [M+H]$^+$. **2-Bromo-5-((5-methylpyridin-3-yl)methyl)pyridine.** ^{1}H NMR (CDCl$_3$, 300 MHz): δ$_H$ (ppm) = 8.31 (d, J = 1.6 Hz, 1 H), 8.28 (d, J = 1.7 Hz, 1 H), 8.24 (d, J = 2.0 Hz, 1 H), 7.39 (d, J = 7.9 Hz, 1 H), 7.30 (dd, J = 8.2, 2.5 Hz, 1 H), 7.21 (m, 1 H), 3.88 (s, 2 H), 2.28 (s, 3 H). ^{13}C NMR (CDCl$_3$, 75 MHz): δ$_C$ (ppm) = 150.2, 148.8, 147.1, 140.2, 138.9, 136.7, 134.8, 134.0, 133.2, 128.0, 35.2, 18.2. (ESI): m/z = 263 [M+H]$^+$.

Ethyl 3-Phenylisothiazole-4-carboxylate (97). A mixture of **96** (877 mg, 4.89 mmol) and ethyl
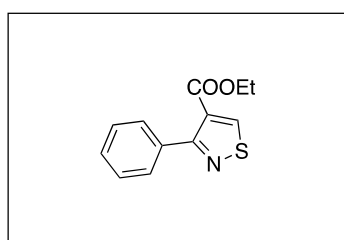
propiolate (4.90 mL, 4.80 g, 48.9 mmol) in CHCl$_3$ (3 mL/mmol) was irradiated for 25 min at 160 °C and 300 W in the microwave oven. The solvent was evaporated and the regioisomers **97** and **98** were obtained. The mixture was purified by flash chromatography on silica-gel using a mixture of hexane/ethyl acetate (25:1) as eluent. A

mixture of **97** and an impurity (3:1) was isolated, which was not further purified and directly used in the next step. Light yellow oil. Yield: 403 mg. **Ethyl 3-Phenylisothiazole-4-carboxylate (97).** ^{1}H NMR (500 MHz, CDCl$_3$): δ$_H$ (ppm) = 9.34 (s, 1H), 7.66–7.61 (m, 2H), 7.47–7.41 (m, 3H), 4.27 (q, J = 7.2 Hz, 2H), 1.25 (t, J = 7.3 Hz, 3H). ^{13}C NMR (125 MHz, CDCl$_3$,): δ$_C$ (ppm) = 168.6, 162.0, 155.7, 135.0, 129.3, 129.1, 129.0, 127.7, 61.1, 14.0. (ESI): m/z = 234 [M+H]$^+$.

Ethyl 3-Phenylisothiazole-5-carboxylate (98). A mixture of **96** (877 mg, 4.89 mmol) and ethyl
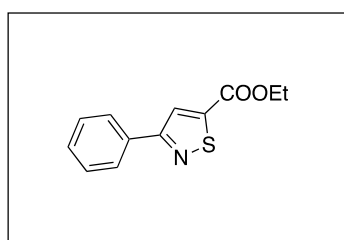
propiolate (4.90 mL, 4.80 g, 48.9 mmol) in CHCl$_3$ (3 mL/mmol) was irradiated for 25 min at 160 °C and 300 W in the microwave oven. The solvent was evaporated and the regioisomers **97** and **98** were obtained. The mixture was purified by flash chromatography on silica-gel using a mixture of hexane/ethyl acetate (25:1) as eluent.

White solid. Yield: 427 mg, 37%. Mp 70–72 °C. ^{1}H NMR (500 MHz, CDCl$_3$): δ$_H$ (ppm) = 8.12 (s, 1H), 7.99–7.95 (m, 2H), 7.50–7.41 (m, 3H), 4.43 (q, J = 7.0 Hz, 2H), 1.43 (t, J = 7.3 Hz, 3H). ^{13}C NMR (125 MHz, CDCl$_3$,): δ$_C$ (ppm) = 168.3, 160.4, 158.0, 134.3, 129.9, 129.2, 127.1, 125.1, 62.3, 14.5. (ESI): m/z = 234 [M+H]$^+$.

4-(Bromomethyl)-3-phenylisothiazole (99). To a solution of **97** (403 mg, 1.73 mmol) in dry THF (10 mL/mmol) was added lithiumaluminiumhydrid (131 mg, 3.45 mmol) in portions at -40 °C. After 1 h stirring saturated NaHCO$_3$-solution (10 mL/mmol) was added slowly at -40 °C and the obtained mixture was extracted with ethyl acetate twice. The combined organic phases were dried over MgSO$_4$ and concentrated under reduced pressure. Without further purification the residue (263 mg) was dissolved in CH$_2$Cl$_2$ (15 mL/mmol) and triphenylphosphine (563 mg, 2.15 mmol) and tetrabrommethane (913 mg, 2.75 mmol) were added under stirring at 0 °C. The reaction mixture was then stirred for 1 h at room temperature, concentrated under reduced pressure and purified by flash chromatography on silica-gel using a mixture of hexane/ethyl acetate (16:1) as eluent. Obtained mixture of **99** and an impurity was directly used in the next step without further purification. Colorless oil. Yield: 295 mg.
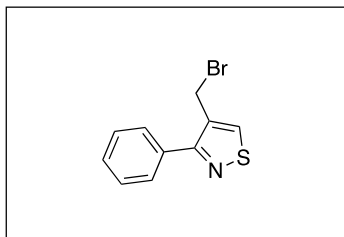
5-(Bromomethyl)-3-phenylisothiazole (100). To a solution of **98** (360 mg, 1.54 mmol) in dry THF (10 mL/mmol) was added lithiumaluminiumhydrid (117 mg, 3.08 mmol) in portions at -40 °C. After 1 h stirring saturated NaHCO$_3$-solution (10 mL/mmol) was added slowly at -40 °C and the mixture was extracted with ethyl acetat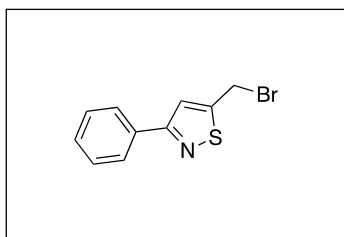e twice. The combined organic phases were dried over MgSO$_4$ and concentrated under reduced pressure resulting in (3-phenylisothiazol-5-yl)methanol as a white solid (291 mg). Without further purification (3-phenylisothiazol-5-yl)methanol (202 mg, 1.06 mmol) was dissolved in CH$_2$Cl$_2$ (15 mL/mmol) and triphenylphosphine (433 mg, 1.65 mmol) and tetrabrommethane (701 mg, 2.11 mmol) were added under stirring at 0 °C. The reaction mixture was then stirred for 1 h at room temperature, concentrated under reduced pressure and purified by flash chromatography on silica-gel using a mixture of hexane/ethyl acetate (16:1) as eluent. Brown solid. Yield: 208 mg, 77%. Mp 67–70 °C. ^{1}H NMR (500 MHz, CDCl$_3$): δ_H (ppm) = 7.97–7.90 (m, 2H), 7.60 (t, J = 0.8 Hz, 1H), 7.49–7.40 (m, 3H), 4.75 (d, J = 1.0 Hz, 2H). ^{13}C NMR (125 MHz, CDCl$_3$,): δ_C (ppm) = 168.1, 164.9, 134.7, 129.6, 129.1, 127.1, 122.2, 21.9. (ESI): m/z = 254 [M+H]$^+$.

N-allylbenzamide (102). To a mixture of benzoyl chloride (2.40 mL, 2.88 g, 20.5 mol) in CH_2Cl_2 (80 mL) was added a solution of allylamine and Et_3N in CH_2Cl_2 (20 mL) at 0 °C. The reaction mixture was stirred for 12 h at room temperature and quenched with water (50 mL) afterwards. The aqueous phase was extracted with CH_2Cl_2 twice followed by evaporation of the organic phase under reduced pressure. The obtained crude product was purified by flash chromatography on silica-gel using a mixture of hexane/ethyl acetate (2:1) as eluent. Colorless liquid. Yield: 3.13 g, 96%. ^{1}H NMR (CDCl$_3$, 500 MHz): δ_H (ppm) = 7.84–7.77 (m, 2H), 7.51–7.43 (m, 1H), 7.42–7.35 (m, 2H), 6.78 (br s, 1H), 5.90 (m, 1H), 5.22 (m, 1H), 5.13 (m, 1H), 4.04 (m, 2H). ^{13}C NMR (CDCl$_3$, 125 MHz): δ_C (ppm) = 167.4, 134.3, 134.1, 131.3, 128.4, 126.9, 116.3, 42.3. (ESI): m/z = 162 [M+H]$^+$.
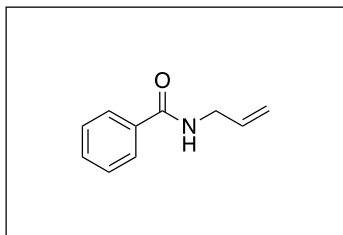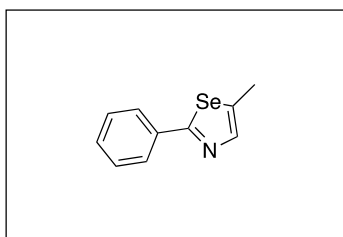
5-Methyl-2-phenyl-1,3-selenazole (104). A suspension of lithium aluminium hydride (490 mg, 12.9 mmol) in dry THF (10 mL) was added to a suspension of selenium powder (1.02 g, 12.9 mmol) in dry THF (10 mL) under nitrogen at 0 °C. The resulting mixture was stirred for 40 min at the same temperature. Lithium hydrogen selenide was formed in situ. Meanwhile PCl$_5$ (3.84 g, 18.4 mmol) and DMF (0.03 mL, 0.40 mmol) were added to a solution of N-(prop-2-yn-1-yl)benzamide (1.47 g, 9.23 mmol) in dry PhMe (35 mL) at room temperature. After 30 min stirring at room temperature freshly prepared lithium hydrogen selenide solution (0.65 M, 20 mL, 12.9 mmol) was added dropwise. After 1 h stirring piperidinium acetate (1.34 g, 9.23 mmol) was added and the mixture was heated under reflux for 2 h. Subsequently, reaction mixture was stirred for 24 h at room temperature followed by evaporation of the solvent. The residue was suspended in water followed by neutralization with NaHCO$_3$-solution. The mixture was extracted with ethyl acetate twice, the combined organic layers were dried over MgSO$_4$, filtered, and concentrated under reduced pressure. Crude product was purified by flash chromatography on silica-gel using a mixture of hexane/ethyl acetate (12:1→8:1) as eluent. Yellow oil. Yield: 643 mg, 31%. ^{1}H NMR (CDCl$_3$, 500 MHz): δ_H (ppm) = 7.83–7.86 (m, 2H), 7.52 (q, J = 1.3 Hz, 1H), 7.40–7.44 (m, 3H), 2.60 (d, J = 1.6 Hz, 3H). (ESI): m/z = 224 [M+H]$^+$.

5-(Bromomethyl)-2-phenylthiazole (107). Synthesized using 2-bromo-5-methylthiazole (**101**) (945 mg, 5.31 mmol) and phenylboronic acid (970 mg, 7.96 mmol) according to method A. Crude product was purified by flash chromatography on silica-gel using a mixture of hexane/ethyl acetate (16:1) as eluent. After flash chromatography product was used for the next step. 5-Methyl-2-phenylthiazole was obtained as colorless oil. Yield: 643 mg, 69%. ^{1}H NMR (CDCl$_3$, 500 MHz): δ_H (ppm) = 7.93–7.87 (m, 2H, Ph H), 7.51 (s, 1H, thiazole H-4), 7.46–7.37 (m, 3H, Ph H), 2.51 (d, J = 0.9 Hz, 3H, CH_3). ^{13}C NMR (CDCl$_3$, 125 MHz): δ_C (ppm) = 166.7 (thiazole C-2), 141.4 (thiazole C-4), 133.9 (Ph C), 133.8 (thiazole C-5), 129.6 (Ph C$_q$), 128.9 (Ph C), 126.2 (Ph C), 12.1 (CH$_3$). (ESI): m/z = 176 [M+H]$^+$. 5-Methyl-2-phenylthiazole (555 mg, 3.17 mmol) was dissolved in 30 mL dry carbon tetrachloride. To this solution NBS (621 mg, 3.49 mmol) and benzoyl peroxide (77.0 mg, 0.317 mmol) were added and the mixture was refluxed over night. After cooling, the succinimide was removed by filtration and the filtrate was concentrated under reduced pressure. Crude product was purified by flash chromatography on silica-gel using a mixture of hexane/ethyl acetate (8:1) as eluent. Orange solid. Yield: 523 mg, 65%. Mp 75–77 °C. ^{1}H NMR (CDCl$_3$, 500 MHz): δ_H (ppm) = 7.96–7.89 (m, 2H), 7.79 (s, 1H), 7.49–7.43 (m, 3H), 4.76 (d, J = 0.6 Hz, 2H). ^{13}C NMR (CDCl$_3$, 125 MHz): δ_C (ppm) = 169.9, 143.3, 135.6, 133.4, 130.4, 129.0, 126.5, 23.3. (ESI): m/z = 254 [M+H]$^+$.
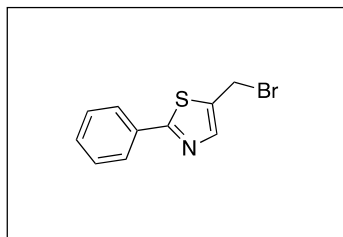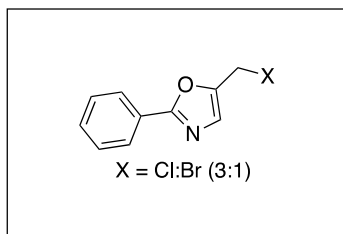
Mixture of 5-(Bromomethyl)-2-phenyloxazole and 5-(Chloromethyl)-2-phenyloxazole (108). A solution of **102** (2.88 g, 17.9 mmol) and NBS (9.54 g, 53.6 mmol) in 1,2-dichloroethane (100 mL) was stirred for 24 h at 100 °C. Afterwards reaction mixture was quenched with saturated aqueous Na$_2$SO$_3$ solution followed by extraction with CH$_2$Cl$_2$ twice. Combined organic phases were washed with brine, dried over MgSO$_4$ and concentrated in vacuum. Crude product was purified by flash chromatography on silica-gel using a mixture of hexane/ethyl acetate (6:1→ 1:1) as eluent to yield an inseparable mixture of 5-(chloromethyl)-2-phenyloxazole and 5-(bromomethyl)-2-phenyloxazole (3:1). White solid. Yield: 1.57 g, 85%. ^{1}H NMR (CDCl$_3$, 500 MHz): δ_H (ppm) = 8.09–8.03 (m, 9H), 7.49–7.43 (m, 12H), 7.19–7.15 (m, 3H), 4.68 (CH_2Cl, d, J = 0.63 Hz, 6H), 4.56 (CH_2Br, d, J = 0.95 Hz, 2H). ^{13}C NMR (CDCl$_3$, 125 MHz): δ_C (ppm) = 162.6, 162.5, 147.4, 147.2, 130.7, 130.7, 128.7, 127.4, 127.4, 126.9, 126.9, 126.4, 125.9, 34.8, 20.1.

Mixture of 5-(Bromomethyl)-3-phenylisoxazole and 5-(Chloromethyl)-3-phenylisoxazole

X = Cl:Br (1:3)
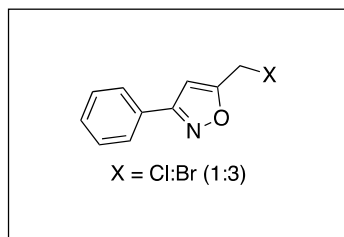
(109). To a stirred solution of (*E*)-benzaldehyde oxime (**104**, 1.80 mL, 2.00 g, 16.5 mmol), propargyl bromide (80% in toluene, 2.20 mL, 2.35 g, 19.8 mmol) and triethylamine (2.30 mL, 1.68 g, 16.6 mmol) in CH_2Cl_2 (30 mL) was added 12% aqueous sodium hypochlorite (49.5 mL, 79.8 mmol) dropwise. After 8 h stirring at room temperature phases were separated and aqueous phase was extracted with CH_2Cl_2 twice. The combined organic phases were washed with water, dried over $MgSO_4$, filtered and concentrated in vacuum. Crude product was purified by flash chromatography on silica-gel using a mixture of hexane/ethyl acetate (9:1) as eluent to yield an inseparable mixture of 5-(chloromethyl)-3-phenylisoxazole and 5-(bromomethyl)-3-phenylisoxazole (1:3). Orange solid. Yield: 1.48 g, 40%. ^{1}H NMR (CDCl$_3$, 500 MHz): δ_H (ppm) = 7.79–7.84 (m, 9H), 7.45–7.50 (m, 12H), 6.63–6.66 (m, 3H), 4.67 (CH_2Cl, d, J = 0.95 Hz, 2H), 4.52 (CH_2Br, d, J = 0.63 Hz, 6H). ^{13}C NMR (CDCl$_3$, 125 MHz): δ_C (ppm) = 167.9, 162.7, 130.2, 129.9, 129.0, 128.5, 128.5, 126.8, 101.9, 101.8, 34.5, 18.6.

(1-Methyl-2-phenyl-1*H*-imidazol-5-yl)methanol (111). To a solution of methyl 1-methyl-1*H*-

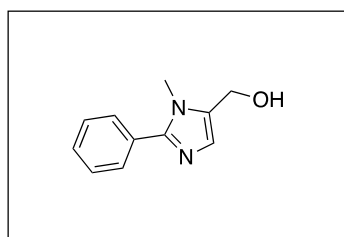imidazole-5-carboxylate (**105**, 1.97 g, 14.0 mmol) in dry CCl$_4$ (150 mL) was added NBS (2.75g, 15.5 mmol) and benzoyl peroxide (170 mg, 0.70 mmol). The reaction mixture was stirred at 60 °C for 48 h and was subsequently filtered. The filtrate was concentrated under reduced pressure and the obtained residue was purified by flash chromatography on silica-gel using a mixture of hexane/ethyl acetate (6:1→ 4:1) as eluent. Methyl 2-bromo-1-methyl-1*H*-imidazole-5-carboxylate was gained as yellow solid. Yield: 1.23 g, 40%. Mp 64–67 °C. ^{1}H NMR (CDCl$_3$, 500 MHz): δ_H (ppm) = 7.68 (s, 1H), 3.91 (s, 3H), 3.86 (s, 3H). (ESI): *m/z* = 219 [M+H]$^+$. Afterwards according to method A reaction of Methyl 2-bromo-1-methyl-1*H*-imidazole-5-carboxylate (1.01 g, 4.61 mmol) with phenylboronic acid (840 mg, 6.89 mmol) was performed. Crude product was purified by flash chromatography on silica-gel using a mixture of hexane/ethyl acetate (7:1→ 3:1) as eluent. Methyl 1-methyl-2-phenyl-1*H*-imidazole-5-carboxylate was gained as white solid. Yield: 466 mg, 47%. Mp 73–76 °C. ^{1}H NMR (CDCl$_3$, 500 MHz): δ_H (ppm) = 7.89 (s, 1H), 7.59–7.56 (m, 2H), 7.50–7.48 (m, 3H), 3.93 (s, 3H), 3.89 (s, 3H). (ESI): *m/z* = 217 [M+H]$^+$. To a stirred suspension of Methyl 1-methyl-2-phenyl-1*H*-imidazole-5-carboxylate (364 mg, 1.68 mmol) in dry THF (24 mL) was added lithium aluminium hydride (128 mg, 3.37 mmol) at 0 °C. After 1 h stirring water (10 mL) was added slowly at 0 °C and the obtained mixture was extracted with ethyl acetate twice. The combined organic phases were dried over

MgSO$_4$ and concentrated under reduced pressure. Crude product was recrystallized from ethyl acetate. White solid. Yield: 273 mg, 86%. Mp 155–157 °C. ^{1}H NMR (DMSO-d$_6$, 500 MHz): δ$_H$ (ppm) = 7.67–7.61 (m, 2H), 7.52–7.46 (m, 2H), 7.45–7.40 (m, 1H), 6.91 (s, 1H), 5.12 (t, J = 5.2 Hz, 1H), 4.50 (d, J = 5.0 Hz, 2H), 3.68 (s, 3H). ^{13}C NMR (DMSO-d$_6$, 125 MHz): δ$_C$ (ppm) = 147.4, 133.6, 131.0, 128.4, 128.4, 128.3, 126.8, 53.0, 31.8. (ESI): m/z = 189 [M+H]$^+$.
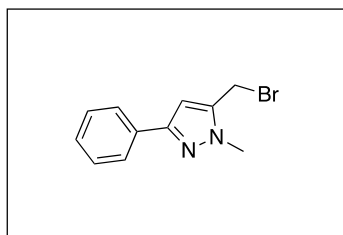
5-(Bromomethyl)-1-methyl-3-phenyl-1H-pyrazole (112). To a stirred suspension of

1-Methyl-3-phenyl-1H-pyrazole-5-carboxylic acid (**106**, 927 mg, 4.58 mmol) in dry THF (35 mL) lithium aluminium hydride (348 mg, 9.17 mmol) was added at 0 °C. Reaction mixture was allowed to warm to room temperature and was stirred for 12 h. Afterwards ice water (20 mL) was added slowly and the obtained mixture was extracted with ethyl acetate twice. The combined organic phases were dried over MgSO$_4$ and concentrated under reduced pressure. Crude product was purified by flash chromatography on silica-gel using ethyl acetate as eluent. (1-Methyl-3-phenyl-1H-pyrazol-5-yl)methanol was obtained as white solid. Yield: 634 mg, 74%. Mp 124–126 °C. ^{1}H NMR (CDCl$_3$, 500 MHz): δ$_H$ (ppm) = 7.78–7.73 (m, 2H), 7.42–7.36 (m, 2H), 7.32–7.28 (m, 1H), 6.44 (s, 1H), 4.65 (s, 2H), 3.90 (s, 3H), 2.39 (br s, 1H). ^{13}C NMR (CDCl$_3$, 125 MHz): δ$_C$ (ppm) = 150.1, 142.6, 133.3, 128.6, 127.6, 125.4, 102.9, 55.6, 36.6. (ESI): m/z = 189 [M+H]$^+$. To a solution of (1-Methyl-3-phenyl-1H-pyrazol-5-yl)methanol (719 mg, 3.82 mmol) in dry THF (50 mL) was added phosphorus tribromide (0.72 mL, 2.07 g, 7.65 mmol) dropwise at 0 °C. Reaction mixture was allowed to warm to room temperature and was stirred for 20 h. Afterwards ice water (30 mL) was added slowly and the obtained mixture was extracted with ethyl acetate twice. The combined organic phases were dried over MgSO$_4$ and concentrated under reduced pressure. Crude product was purified by flash chromatography on silica-gel using a mixture of hexane/ethyl acetate (6:1) as eluent. White solid. Yield: 775 mg, 81%. Mp 127–130 °C. ^{1}H NMR (CDCl$_3$, 500 MHz): δ$_H$ (ppm) = 7.78–7.72 (m, 2H, Ph H), 7.43–7.37 (m, 2H, Ph H), 7.34–7.29 (m, 1H, Ph H), 6.60 (s, 1H, pyrazole H-4), 4.59 (s, 2H, CH_2), 4.05 (s, 3H, CH_3). ^{13}C NMR (CDCl$_3$, 125 MHz): δ$_C$ (ppm) = 150.2 (pyrazole C-3), 138.8 (pyrazole C-5), 132.9 (Ph C$_q$), 128.6 (Ph C), 127.7 (Ph C), 125.4 (Ph C), 104.0 (pyrazole C-4), 36.6 (CH$_3$), 20.6 (CH$_2$). (ESI): m/z = 251 [M+H]$^+$.

5-((3-Phenylisoxazol-5-yl)methyl)pyridin-3-ol **(115).** 5-((5-Methoxypyridin-3-yl)methyl)-3-phenylisoxazole (**90**) (80 mg, 0.30 mmol) was suspended in HBr (48 % in water, 10 mL) and the mixture was stirred at 130 °C overnight. After cooling to RT, the aqueous phase was washed with EtOAc and then neutralized with saturated Na_2CO_3 solution. After extraction with EtOAc, the combined organic phases were dried over $MgSO_4$, filtered and concentrated under reduced pressure. Crude product was purified by flash chromatography on silica-gel using a mixture of ethyl acetate / methanol (9:1) as eluent. White solid. Yield: 18 mg, 24%. Mp degradation >185 °C. ^{1}H NMR (DMSO-d_6, 500 MHz): δ_H (ppm) = 9.95 (s, 1 H, OH), 8.06 (d, J = 2.8 Hz, 1 H, pyridinyl H-6), 8.04 (d, J = 1.6 Hz, 1 H, pyridinyl H-2), 7.87–7.82 (m, 2 H, Ph H), 7.51–7.46 (m, 3 H, Ph H), 7.11 (dd, J = 2.5, 1.9 Hz, 1 H, pyridinyl H-4), 6.83–6.80 (m, 1 H, isoxazol H-4), 4.18 (s, 2 H, CH_2). ^{13}C NMR (DMSO-d_6, 125 MHz): δ_C (ppm) = 172.5 (isoxazol C_q), 162.5 (isoxazol C_q), 154.1 (C_q), 140.9 (pyridinyl C-2), 137.3 (pyridinyl C-6), 133.2 (C_q), 130.7 (Ph C), 129.6 (Ph C), 129.1 (C_q), 127.1 (Ph C), 122.7 (pyridinyl C-4), 100.9 (isoxazol C-4), 29.7 (CH$_2$). (ESI): m/z = 253 [M+H]$^+$. HRMS: [$C_{15}H_{12}N_2O_2$+H]$^+$ calcd: 253.0972, found: 253.0974.
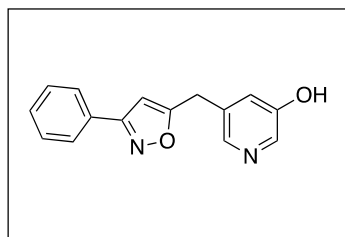
5-((2-Phenylthiazol-5-yl)methyl)pyridin-3-ol **(116).** Synthesized using 5-(bromomethyl)-2-phenylthiazole (**107**) (297 mg, 1.17 mmol), (5-methoxypyridin-3-yl)boronic acid pinacol ester (330 mg, 1.40 mmol), Cs_2CO_3 (1.63 g, 5.00 mmol) and $PdCl_2$(dppf) (61.0 mg, 0.08 mmol) according to method H. Crude product was purified by flash chromatography on silica-gel using a mixture of hexane / ethyl acetate (4:1) as eluent. Light yellow solid. Yield: 22 mg, 7%. Mp 153–155 °C. ^{1}H NMR (DMSO-d_6, 500 MHz): δ_H (ppm) = 9.92 (s, 1 H, OH), 8.03 (dd, J = 2.4, 3.6 Hz, 2 H, pyridinyl H), 7.85–7.89 (m, 2 H, Ph H), 7.74 (s, 1 H, thiazol H-4), 7.42–7.49 (m, 3 H, Ph H), 7.06 (t, J = 2.4 Hz, 1 H, pyridinyl H-4), 4.20 (s, 2 H, CH_2). ^{13}C NMR (DMSO-d_6, 125 MHz): δ_C (ppm) = 166.4 (thiazol C-2), 153.6 (pyridinyl C-3), 141.7 (thiazol C-4), 140.1 (pyridinyl C), 138.3 (C_q), 136.5 (pyridinyl C), 136.2 (C_q), 133.1 (C_q), 130.0 (Ph C), 129.2 (Ph C), 125.8 (Ph C), 121.8 (pyridinyl C-4), 29.0 (CH$_2$). (ESI): m/z = 269 [M+H]$^+$. HRMS: [$C_{15}H_{12}N_2OS$+H]$^+$ calcd: 269.0743, found: 269.0745.
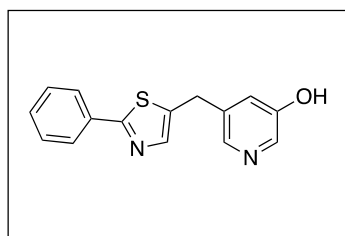
5-((1-Methyl-3-phenyl-1*H*-pyrazol-5-yl)methyl)pyridin-3-ol (117). Synthesized using 5-(bromomethyl)-1-methyl-3-phenyl-1*H*-pyrazole (**112**) (245 mg, 0.98 mmol), (5-methoxypyridin-3-yl)boronic acid pinacol ester (275 mg, 1.17 mmol), Cs_2CO_3 (958 mg, 2.94 mmol) and $PdCl_2$(dppf) (36.0 mg, 0.05 mmol) according to method H. Crude product was purified by flash chromatography twice on silica-gel using ethyl acetate and subsequent a mixture of hexane / EtOAc (1:3) as eluent. Off-white solid. Yield: 17 mg, 7%. Mp degradation >205 °C. ^{1}H NMR (DMSO-d$_6$, 500 MHz): δ_H (ppm) = 9.87 (br. s., 1 H, OH), 8.02 (d, J = 2.5 Hz, 1 H, pyridinyl H), 8.00 (d, J = 1.9 Hz, 1 H, pyridinyl H), 7.71–7.76 (m, 2 H, Ph H), 7.33–7.39 (m, 2 H, Ph H), 7.23–7.29 (m, 1 H, Ph H), 6.99 (dd, J = 1.9, 2.5 Hz, 1 H, pyridinyl H-4), 6.46 (s, 1 H, pyrazole H-4), 4.03 (s, 2 H, C*H*$_2$), 3.75 (s, 3 H, C*H*$_3$). ^{13}C NMR (DMSO-d$_6$, 125 MHz): δ_C (ppm) = 153.6 (C$_q$), 148.5 (C$_q$), 142.4 (C$_q$), 140.3, 136.3, 134.3 (C$_q$), 133.3 (C$_q$), 128.6, 127.2, 124.8, 121.9, 102.6 (pyrazole C-4), 36.3 (CH$_3$), 27.8 (CH$_2$). (ESI): m/z = 266 [M+H]$^+$. HRMS: [C$_{16}$H$_{15}$N$_3$O+H]$^+$. calcd: 266.1288, found: 266.1289.
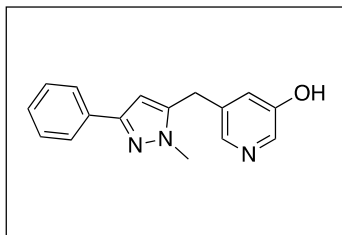
2-(2-Fluorophenyl)-5-((5-methoxypyridin-3-yl)methyl)pyridine (118). To a solution of **121** (900 mg, 3.38 mmol), (5-methoxypyridin-3-yl)boronic acid pinacol ester (1.02 g, 4.34 mmol) and Pd(PPh$_3$)$_4$ (197mg, 0.17 mmol) in degassed toluene/EtOH (27 mL, 1:1), a degassed solution of 2 M Na$_2$CO$_3$ (7.8 mL, 15.7 mmol) was added and the reaction mixture was stirred for 22 h at 100 °C. After cooling to room temperature, water was added and the mixture was extracted with EtOAc. The combined organic layer was dried over Na$_2$SO$_4$, filtered and concentrated under reduced pressure. The crude product was purified by flash chromatography on silica-gel using a mixture of hexane/EtOAc (1:1) as eluent. The obtained impure product was dissolved in EtOAc and extracted with 1 M HCl. The aqueous phase was washed with DCM, basified with saturated Na$_2$CO$_3$ solution. The aq. layer was extracted with DCM (×3) and the combined organic phases were dried over MgSO$_4$, filtered and concentrated under reduced pressure. Beige solid. Yield: 367 mg, 38%. Mp 69–71 °C. ^{1}H NMR (CDCl$_3$, 500 MHz): δ_H (ppm) = 8.61 (d, J = 2.0 Hz, 1 H), 8.21 (d, J = 2.7 Hz, 1 H), 8.16 (d, J = 1.1 Hz, 1 H), 7.96 (td, J = 7.9, 1.8 Hz, 1 H), 7.73 (dd, J = 8.1, 1.8 Hz, 1 H), 7.53 (dd, J = 8.2, 2.3 Hz, 1 H), 7.37 (m, 1 H), 7.26 (td, J = 7.5, 1.1 Hz, 1 H), 7.15 (ddd, J = 11.4, 8.2, 1.1 Hz, 1 H), 7.00 (m, 1 H), 4.01 (s, 2 H), 3.83 (s, 3 H). ^{13}C NMR (CDCl$_3$, 125 MHz): δ_C (ppm) = 160.6 (d, $J_{C,F}$ = 249.6 Hz), 156.2, 152.0, 150.0, 141.7, 136.9, 136.5, 135.0, 133.8, 131.0 (d, $J_{C,F}$ = 3.1 Hz), 130.6 (d, $J_{C,F}$ = 8.6 Hz), 127.1 (d, $J_{C,F}$ = 12.0 Hz), 124.7 (d, $J_{C,F}$ = 3.6 Hz), 124.6 (d, $J_{C,F}$ = 9.2 Hz),

122.0, 116.3 (d, $J_{C,F}$ = 23.1 Hz), 55.8, 35.9. (ESI): m/z = 295 [M+H]$^+$. HRMS: [C$_{18}$H$_{15}$FN$_2$O+H]$^+$ calcd: 295.1241, found: 295.1244.

5-((6-(2-Fluorophenyl)pyridin-3-yl)methyl)pyridin-3-ol (119). To a solution of **118** (74.0 mg,
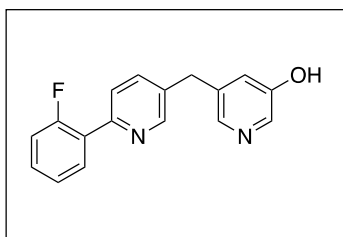
0.25 mmol) in DCM was added a solution of BBr$_3$ in DCM (1 M, 2,5 mL) at -78 °C and the reaction mixture was allowed to warm up to room temperature overnight (21 h). The reaction mixture was quenched with ice-water and the aqueous phase washed twice with DCM. The aqueous phase was neutralized (pH ~ 8) with saturated

aq. NaHCO$_3$ solution and extracted with DCM (×3). The combined organic layers were dried over Na$_2$SO$_4$, filtered and concentrated *in vacuo*. Crude product was purified by flash chromatography on silica-gel using EtOAc as eluent. White solid. Yield: 11 mg, 16%. Mp 134–135 °C. ^{1}H NMR (CDCl$_3$, 500 MHz): δ$_H$ (ppm) = 8.53 (s, 1 H), 8.07 (s, 1 H), 7.99 (s, 1 H), 7.86 (t, J = 7.8 Hz, 1 H), 7.70 (d, J = 8.1 Hz, 1 H), 7.54 (d, J = 8.2 Hz, 1 H), 7.35 (m, 1 H), 7.22 (m, 1 H), 7.13 (m, 1 H), 7.00 (s, 1 H), 3.94 (s, 2 H). ^{13}C NMR (CDCl$_3$, 125 MHz): δ$_C$ (ppm) = 160.3 (d, $J_{C,F}$ = 249.6 Hz), 154.9, 151.8 (d, $J_{C,F}$ = 2.1 Hz), 149.5, 139.6, 137.2, 136.8, 135.7, 134.1, 130.8 (d, $J_{C,F}$ = 2.7 Hz), 130.6 (d, $J_{C,F}$ = 8.4 Hz), 126.7 (d, $J_{C,F}$ = 11.7 Hz), 124.7 (d, $J_{C,F}$ = 8.3 Hz), 124.5 (d, $J_{C,F}$ = 3.6 Hz), 124.4, 116.2 (d, $J_{C,F}$ = 7.8 Hz), 35.6. (ESI): m/z = 281 [M+H]$^+$. HRMS: [C$_{17}$H$_{13}$FN$_2$O+H]$^+$ calcd: 281.1085, found: 281.1086.

2-(2-Fluorophenyl)-5-methylpyridine (120). To a solution of 2-bromo-5-methylpyridine (3.00 g,
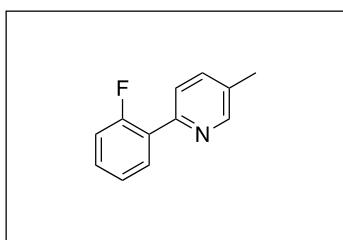
17.4 mmol), (2-fluoro-phenyl)boronic acid (3.65 g, 26.1 mmol) and Pd(PPh$_3$)$_4$ (780 mg, 0.67 mmol) in degassed toluene/EtOH (160 mL, 1:1), a degassed aqueous solution of Na$_2$CO$_3$ (2 M, 40 mL, 80.0 mmol) was added and the reaction mixture was stirred for 20 h at 100 °C under nitrogen. After cooling to room temperature, water

was added and the mixture was extracted three times with ethyl acetate. The combined organic layers were dried over Na$_2$SO$_4$, filtered and concentrated under reduced pressure. The crude product was purified by flash chromatography on silica-gel using a mixture of hexane/EtOAc (9:1) as eluent. Colorless oil. Yield: 3.16 g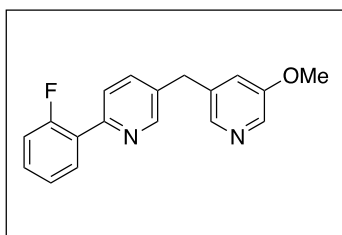, 97%. ^{1}H NMR (CDCl$_3$, 500 MHz): δ$_H$ (ppm) = 8.55 (m, 1 H), 7.95 (td, J = 7.9, 1.9 Hz, 1 H), 7.68 (dd, J = 8.1, 2.2 Hz, 1 H), 7.56 (dd, J = 8.1, 2.2 Hz, 1 H), 7.35 (m, 1 H), 7.25 (td, J = 7.5, 1.2 Hz, 1 H), 7.15 (ddd, J = 11.4, 8.2 Hz, 1.2 Hz, 1 H), 2.38 (s, 3 H). ^{13}C NMR (CDCl$_3$, 125 MHz): δ$_C$ (ppm) = 160.4 (d, $J_{C,F}$ = 249.2 Hz), 150.6 (d, $J_{C,F}$ = 1.8 Hz), 150.2, 136.9, 132.0, 130.8 (d, $J_{C,F}$ = 8.6 Hz), 130.0 (d, $J_{C,F}$ = 8.6 Hz), 127.5 (d, $J_{C,F}$ = 11.9 Hz), 124.4 (d, $J_{C,F}$ = 3.3 Hz), 123.9 (d, $J_{C,F}$ = 8.8 Hz), 116.1 (d, $J_{C,F}$ = 23.1 Hz), 18.2.

5-(Bromomethyl)-2-(2-fluorophenyl)pyridine (121). Compound **120** (1.10 g, 5.88 mmol) was
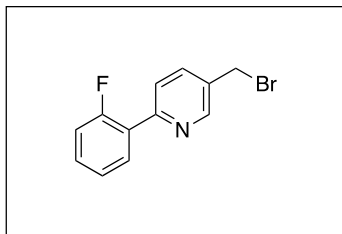
dissolved in carbon tetrachloride, and NBS (1.05 g, 5.90 mmol) and AIBN (49.0 mg, 0.30 mmol) were added. The reaction mixture was stirred for 7 h at 80 °C. After cooling to room temperature, the suspension was filtered and the filtrate concentrated in vacuum. The crude product was purified by flash chromatography on silica-gel using a mixture of hexane/EtOAc (95:5→ 9:1) as eluent. Orange oil. Yield: 1.02 g, 65%. ^{1}H NMR (CDCl$_3$, 500 MHz): δ_H (ppm) = 8.73 (t, J = 1.6 Hz, 1 H), 7.99 (td, J = 7.9, 1.9 Hz, 1 H), 7.80 (m, 2 H), 7.39 (m, 1 H), 7.27 (m, 1 H), 7.16 (ddd, J = 11.5, 8.2, 1.1 Hz, 1 H), 4.53 (s, 2 H). ^{13}C NMR (CDCl$_3$, 125 MHz): δ_C (ppm) = 160.5 (d, $J_{C,F}$ = 250.2 Hz), 153.3 (d, $J_{C,F}$ = 2.7 Hz), 149.7, 137.0, 132.3, 131.0 (d, $J_{C,F}$ = 2.7 Hz), 130.7 (d, $J_{C,F}$ = 8.8 Hz), 126.8 (d, $J_{C,F}$ = 11.2 Hz), 124.6 (d, $J_{C,F}$ = 3.5 Hz), 124.4 (d, $J_{C,F}$ = 9.3 Hz), 116.2 (d, $J_{C,F}$ = 22.9 Hz), 29.5.

7. References

1   Voet, D.; Voet, J. G.; Pratt, C. W.; Beck-Sickinger, A., *Lehrbuch der Biochemie*. Wiley-VCH: Weinheim, **2002**, p 1062 S.

2   Smith, S. M.; Vale, W. W., The role of the hypothalamic-pituitary-adrenal axis in neuroendocrine responses to stress. *Dialogues Clin Neurosci* **2006,** *8* (4), 383.

3   Miller, W. L.; Auchus, R. J., The molecular biology, biochemistry, and physiology of human steroidogenesis and its disorders. *Endocrine Reviews* **2011,** *32* (1), 81.

4   Ballantyne, S., *The paleo approach : reverse autoimmune disease and heal your body*. 1st ed.; Victory Belt Publishing: **2014**.

5   Hakki, T.; Bernhardt, R., CYP17- and CYP11B-dependent steroid hydroxylases as drug development targets. *Pharmacology & Therapeutics* **2006,** *111* (1), 27.

6   Strushkevich, N.; Gilep, A. A.; Shen, L.; Arrowsmith, C. H.; Edwards, A. M.; Usanov, S. A.; Park, H. W., Structural insights into aldosterone synthase substrate specificity and targeted inhibition. *Molecular Endocrinology* **2013,** *27* (2), 315.

7   Funder, J. W., Glucocorticoid and mineralocorticoid receptors: biology and clinical relevance. *Annual Review of Medicine* **1997,** *48*, 231.

8   Magiakou, M. A.; Smyrnaki, P.; Chrousos, G. P., Hypertension in Cushing's syndrome. *Best Practice and Research. Clinical Endocrinology and Metabolism* **2006,** *20* (3), 467.

9   Tomlinson, J. W.; Walker, E. A.; Bujalska, I. J.; Draper, N.; Lavery, G. G.; Cooper, M. S.; Hewison, M.; Stewart, P. M., 11beta-hydroxysteroid dehydrogenase type 1: a tissue-specific regulator of glucocorticoid response. *Endocrine Reviews* **2004,** *25* (5), 831.

10   Anagnostis, P.; Katsiki, N.; Adamidou, F.; Athyros, V. G.; Karagiannis, A.; Kita, M.; Mikhailidis, D. P., 11beta-Hydroxysteroid dehydrogenase type 1 inhibitors: novel agents for the treatment of metabolic syndrome and obesity-related disorders? *Metabolism: Clinical and Experimental* **2013,** *62* (1), 21.

11   Smets, P.; Meyer, E.; Maddens, B.; Daminet, S., Cushing's syndrome, glucocorticoids and the kidney. *General and Comparative Endocrinology* **2010,** *169* (1), 1.

12   Newell-Price, J.; Bertagna, X.; Grossman, A. B.; Nieman, L. K., Cushing's syndrome. *Lancet* **2006,** *367* (9522), 1605.

13   Tritos, N. A.; Biller, B. M., Medical management of Cushing's disease. *Journal of Neuro-Oncology* **2014,** *117* (3), 407.

14   Boscaro, M.; Barzon, L.; Fallo, F.; Sonino, N., Cushing's syndrome. *Lancet* **2001,** *357* (9258), 783.

15   Hatipoglu, B. A., Cushing's syndrome. *Journal of Surgical Oncology* **2012,** *106* (5), 565.

16   Krikorian, A.; Khan, M., Is metabolic syndrome a mild form of Cushing's syndrome? *Reviews in Endocrine and Metabolic Disorders* **2010,** *11* (2), 141.

17   Hermanowski-Vosatka, A.; Balkovec, J. M.; Cheng, K.; Chen, H. Y.; Hernandez, M.; Koo, G. C.; Le Grand, C. B.; Li, Z.; Metzger, J. M.; Mundt, S. S.; Noonan, H.; Nunes, C. N.; Olson, S. H.; Pikounis, B.; Ren, N.; Robertson, N.; Schaeffer, J. M.; Shah, K.; Springer, M. S.; Strack, A. M.; Strowski, M.; Wu, K.; Wu, T.; Xiao, J.; Zhang, B. B.; Wright, S. D.; Thieringer, R., 11beta-HSD1 inhibition ameliorates metabolic syndrome and prevents progression of atherosclerosis in mice. *Journal of Experimental Medicine* **2005,** *202* (4), 517.

18   Ten, S.; New, M.; Maclaren, N., Clinical review 130: Addison's disease 2001. *Journal of Clinical Endocrinology and Metabolism* **2001,** *86* (7), 2909.

19   Fleseriu, M.; Petersenn, S., Medical management of Cushing's disease: what is the future? *Pituitary* **2012,** *15* (3), 330.

20   Feelders, R. A.; Hofland, L. J., Medical treatment of Cushing's disease. *Journal of Clinical Endocrinology and Metabolism* **2013,** *98* (2), 425.

21   Dang, C. N.; Trainer, P., Pharmacological management of Cushing's syndrome: an update. *Arquivos Brasileiros de Endocrinologia e Metabologia* **2007,** *51* (8), 1339.

22   Molitch, M. E., Current approaches to the pharmacological management of Cushing's disease. *Molecular and Cellular Endocrinology* **2015,** *408*, 185.

23   Bertagna, X.; Pivonello, R.; Fleseriu, M.; Zhang, Y.; Robinson, P.; Taylor, A.; Watson, C. E.; Maldonado, M.; Hamrahian, A. H.; Boscaro, M.; Biller, B. M., LCI699, a potent 11beta-hydroxylase inhibitor, normalizes urinary cortisol in patients with Cushing's disease: results from a multicenter, proof-of-concept study. *Journal of Clinical Endocrinology and Metabolism* **2014,** *99* (4), 1375.

24   Alexandraki, K. I.; Grossman, A. B., Medical therapy of Cushing's disease: where are we now? *Frontiers of Hormone Research* **2010,** *38*, 165.

25   Petersenn, S.; Fleseriu, M., Pituitary-directed medical therapy in Cushing's disease. *Pituitary* **2015,** *18* (2), 238.

26   Ceccato, F.; Barbot, M.; Zilio, M.; Albiger, N.; Mantero, F.; Scaroni, C., Therapeutic strategies for Cushing's syndrome: an update. *Expert Opinion on Orphan Drugs* **2015,** *3* (1), 45.

27   Wondisford, F. E., A new medical therapy for Cushing disease? *Journal of Clinical Investigation* **2011,** *121* (12), 4621.

28	Cuevas-Ramos, D.; Lim, D. S. T.; Fleseriu, M., Update on medical treatment for Cushing's disease. *Clin Diabetes Endocrinol* **2016,** *2*, 16.

29	Roumen, L.; Sanders, M. P.; Pieterse, K.; Hilbers, P. A.; Plate, R.; Custers, E.; de Gooyer, M.; Smits, J. F.; Beugels, I.; Emmen, J.; Ottenheijm, H. C.; Leysen, D.; Hermans, J. J., Construction of 3D models of the CYP11B family as a tool to predict ligand binding characteristics. *Journal of Computer-Aided Molecular Design* **2007,** *21* (8), 455.

30	Hu, Q.; Yin, L.; Hartmann, R. W., Aldosterone synthase inhibitors as promising treatments for mineralocorticoid dependent cardiovascular and renal diseases. *Journal of Medicinal Chemistry* **2014,** *57* (12), 5011.

31	Schenkman, J. B.; Sligar, S. G.; Cinti, D. L., Substrate interaction with cytochrome P-450. *Pharmacology & Therapeutics* **1981,** *12* (1), 43.

32	Tanaka, E., Clinically important pharmacokinetic drug-drug interactions: role of cytochrome P450 enzymes. *Journal of Clinical Pharmacy and Therapeutics* **1998,** *23* (6), 403.

33	Alexandraki, K. I.; Kaltsas, G. A., Pharmacological Management of Cushing's Disease. *JSM Thyroid Disord Manag* **2017,** *2* (1), 1006.

34	Gower, D. B., Modifiers of steroid-hormone metabolism: a review of their chemistry, biochemistry and clinical applications. *Journal of Steroid Biochemistry* **1974,** *5* (5), 501.

35	Miller, J. W.; Crapo, L., The medical treatment of Cushing's syndrome. *Endocrine Reviews* **1993,** *14* (4), 443.

36	Jameson, J. L.; DeGroot, L. J.; De Kretser, D. M.; Giudice, L.; Grossman, A.; Melmed, S.; Potts, J. T.; Weir, G. C., *Endocrinology adult & pediatric*. 7th edition ed.; Elsevier/Saunders: Philadelphia, PA, **2016**, p Online.

37	Newell-Price, J., Ketoconazole as an adrenal steroidogenesis inhibitor: effectiveness and risks in the treatment of Cushing's disease. *Journal of Clinical Endocrinology and Metabolism* **2014,** *99* (5), 1586.

38	Gadelha, M. R.; Vieira Neto, L., Efficacy of medical treatment in Cushing's disease: a systematic review. *Clinical Endocrinology* **2014,** *80* (1), 1.

39	Fleseriu, M.; Pivonello, R.; Young, J.; Hamrahian, A. H.; Molitch, M. E.; Shimizu, C.; Tanaka, T.; Shimatsu, A.; White, T.; Hilliard, A.; Tian, C.; Sauter, N.; Biller, B. M.; Bertagna, X., Osilodrostat, a potent oral 11beta-hydroxylase inhibitor: 22-week, prospective, Phase II study in Cushing's disease. *Pituitary* **2016,** *19* (2), 138.

40	Roumen, L.; Peeters, J. W.; Emmen, J. M.; Beugels, I. P.; Custers, E. M.; de Gooyer, M.; Plate, R.; Pieterse, K.; Hilbers, P. A.; Smits, J. F.; Vekemans, J. A.; Leysen, D.; Ottenheijm, H. C.; Janssen, H. M.; Hermans, J. J., Synthesis, biological evaluation, and molecular

modeling of 1-benzyl-1H-imidazoles as selective inhibitors of aldosterone synthase (CYP11B2). *Journal of Medicinal Chemistry* **2010,** *53* (4), 1712.

41   Hille, U. E.; Zimmer, C.; Vock, C. A.; Hartmann, R. W., First Selective CYP11B1 Inhibitors for the Treatment of Cortisol-Dependent Diseases. *ACS Medicinal Chemistry Letters* **2011,** *2* (1), 2.

42   Emmerich, J.; Hu, Q.; Hanke, N.; Hartmann, R. W., Cushing's syndrome: development of highly potent and selective CYP11B1 inhibitors of the (pyridylmethyl)pyridine type. *Journal of Medicinal Chemistry* **2013,** *56* (15), 6022.

43   Hille, U. E.; Zimmer, C.; Haupenthal, J.; Hartmann, R. W., Optimization of the First Selective Steroid-11beta-hydroxylase (CYP11B1) Inhibitors for the Treatment of Cortisol Dependent Diseases. *ACS Medicinal Chemistry Letters* **2011,** *2* (8), 559.

44   Guo, S.; Dipietro, L. A., Factors affecting wound healing. *Journal of Dental Research* **2010,** *89* (3), 219.

45   Menke, N. B.; Ward, K. R.; Witten, T. M.; Bonchev, D. G.; Diegelmann, R. F., Impaired wound healing. *Clinics in Dermatology* **2007,** *25* (1), 19.

46   Vukelic, S.; Stojadinovic, O.; Pastar, I.; Rabach, M.; Krzyzanowska, A.; Lebrun, E.; Davis, S. C.; Resnik, S.; Brem, H.; Tomic-Canic, M., Cortisol synthesis in epidermis is induced by IL-1 and tissue injury. *Journal of Biological Chemistry* **2011,** *286* (12), 10265.

47   Hannen, R. F.; Michael, A. E.; Jaulim, A.; Bhogal, R.; Burrin, J. M.; Philpott, M. P., Steroid synthesis by primary human keratinocytes; implications for skin disease. *Biochemical and Biophysical Research Communications* **2011,** *404* (1), 62.

48   Tiganescu, A.; Hupe, M.; Uchida, Y.; Mauro, T.; Elias, P. M.; Holleran, W. M., Increased glucocorticoid activation during mouse skin wound healing. *Journal of Endocrinology* **2014,** *221* (1), 51.

49   Tomic-Canic, M.; Brem, H.; Samuels, H. H., De novo synthesis of glucocorticoids in the epidermis and its uses and applications. *US2008274079 (A1)* **2008**.

50   van Koppen, C. J.; Hartmann, R. W., Advances in the treatment of chronic wounds: a patent review. *Expert Opinion on Therapeutic Patents* **2015,** *25* (8), 931.

51   Slominski, A.; Zbytek, B.; Nikolakis, G.; Manna, P. R.; Skobowiat, C.; Zmijewski, M.; Li, W.; Janjetovic, Z.; Postlethwaite, A.; Zouboulis, C. C.; Tuckey, R. C., Steroidogenesis in the skin: implications for local immune functions. *Journal of Steroid Biochemistry and Molecular Biology* **2013,** *137*, 107.

52   Zhu, W.; Hu, Q.; Hanke, N.; van Koppen, C. J.; Hartmann, R. W., Potent 11beta-hydroxylase inhibitors with inverse metabolic stability in human plasma and hepatic S9 fractions to promote wound healing. *Journal of Medicinal Chemistry* **2014,** *57* (18), 7811.

53   Morton, N. M., Obesity and corticosteroids: 11beta-hydroxysteroid type 1 as a cause and therapeutic target in metabolic disease. *Molecular and Cellular Endocrinology* **2010,** *316* (2), 154.

54   White, P. C.; Curnow, K. M.; Pascoe, L., Disorders of steroid 11 beta-hydroxylase isozymes. *Endocrine Reviews* **1994,** *15* (4), 421.

55   Mornet, E.; Dupont, J.; Vitek, A.; White, P. C., Characterization of two genes encoding human steroid 11 beta-hydroxylase (P-450(11) beta). *Journal of Biological Chemistry* **1989,** *264* (35), 20961.

56   Lucas, S.; Heim, R.; Ries, C.; Schewe, K. E.; Birk, B.; Hartmann, R. W., In vivo active aldosterone synthase inhibitors with improved selectivity: lead optimization providing a series of pyridine substituted 3,4-dihydro-1H-quinolin-2-one derivatives. *Journal of Medicinal Chemistry* **2008,** *51* (24), 8077.

57   Lucas, S.; Heim, R.; Negri, M.; Antes, I.; Ries, C.; Schewe, K. E.; Bisi, A.; Gobbi, S.; Hartmann, R. W., Novel aldosterone synthase inhibitors with extended carbocyclic skeleton by a combined ligand-based and structure-based drug design approach. *Journal of Medicinal Chemistry* **2008,** *51* (19), 6138.

58   Heim, R.; Lucas, S.; Grombein, C. M.; Ries, C.; Schewe, K. E.; Negri, M.; Müller-Vieira, U.; Birk, B.; Hartmann, R. W., Overcoming undesirable CYP1A2 inhibition of pyridylnaphthalene-type aldosterone synthase inhibitors: influence of heteroaryl derivatization on potency and selectivity. *Journal of Medicinal Chemistry* **2008,** *51* (16), 5064.

59   Lucas, S.; Negri, M.; Heim, R.; Zimmer, C.; Hartmann, R. W., Fine-tuning the selectivity of aldosterone synthase inhibitors: structure-activity and structure-selectivity insights from studies of heteroaryl substituted 1,2,5,6-tetrahydropyrrolo[3,2,1-ij]quinolin-4-one derivatives. *Journal of Medicinal Chemistry* **2011,** *54* (7), 2307.

60   Yin, L.; Lucas, S.; Maurer, F.; Kazmaier, U.; Hu, Q.; Hartmann, R. W., Novel imidazol-1-ylmethyl substituted 1,2,5,6-tetrahydropyrrolo[3,2,1-ij]quinolin-4-ones as potent and selective CYP11B1 inhibitors for the treatment of Cushing's syndrome. *Journal of Medicinal Chemistry* **2012,** *55* (14), 6629.

61   Yin, L.; Hu, Q.; Hartmann, R. W., Tetrahydropyrroloquinolinone type dual inhibitors of aromatase/aldosterone synthase as a novel strategy for breast cancer patients with elevated cardiovascular risks. *Journal of Medicinal Chemistry* **2013,** *56* (2), 460.

62   Tosco, P.; Balle, T., Open3DQSAR: a new open-source software aimed at high-throughput chemometric analysis of molecular interaction fields. *Journal of Molecular Modeling* **2011,** *17* (1), 201.

63   Hu, Q.; Negri, M.; Jahn-Hoffmann, K.; Zhuang, Y.; Olgen, S.; Bartels, M.; Müller-Vieira, U.; Lauterbach, T.; Hartmann, R. W., Synthesis, biological evaluation, and molecular modeling studies of methylene imidazole substituted biaryls as inhibitors of human 17alpha-hydroxylase-17,20-lyase (CYP17)--part II: Core rigidification and influence of substituents at the methylene bridge. *Bioorganic & Medicinal Chemistry* **2008,** *16* (16), 7715.

64   Hille, U. E.; Hu, Q.; Vock, C.; Negri, M.; Bartels, M.; Muller-Vieira, U.; Lauterbach, T.; Hartmann, R. W., Novel CYP17 inhibitors: synthesis, biological evaluation, structure-activity relationships and modelling of methoxy- and hydroxy-substituted methyleneimidazolyl biphenyls. *European Journal of Medicinal Chemistry* **2009,** *44* (7), 2765.

65   Leze, M. P.; Le Borgne, M.; Pinson, P.; Palusczak, A.; Duflos, M.; Le Baut, G.; Hartmann, R. W., Synthesis and biological evaluation of 5-[(aryl)(1H-imidazol-1-yl)methyl]-1H-indoles: potent and selective aromatase inhibitors. *Bioorganic & Medicinal Chemistry Letters* **2006,** *16* (5), 1134.

66   Gobbi, S.; Cavalli, A.; Negri, M.; Schewe, K. E.; Belluti, F.; Piazzi, L.; Hartmann, R. W.; Recanatini, M.; Bisi, A., Imidazolylmethylbenzophenones as highly potent aromatase inhibitors. *Journal of Medicinal Chemistry* **2007,** *50* (15), 3420.

67   Stefanachi, A.; Favia, A. D.; Nicolotti, O.; Leonetti, F.; Pisani, L.; Catto, M.; Zimmer, C.; Hartmann, R. W.; Carotti, A., Design, synthesis, and biological evaluation of imidazolyl derivatives of 4,7-disubstituted coumarins as aromatase inhibitors selective over 17-alpha-hydroxylase/C17-20 lyase. *Journal of Medicinal Chemistry* **2011,** *54* (6), 1613.

68   Gobbi, S.; Hu, Q.; Negri, M.; Zimmer, C.; Belluti, F.; Rampa, A.; Hartmann, R. W.; Bisi, A., Modulation of cytochromes P450 with xanthone-based molecules: from aromatase to aldosterone synthase and steroid 11beta-hydroxylase inhibition. *Journal of Medicinal Chemistry* **2013,** *56* (4), 1723.

69   Feelders, R. A.; Pulgar, S. J.; Kempel, A.; Pereira, A. M., The burden of Cushing's disease: clinical and health-related quality of life aspects. *European Journal of Endocrinology* **2012,** *167* (3), 311.

70   Biller, B. M.; Grossman, A. B.; Stewart, P. M.; Melmed, S.; Bertagna, X.; Bertherat, J.; Buchfelder, M.; Colao, A.; Hermus, A. R.; Hofland, L. J.; Klibanski, A.; Lacroix, A.; Lindsay, J. R.; Newell-Price, J.; Nieman, L. K.; Petersenn, S.; Sonino, N.; Stalla, G. K.; Swearingen, B.; Vance, M. L.; Wass, J. A.; Boscaro, M., Treatment of adrenocorticotropin-dependent Cushing's syndrome: a consensus statement. *Journal of Clinical Endocrinology and Metabolism* **2008,** *93* (7), 2454.

71   Sigalas, P. D.; Garg, H.; Watson, S.; McAllister-Williams, R. H.; Ferrier, I. N., Metyrapone in treatment-resistant depression. *Ther Adv Psychopharmacol* **2012,** *2* (4), 139.

72   Hu, Q.; Yin, L.; Jagusch, C.; Hille, U. E.; Hartmann, R. W., Isopropylidene substitution increases activity and selectivity of biphenylmethylene 4-pyridine type CYP17 inhibitors. *Journal of Medicinal Chemistry* **2010,** *53* (13), 5049.

73   Hu, Q.; Negri, M.; Olgen, S.; Hartmann, R. W., The role of fluorine substitution in biphenyl methylene imidazole-type CYP17 inhibitors for the treatment of prostate carcinoma. *ChemMedChem* **2010,** *5* (6), 899.

74   Yin, L.; Hu, Q.; Emmerich, J.; Lo, M. M.; Metzger, E.; Ali, A.; Hartmann, R. W., Novel pyridyl- or isoquinolinyl-substituted indolines and indoles as potent and selective aldosterone synthase inhibitors. *Journal of Medicinal Chemistry* **2014,** *57* (12), 5179.

75   Grombein, C. M.; Hu, Q.; Heim, R.; Rau, S.; Zimmer, C.; Hartmann, R. W., 1-Phenylsulfinyl-3-(pyridin-3-yl)naphthalen-2-ols: a new class of potent and selective aldosterone synthase inhibitors. *European Journal of Medicinal Chemistry* **2015,** *89*, 597.

76   Stefanachi, A.; Hanke, N.; Pisani, L.; Leonetti, F.; Nicolotti, O.; Catto, M.; Cellamare, S.; Hartmann, R. W.; Carotti, A., Discovery of new 7-substituted-4-imidazolylmethyl coumarins and 4'-substituted-2-imidazolyl acetophenones open analogues as potent and selective inhibitors of steroid-11beta-hydroxylase. *European Journal of Medicinal Chemistry* **2015,** *89*, 106.

77   Grombein, C. M.; Hu, Q.; Rau, S.; Zimmer, C.; Hartmann, R. W., Heteroatom insertion into 3,4-dihydro-1H-quinolin-2-ones leads to potent and selective inhibitors of human and rat aldosterone synthase. *European Journal of Medicinal Chemistry* **2015,** *90*, 788.

78   Hu, Q.; Yin, L.; Ali, A.; Cooke, A. J.; Bennett, J.; Ratcliffe, P.; Lo, M. M.; Metzger, E.; Hoyt, S.; Hartmann, R. W., Novel pyridyl substituted 4,5-dihydro-[1,2,4]triazolo[4,3-a]quinolines as potent and selective aldosterone synthase inhibitors with improved in vitro metabolic stability. *Journal of Medicinal Chemistry* **2015,** *58* (5), 2530.

79   ACD/Labs, Advanced Chemistry Development. *Inc., Toronto, ON, Canada, www. acdlabs.com* **2016**.

80   Bingham, E.; Attfield, M.; Albert, R. E.; Baxter, C. S.; Bus, J. S.; Barter, R. A.; Boatman, R. J.; Adams, T., *"Patty's toxicology" Woo, Y. T.; Lai, D. Y. Aromatic amino and nitro-amino compounds and their halogenated derivatives.* 5th ed.; John Wiley: New York, 2001, p 969.

81   Fordyce, E. A. F.; Morrison, A. J.; Sharp, R. D.; Paton, R. M., Microwave-induced generation and reactions of nitrile sulfides: an improved method for the synthesis of isothiazoles and 1,2,4-thiadiazoles. *Tetrahedron* **2010,** *66* (35), 7192.

82   Zhou, W.; Xie, C.; Han, J. L.; Pan, Y., Catalyst-free intramolecular oxidative cyclization of N-allylbenzamides: a new route to 2,5-substituted oxazoles. *Organic Letters* **2012,** *14* (18), 4766.

83   Liu, Y. X.; Cui, Z. P.; Bin, L.; Cai, B. L.; Li, Y. H.; Wang, Q. M., Design, synthesis, and herbicidal activities of novel 2-cyanoacrylates containing isoxazole moieties. *Journal of Agricultural and Food Chemistry* **2010,** *58* (5), 2685.

84   Pizzo, C.; Mahler, S. G., Synthesis of selenazoles by in situ cycloisomerization of propargyl selenoamides using oxygen-selenium exchange reaction. *Journal of Organic Chemistry* **2014,** *79* (4), 1856.

85   Yanase, T.; Simpson, E. R.; Waterman, M. R., 17 alpha-hydroxylase/17,20-lyase deficiency: from clinical investigation to molecular definition. *Endocrine Reviews* **1991,** *12* (1), 91.

86   Jacobsen, N. W.; Halling-Sorensen, B.; Birkved, F. K., Inhibition of human aromatase complex (CYP19) by antiepileptic drugs. *Toxicology in Vitro* **2008,** *22* (1), 146.

87   Ehmer, P. B.; Jose, J.; Hartmann, R. W., Development of a simple and rapid assay for the evaluation of inhibitors of human 17alpha-hydroxylase-C(17,20)-lyase (P450cl7) by coexpression of P450cl7 with NADPH-cytochrome-P450-reductase in Escherichia coli. *Journal of Steroid Biochemistry and Molecular Biology* **2000,** *75* (1), 57.

88   Hutschenreuter, T. U.; Ehmer, P. B.; Hartmann, R. W., Synthesis of hydroxy derivatives of highly potent non-steroidal CYP 17 inhibitors as potential metabolites and evaluation of their activity by a non cellular assay using recombinant human enzyme. *Journal of Enzyme Inhibition and Medicinal Chemistry* **2004,** *19* (1), 17.

89   Hartmann, R. W.; Batzl, C., Aromatase inhibitors. Synthesis and evaluation of mammary tumor inhibiting activity of 3-alkylated 3-(4-aminophenyl)piperidine-2,6-diones. *Journal of Medicinal Chemistry* **1986,** *29* (8), 1362.

90   Machala, M.; Vondracek, J.; Blaha, L.; Ciganek, M.; Neca, J. V., Aryl hydrocarbon receptor-mediated activity of mutagenic polycyclic aromatic hydrocarbons determined using in vitro reporter gene assay. *Mutation Research* **2001,** *497* (1-2), 49.

91   Piper, D. R.; Duff, S. R.; Eliason, H. C.; Frazee, W. J.; Frey, E. A.; Fuerstenau-Sharp, M.; Jachec, C.; Marks, B. D.; Pollok, B. A.; Shekhani, M. S.; Thompson, D. V.; Whitney, P.; Vogel, K. W.; Hess, S. D., Development of the predictor HERG fluorescence polarization assay using a membrane protein enrichment approach. *Assay and Drug Development Technologies* **2008,** *6* (2), 213.

92   Rigel, D. F.; Fu, F.; Beil, M.; Hu, C. W.; Liang, G.; Jeng, A. Y., Pharmacodynamic and pharmacokinetic characterization of the aldosterone synthase inhibitor FAD286 in two

rodent models of hyperaldosteronism: comparison with the 11beta-hydroxylase inhibitor metyrapone. *Journal of Pharmacology and Experimental Therapeutics* **2010,** *334* (1), 232.

93   Gosain, A.; DiPietro, L. A., Aging and wound healing. *World Journal of Surgery* **2004,** *28* (3), 321.

94   Wild, T.; Rahbarnia, A.; Kellner, M.; Sobotka, L.; Eberlein, T., Basics in nutrition and wound healing. *Nutrition* **2010,** *26* (9), 862.

95   Sen, C. K.; Gordillo, G. M.; Roy, S.; Kirsner, R.; Lambert, L.; Hunt, T. K.; Gottrup, F.; Gurtner, G. C.; Longaker, M. T., Human skin wounds: a major and snowballing threat to public health and the economy. *Wound Repair and Regeneration* **2009,** *17* (6), 763.

96   Tricco, A. C.; Cogo, E.; Isaranuwatchai, W.; Khan, P. A.; Sanmugalingham, G.; Antony, J.; Hoch, J. S.; Straus, S. E., A systematic review of cost-effectiveness analyses of complex wound interventions reveals optimal treatments for specific wound types. *BMC Med* **2015,** *13*, 90.

97   Cirillo, N.; Prime, S. S., Keratinocytes synthesize and activate cortisol. *Journal of Cellular Biochemistry* **2011,** *112* (6), 1499.

98   Lee, B.; Vouthounis, C.; Stojadinovic, O.; Brem, H.; Im, M.; Tomic-Canic, M., From an enhanceosome to a repressosome: molecular antagonism between glucocorticoids and EGF leads to inhibition of wound healing. *Journal of Molecular Biology* **2005,** *345* (5), 1083.

99   de Almeida, T. F.; de Castro Pires, T.; Monte-Alto-Costa, A., Blockade of glucocorticoid receptors improves cutaneous wound healing in stressed mice. *Exp Biol Med (Maywood)* **2016,** *241* (4), 353.

100   Tice, C. M.; Zhao, W.; Xu, Z.; Cacatian, S. T.; Simpson, R. D.; Ye, Y. J.; Singh, S. B.; McKeever, B. M.; Lindblom, P.; Guo, J.; Krosky, P. M.; Kruk, B. A.; Berbaum, J.; Harrison, R. K.; Johnson, J. J.; Bukhtiyarov, Y.; Panemangalore, R.; Scott, B. B.; Zhao, Y.; Bruno, J. G.; Zhuang, L.; McGeehan, G. M.; He, W.; Claremon, D. A., Spirocyclic ureas: orally bioavailable 11 beta-HSD1 inhibitors identified by computer-aided drug design. *Bioorganic & Medicinal Chemistry Letters* **2010,** *20* (3), 881.

101   Terao, M.; Murota, H.; Kimura, A.; Kato, A.; Ishikawa, A.; Igawa, K.; Miyoshi, E.; Katayama, I., 11beta-Hydroxysteroid dehydrogenase-1 is a novel regulator of skin homeostasis and a candidate target for promoting tissue repair. *PLoS One* **2011,** *6* (9), e25039.

102   Preissner, S.; Kroll, K.; Dunkel, M.; Senger, C.; Goldsobel, G.; Kuzman, D.; Guenther, S.; Winnenburg, R.; Schroeder, M.; Preissner, R., SuperCYP: a comprehensive database on

Cytochrome P450 enzymes including a tool for analysis of CYP-drug interactions. *Nucleic Acids Res* **2010,** *38* (Database issue), D237.

103   Hu, Q.; Kunde, J.; Hanke, N.; Hartmann, R. W., Identification of 4-(4-nitro-2-phenethoxyphenyl)pyridine as a promising new lead for discovering inhibitors of both human and rat 11beta-Hydroxylase. *European Journal of Medicinal Chemistry* **2015,** *96*, 139.

104   Emmerich, J.; van Koppen, C. J.; Burkhart, J. L.; Hu, Q.; Siebenburger, L.; Boerger, C.; Scheuer, C.; Laschke, M. W.; Menger, M. D.; Hartmann, R. W., Lead optimization generates CYP11B1 inhibitors of pyridylmethyl isoxazole type with improved pharmacological profile for the treatment of Cushing's disease. *Journal of Medicinal Chemistry* **2017,** *60* (12), 5086.

105   Voets, M.; Antes, I.; Scherer, C.; Muller-Vieira, U.; Biemel, K.; Marchais-Oberwinkler, S.; Hartmann, R. W., Synthesis and evaluation of heteroaryl-substituted dihydronaphthalenes and indenes: potent and selective inhibitors of aldosterone synthase (CYP11B2) for the treatment of congestive heart failure and myocardial fibrosis. *Journal of Medicinal Chemistry* **2006,** *49* (7), 2222.

106   Nikolakis, G.; Stratakis, C. A.; Kanaki, T.; Slominski, A.; Zouboulis, C. C., Skin steroidogenesis in health and disease. *Reviews in Endocrine and Metabolic Disorders* **2016,** *17* (3), 247.

107   Hardman, M. J.; Ashcroft, G. S., Hormonal influences on wound healing: a review of current experimental data. *Wounds* **2005,** *17*, 313.

108   Trengove, N. J.; Langton, S. R.; Stacey, M. C., Biochemical analysis of wound fluid from nonhealing and healing chronic leg ulcers. *Wound Repair and Regeneration* **1996,** *4* (2), 234.

109   Denner, K.; Doehmer, J.; Bernhardt, R., Cloning of CYP11B1 and CYP11B2 from normal human adrenal and their functional expression in COS-7 and V79 Chinese hamster cells. *Endocrine Research* **1995,** *21* (1-2), 443.

110   Kerns, E. H.; Di, L., *Drug-like properties concepts, structure design and methods from ADME to toxicity optimization*. Elsevier: Amsterdam, **2008**, p 526 S.

111   Vuorinen, A.; Engeli, R.; Meyer, A.; Bachmann, F.; Griesser, U. J.; Schuster, D.; Odermatt, A., Ligand-based pharmacophore modeling and virtual screening for the discovery of novel 17beta-hydroxysteroid dehydrogenase 2 inhibitors. *Journal of Medicinal Chemistry* **2014,** *57* (14), 5995.

112   Pullar, C. E.; Grahn, J. C.; Liu, W.; Isseroff, R. R., Beta2-adrenergic receptor activation delays wound healing. *FASEB Journal* **2006,** *20* (1), 76.

136

113   Kratz, G., Modeling of wound healing processes in human skin using tissue culture. *Microscopy Research and Technique* **1998,** *42* (5), 345.

114   Papillon, J. P. N.; Adams, C. M.; Hu, Q.-Y.; Lou, C.; Singh, A. K.; Zhang, C.; Carvalho, J.; Rajan, S.; Amaral, A.; Beil, M. E.; Fu, F.; Gangl, E.; Hu, C. W.; Jeng, A. Y.; LaSala, D.; Liang, G.; Logman, M.; Maniara, W. M.; Rigel, D. F.; Smith, S. A.; Ksander, G. M., Structure−Activity Relationships, Pharmacokinetics, and in Vivo Activity of CYP11B2 and CYP11B1 Inhibitors. *Journal of Medicinal Chemistry* **2015,** *58*, 4749−4770.

115   Ehmer, P. B.; Bureik, M.; Bernhardt, R.; Muller, U.; Hartmann, R. W., Development of a test system for inhibitors of human aldosterone synthase (CYP11B2): screening in fission yeast and evaluation of selectivity in V79 cells. *Journal of Steroid Biochemistry and Molecular Biology* **2002,** *81* (2), 173.

116   Haupenthal, J.; Baehr, C.; Zeuzem, S.; Piiper, A., RNAse A-like enzymes in serum inhibit the anti-neoplastic activity of siRNA targeting polo-like kinase 1. *International Journal of Cancer* **2007,** *121* (1), 206.

117   Lu, C.; Kirsch, B.; Maurer, C. K.; de Jong, J. C.; Braunshausen, A.; Steinbach, A.; Hartmann, R. W., Optimization of anti-virulence PqsR antagonists regarding aqueous solubility and biological properties resulting in new insights in structure-activity relationships. *European Journal of Medicinal Chemistry* **2014,** *79*, 173.